Solubility limits of fission and activation products in saline near field solutions

GRS

Gesellschaft für Anlagen-
und Reaktorsicherheit
(GRS) gGmbH

Solubility limits of fission and activation products in saline near field solutions

Sven Hagemann
Thorsten Meyer
Heike Mönig
Barbara Bischofer
Kyra Jantschik

February 2024

Table of Contents

Kurzfassung

Ereignisabläufe im Endlagersystem, die zu einem Kontakt von Lösungen mit den eingelagerten Abfallbehälter führen, können dazu führen, dass von einer sicheren Isolation der im Abfall vorhandenen Radionuklide im einschlusswirksamen Gebirgsbereich nicht mehr ausgegangen werden kann. Dies kann erfolgen, wenn die eingesetzten Behälter aus mechanischen Gründen oder aufgrund von Korrosion ausfallen, also undicht werden, so dass eindringende Lösung zum Abfall vordringt und die Abfallstoffe aus ihrer Matrix mobilisiert werden. Derartige Entwicklungsmöglichkeiten des Endlagersystems sind nach heutigem Kenntnisstand selbst bei konsequenter Umsetzung des Sicherheitskonzeptes innerhalb eines Endlagers in einer Tonformation zu erwarten. Zur Bewertung dieser Ereignisabläufe sind langzeitsicherheitsanalytische Modellrechnungen durchzuführen.

Der Austrag von Radionukliden aus dem Nahfeld wird häufig durch Löslichkeitsgrenzen bestimmt[1]. Löslichkeitsgrenzen sind jedoch keine starren Größen, sondern hängen stark vom lokalen chemischen Milieu ab (z.B. Salzgehalt, pH, Redoxniveau). In probabilistischen Langzeitsicherheitsanalysen werden in der Regel die Ungewissheiten bezüglich des chemischen Milieus durch Bandbreiten der Löslichkeitsgrenzen abgebildet.

Löslichkeitsgrenzen, die für norddeutsche Unterkreidetonformationen anwendbar sind, wurden bislang nicht abgeleitet. Somit ist die Berücksichtigung chemischer Rückhalteeffekte bei Radionuklid-Ausbreitungsrechnungen derzeit nicht belastbar. Für Endlagerstandorte in Steinsalzformationen liegen aktuelle pH-abhängige Löslichkeitsgrenzen bislang nur für wichtige Aktiniden (u.a. Uran, Plutonium, Thorium), Technetium und Zirkonium vor. Für andere Spalt- und Aktivierungsprodukte (u.a. Nb, Ni, Se, Sn) wurden experimentelle Untersuchungen bislang nicht durchgeführt. Die bislang einzige für salinare Lösungen relevante Studie, in der Löslichkeitsgrenzen für solche Elemente abgeleitet wurden, ist über 30 Jahre alt /BUH 91/. Sie beinhaltet vor allem Schätzungen und spiegelt nicht mehr den Stand der Wissenschaft wider. Mit der vorliegenden Arbeit wurde für viele Spalt- und Aktivierungsprodukte erstmals eine experimentelle Grundlage zur Abschätzung von Löslichkeitsgrenzen für relevante Spaltelemente geschaffen.

---

[1] In Gegenwart von Komplexbildnern sowie durch Sorption an Kolloiden kann aber lokal die maximal mögliche Konzentration an Radionukliden in Lösung über die jeweilige Löslichkeitsgrenze erhöht werden.

Gegenstand der vorliegenden Arbeiten waren folgende chemischen Elemente: Ni, Se, Rb, Sr, Nb, Mo, Pd, Sn, I, Cs, Sm, Zr, Ag und Pb. Radionuklide dieser Elemente werden in langfristigen Sicherheitsanalysen berücksichtigt. Einige tragen in bestimmten Zeitbereichen zu den berechneten Indikatorwerten für die Bewertung der Sicherheit des Sicherheitsbehälters von Radionukliden bei.

Berücksichtigt wurden nur solche Elemente, die auch nicht radioaktive Isotope aufweisen, so dass eine Untersuchung auch ohne strahlenschutzrechtliche Auflagen möglich war. Einige Elemente können unter den erwarteten geochemischen Bedingungen im Nahfeld in mehreren Oxidationsstufen auftreten. Dies betrifft Ag, Mo, Ni, Pd, Se und Sn.

Als Einstieg in das Thema wurden Löslichkeitsgrenzen und löslichkeitsbestimmende Festphasen aus verschiedenen internationalen Endlagerprojekten zusammengetragen. Einige dieser Studien leiteten auch Werte für salinare Lösungen ab, die als Orientierung für Lösungstypen dienen können, die für potentielle Endlagerformationen in Deutschland relevant sind.

Die Zusammensetzung von Lösungen, die im Nahfeld eines Endlagers auftreten können, ist stets standortabhängig. Da in Deutschland noch kein Standort für Endlager für wärmeentwickelnde Abfälle festgelegt wurde, kann derzeit keine Eingrenzung der möglichen Zusammensetzungen erfolgen. Auf Grundlage von historischen Lösungsdaten aus einer Vielzahl von vornehmlich mitteldeutschen Salzbergwerken wurde eine grobe Typisierung vorgenommen. Insgesamt wurden zehn Lösungstypen beschrieben, die grundsätzlich in Salzbergwerken auftreten können. Am häufigsten sind Lösungen mit einem mittleren bis hohen $MgCl_2$-Gehalt (etwa 1 bis 4 mol/kg), teils auch mit erheblichen Mengen an $CaCl_2$ (bis 1.9 mol/kg).

Angesichts fehlender publizierter Daten für Porenwässer im norddeutschen Unterkreideton kann über deren Zusammensetzung nur spekuliert werden. Ergebnisse des parallel abgeschlossenen Projektes KORPHA zeigen jedoch, dass in Unterkreide-Formationen des Apt und älter (≥ 113 Millionen Jahre) wahrscheinlich mit stark salinaren Porenwässern zu rechnen ist[2].

---

[2] Hagemann S.; Mönig H. (2021) Stability of iron corrosion phases expected in a repository in Lower Cretaceous clay. GRS-Bericht 587

Zur experimentellen Bestimmung der Löslichkeit von Spalt- und Aktivierungsprodukten wurden vier Lösungstypen ausgewählt und im Labor synthetisiert:

- Eine Salzlösung, die an Halit und Anhydrit gesättigt ist

- IP9-Lösung, die sich durch Auflösung von polyhalitischem Steinsalz ergibt. Sie weist einen erhöhten $MgCl_2$-Gehalt auf, ist aber nicht an Kalimineralen gesättigt. Lösungen dieses Typs werden häufig in Reservoiren angetroffen. Auch zur IP9-Lösung wurde eine Variante eingesetzt, die sich durch Ausfällung von Magnesium aufgrund der Eisen-Korrosion ergibt. Eine weitere Variante beschreibt eine IP9-Lösung nach Kontakt mit Sorelbeton, welcher für Streckenverschlüssen diskutiert wird.

- IP21-Lösung, eine $MgCl_2$-reiche Lösung, die durch Kontakt von Salzlösungen mit den Kaligesteinen Sylvin, Carnallit und Kainit sowie Polyhalit entsteht. Lösungen ähnlicher Zusammensetzung treten auch als begrenztes Lösungsreservoiren in Salzformationen auf, selbst wenn die genannten Kaligesteine nicht oder nur teilweise in der Umgebung vorhanden sind. Als Variante wurde eine Reaktionslösung eingesetzt, die sich ergibt, wenn IP21-Lösung aufgrund der Korrosion von Eisen basischer wird und es zur Ausfällung von Magnesium kommt.

- Ein Modell-Porenwasser, dessen Zusammensetzung aufgrund eines in Norddeutschland angetroffenen Salinitäts-Gradienten für einen generischen Standort im Unterkreide-Ton berechnet wurde. Es handelt sich um eine $NaCl/CaCl_2$ dominierte Lösung, die im Gleichgewicht mit den im Ton angetroffenen Mineralen steht. Als Variante wurde eine alkalische Lösung eingesetzt, die sich durch Kontakt des Porenwassers mit Portlandit ergibt. Dieses Mineral ist der Hauptbestandteil von Portlandit-Zement, der für den Streckenausbau und die Bohrlochabdichtung in Frage kommt.

Zur Bestimmung der Spaltprodukt-Löslichkeiten wurden die genannten Salzlösungen mit einer geeigneten Festphase des Spaltproduktes versetzt (möglichst diejenige, die aufgrund früherer Untersuchungen wahrscheinlich löslichkeitsbestimmend ist). Anschließend wurde der pH-Wert durch Zugabe von Säure oder Base auf den Zielwert verändert. Die Versuche liefen mindestens einige Monate, die Gleichgewichtseinstellung wurde durch pH-Messung und Analyse des Schadstoffgehaltes kontrolliert.

Für die untersuchten Element/ Lösungskombinationen konnte aufgrund der experimentellen Befunde ein pH-abhängiges Löslichkeitsprofil erstellt werden. Aufgrund teils langwieriger Umwandlungsprozesse in den Versuchsansätzen sind innerhalb des Projektzeitraumes nicht alle Versuche zu einem Gleichgewicht gekommen. In anderen Fällen könnte das geplante pH-Spektrum nicht vollständig abgedeckt werden, weil sich die pH-

Werte aufgrund von Umwandlungsprozessen zu weit von den geplanten Werten entfernt hatten.

Die jeweils löslichkeitsbestimmenden Festphasen wurde in den meisten Fällen per Röntgendiffraktometrie identifiziert. Bei einigen Elementen war eine eindeutige Zuordnung nicht möglich, wahrscheinlich weil nur röntgenamorphe Phasen auftraten. Dies betraf Versuche mit Palladium, Samarium, Zinn, Niob und Zirkonium.

Die Ergebnisse dienten in Kombination mit unabhängigen Informationen zur Ableitung von Löslichkeitsgrenzen für die Lösungstypen Halit/Anhydrit-gesättigte Lösungen, IP9-Lösung, IP21-Lösung und Unterkreidetonwasser jeweils für Lösungen im pH-Bereich von etwa 6 bis 12.

Die Experimente und die Ableitung der Löslichkeitsgrenzen wurden durch geochemische Modellierungen unterstützt. Die hierfür notwendigen thermodynamischen Daten lagen größtenteils nicht in der THEREDA-Datenbasis vor. Sie wurden, soweit möglich, mit verfügbaren Daten aus der Literatur ergänzt. Insbesondere die für salinare Lösungen erforderlichen Pitzer-Ionenwechselwirkungsparameter wiesen für viele relevante Lösungsspezies signifikante Datenlücken auf. In der Literatur beschriebene Methoden zur Abschätzung von Wechselwirkungsparameter wurden dargestellt, diskutiert und an einer Vielzahl von Beispielsystemen getestet. Für 1:1, 1:2 und 2:1-Systeme, also Systeme, die nur einfach oder doppelt geladene Ionen enthalten, ist zum derzeitigen Zeitpunkt die Verwendung von festen Referenzwerten am robustesten. Der vielversprechende Ansatz zur Ableitung von Werten aus Ladung und Ionenradius erwies sich in der Praxis als zu fehleranfällig und zeigt Vorteile nur bei 2:2-Systemen sowie in Systemen, die ein mindestens dreifach geladenes Ion enthalten. Testmodelle zeigen jedoch, dass dieser Ansatz noch erhebliches Potential hat. Mit Hilfe der ausgewählten Schätzverfahren wurden die fehlenden Modellparamater ergänzt, um eine Modellierung in den relevanten pH- und Salinitätsbereichen zu ermöglichen.

Bei einigen Elementen ergaben sich dabei gute Übereinstimmungen zwischen den Modellierungen und den in den Versuchen beobachteten Löslichkeiten. In einigen Fällen kamen dabei aber Annahmen zur Anwendung, die noch durch zusätzliche wissenschaftliche Untersuchungen bestätigt werden müssen. In anderen Fällen bestehen auch nach den Versuchen noch Unsicherheiten bei der Identifizierung der löslichkeitsbestimmenden Phasen und der vorherrschenden Lösungsspezies. Dies machte sich in erheblichen Abweichungen zwischen Experiment und Modellierung bemerkbar.

Auf der Grundlage der experimentellen Ergebnisse und der derzeitigen Möglichkeiten der geochemischen Modellierung wurden in dieser Studie kritische Wissenslücken ermittelt, die im Rahmen künftiger Forschungsaktivitäten geschlossen werden sollten. Hierzu gehören u.a.:

- Erstellung eines vollständigen chemischen Inventars in Abfällen und Behältern unter Einschluss nicht-radioaktiver Bestandteile
- Für die redoxsensitiven Elemente, z.B. Molybdän, Selen, Zinn, Palladium, sollte geklärt werden, mit welchen Oxidationsstufen nach Durchgang durch die Behälter-Korrosionszone tatsächlich zu rechnen ist.
- In einigen Fällen ist die Zusammensetzung der löslichkeitsbestimmenden Phase noch unklar, z.B. bei Sn(IV), Zr, Nb, Pd
- Für einige identifizierte oder angenommene Festphasen liegen nur unzuverlässige oder keine Daten zur Löslichkeit und zur Löslichkeitskonstante vor, z.B. für $MoO_2 \cdot xH_2O$, $Na_2Sn(OH)_6$, $Ni(OH)_3Cl$
- Für die relevanten Oxidationsstufen sind die Spezies zu identifizieren, die im relevanten pH-Bereich und in den betrachteten Lösungstypen vorherrschen, z.B. Sn(IV) bei höheren pH-Werten, Sn(II), Mo(III, IV, V), Nb
- Für calciumreiche Lösungen gibt es Hinweise auf die Bildung von ternären Calciumhydroxo-Komplexen, die die Löslichkeit von Spaltelementen in alkalischen Lösungen stark erhöhen. Solche Komplexe sind für drei- und vierwertige Radionuklidionen bekannt, für zweiwertige Metallionen sollte ihre Relevanz aber noch näher betrachtet werden
- Es werden Wechselwirkungsparameter benötigt, die die Berechnung von Aktivitätskoeffizienten von Spezies erlauben, die unter alkalischen Bedingungen auftreten. Für einige Spezies wurden solche Parameter durch Analogieschluss bereits abgeleitet. Die Datenbasis ist aber besonders bei mittelschweren Hydroxospezies noch lückenhaft, sodass die Analogieschlüsse recht unsicher sind.

Die neu bestimmten Löslichkeitsgrenzen erlauben es die bislang sehr vagen Annahmen zur Löslichkeit der betrachteten Radionuklide in relevanten salinaren Lösungen enger zu fassen. Für viele Elemente konnte die Obergrenze der anzunehmenden Löslichkeit erheblich reduziert werden.

Weiterhin wurde der Einfluss von metallischem Eisen oder Eisen(II)-Korrosionsphasen auf die Löslichkeit einiger redoxaktiver Elemente untersucht. Es konnte gezeigt werden,

dass die Löslichkeit von Palladium, Blei, Silber und Nickel stark vermindert wird, wenn diese Elemente, wie zu erwarten ist, in den elementaren Zustand reduziert werden. Für Molybdän wird nur eine geringe Löslichkeitsänderung vorhergesagt, obwohl es zu einer erheblichen Verschiebung der Oxidationsstufen kommt. Bei Zinn hängt die Löslichkeit oberhalb von pcH 9 stark davon ab, welche Oxidationsstufe (II oder IV) tatsächlich vorherrscht. Die thermodynamische Modellierung sagt die Oxidation zu Sn(IV) und eine starke Abnahme der Löslichkeit durch die Bildung von Calciumstannat (IV) voraus. Im Experiment war aber offensichtlich noch Sn(II) vorhanden, was zu einem deutlich höheren Zinngehalt in der Lösung führte. Zumindest oberhalb von pcH 7 wird die Löslichkeit von Selen durch Eisenselenide bestimmt, die sich sowohl in Gegenwart von metallischem Eisen als auch von Fe(II)-Korrosionsphasen bilden. Stärker reduzierende Bedingungen zwingen Selen ggf. in löslichere Se(-II)-haltige Phasen. Für alle diese sechs betrachteten Elemente ist die Kinetik der Redoxreaktion in Gegenwart von Fe(s)- und Fe(II)-Korrosionsphasen unbekannt. Geschwindigkeit und Produkt der Redoxreaktionen müssen weiter untersucht werden, bevor von den vorhergesagten, oft stark reduzierten Löslichkeiten, Kredit genommen werden kann.

Executive summary

Event sequences in the repository system that lead to a contact of solutions with the stored waste containers can lead to a situation where a safe isolation of the radionuclides present in the waste in the containment-effective rock area can no longer be assumed. This can occur if the containers fail for mechanical reasons or due to corrosion, i.e., if they become leaky, so that intruding solution penetrates to the waste and mobilizes the waste materials from their matrix. According to the current state of knowledge, such developments of the repository system are to be expected in a clay formation even with consistent implementation of the safety concept for a repository. In order to evaluate these event sequences, long-term safety-analytical model calculations must be carried out.

The discharge of radionuclides from the near field is often determined by solubility limits[3]. However, solubility limits are not rigid quantities, but depend strongly on the local chemical environment (e.g., salinity, pH, redox level). In probabilistic long-term safety analyses, the uncertainties regarding the chemical environment are usually represented by ranges of solubility limits.

Solubility limits applicable to North German Lower Cretaceous formations have not yet been derived. Thus, the consideration of chemical retention effects in radionuclide dispersion calculations is currently not reliable. For repository sites in rock salt formations, current pH-dependent solubility limits are only available for important actinides (e.g., uranium, plutonium, thorium), technetium and zirconium. Experimental investigations have not yet been carried out for other fission and activation products (e.g., niobium, nickel, selenium, tin). The only study relevant to saline solutions so far in which solubility limits for such elements were derived is over 30 years old /BUH 91/. It mainly contains estimates and no longer reflects the state of the art. With the present work, an experimental basis was created that supports the estimation of solubility limits for many fission and activation products,

The following chemical elements were the subject of the present work: Ni, Se, Rb, Sr, Nb, Mo, Pd, Sn, I, Cs, Sm, Zr, Ag and Pb. Radionuclides of these elements are

---

[3] In the presence of complexing agents and through sorption on colloids, however, the maximum possible concentration of radionuclides in solution can be locally increased above the respective solubility limit.

considered in long-term safety analyses, and some contribute to the calculated indicator values for the containment safety assessment of radionuclides in certain time ranges. Lead was included in the study because of its high toxicity and considerable mass (over 15.000 t) in repository-relevant waste.

Only elements with non-radioactive isotopes were considered, so that an investigation was possible without radiation protection regulations. Some elements can occur in several oxidation states under the expected geochemical conditions in the near field. This concerns Ag, Mo, Ni, Pd, Se and Sn.

As an introduction to the topic, solubility limits and solubility-determining solid phases were compiled from various international repository projects. Some of these studies also derived values for saline solutions that can serve as orientation for solution types relevant for potential repository formations in Germany.

The composition of solutions that can occur in the near field of a repository is always site-dependent. Since no site for a repository for heat-generating waste has yet been defined in Germany, it is not possible at present to narrow down the possible compositions. Based on historical solution data from a large number of salt mines, mainly in central Germany, a rough typification was made. A total of ten solution types were described, which can basically occur in salt mines. Most common are solutions with a medium to high $MgCl_2$ content (about 1 to 4 mol/kg), partly also with considerable amounts of $CaCl_2$ (up to 1.9 mol/kg).

In view of the lack of published data on pore waters in the North German Lower Cretaceous, we can only speculate about their composition. However, results from the KOR-PHA project, which was completed in parallel, show that in formations of the Apt and older (≥ 113 million years), strongly saline pore waters are probably to be expected[4].

For the experimental determination of the solubility of fission and activation products, four solution types were selected and prepared in the laboratory:

- A salt solution saturated in halite and anhydrite

---

[4] Hagemann S.; Mönig H. (2021) Stability of iron corrosion phases expected in a repository in Lower Cretaceous clay. GRS-Bericht 587

- IP9 solution resulting from dissolution of polyhalitic rock salt. It has an increased $MgCl_2$ content but is not saturated in potash minerals. Solutions of this type are also frequently encountered in reservoirs. A variant was also used for the IP9 solution, which results from the precipitation of magnesium due to iron corrosion. Another variant describes an IP9 solution after contact with Sorel concrete, which is discussed for roadway closures.

- IP21 solution, an $MgCl_2$-rich solution formed by contact of salt solutions with the potash minerals sylvite, carnallite, kainite, and polyhalite. Solutions of similar composition also occur as confined solution reservoirs in salt formations, even if the aforementioned potash minerals are not or only partially present in the environment. As a variant, a reaction solution was used that results when IP21 solution becomes more basic due to the corrosion of iron and magnesium precipitation.

- A model pore water whose composition was calculated based on a salinity gradient encountered in northern Germany for a generic site in Lower Cretaceous clay. It is a $NaCl/CaCl_2$ dominated solution in equilibrium with the minerals encountered in the clay. An alkaline solution was used as a variant, which results from contact of the pore water with portlandite. This mineral is the main constituent of portlandite cement, which is considered for roadway lining and borehole sealing.

To determine the solubilities of the fission products, a suitable solid phase of the fission product was added to the salt solutions (preferably that which, based on previous investigations, is likely to determine the solubility). Subsequently, the pH value was changed to the target value by adding acid or base. The experiments ran for at least a few months, the equilibrium setting was controlled by pH measurement and analysis of the pollutant content.

Based on the experimental findings, a pH-dependent solubility profile could be established for the investigated element/solution combinations. Due to partly lengthy transformation processes in the experimental approaches, not all experiments reached equilibrium within the project period. In other cases, the planned pH spectrum could not be fully covered because the pH values had moved too far away from the planned values due to conversion processes.

The solubility-determining solid phases were identified in most cases by X-ray diffraction. For some elements, however, a clear assignment was not possible, probably because only X-ray amorphous phases occurred. This concerned experiments with palladium, samarium, tin, niobium, and zirconium.

The results, in combination with independent information, were used to derive solubility limits for the solution types of halite/anhydrite-saturated solutions, IP9 solution, IP21 solution and Lower Cretaceous clay water, each for solutions in the pH range of about 6 to 12.

The experiments and the derivation of the solubility limits were supported by geochemical modelling. Most of the thermodynamic data required for this were not yet available in the THEREDA database. They were supplemented as far as possible with available data from the literature. In particular, the Pitzer ion interaction parameters required for saline solutions were not available for many relevant solution species. Methods described in the literature for estimating interaction parameters were presented, discussed, and tested on many example systems. For 1:1, 1:2 and 2:1 systems, i.e., systems containing only singly or doubly charged ions, the use of fixed reference values is currently the most robust. The promising approach of deriving values from charge and ion radius proved to be too error-prone in practice and showed advantages only in 2:2 systems and in systems containing an ion with at least three charges. However, test models show that this approach still has considerable potential. With the help of the selected estimation methods, the missing model parameters were supplemented to enable modelling in the relevant pH and salinity ranges.

For some elements, there was good agreement between the models and the solubilities observed in the experiments. In some cases, however, assumptions were used that still need to be confirmed by additional scientific investigations. In other cases, there are still uncertainties in the identification of the solubility-determining phases and the predominant solution species even after the experiments. This became noticeable in considerable deviations between experiment and modelling.

Based on the experimental results and current geochemical modelling capabilities, this study identified critical knowledge gaps that should be addressed in future research activities. These include:

- Establish a complete chemical inventory in waste and containers including non-radioactive components.

- For the redox-sensitive elements, e.g., molybdenum, selenium, tin, palladium, it should be clarified which oxidation states are expected to be present after passing through the container corrosion zone.

- In some cases, the composition of the solubility-determining phase is still unclear, e.g. for Sn(IV), Zr, Nb, Pd

- For some identified or assumed solid phases only unreliable or no data on solubility and solubility constant are available, e.g. for MoO_2-xH_2O, $Na_2Sn(OH)_6$, $Ni_2(OH)_3Cl$

- For the relevant oxidation states, identify the species that predominate in the relevant pH range and in the solution types considered, e.g. Sn(IV) at higher pH values, Sn(II), Mo(III, IV, V), Nb

- For calcium-rich solutions, there is evidence for the formation of ternary calcium hydroxo complexes, which strongly increase the solubility of fission elements in alkaline solutions. Such complexes are known for trivalent and tetravalent radionuclide ions, but for divalent metal ions their relevance should be considered in more detail.

- Interaction parameters are needed that allow the calculation of activity coefficients of species occurring under alkaline conditions. For some species, such parameters have already been derived by analogy. However, the data basis is still incomplete, especially for medium-heavy hydroxo species, so that the analogy conclusions are rather uncertain.

The newly determined solubility limits allow the previously very vague assumptions on the solubility of the radionuclides under consideration in relevant saline solutions to be defined more narrowly. For many elements, the upper limit of the solubility to be assumed could be considerably reduced.

Furthermore, the influence of metallic iron or iron(II) corrosion phases on the solubility of some redox-active elements was investigated. It could be shown that the solubility of palladium, lead, silver, and nickel is strongly reduced if, as expected, these elements are reduced to the elemental state. For molybdenum, only a small change in solubility is predicted, although there is a significant shift in oxidation states. For tin, the solubility above pcH 9 depends strongly on which oxidation state (II or IV) dominates. Thermodynamic modelling predicts oxidation to Sn(IV) and a strong decrease in solubility due to the formation of calcium stannate (IV). In the experiment, however, Sn(II) was obviously still present, which led to a significantly higher tin content in the solution. At least above pcH 7, the solubility of selenium is determined by iron selenides, which form in the presence of both metallic iron and Fe(II) corrosion phases. More reducing conditions may force selenium into more soluble Se(-II)-containing phases. For all these six elements considered, the kinetics of the redox reaction in the presence of Fe(s) and Fe(II)

corrosion phases is unknown. The rate and product of the redox reactions must be further investigated before credit is taken from the predicted, often greatly reduced solubilities.

1 Introduction

1.1 The role of solubility limits in radionuclide migration calculations

Event sequences in the repository system that lead to a contact of solutions with the stored waste containers can lead to a situation where a safe isolation of radionuclides in the containment-effective rock area can no longer be assumed. This can occur if the containers fail for mechanical reasons or due to corrosion, so that an intruding solution mobilizes the waste materials from their matrix. According to the current state of knowledge, such developments of the repository system are to be expected in a clay formation even with consistent implementation of the safety concept for a repository. To evaluate these event sequences, long-term safety-analytical model calculations must be carried out.

Long-term safety analyses for repositories are based on models and data that help to describe expected or at least possible processes. This is often done at high level of abstraction to reduce computation time. In typical codes used for long-term safety analysis, radionuclide mobilization is represented by the variables radionuclide inventory, mobilisation rates (source term), solubility limits, diffusion coefficients and sorption coefficients. Solubility limits define the concentrations of radionuclides and other hazardous substances that are limited by mineral saturation at the sites under consideration. They depend strongly on the local chemical environment (e.g., salinity, pH). Solubility limits are often given in ranges to reflect uncertainties in the chemical milieu and the chemical behaviour of individual chemical elements.

1.2 Occurrence of saline solutions in clay formations and crystalline rock

In Germany, an important part of clay formations that are considered worthy of further investigation are mainly found in the North German Basin in Lower Cretaceous formations, as the "BGR Clay Study" /HOT 07/ as well as the project AnSichT have shown /REI 13/. These findings were later confirmed by the BGE report of sub-areas with favourable geological conditions /BUN 20/.A particular feature of these formations is the high salinity of the pore water. Depending on location and depth, salinity levels can exceed 300 g/l /ENG 63/. This is close to values found for solutions in the vicinity of salt formations. For the model site North, the AnSichT project assumes a value of 150 g/l at the level of the disposal horizon /NOW 13/.

The chemical properties of the pore solutions in the North German Lower Cretaceous formations are therefore fundamentally different from the weakly mineralised waters found in other European study areas. These include the Boom Clay in Mol, Belgium, the Callovo Oxfordian Clay Formation in Bure, France, and the Opalinus Clay in Switzerland. The chemical investigations on the solubility of radionuclides carried out in these international projects cannot be transferred to German sites, especially those in the northern part of the country. Solubility limits applicable to North German Lower Cretaceous clay formations have not yet been derived. For this reason, a reliable consideration of chemical retention effects in radionuclide transport calculations is not possible at the present time.

Previous generic studies for the development of tools for long-term safety analysis and methods for the comparison of repository systems (e.g. projects TONI - /RÜB 07/[5] and VerSi, /RES 10/) have used data sets developed for weakly mineralised waters (e.g. for Swiss Opalinus Clay sites, /NAG 02/) due to a lack of suitable information. Because of the strong influence of salinity on the solubility of elements, such an approach leads to large uncertainties in long-term safety analyses, or possibly even to incorrectly calculated safety indicators, such as the radiological insignificance indicator[6] value at the edge of the effective containment area /MÖN 12/ or the potential radiation exposure in the biosphere.

Saline waters may also occur in some German crystalline rock formations currently under consideration. If they are or have been in hydrological contact with saline deposits or seawater, high salinities may occur /STO 99/, /BUC 16/. Therefore, saline conditions should be considered until a specific site has been selected.

1.3 Solubility limits for rock salt

Although salt formations have been discussed and investigated for the construction of repositories since the 1960s, surprisingly little work has been done on characterising and typing the potentially occurring solutions and determining solubility limits for relevant radionuclides. The situation still looks best for actinides, technetium, zirconium and

---

[5] FKZ (BMWi) 02 E 9813

[6] German: Radiologischer Geringfügigkeitsindikator (RGI)

neodymium, for which Kienzler et al. (2012) derived solubility limits based on experimental investigations and modelling for two simplified solution types within the framework of the VSG project for Gorleben /KIE 12/. The authors pointed out that the solubility of other radionuclides cannot be predicted at present and that there is a need for further research.

For such radionuclides, only the compilation from Buhmann et al. (1990) is available. This study was based on expert estimates reflecting the state of knowledge in the 1980s and was not linked to a specific solution composition, but only to the "saline rock system" and three not further defined acidity ranges ('acidic', 'neutral, 'alkaline'). The study does not contain any hint how the solubility limits were derived.

In lack of other data, radionuclide migration studies for salt formations utilised the data of Buhmann et al. (1990) (e.g. /KEE 05/, /BUH 08/, /RÜB 10/). After the release of the study of Kienzler et al. (2012) several studies referred to the data therein and set the solubility of other radionuclides to unlimited /KÜP 11/, /BER 20/. However, the lighter fission and activation products (depending on the scenario, ^{135}Cs, ^{129}I, ^{79}Se, ^{59}Ni, ^{36}Cl, ^{14}C, among others) play a special role in release scenarios, since, in contrast to the main components of heat-generating waste (U, Pu), they strongly contribute to the respective safety indicators /KEE 05/: granite/clay, /GRA 08/: clay, /SKB 11/: granite, /AND 05a/: clay).

A new quantification of solubility limits, considering the findings of the last 30 years, therefore seems necessary. This may lead to a significant reduction of the maximum concentrations for individual elements assumed so far. In some cases, higher solubility limits cannot be excluded, e.g., due to the formation of previously unknown or overlooked complexes. Lower solubilities significantly reduce the number of transportable radionuclides. A better knowledge of solubilities helps to reduce conservative assumptions in safety analyses and to document additional safety reserves.

1.4   Study objectives

The overall aim of the project was to determine the solubility limits of fission and activation products in saline waters of North German Lower Cretaceous clay and rock salt formations. This should be achieved primarily on the basis of experimental data. Furthermore, theoretical methods should be tested and applied to obtain information on fission

and activation products for which no experimental data are available, or which can only be obtained with great experimental effort.

The project should contribute to a better understanding of the chemical processes in the near-field of heat-generating radioactive waste and their significance for the long-term safety of a repository system. This will reduce uncertainties in the geochemical properties of these chemical elements and improve the robustness of the results of geochemical modelling calculations.

1.5   Conceptual approach

The derivation of solubility limits is carried out in a multi-stage process. Initially, potentially occurring saline solutions in salt formations and northern German clay formations are discussed and typified as far as possible. This will give an idea of the type of solutions for which solubility limits need to be developed. An overview of solubility limits and solubility-limiting solid phases for selected radionuclides derived from other repository studies is then given. Although the geochemical boundary conditions at European and non-European sites are generally different, these studies provide a useful basis for the selection of solid phases and the classification of our own results. This is followed by a brief review of corrosion studies on nuclear fuel and vitrified waste. Maximum radionuclide concentrations and solid phases have been documented, which can be used as a guide.

The core of the project is the experimental determination of the pH-dependent solubility of radionuclides in selected salt solutions. To support the evaluation of the experiments, geochemical modelling will be performed. For this purpose, thermodynamic data for relevant radionuclides not yet included in the THEREDA database will be collected. Gaps, especially in ion interaction parameters, will be filled as far as possible by estimation methods. For this purpose, different estimation methods will be presented, tested, compared, and evaluated.

The work leads to the derivation of solubility limits for selected radionuclides. These are given both for specific solution types and in combination when the specific solution type is not known a priori.

2 Composition of aqueous solutions potentially occurring salt formations

2.1 Potentially suitable salt formations

Among the evaporate deposits that occur in northern and central Germany the Zechstein deposits have the most promising properties. They are the remnants of the Permian Zechstein Sea that 258 to 250 million years ago covered large parts of Central and Northern Europe (Fig. 2.1).

Fig. 2.1   Extension of Zechstein Sea, Central Europe, 255 million years ago[7]

Zechstein evaporites form mighty deposits of sometimes more than one km thickness. Within the Zechstein seven sequences may be distinguished (Fig. 2.2). Their occurrence and strength vary from region to region. For example, salt deposits of the Werra sequence are typically found only south of the Harz mountains, whereas Leine and later deposits are typically found north of them.

---

[7] Source: San Jose and Drdoht (https://de.wikipedia.org/wiki/Zechsteinmeer) in the German language Wikipedia [GFDL (http://www.gnu.org/copyleft/fdl.html) or CC-BY-SA-3.0 (http://creativecommons.org/licenses/by-sa/3.0/)], via Wikimedia Commons

Among the seven sequences, the Staßfurt sequence is often the mightiest. In Northern Germany where the salt deposits were covered by large sediments layers of higher density, the salt deposits became mobile. Due to the combined action of pressure and density difference the salt deposits deformed and began to flow vertically. The salt structures changed from vertical beds into salt pillows and later diapirs.

In some regions, the Leine sequence also forms significant deposits. For the disposal of radioactive waste, the main rock salt strata z2HS (Staßfurt Hauptsalz) and z3LS to z3OS (Leine Liniensalz to Orangesalz) within the sequences are of special interest /BUN 95/ because they may form layers up to several 100 m thickness. In some regions (Werra/ South Thuringia, Thuringian Basin, South Brandenburg) the Werra rock salt may amount to several hundred meters as well.

Buntsandstein

Mölln-Steinsalz   **Fulda-Folge (z7)**

Friesland-Steinsalz   **Friesland-Folge (z6)**

Ohre-Steinsalz   **Ohre-Folge (z5)**

Aller-Steinsalz   **Aller-Folge (z4)**

oberes Leine-Steinsalz
Kalisalzflöz Riedel

oberes Leine-Steinsalz

mittleres Leine-Steinsalz

Kalisalzflöz Bergmannssegen

Kalisalzflöz Ronnenberg

Leine-Folge (z3)

unteres Leine-Steinsalz

Kalisalzflöz Staßfurt

Staßfurt-Steinsalz

Staßfurt-Folge (z2)

oberes Werra-Steinsalz

Werra-Folge (z1)

Kalisalzflöz Hessen

mittleres Werra-Steinsalz

Kalisalzflöz Thüringen

unteres Werra-Steinsalz

Rotliegend / Grundgebirge

Sandstein   Steinsalz   Gips / Anhydrit   Kalisalz

Tonstein   Karbonat   Konglomerat   Rotliegend / Grundgebirge

Fig. 2.2   Generalized schematic stratigraphic column of the Zechstein series /BGR 16/.

2.2   The occurrence of aqueous solutions in a repository in salt rock

2.2.1   Natural deposits of water

All salt formations contain aqueous solutions, most of them, however, in very small quantities. The rock salt preferred for final storage is selected in such a way that it contains neither crevices nor significant quantities of temporarily stored porous storage rock. The water content of the host formations is then limited to tiny liquid inclusions surrounded by salt crystals. They contain residual solutions or metamorphosis solutions of up to several 100 µl per inclusion /VON 92/. If the rock salt is heated, e.g. by heat-generating waste, a part of the enclosed solution volumes moves towards the heat source /BAA 77/.

Larger amounts of solution are present in porous rocks that are located within or at the edge of the salt formation /VON 92/:

- Gypsum hat: Formed by subrosion of the salt formation. Existing anhydrite is largely converted into gypsum
- Kainite hat: By conversion of minerals containing $MgSO_4$
- Salt level: upper edge of the salt formation, where the dissolution of the salt mines by undersaturated groundwater occurs. At the limits of formations, the dissolution also takes place from the edges (salt slope)
- Buntsandstein: mainly in the Werra-Fulda deposit district above the Zechstein
- Leine carbonate (Ca3, platy dolomite) with a fissure volume of around 10 %.
- Leine anhydrite (A3, main anhydrite), partly embedded, partly in contact with the salt level
- Lower Leine clay (T3, grey salt clay): solution storage but also the location of pathways
- Lower Staßfurth anhydrite (A2, basal anhydrite): Stored below the Staßfurth rock salt (Na2): Solution-filled and possibly in contact with pathways in the horizontal
- Staßfurth carbonate (Ca2, main dolomite): located below the Staßfurth anhydrite, solution or gas-filled, partly also with petroleum

2.2.2   Dispersed water in the host rock and the backfill

In the reference scenario for the post-closure development of a repository at the Gorleben site, it was assumed that there is no inflow of external water to the storage

areas /BEU 12/. However, the salt rock itself contains limited amounts of water (about 0.02 wt.- % /KEL 07a/ p. 53, /HER 01/). Consequently, the crushed rock salt used to backfill the storage drifts will contain similar amounts of water as well. This water is not fully mobile but located finely dispersed at grain boundaries or in fluid inclusions. In one storage concept the crushed salt used to backfill the storage areas was intended to be wetted with brine (max. 1 wt.- % according to /BOL 11/, max. 0.6 wt.- % according to /BOL 12/).

2.2.3 Isolated solution deposits in the host rock

Isolated brine volumes are not expected to occur in the vicinity of the storage drifts /BEU 12/. This assumption may be valid for the Gorleben salt dome but cannot be generalized for all rock salt formations that may be considered as candidate sites for a repository. Currently, it is unclear whether the absence of potentially mobile solution volumes would be a decisive criterion for determining the suitability of a site. Therefore, it is necessary to consider the presence of limited volumes of isolated solutions in the vicinity of the storage drift. In the reference scenario of the Gorleben VSG study, the occurrence of up to 5 100 m^3 isolated solution was considered to be possible near the infrastructure area, where it could be located in a permeable fault consisting of anhydrite /KOC 12/. The volume could potentially be mobilized by movements of the rock salt body and enter the infrastructure area. It would be filled with crushed rock that has a sufficiently high pore volume to consume any limited water inflow from the salt rock or the shaft.

In a less probable scenario, this volume was increased to 20 200 m^3. No further information was given about the possible composition of the solution besides the assumption that it would be a NaCl solution. It is stored in an anhydrite layer where it would be in equilibrium with halite and anhydrite.

If the anhydrite layer is or was also in hydraulic contact with a potash formation other solution types could occur, for example the IP21 solution that is in equilibrium with halite, polyhalite and the potash minerals sylvite, kainite and carnallite.

2.2.4 Water content of radioactive waste

Also, the waste itself may contain water in small amounts. The total amount of water per waste container has been calculated by /LAR 13/. It strongly depends on the waste type.

Waste containers filled with with spent fuel and vitrified waste contain about 14 to 52 kg water (Tab. 2.1). This figure is very small in comparison to the total mass of waste containers (POLLUX: 65 t, CASTOR: 16 to 26 t) /BOL 11/.

Tab. 2.1 Water content of waste containers in an HLW repository in salt (water content of waste and crushed salt, /LAR 13/)

Waste type	Container type	Containers in repository	Water content per container [kg]	Total amount of water in all containers [kg]
Waste from experimental, prototype and research reactors	Castor	511	14.58	7450
Waste from reprocessing	Pollux-9	906	51.47	46632
Spent Fuel	Pollux-10	2120	37.68	79882
Compressed structure parts	Cast steel containers Type II	2620	2.23	5843
Uranium tails	Container VI (steel)	7217	78.74	568267
Graphite waste	Container IV (Concrete)	313	37.23	11653
Other waste	Container Type IV (steel)	1695	507.49	860196
Other waste	Cast steel containers Type II	1150	48.14	55361
Other waste	Concrete Container Type I	800	20.615	16492
Total water in the repository				**1651776**

2.2.5 Groundwaters outside the host rock formation

Two other hyopthetical sources of waters are excluded from further discussions. These are external solutions entering the salt formation through crevices and fissures and freshwater entering the mine through a shaft. The absence of active crevices and fissures and the sealing of human-made shafts, drifts and boreholes is a precondition for showing the isolating performance of a repository site. Only in the hypothetical case of an

independent failure of several consecutive technical barriers unlimited groundwater from outside the formation may enter the repository. The residual risk is so low that such a scenario is not considered in the long-term safety analysis. It may be part of what-if evaluations.

In the same manner, uncontrolled inflow of groundwater during the active operation of the mine or during intended long-term surveillance periods are not included in further discussions as they are thought to be avoidable or manageable through preventive and active measures that are prepared and documented in the incident analysis /WOL 12/.

2.3   Chemical composition of salt solutions

2.3.1   Naturally occurring solutions: major components (Na, K, Mg, Ca, Cl, SO$_4$)

As all salt minerals that occur in German salt formation mainly consist of a combination of the ions Na, K, Mg, Ca, Cl, SO$_4$. Solutions that accompany these formations primarily consist of the same chemical components. For practical as well as historical reasons, the solution composition is often expressed with the help of formal salt contents (NaCl, KCl, MgCl$_2$, MgSO$_4$, CaSO$_4$/ CaCl$_2$), which can be derived from the concentrations of the ions mentioned above according to certain calculation rules:

$c_{NaCl} = I$

$c_{KCl} = c_K$

$c_{MgCl2} = c_{-g} - c_{SO4}$

$c_{MgSO4} = c_{S-4} - c_{CaSO4}$

$c_{CaSO4} = c_{-a} - c_{CaCl2}$

$c_{CaCl2} = (c_{Cl} - c_{NaCl} - c_{KCl} - 2c_{MgCl2})/2$ (either c_{CaCl2} or c_{MgSO4} is zero)

The composition of naturally occurring solutions depends on various factors. First of all, their origin is decisive (e.g., evaporation solution, overburden solution, thermal metamorphosis solution). Subsequently, the entire history of interactions with surrounding salt minerals plays an important role. The composition of the last reservoir rock or the rocks along the inflow path can then change the composition again. Given the large number of possible origins and transformation processes and contact possibilities, the range of possible final solution compositions will be quite broad.

Herbert and Schwand /HER 07/ summarized more than 5800 solution analyses from salt mines in central Germany, especially the Northern Harz, Southern Harz, Saale-Unstrut, Werra-Thüringen and the Calvörde districts. The solutions were observed in different geological strata of the salt formations and thus represent a comprehensive picture of geochemical situations that may occur. They occupy a more or less continuous sector in the five-dimensional space ($NaCl$, KCl, $MgCl_2$, $MgSO_4$, $CaSO_4$/ $CaCl_2$).

Fig. 2.4 shows an overview of those solutions that are saturated with halite, i.e., have been in contact with salt rock for a long time and do not originate from the overburden. They can generally be characterised as follows: The majority of the solutions observed have compositions along the development path F-N-M-P-Q-R-Z (Fig. 2.3: Jänecke diagram). Depending on the formation and ambient temperatures, the compositions can be shifted towards the low-sulphate triangular axis (right). It should be noted that incomplete metamorphosis of salt rocks due to exhaustion of minerals available for reaction or mixing of solutions with higher and lower $MgCl_2$ content may lead to solutions that are between these types.

As a subtype, solutions occur which are more or completely depleted in $MgSO_4$ because of contact with carbonate or calcium sources (calcite, $CaCl_2$ solutions). In such cases, $CaCl_2$ concentrations of up to 180 g/l are possible. This concerns almost 700 of the 5800 solution analyses described.

Following the data in /HER 07/, the observed solutions can be roughly divided into six main groups and ten subtypes:

a) Type A and A': solutions along the R-Z axis. They are in equilibrium with carnallite, kieserite and halite (type A) and additionally with kainite (R) or bischofite (Z). Their $MgCl_2$ content is very high (> 400 g/l). Some solutions of this type have high $CaCl_2$ contents (up to 50 g/l, subtype A').

b) type B and B': solutions around point Q. They are in balance with carnallite, kainite, sylvite, halite and polyhalite. Their $MgCl_2$ content is between 320 and 400 g/l. In some cases ('type B') a part of the $MgCl_2$ is replaced by $CaCl_2$ and the SO_4 content is zero.

c) Type C1 and C1': solutions in the sylvite field between points P and Q. The broad scattering in the direction of the SO_4-free (right) triangular axis is striking. In extreme cases, the SO_4 content is close to zero and high $CaCl_2$ concentrations occur (subtype C1'). They are saturated with sylvite and halite, sometimes also with

kainite or possibly langbeinite (depending on the temperature). It should be noted that the stability limit sylvite/ kainite or sylvite/ langbeinite (25-35 °C: P-Q, 55 °C N-Q, 83 °C: M-R) shifts strongly in the direction of the right triangular axis with temperature. Therefore, a large part of type C (and D) solutions should originate from a three-mineral paragenesis (four if the Ca salts are included), even if this is not obvious when plotted in the Jänecke diagram at 25 °C. The sampling temperature of the solution is often not recorded, and at first, it says little about the historical temperatures to which the solutions were once exposed. The $MgCl_2$ concentration of these solutions lies between 160 and 350 g/l.

d) Type C2 and C2': solutions in the sylvite field along the axis F-M-N-P. Like the type C1 solutions, they are saturated with sylvite and halite, but also with leonite (or langbeinite) and aphthitalite. At least an earlier saturation with these minerals can be assumed since the solution compositions are grouped in a narrow range around this line. Solutions of the type C2' are nearly SO_4-free but contain Ca. The $MgCl_2$ content is between 50 and 250 g/l.

e) Type D: In this group there are several solutions compositions with exceptionally high potassium to magnesium ratio, typically very low sulphate but high Ca concentration. Most documented samples originate from one salt mine.

f) Type E: these are solutions saturated with halite but not with any Ca-free potassium or magnesium mineral (calculated saturation index <0.5 kcal/mol for all relevant solid phases). They have a $MgCl_2$ concentration of 1.5 to 150 g/l. The concentration of NaCl is between 300 and 100 g/l. They typically occur in or near rock salt, anhydrite, or calcite formations. These solutions had only short or limited contact with potash minerals so that saturation did not occur. It is also possible that these are solutions previously saturated with potash minerals but later diluted by NaCl solutions. The IP9 solution, which results from the dissolution of polyhalitic rock salt, also belongs to this group, as well as a solution saturated exclusively with halite and anhydrite as a theoretical limit case. In practice, all salt solutions have a $MgCl_2$ content, albeit small. Formally, these solutions are scattered throughout the Jänecke Triangle. However, due to the lack of saturation of potash minerals, their respective positions only reflect the element ratio. Most E solutions are in the field of C2.

Solutions that are not saturated with halite are very critical. These may be groundwaters from the overburden that penetrate the mine quickly through fissures or shafts. Along their way, they can dissolve salt rock and cause increasing instability of the rock

structure. In a repository, the occurrence of groundwater inflow is avoided by technical measures. Such solutions are not considered here.

A comparison with data from other districts and mines not considered in /HER 07/ (among others Gorleben, Asse, Morsleben) does not reveal fundamentally different types of solutions /BAU 28/, /HER 61/, /HER 00/, /KLA 08/, /SCH 09/, /XIE 12/, /BOH 13/. This also applies to the liquid inclusions found in salt minerals /VON 92/. Typical ranges of solution compositions for each type are shown in Tab. 2.2. They have been extracted from the compilation of /HER 07/ and represent all data sets that are in equilibrium with halite (calculated saturation index above -0.5 kcal/mol).

The following rules have been applied to select the solutions:

- Saturation index for halite > -0.5 kcal/mol
- A-D: at least one K or Mg mineral is saturated (calculated saturation index >-0.5 kcal/ mol)
- D: Mg<35 % and K_2>40 % (Jänecke coordinates)
- E: no K or Mg mineral is saturated (calculated saturation index ≤-0.5 kcal/ mol)
- A: K_2<4 %, M>90 % $CaCl_2$ content = 0 g/l
- A': like A, but $CaCl_2$ content > 0 g/l
- B: 9>K_2≥4 %, Mg>85 %, $CaCl_2$ content = 0 g/l
- B': like B, but $CaCl_2$ content > 0 g/l
- C1: 22>K_2≥9 %, Mg>71 %, $CaCl_2$ content = 0 g/l
- C1': like C1, but $CaCl_2$ content > 0 g/l
- C2: 71≥Mg>39 %, SO_4<25 %, $CaCl_2$ content = 0 g/l
- C2': like C2, but $CaCl_2$ content > 0 g/l

277 solution samples did not fit into this pattern. Further 1413 solution were not saturated with halite and were not considered in this evaluation. Among the solution types C1+C1' is by far the most common (68 %), followed by C2+C2' (16 %) and E (9 %). Solutions with a very high $MgCl_2$ content (A+A', B+B') are far less frequent (6 %) (Fig. 2.5).
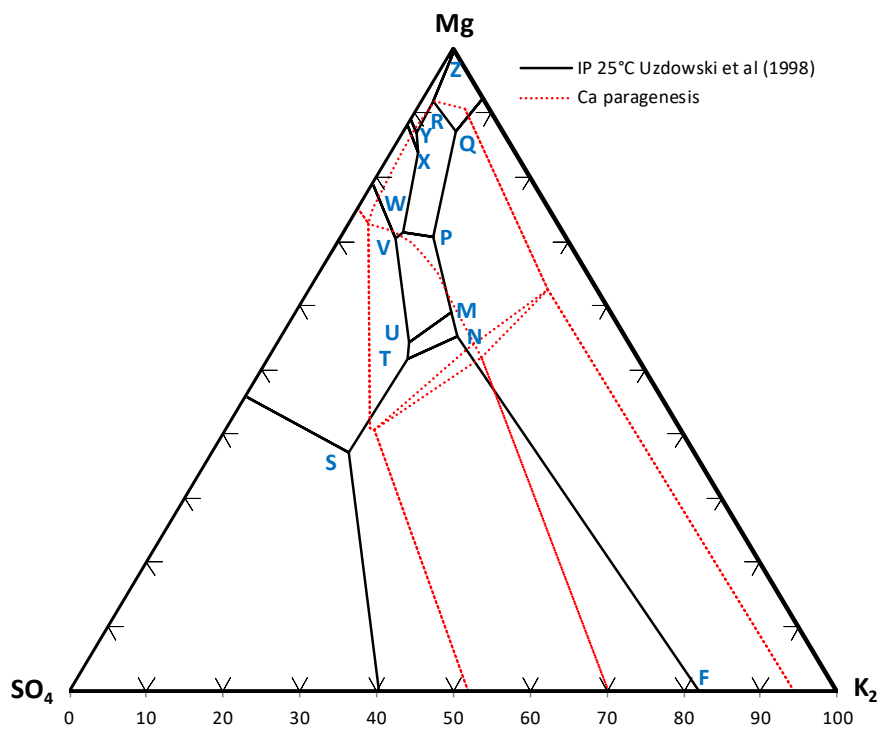
Fig. 2.3   Jänecke projection of invariant points in the halite saturated salt solutions of the system Ca,Na,K,Mg,Ca || Cl,SO$_4$-H$_2$O at 25 °C according to /USD 98/
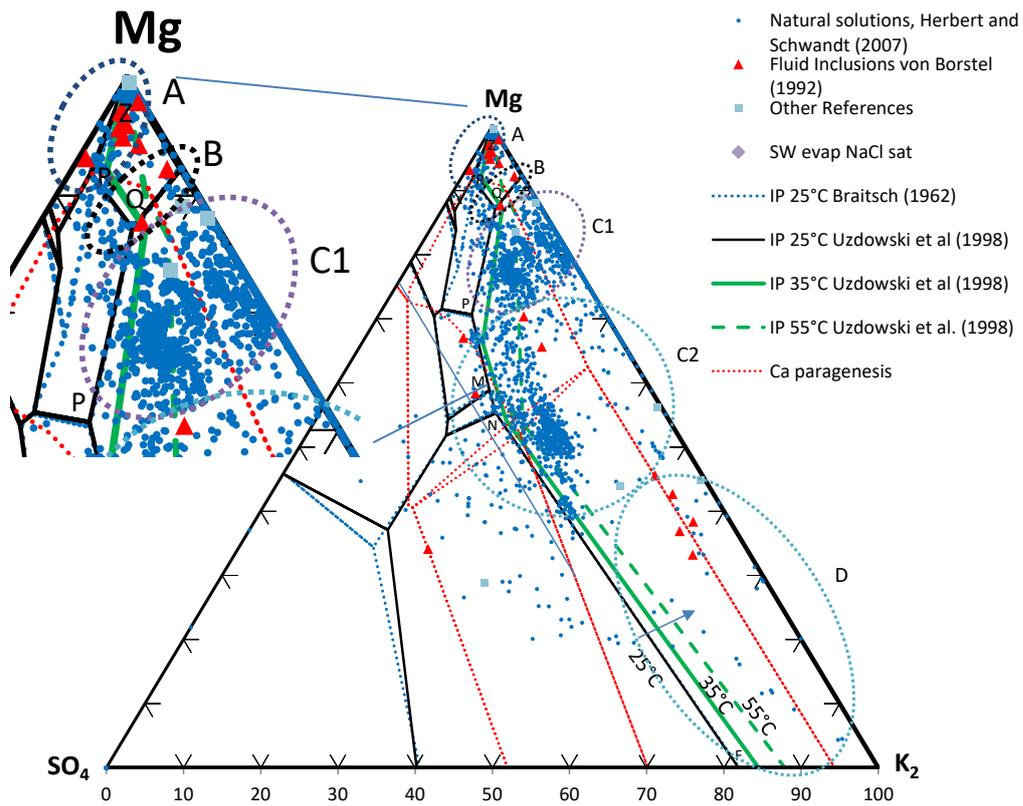
Fig. 2.4 Naturally occurring solutions in German salt mines according to data collected by Herbert and Schwand /HER 07/. Only solutions that are saturated with halite are shown
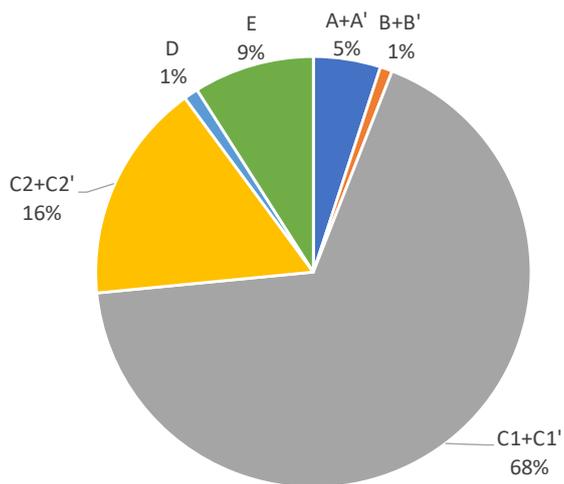
Fig. 2.5 Relative frequency of solution types

Tab. 2.2 Ranges of compositions salt solution types in salt rock (calculated halite saturation index > 0.5 kcal)

Ranges include all data the lie within a confidence interval of 95 %. The median values are in brackets

Group	Near IP	No of sam-ples	K [mol/kg]	Mg [mol/kg]	Na [mol/kg]	SO$_4$ [mol/kg]	Ca [mol/kg]
A	R-Z	173	0.001 – 0.18 (0.046)	4.59 – 5.68 (5.31)	0.08 – 0.76 (0.23)	0 – 0.34 (0.06)	0 – 0.0039 (0)
A'	A	37	0.03 – 0.15 (0.10)	3.44 – 5.26 (4.82)	0.10 – 0.57 (0.19)	0 – 0.005 (0)	0.08 – 1.79 (0.2)
B	Q	33	0.22 – 0.43 (0.31)	3.75 – 5.40 (4.30)	0.15 – 1.98 (0.53)	0.02 – 0.48 (0.35)	0 – 0.007 (0)
B'	E	5	0.23 – 0.36 (0.321)	3.31 – 4.31 (3.68)	0.27 – 0.57 (0.44)	0	0.12 – 0.59 (0.46)
C1	P-Q	2331	0.52 – 0.83 (0.63)	3.06 – 4.13 (3.84)	0.38 – 1.49 (0.60)	0.03 – 0.58 (0.27)	0 *
C1'		514	0.45 – 0.87 (0.71)	1.69 – 3.49 (3.00)	0.43 – 1.92 (1.06)	0 – 0.043 (0)	0.04 – 1.50 (0.44)
C2	(E)-N-P	653	0.71 – 1.43 (1.08)	1.17 – 3.51 (1.79)	0.82 – 3.98 (2.95)	0.01 – 0.81 (0.56)	0 -0.003 (0)
C2'		42	0.65 – 1.72 (0.73)	1.23 – 2.70 (1.42)	0.95 – 2.57 (1.64)	0 – 0.30 (0)	0.21 – 1.86 (1.54)
D	E-(N)	45	1.09 – 1.74 (1.12)	0.06 – 0.59 (0.46)	3.87 – 5.43 (4.31)	0.003 – 0.30 (0.01)	0.01 – 0.38 (0.35)
E	IP9	378	0.03 – 0.86 (0.41)	0.05 – 3.49 (1.12)	0.62 – 5.97 (3.96)	0 – 0.62 (0.26)	0 – 0.9 (0)

)* Ca was not or could not be measured frequently. Analytical values range from near zero to 0.191

2.3.2　　　Minor components

All chemical elements that were listed as minor components of rock salt principally may occur in salt solution as well /HER 61/, /BRA 62/, /BOH 13/. Their concentration strongly varies from sample to sample. The history of an individual salt solution, its contact with different evaporates, the region and location of a salt deposit have a strong impact on the composition as well. No attempt is made to classify the rather scattered information on minor elements concentrations. Instead, the range of possible concentrations is aggregated from different sources /HER 61/: 24 solutions, /HER 07/: 5901 solutions) as to give an idea about the order of magnitude a concentration for an individual element could probably achieve. Tab. 2.3 lists the maximum reported values for 19 components as well as the 95 % quantile. Minimum values are not included because in many analyses report only a few if any trace compounds were mentioned. Some of them have not been analysed, for some the concentration was below the detection limit. If only solutions are selected that occur in rock salt (without discussion of their origin that may be a different formation) then the concentrations in the right part of Tab. 2.3 are found. It is evident that several complex-forming anions always occur: bromide (median 2000 mg/l), boron (median 14 mg/l, but frequently much higher), hydrogen carbonate (median 0.32 mg/l). In some cases, iodine and H_2S are detected. The rather frequent occurrence of 'oil' = organics/ hydrocarbons relates to oil and gas deposits below or near the salt formations.

Tab. 2.3   Maximum Concentrations of minor components in salt solutions

Ele-ment/com-po-nent	All solutions Concentration [mg/l]		Solutions occurring in rock salt formations (Na1α, Na1β, Na1γ, Na2, Na3) Concentration [mg/l]			
	95 % quantile	maximum	median	95 % quan-tile	maximum	No. of an-alysed samples
B	880.8	2500	14	1198	1339.3	34
Ba	16.425	21				
Br	7191	8130	2075	4997	7790	34
Cu	4910	6.8				
Fe to-tal	1610	2300	9	337	510	33
Fe(II)	313.2	1100	8.65	256.8	444	32
Fe(III)	44.6	2300	1.5	49.1	168	33
H_2S	0.673	432	0	18.4	23	5
HCO_3	1900	22150	0.32	1.16	1.94	34
Hg	1	3	0	0.765	0.9	4
I	0.6	14	0	3.8275	10	21
Li	245.6	6000	11.4	254.5	262	31
Mn	409	470				
NH_4	505.2	760	14.09	544.4	563	28
NO_3	72.49	832	6.3	8.28	8.5	2
P	1.6	4.4				
Pb	8	10				
Rb	4.45	140				
Sn	0.2	0.2				
Sr	1052.5	4170	29	1130.25	1280	31
Zn	5.05	12				
Oil	0.673	1500	0	107.95	259	19

The presentation in Tab. 2.3 is only indicative and by no means representative for all potentially occurring salt solutions. Of particular importance for the mobility of radionuclides are potentially bromide, borate, and iodide, as they can form solubility increasing complexes with metal cations. The maximum concentration of bromide shown (8 g/l) is by far not the highest naturally occurring value. For example, a solution with up to 120 g/l bromide was found during the exploration of the carnallite deposit in the Conow mine /PIN 15/. This corresponds to 1.5 mol/l.

2.3.3 Technical solutions

To eliminate or at least the corrosion potential of halite saturated solutions towards Sorel cement, concepts are considered to mix crushed salt used as a backfill in the drifts with concentrated $MgCl_2$ solution. The maximum solution content is 1 wt.- % (see chapter 2.2.1). The composition of this solution is not been defined in /BOL 12/. From a practical point of view, it would make sense to use the same solution as it is needed for the preparation of Sorel cement A1 (Tab. 2.4, /XIE 12/).

Tab. 2.4 Technical $MgCl_2$ solution used to prepare Sorel cement /XIE 12/.

Component	Concentration range [wt.- %]	Averaged concentration [wt.- %]	Averaged concentration [mol/kg]
$MgCl_2$	28.6 – 31.6	30.1	4.72
$MgSO_4$	2.3 – 2.5	2.4	0.30
$CaSO_4$	0.07 – 0.1	0.1	0.011
KCl	0.1 – 0.11	0.1	0.02
NaCl	0.3 – 0.36	0.3	0.08
H_2O	balance	67.0	
Density	1.32 kg/l		

3 Pore water composition and development in the near-field of a repository in clay

3.1 Geology and mineralogy of Lower Cretaceous (Northern Central Europe)

The Lower Cretaceous shows an age o– 144 - 99 million years and is divided into six stages:

- Berriasian/ Weald (144 – 137 million years)
- Valanginian (137 – 132 million years.)
- Hauterivian (132 – 127 million years.)
- Barremian (127 – 121 million years.)
- Aptian (121 – 112 million years.)
- Albian (112 – 99 million years.)

At the beginning of the Lower Cretaceous, the sea level rose worldwide. At that time, there was a large epicontinental area in northern Central Europe, stretching from England across what is now the North Sea, Holland, northern Germany, Poland and far into Belarus/ Russia. This area showed itself to be highly differentiated in detail. Highlands or mainland areas such as the Central European, the English-Armorican and the Fennoscan-Sarmatian land masses lined this area, which is subdivided into several partial depressions alongside the mainland. These are the Danish, Polish, Dutch, and North German depressions. The latter is subdivided into the Lower Saxonian Basin and the Pompeckj Plain, among others. These depressions largely show a comprehensive sedimentation sequence of the entire Lower Cretaceous /WAL 07/, /AME 07/.

3.1.1 The Lower Cretaceous in the Lower Saxony basin

The Lower Saxon Basin is characterized by a great thickness and a wide distribution of Lower Cretaceous sediments such as clays /AME 07/. The basin is divided into three parts due to different sediment thickness and lithological changes: a western part in the area of the Emsland, a central part in the area of Osnabrück-Bielefeld-Minden-Vechta-Sulingen and an eastern part, which extends to the area of Hannover-Braunschweig.

While at the beginning of the Lower Cretaceous (Wealden) the basin was sweetened to a greater or lesser extent by a strong cut-off from the Cretaceous North Sea, the first

extensive marine intrusion occurred during the Valanginian. In the Hauterivian, the intrusion extended to parts of the Pompeckj Block. Water exchange also took place with the Polish-Danish Basin in Wealden and Hauterivian. In the further course of the Barremian, regressions in the south-eastern and eastern parts of the basin led to an interruption of the marine connection to the east. In the western part of the basin, oxygen-rich water continued to be supplied from the north. These waters hardly reached the central or eastern part of the Lower Saxon Basin, because the Pompeckj Block did not allow a significant seaway to the Cretaceous North Sea. Thus, bituminous sediments could form in these basins under reducing conditions. This changed in the Lower Aptian. The Pompeckj Block subsided, and a connection was established between the Cretaceous North Sea and the central and eastern part of the Lower Saxony Basin. The sediments from these areas show a change of sedimentation conditions and an oceanic influence. In the Albian, the sea space in north-western Germany continues to expand /AME 07/. Fig. 3.1 offers an overview of the Lower Saxony Lower Cretaceous Basin.
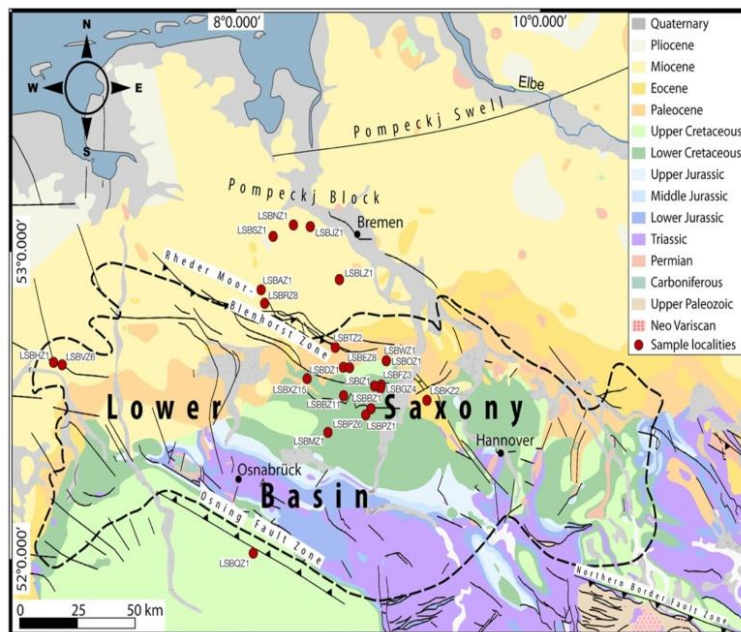
Fig. 3.1   Lower Cretaceous formation (green) in the Lower Saxony basin /NAD 19/[8]

---

[8] Open Access under a Creative Commons licence (https://creativecommons.org/licenses/by/4.0/)

Fig. 3.2   Lower Cretaceous clay formations in Northern Germany where favorable geological conditions can be expected /BUN 20/[9]

3.1.2   Mineralogy of the Lower Cretaceous clay formations

The mineralogical composition of the clay rocks from the Lower Cretaceous is known from several localities in the eastern part of the Lower Saxony Lower Cretaceous Basin. The restriction to this part of the basin follows from the fact that model sites for this area have been developed /AME 07/, /REI 13/, /JAH 13/ and therefore the descriptions of the upcoming formations are very detailed. The drillings Wichendorf 1/86, Hoheneggelsen KB9 and Ahlum 1 /MÜL 95/, the clay pit Hoheneggelsen /LIP 55/ and Sarstedt /KEM 78/ and the drillings Konrad 1 as well as the shaft drillings Konrad 1 and 2 were used among others for this purpose.

Both in the Hauterivian and the Barremian, layered silicates (35 % to 52 %), quartz (13 % to 30 %) and carbonates (calcite, dolomite, and siderite, 7 % to 55 %) were found as main components in the drilling around the Konrad mine. The transition zone Barremian/ Aptian shows increased smectite and alternating storage mineral contents. These again increase from the sub-Albian /JAH 13/. The compositions of the clay rocks in the Hauterivian and the Barremian is described in detail in /HAG 21/.

---

[9]   Graphic prepared by the interactive viewer provided by BGE on https://www.bge.de/de/endlagersu-che/zwischenbericht-teilgebiete/

35

3.2   Composition of fluids

3.2.1   Origin and salinity of fluids in the North German Basin

The fluids in the Lower Cretaceous clays were primarily formed a) during sedimentation as trapped pore water and b) as enriched saline solutions during evaporation. The trapped pore water mostly originates from brackish or seawater with primarily high salinities. These compositions can be changed by secondary processes. These processes are diagenetic or, at higher temperatures, also metamorphic. Furthermore, the supply and mixing with fluids from other stratigraphic horizons have to be mentioned /WOL 11/.

For clay formations in northern Germany, salinity depends on location and depth. Also, the chemical composition is typified by depth /MÜL 75/ /HOT 97/ /WOL 11/.

This results in a range of possible characteristics for the siting regions and repository depths in question, which is an essential factor in the prediction of radionuclide solubilities. To date, however, no measured data are available for the pore solution in deep Lower Cretaceous formations in northern Germany. Within the framework of the KOR-PHA project /HAG 21/, model-based considerations were made to derive reasonable assumptions about the probable composition of pore solutions.

Diagenetic processes are caused by increasing pressure and temperature so that the salinity increases with depth due to the clay membrane effect. At a depth > 1000 m and a temperature > 50 °C chemical diagenesis starts, which leads to a change in the salinity trend /WOL 11/. Also, the compaction and selective displacement of ions from the clay pores into the surrounding water-bearing rocks over millions of years affect the composition of the pore waters /HAG 21/

a) If the mineral kaolinite predominates, the pore solution remains saline. Near salt formations, the salt concentration can even rise to the saturation limit. According to current knowledge, such conditions can be expected in the layers of the Aptian and older (≥113 million years) in the North German Lower Cretaceous. This is the area in which e.g., the Generic Model Site North is located, which is referred to in various projects of GRS and BGR.

b) If smectites predominate, salinity levels may fall to levels well below those of the original seawater. Ions are pressed out into the surrounding sandstones. The salinity there can then be very high (up to 10-20 times higher than in the clay pore

waters). This is probably the case in northern Germany in the layers from Albian and younger (≤113 million years)

Further considerations may be found in the report of the project KORPHA /HAG 21/.

3.2.2 Model pore water composition of a Lower Cretaceous clay

At present, there are no analytical data available from Northern Germany on the pore water for the Lower Cretaceous clays. Engelhardt and Gaida (1963) provided some values for kaolinitic dominated Jurassic clays /ENG 63/. Concentrated salt solutions are present in these clays. This is consistent with the findings from other clay deposits where it could be shown that compacted marine kaolinitic clays tend to have high saline pore waters (see above). Since the mineralogical composition of the lower Hauterivian, the host rock in the North Repository Site Model North is similar to that of the Upper Jurassic, likely, high saline solutions are also present here. The actual composition of the pore waters in the Lower Cretaceous can currently only be estimated.

Further details can be found in the final report of the KORPHA project /HAG 21/. They are based on the following assumptions:

- The model solutions were calculated for the generic model repository "NORD". It is located at a depth of 770 m in the Lower Hauterivian claystone /REI 13/, /LOM 15/. This claystone is rich in kaolinite.
- Since the pore waters in kaolinitic clays differ only slightly from the formation waters in the accompanying water-bearing sandstones, it is possible to rely on measured data in these formations.
- At least for the Konrad shaft and some surrounding boreholes, evaluations are available for the correlation between depth, salinity, and solution components (total salt content).
- Klinge et al. found that all mine waters of Konrad are of the Na-Ca-Cl type. The ion ratios Na/Cl, Ca/Cl, Mg/Cl and Br/Cl all show a linear correlation with depth, so that it is possible to predict the total composition of groundwater at a specific depth within a certain range of uncertainty. /KLI 92/
- No correlations are available for minor ions, but chemical analyses of the waters from the Hils sandstone aquifer provide some valuable insight even though the

calculated salinity of the model water is a proximately 10 % higher than the Hils water.

- Using geochemical modelling, the water formulated in this way was mathematically brought into contact with minerals known to be present in the claystone - goethite, pyrite, calcite, dolomite, gypsum, and siderite

The resulting composition may be found in Tab. 3.1.

Tab. 3.1 Lower Cretaceous formation water at a depth of 770 m (calculated based on the relationships in and around Konrad shaft

Ion	Concentration [mol/l]	Concentration [mol/kg]	Concentration [mol/kg] After saturation with goethite, pyrite, calcite, dolomite, gypsum, and siderite
Li^+	0.01288	0.01369	-
Na^+	2.48472	2.64095	2.64
K^+	0.00455	0.00484	0.00484
Mg^{2+}	0.06751	0.07176	0.0806
Ca^{2+}	0.17841	0.18963	0.194
Fe^{2+}	0.00034738	0.00037	0.000495
Fe^{3+}			$4.25 \cdot 10^{-11}$
Sr^{2+}	0.00502454	0.00534	-
$B(OH)_4^-$	0.00083	0.00088	-
HCO_3^-	0.00257878	0.00274	0.0021
Cl^-	2.98642	3.17420	3.16
SO_4^{2-}	0.00491	0.00522	0.0191
Br^-	0.00503	0.00534	-
I^-	0.00006	0.00006	-
HS^-			$2.28 \cdot 10^{-10}$
-log cH			6.41
TDS	173.6		
pH	6.5		

To carry out solubility tests, a model pore water was prepared according to the concentrations shown above. For this purpose, the salts listed in Tab. 3.2 were dissolved in water. After that calcite and gypsum in solid form were added.

Tab. 3.2 Recipe for preparing a model pore water at a depth of 770 m in Lower Hauterivian clay

Ion	Concentration [mol/kg]	Salt/ Solution	Mass for preparing a solution with 4 kg H_2O
Na^+	2.64	NaCl (Sigma Aldrich 31434)	617
K^+	0.00484	KCl (Merck 1.04933)	1.44
Mg^{2+}	0.0806	$MgCl_2 \cdot 6H_2O$ (Merck 1.05833)	65.5
Ca^{2+}	0.194	$CaCl_2 \cdot 2H_2O$ (Merck 1.42000)	114
Fe^{2+}	0.000495	Fresh $FeCl_2$-solution, free of Fe^{3+} (11.49 wt.- %)	2.231
HCO_3^-	0.0021	$NaHCO_3$ (p.a. Merck 1.06329)	0.706
Cl^-	3.16	Charge balance	
SO_4^{2-}	0.0191	$Na_2SO_4 \cdot 10H_2O$ (Merck 1.06648)	24.6
Br^-	0.00534	NaBr (Merck 1.5833)	2.20
H_2O			3921
-log cH	6.41		
pH	6.5		
Calcite		$CaCO_3$ (Merck 2066)	20
Gypsum		$CaSO_4 \cdot 2H_2O$ (Merck 1.02161)	20

4 Radioactive inventory and hypothetical maximum radionuclide concentrations

4.1 Elements considered in this study

In a repository, a large number of radionuclides may occur. They include the elements of the primary nuclear fuel (mainly U) as well as fission, activation, and decay products. Some of them are very short-lived and play no important role in safety considerations. Within the present study, the following elements were further investigated:

Ni, Se, Rb, Sr, Nb, Mo, Pd, Sn, I, Cs, Sm[10], Zr, Ag, Pb

Radionuclides of these elements are listed national regulatory guidelines /BUN 06/ or were considered in long-term safety analyses (e.g. /KEE 05/, /AND 05a/, /GRA 08/, /SKB 11/). Lead was included because of its high toxicity and its considerable mass in radioactive waste (above 15.000 t, /PFE 11/).

Some other radionuclides were not investigated further:

- ^{36}Cl has the same well understood properties as the two naturally occurring isotopes ^{35}Cl und ^{37}Cl.
- For ^{14}C in its simple forms (carbonate and methane) the solubility can already be derived with existing databases. The range of possible organic carbon compounds that could contain radioactive ^{14}C is too wide to be characterized by a general solubility limit.
- For the same reason ^{41}Ca was not included because Ca is a rock forming element and naturally present in all potential host rock formations.
- Elements that have no stable isotopes and cannot not be managed in the GRS laboratory ^{99}Tc, ^{226}Ra as well as all actinides.

---

[10] Also as an analogue for other rare earth isotopes such as ^{144}Ce, ^{143}Nd, ^{145}Nd, ^{152}Eu.1^{54}Eu, ^{155}Gd

4.2 Radioactive inventory

The radioactive inventory of a German repository in Salt rock has been evaluated by /PFE 11/ and summarized by /LAR 13/ within the preliminary safety analysis for Gorleben (VSG). It depends among other things on the storage time of the waste before its emplacement in a repository. Moreover, the types of waste to be transported to an HLW repository may change according to regulatory requirements. Recent considerations to include non-heat-generating waste into a single repository /BUN 15/ will likely not lead to a significant change of the total radioactive inventory since the total amount of radionuclides in LLW and ILW is low in comparison to the HLW inventory. However, the volume of waste, the water content in waste as well as the amount of non-radioactive waste and stable isotopes would considerably increase. No new calculations of the total radioactive and non-radioactive inventory for a combined HLW/LLW/ILW repository are available so that the inventory from the Gorleben study is taken as a basis. For a repository in clay, the same radioactive inventory is assumed.

The calculated inventory is shown in Tab A. 49 along with the radionuclides' half-lives and total masses. These were calculated from their respective activities by using formula (4.1):

$$m_i = \frac{M_i \, A_i \, T_i}{N_A \, \ln(2)}$$

(4.1)

m_i mass of radionuclide I [g]
A_i activity of radionuclide [Bq]
T_i half-live of radionuclide I [s^{-1}]
N_A Avogadro constant (6.0221×10^{23} mol^{-1})

98 % and more of all fission products are concentrated in spent fuel and vitrified waste (CSD-V). Relevant percentages of activation products (Ni, Nb, Mo) are also found in CSD-C waste. A key problem of this as well as other inventories is that they concentrate on radioactive fission and activation products. A very considerable amount of these products is inactive. In the case of lanthanides there are much more inactive than active isotopes in the glass /GRA 97a/. In addition to that, materials used for the construction of containers may also contain significant amounts of the same elements. This especially applies to metallic materials: Mo (up to 3 wt.- % in structural parts of fuel elements), Ni (up to 72 wt.- % in structural parts of fuel elements), Nb (1 wt.- % in zircaloy 4), Sn (1.5

wt.- % in zircaloy 4), Zr (97 wt.- % in zircaloy 4). Lead is no major part of spent fuel or vitrified waste but occurs as the final and inactive decay product of uranium and plutonium. However, quite enormous quantities may be present in MOSAIK containers used for compressed structural elements (about 9.4 t in each container, in total 13700 t) and in other non-heat-generating waste (1700 t) /PFE 11/.

Omitting this contribution may lead to incorrect prediction of the nearfield geochemistry. For example, the concentration of a radionuclide may be assumed to below the solubility limit and entirely in the liquid phase while in reality the limit is exceeded, and part of radionuclide is bound in a solid phase. On the one hand, this is advantageous with regards to radionuclide retention. On the other hand, this may become a problem when assessing the risk of criticality in the nearfield.

4.3   Inventory controlled upper limit of radionuclide concentration

The maximum concentration of radionuclides in the pore water of the surrounding backfill may be calculated by dividing the radionuclide inventory with the pore volume available at the time of the first radionuclide release. The calculation is of hypothetical nature as it assumes that there is enough solution to fill these pores, all waste containers become penetrable without any water being lost because of corrosion and the full radionuclide inventory is mobilised into the liquid phase. The calculation is unrealistic because:

- Only a small fraction of containers (0.1 %) is considered to fail without prior corrosion /WOL 12/.

- Only part of the radionuclides is mobilized immediately or shortly after the first contact with water (instant release fraction). Much of the inventory is retained in the waste matrix and will be released only slowly. If there is a transport path leading out of the emplacement areas part of released radionuclides will leave the area before further amounts are added to the solution inventory.

- Significant amounts of water are consumed by corrosion and secondary formation of hydrated salts and cannot support corrosion of the waste matrix and mobilization of radionuclides.

Nevertheless, the calculation allows to identify those radionuclides whose maximum concentration is probably so low that is not controlled by solubility.

In rock salt, the maximum amount of water that could theoretically be present in the emplacements drifts is limited by the pore volume of the salt backfill. Kienzler et al.

calculated the maximum concentration of radionuclides in a repository in salt rock based on the inventory in spent fuel and a void volume of 2 m^3 per container /KIE 13/. The results are summarized in Tab. 4.2. It should be noted that the underlying inventory only listed radioactive fission and activation products but no inactive isotopes.

There are multiple potential combinations of waste types, host rocks and emplacement concepts. For comparison with the above-mentioned study on rock salt, two calculations were performed for a repository in clay rock. It was based on the concept of borehole emplacement in a clay rock formation of high thickness (variant C in the RESUS project /ALF 20/). In this concept three BSK containers are placed in a vertical borehole surrounded by a steel liner. The void between containers and liner is filled with sand.

Two variants are considered

- Three triple-pack BSK containers each containing vitrified waste in 2 CSD-V moulds (in total there are 1868 BSK containers with CSD-V waste)

- Three BSK containers each containing either three fuel elements from pressurized water reactors or nine fuel elements from boiling water reactors (in total there are 11159 BSK containers with spent fuel from commercial reactors)

The diameters and volumes per borehole are listed in Tab. 4.1. The maximum total pore volume per borehole (without considering the formation of any secondary corrosion phases) is 3.51 m^3. The radionuclide inventory per borehole was calculated by dividing the total inventories per waste type in A 1.1 by the number of BSK containers and multiplying the result with three (the number of BSK containers per borehole). A comparison between experimentally determined solubility limits and inventory controlled maximum concentrations will be done in chapter 8.11.2.

Tab. 4.1 Characteristics of a vertical borehole for the storage of vitrified waste and spent fuel in clay rock

Parameter	Value
Length of the borehole	32.4 m
Inner diameter of the bore-hole	0.62 m
Total inner volume of the liner	9.8 m^3
Volume of three BSK con-tainers	0.99 m^3
Volume of sand	8.8 m^3
Porosity of sand	35.8 %
Total pore volume	3.51 m^3

Tab. 4.2   Radionuclide inventory and hypothetical maximum concentrations for a generic repository in salt rock (bold: elements considered in this study) - I

Radionu-clide	Inventory [Bq] /LAR 13/	Inventory in repository [log mol]	Clay rock vertical borehole CSD-V [log mol/l]	Clay rock vertical borehole SF [log mol/l]	Salt rock drifts SF [log mol/l] /KIE 12/
Be-10	1.91E+11	1.36	-5.7	-5.9	no data
C-14	8.14E+14	2.55	-4.9	-4.9	no data
Cl-36	1.58E+13	2.55	-4.7	-4.7	no data
Ca-41	8.51E+11	0.82	-6.3	-6.4	no data
Ni-59	3.55E+15	4.30	-6.1	-3.0	no data
Ni-63	3.26E+17	3.39	-7.0	-3.9	
Se-79	3.84E+13	3.14	-3.8	-4.1	-2.6
Rb-87	1.75E+10	4.80	-2.2	-2.4	-1.8
Sr-90	1.37E+19	4.47	-2.7	-2.7	-1.8
Y	No data	No data	No data	No data	-1.6
Zr-93	1.58E+15	5.25	-1.8	-2.0	-0.7
Nb-94	4.68E+15	3.85	-7.4	-3.4	-5.1
Mo-93	6.44E+13	1.23	-7.7	-6.0	-0.8
Tc-99	1.18E+16	5.27	-1.7	-2.0	-2.5
Ru	No data	No data	No data	No data	-1.1
Rh	No data	No data	No data	No data	-1.8
Pd-107	1.13E+14	4.74	-2.4	-2.5	-1.5
Ag-108m	5.52E+13	0.24	-6.7	-7.0	-2.8
Cd	No data	No data	No data	No data	-1.5
In	No data	No data	No data	No data	-4.1
Sn-126	4.87E+14	3.94	-3.1	-3.3	-2.7
Sb	No data	No data	No data	No data	-3.4
Te	No data	No data	No data	No data	-2.0
I-129	2.76E+13	4.52	-2.6	-2.8	-2.2
Xe	No data	No data	No data	No data	gas
Cs-135	4.02E+14	4.78	-2.2	-2.4	-1.3
Cs-137	2.26E+19	4.71	-2.5	-2.5	
Ba	No data	No data	No data	No data	-1.1
La	No data	No data	No data	No data	-1.4
Ce	No data	No data	No data	No data	-1.2
Pr	No data	No data	No data	No data	-1.5

Tab. 4.3 Radionuclide inventory and hypothetical maximum concentrations for a generic repository in salt rock (bold: elements considered in this study) – II

Radionuclide	Inventory [Bq] /LAR 13/	Inventory [log mol]	Clay rock vertical borehole CSD-V [log mol/l]	Clay rock vertical borehole SF [log mol/l]	Salt rock drifts SF [log mol/l] /KIE 13/
Nd	No data	No data	No data	No data	-1.0
Sm-147	4.21E+09	4.53	-2.4	-2.7	-1.6
Sm-151	1.96E+17	3.14	-4.0	-4.1	
Eu	No data	No data	No data	No data	-2.4
Gd	No data	No data	No data	No data	-2.3
Ho-166m	9.52E+11	-1.06	-8.5	-8.2	no data
Ra-226+	1.36E+11	-1.78	-10.5	-10.4	-5.8
Ac-227	1.27E+11	-3.68	-11.3	-11.5	no data
Th-229	4.24E+11	-0.60	-10.1	-9.5	-3.9
Th-230	5.17E+11	0.47	-7.4	-6.8	
Th-232	2.72E+11	5.46	-4.3	-4.7	
Pa-231	1.49E+11	-0.43	-8.1	-8.2	-6.3
U-232	5.15E+13	-0.57	-10.7	-8.0	1.0
U-233	5.80E+13	2.84	-6.9	-6.0	
U-234	1.11E+15	4.31	-5.1	-2.9	
U-235	2.15E+13	6.06	-3.8	-1.6	
U-236	1.39E+14	5.39	-4.2	-1.7	
U-238	1.31E+15	8.65	-1.9	0.5	
Np-237	3.50E+14	4.75	-2.3	-2.5	-1.5
Pu-238	2.78E+18	4.27	-5.2	-2.9	-1.0
Pu-239	2.08E+17	5.58	-3.5	-1.5	
Pu-240	4.58E+17	5.36	-3.6	-1.8	
Pu-242	2.78E+15	4.90	-4.6	-2.2	
Pu-244+	3.33E+11	3.30	-4.6	-3.8	
Am-241+	4.23E+18	5.14	-2.6	-2.0	-1.9
Am-242m	1.43E+16	2.18	-5.4	-5.0	
Am-243	3.89E+16	4.34	-3.2	-2.8	
Cm-245	1.58E+15	3.01	-5.1	-4.1	-4.4
Cm-246	2.59E+14	1.97	-6.3	-5.2	
Cm-247	1.42E+09	0.22	-8.3	-6.9	
Cm-248	3.66E+09	-1.03	-9.7	-8.1	

5 Results of previous waste corrosion studies

5.1 General overview

The intrusion of aqueous solutions to vitrified waste and spent fuel causes to corrosion and mobilisation processes that lead to continuous release of radionuclides into the liquid and in some cases to the gas phase. Experimental investigations of corrosion processes in saline solutions were mainly conducted in the late 1980s to early 2000s at the For-schungszentrum Karlsruhe (FZKA, now KIT) and in France. On the background of the then planned construction of a repository in the salt dome of Gorleben and the scenarios discussed at that time, most experiments were conducted at high temperatures (e.g., 190°) and in contact with one of three saline solutions that were considered relevant for Gorleben (solutions I to III, see Tab. 5.1). The results gave valuable insights into the kinetics of glass and SF corrosion, the release and fate of radionuclides and the type of secondary phases that may bind radionuclides. However, the experimental temperature was often quite far away from the conditions that are expected in the medium to long-term when the hypothetical release of radionuclides is considered to take place in current safety studies. Processes, solid phases, kinetics, and element concentrations may be substantially different at moderately increased temperatures than observed in such ex-periments.

Tab. 5.1   Composition of Gorleben solutions I, II, and III

Component	Solution I MgCl$_2$-rich Q solution (55 °C)	Solution II	Solution III NaCl solution
Na$^+$	0.378	0.083	6.036
K$^+$	0.967	0.022	0.037
Mg^{2+}	4.471	5.401	0.018
Ca^{2+}	-	0.316	0.021
Cl$^-$	9.933	11.538	6.036
SO$_4^{2-}$	0.177	0.0006	0.058
pH	6.53	6.28	6.85

5.2 Corrosion of vitrified waste

Most experiments at the FZKA were conducted with inactive materials, especially a simulate of R7T7, the vitrified waste product from COGEMA. To this group of glass types also belongs the SON68 glass, another inactive simulate of R7T7 as well as the MW (Magnox waste) glass which represents vitrified waste produced by BNFL.

Specimens from these experiments were analysed over a period of more than seven years by various authors (Tab. 5.2). In the centre of the second line of experiments was an inactive simulate of GP-WAK I, a glass produced in the reprocessing pilot plant in Karlsruhe (until 1990). Finally, active R7T7 glass was investigated by Grambow et al. /GRA 96a/.

All five borosilicate glass types have a similar chemical composition (see A.3) so that the results are generally comparable. Much more data is available on the leaching of glass in pure or weakly mineralized waters (e.g., /CUR 06/, /VAN 06/, /BOS 09/, /GIN 21/, /THO 21/. At this place, no summary is made on these results, but some observed secondary minerals are included in the following discussion.

It should be noted that the corrosion of glass in $MgCl_2$ rich solutions leads to rather low pH values (e.g., pH 3.5) because of the formation of magnesium silicate hydrates that leads to a release of hydrogen ions (simplified):

$$x\ H_4SiO_4 + y\ Mg^{2+} \rightarrow Mg_yH_{4y-z}(SiO_4)_y + z\ H^+$$

Once magnesium is depleted the pH increases. In NaCl solution, mildly alkaline conditions are reached soon (pH 7 to 9) /ZIM 03/.

Tab. 5.2 Glass corrosion experiments in salt solutions

Experiment	Source
Inactive R7T7 simulate in NaCl solutions at 90 °C (concentrations between 0 and saturation) (up to 28 d)	/GOD 88/
Inactive R7T7 simulate in Gorleben solutions I, II and III at 190 °C (solution III also at 110 and 150 °C) (up to 7.5 y)	/GRA 90/, /LUT 93/, /ABD 95/, /ABD 97/, /ZIM 03/
Inactive GP-WAK I simulate in Gorleben solutions I and III at 110 and 190 °C	/LUC 96/
Inactive GP-WAK I simulate in contact with halite at 90 and 180-210 °C (in situ experiment, 10.2 y)	/ZIM 03/
Inactive GP-WAK I simulate in Gorleben solution II at 20, 50 and 80 °C in batches with and without metallic iron (up to 2 y)	/ZIM 03/
Active R7T7 (Cogema) in Gorleben solution II at 190 °C	/GRA 96a/

A general observation in all experiments was that fission products typically did not occur in individual well defined solid phases but rather as components in complex secondary host phases or in solid solutions. Without going too much into detail and not differentiating between experimental conditions, the host phases in Tab. 5.3 were found. The retaining mechanisms may be sorption on fresh surfaces (silicates), solid solutions (baryte, powellite/ molybdates, zircon) and ion exchange processes (zeolites, clay minerals) /ZIM 03/. Up to 99 % of the radionuclide inventory of glass may be retained in secondary phases /CUR 06/.

So far, research concentrated on actinides and a selection of fission products, namely Sr, rare earth elements (REE) and Zr. Little information is available on the fate of other radionuclides present in vitrified waste.

Some long-term studies also showed that some element concentrations (Nd, Mo, U) reached a plateau thus demonstrating the existence of solubility limiting processes /GRA 13/. In some cases solubility limiting phases could be confirmed or identified by thermodynamical modelling (e.g. /RAI 11a/).

The observed maximum solution concentrations depended very much on the starting conditions, the liquid to surface ratio, the corrosion process, and the resulting pH value. They cannot be directly compared with each other or with solubility studies without the presence of glass but provide useful orientating points (Tab. 5.4).

Tab. 5.3   Host phases that were found to bind fission products during the corrosion of vitrified waste with brines

Host phase	Cs	Mo	Ni	REE	Sr	Zr
Secondary silicates (Mg silicates, clay minerals such as smectite, chlorites, saponite)	x	x	x	x		x
Zircon, $ZrSiO_4$				x		x
Baryte, $BaSO_4$/ $(Ba,Sr)SO_4$				x	x	
Powellite, $CaMoO_4$/ REE molybdates, e.g. $(Ca,Na_{0.5}REE_{0.5})MoO_4$		x		x		
'Spherules'		x		x		
Cerianite, CeO_2				x		x
REE sulphates $REE_2(SO_4)_3$				x		
Phosphates/ apatite $(Ca,REE)PO_4$				x		
REE hydroxide carbonates, $REE(OH)CO_3$						
RRE hydroxides, $REE(OH)_3$ *)				x		

)* not found in experiments but assumed to exist in neutral to alkaline solutions based on solubility calculations /RAI 11a/

Tab. 5.4   Observed maximum radionuclide concentrations in long-term glass corrosion studies

Component	MW Water, 90 °C (12 y) (1) [log mol/l]	R7T7 analogue $MgCl_2$-rich (Gorleben I) 190 °C, S/V 10000 m^{-1} 7 y (2) [log mol/l]	R7T7 analogue NaCl-rich (Gorleben III) 190 °C, S/V 10000 m^{-1} 7y (2) [log mol/l]
Ca	-5.7		
Mo	-3.2	-3.3	-3.0
Nd	-5.2	-2.9	-4.7
Ni	-6.8		
SO_4	-6.0		
Sm	-5.9	-2.8	-3.6
Sr	-5.2		
Zr	-4.1		
pH	9.1	2.9	7.9

1 /CUR 09/
2 /ZIM 03/

5.3 Corrosion of spent fuel

As there are no inactive analogues to spent fuel, experiments can only be done with active material. Due to the experimental challenges, the number of studies dealing with the release of radionuclides from SF when in contact with saline waters is low (Tab. 5.5).

In the course of the experiments of Grambow et al. the concentrations of Cs, Sb, Sr, U and Pu constantly increased while that of Ag, Tc (10^{-7} mol/l) and Ru (10^{-8} mol/l) soon approached a constant value /GRA 96b/. The concentration of the trivalent actinides Am and Cm as well as Eu first increased but later decreased. The main observed retention mechanism in these experiments was sorption of radionuclides on iron corrosion phases (REE, trivalent actinides). U and Pu often remained on the surface of the spent fuel matrix. For REE and trivalent Actinides, the formation of a mixed hydroxide (REE,An) or the coprecipitation of An(III) with U(VI) phases were considered to be the solubility limiting processes /GRA 96b/. The release of strontium was constant and served as an indicator of the corrosion process.

In the studies of Metz et al. radionuclide concentrations increased within the first 10 months of the experiment. After that the liquid phase was replaced and most solution concentrations dropped /MET 08/. There is no information on the fate of fission products.

Tab. 5.5 Corrosion experiments with spent fuel in salt solutions

Experiment	Source
High burnup SF from a light water reactor and unirradiated UO_2 in NaCl solution at 25 and 150 °C under anaerobic conditions in batches with and without metallic iron (up to 2 y)	/GRA 96b/, /GRA 97b/
Corrosion of high burnup SF in NaCl brine in presence of H_2	/LOI 05/
Corrosion of SF and γ-irradiated UO_2 in NaCl brine in presence of H_2 and Br (up to 2 y)	/MET 08/

6   Methods for the estimation of ion interaction coefficients

6.1   Introduction

For the calculation of solid-solution equilibria in saline systems, suitable models are required which take into account the specific interactions between the dissolved species. For this application field, the Pitzer theory has become generally accepted for the calculations of activity coefficients /PIT 91/. For a pure solution of the salt MX the Pitzer formula reads as follows:

$$\ln \gamma_\pm = -A_\varphi |z_M z_X| \left[\frac{\sqrt{I}}{1 + b\sqrt{I}} + \frac{2}{b} ln(1 + b\sqrt{I}) \right] + 2m \frac{\nu_M \nu_X}{\nu_M + \nu_X} [B_{MX} + B_{MX}^\varphi] \tag{6.1}$$

$$+ 3m^2 \frac{(\nu_M \nu_X)^{3/2}}{\nu_M + \nu_X} C_{MX}^\varphi$$

γ±   mean activity coefficient of solute MX

z_M, z_X charge of species M and X

A_φ, b   Debye Hückel coefficients

I   Ionic strength

ν_M, ν_X ,stoichiometric coeffjcients of cation M and anion X in salt MX

B, B^φ Pitzer terms, a function of the Pitzer coefficients molality of species j

C^φ Pitzer coefficient

with

$$B_{MX}^\varphi = \beta_{MX}^{(0)} + \beta_{MX}^{(1)} e^{-\alpha_1 \sqrt{I}} + \beta_{MX}^{(2)} e^{-\alpha_2 \sqrt{I}} \tag{6.2}$$

$$B_{MX}^\varphi = \beta_{MX}^{(0)} + \beta_{MX}^{(1)} g\left(\alpha_1 \ \sqrt{I}\right) + \beta_{MX}^{(2)} g\left(\alpha_2 \ \sqrt{I}\right) \tag{6.3}$$

$$g(x) = \frac{2[1 - (1 + x)e^{-x}]}{x^2} \tag{6.4}$$

α_1, α_2 Pitzer coefficients, typically a fixed value for all ion pairs

$\beta^{(0)}$, $\beta^{(1)}$, $\beta^{(2)}$ Pitzer coefficients

More Details may be found in /PIT 91/. In the course of the past decades, several databases have been developed that are able to describe heterogenous gas-solid-liquid as well as complex aqueous equilibria. One of the very first was the model of Harvie, Moeller, and Weare that addressed the equilibria in seawater system, H^+-Na^+-K^+-Mg-Ca^{2+}||$Cl^-$$SO_4^{2-}$-$CO_3$-$OH$-$H_2O$ /HAR 84/.

For a number of radionuclides relevant data were combined in the internally consistent data base THEREDA (currently Am(III), Cm(III), Np(V), Cs, Th(IV), Np(IV), Pu(IV), U(IV/VI), Sr) /MOO 15/. For some other elements consistent databases are also available, but they are not yet part of THEREDA, e.g., Pb, Zr, Ni.

These databases contain solubility constants, complex formation constants, and ion interaction coefficients for relevant combinations of dissolved species.

However, for most fission, activation and decay products, consistent and comprehensive data bases for the relevant pH range are not available. This is mainly due to the fact that medium to heavy fission elements, in contrast to actinides, were much less in the focus of scientific programs, and research on their behaviour in salt solutions is rather an exception. Also, the determination of Pitzer interaction coefficients for complex species is a very demanding experimental task, prone to errors and, moreover, often enough inseparable from the determination of complex formation constants. For many species occurring in medium to high pcH values, activity coefficients are difficult to determine and their dependence on the media concentration is only roughly known, if at all.

In these cases, modelling without ion interaction coefficients is not a suitable approach. The specific interactions can lead to a considerable change in the activity coefficients and thus in the observed solution properties (e.g., solubility). It makes more sense to use estimation methods to arrive at plausible parameters which do not predict the activity coefficients particularly accurately but in the correct magnitude. For this purpose, several methods are available, some of which will be presented here. A systematic comparison and validation of the individual models is not carried out in this study. This should be subject of further investigations.

6.2 Conversion of SIT to Pitzer coefficients

A simpler approach than the Pitzer theory to describe specific ion interactions is the Specific Ion Interaction Theory (SIT) (/BRÖ 22/, /GUG 55/, /CIA 80/). It contains a slightly different Debye-Hückel term and only one adjustable parameter per ion combination.

$$\log \gamma_i = -z_i^2 A \frac{\sqrt{I}}{1 + b\sqrt{I}} + \sum_j \varepsilon_{i,j}\, m_j \tag{6.5}$$

γ_i	activity coefficient of species i
z_i	charge of species i
A,b	Debye Hückel coefficients
I	Ionic strength
$\varepsilon_{i,j}$	ion interaction coefficient for the pair of species i and j
m_j	molality of species j

The approach is mainly used at low and medium ionic strengths to extrapolate conditional equilibrium constants to zero ionic strength. Depending on the salt, the formula provides reliable results up to ionic strengths of around 1 (sometimes even higher). It is not suitable for precise modelling in highly concentrated salt solutions, as the deviations from the actual activity coefficients can then increase dramatically. Fig. 6.1 shows the activity coefficients of NaCl solutions. The difference between the values calculated with SIT and Pitzer at the highest concentration (6.1 mol/kg) is less than 0.08 log units (about 17 %). In contrast, the difference with Na_2CrO_4 solutions (4.5 mol/kg) already reaches 0.5 log units (factor 3), while up to 1 mol/kg the agreement is very good (Fig. 6.2). The reason for that may be that available SIT coefficients were determined on the basis of a limited dataset covering only solutions of rather low ionic strength. Using only one adjustable parameter, the SIT approach by nature has a less powerful ability to describe all the characteristics of a specific salt solution over the entire solubility range (the Pitzer approach uses up to three adjustable parameters).

If SIT parameters have been developed for sufficiently concentrated solutions, they may be transformed into Pitzer ion interaction parameters. Of course, direct optimization of Pitzer coefficients is always preferable, but in several cases original data may not be at hand or requires cumbersome evaluation of experimental data. Moreover, the SIT approach provides some easy estimation methods for interaction coefficients parameters that cannot be used within the Pitzer model. In such cases, calculation of Pitzer from SIT coefficients may have some advantages.

A simple transformation method was presented by Grenthe et al. /GRE 97/. If $\varepsilon_\gamma(M,X) = \varepsilon(M,X) \cdot \ln(10)$ is known, $\beta^{(0)}$ and $\beta^{(1)}$ may be approximated using the following relationships (Tab. 6.1)

Tab. 6.1   Relationship between Pitzer and SIT ion interaction coefficients

Ion combination (M-X)	$\beta^{(0)} - \varepsilon/2$	$\beta^{(1)}$
1-1	0.035	0.34
2-1, 1-2	0.150	1.56
3-1, 1-3	0.366	4.29
4-1, 1-4	0.754	8.89

Instead of using such simplifying conversions, it is also possible to derive Pitzer coefficients numerically. This can be done easily using the following method:

1. The activity coefficients of a salt are calculated over a certain concentration range using known SIT coefficients.
2. On this basis Pitzer coefficients are optimized. Due to the weakness of the SIT model at high ionic strengths, it is sufficient to limit the evaluation to $\beta^{(0)}$ and $\beta^{(1)}$.

With this method, for $\beta^{(1)}$ values are obtained that depend essentially only on the charge type of the salt and the maximum salt concentration used. Values close to the $\beta^{(1)}$ coefficients proposed by /PLY 98/ are only retained if the maximum concentration of the evaluated experimental data was close to one.

How well calculations with Pitzer and SIT parameters agree, depends on several factors. First of all, the maximum concentration of solutes has to be considered that was used for the optimization of parameters. Unfortunately, information on the upper concentration limit is often missing in overview tables (e.g., in the NEA reports) and needs to be researched for each value. If it is unclear whether at least moderate concentrations (up to 3 mol/kg) were used in optimization of parameters, Pitzer coefficients should better not be calculated from SIT coefficients if a later use in saline systems is planned.

Secondly, the SIT approach with one adjustable parameter cannot represent quadratic characteristics of an activity curve. At higher concentrations SIT generated curves always end in a straight line whereas many real systems show a flattening of an initially almost linear trend. The Pitzer formalism addresses this behaviour with the quadratic C Term. If the full concentration range is fitted with one SIT parameter, the flattening can be included to a certain extent but only at cost of weaker agreement at medium concentrations.

Fig. 6.1 Mean activity coefficients of NaCl in aqueous solution at 25 °C calculated with Pitzer and SIT coefficients

Fig. 6.2 Mean activity coefficients of Na_2CrO_4 in aqueous solution at 25 °C calculated with Pitzer and SIT coefficients

6.3 Correlation between chemically similar ions

6.3.1 Pitzer coefficients for complex ions: use of analogues with identical structure

Interactions between ions of similar size and chemical structure can be described by similar interaction coefficients if they are primarily of non-specific electrostatic nature. A simple example would be the pairs K^+, $Fe(CN)_6^{3-}$ and K^+, $Co(CN)_6^{3-}$. The two complex ions $Fe(CN)_6^{3-}$ and $Co(CN)_6^{3-}$ have an almost identical radius and molecular weight, the metal nucleus is not important for the external interactions of the ion, so that the interactions with K^+ are also very similar. Analogues of this kind have been employed in many studies (e.g., Reardon 1990: silica species/ sulphate species; Rai et al. 2018: $Zr(OH)_6^{2-}$ / $Hf(OH)_6^{2-}$).

In principle, groups of chemically similar compounds can be formed, which are suitable for an estimation of ion interaction coefficients (without claiming to be complete), e.g.

Oxoanions:

- $M^{VI}O_4^{2-}$: SO_4^{2-}, SeO_4^{2-}, CrO_4^{2-}, MoO_4^{2-}, WO_4^{2-}
- $M^{VII}O_4^-$: ClO_4^-, BrO_4^-, ReO_4^-, MnO_4^-, TcO_4^-

Hydroxo complexes

- $M^{II}(OH)_3^-$: $Pd(OH)_3^-$, $Pb(OH)_3^-$, $Sn(OH)_3^-$, $Fe(OH)_3^-$, $Ni(OH)_3^-$
- $M^{II}(OH)_4^{2-}$: $Zn(OH)_4^{2-}$, $Cd(OH)_4^{2-}$, $Cu(OH)_4^{2-}$
- $M^{III}(OH)_4^-$: $Al(OH)_4^-$, $Fe(OH)_4^-$, $Sm(OH)_4^-$
- $M^{IV}(OH)_6^{2-}$: $Sn(OH)_6^{2-}$, $Zr(OH)_6^{2-}$, $Pb(OH)_6^{2-}$

Halogeno complexes:

- $M^{II}Cl_3^-$: $PdCl_3^-$, $PbCl_3^-$, $SnCl_3^-$
- $M^{II}Cl_4^{2-}$: $HgCl_4^{2-}$, $PbCl_4^{2-}$, $SnCl_4^{2-}$, $PdCl_4^{2-}$

It is also conceivable to compare ions with slightly different chemistry, but similar ionic radius and charge, e.g.:

$M^{IV}O_3^-/ HM^{VI}O_4^-$, SeO_3^{2-}/ HSO_4^-, $H_3SiO_4^-/ HSO_4^-$

Mixed complexes represent an experimental challenge. For the estimation of Pitzer coefficients, it can be assumed in a first approximation that the interactions with species with only one ligand exchange are similar, e.g.:

$Pd(OH)Cl_3^{2-}$, $PdCl_4^{2-}$

6.3.2 Similarity of activity coefficients of potassium and sodium salts

For modelling in seawater systems, it is important to note that interactions with Na^+ and K^+ are often, though not always, similar, e.g. in selenates /HAG 12a/ and chromates /HAG 15a/:

Na^+, SeO_4^{2-}: $\beta^{(0)}= 0.09771$; $\beta^{(1)}= 0.78265$; $C = 0$

K^+, SeO_4^{2-}: $\beta^{(0)}= 0.09481$; $\beta^{(1)}= 1.62335$; $C = 0.00021$

The differences in the coefficients $\beta^{(1)}$ and C have only a minor impact on the calculated activity coefficients (Fig. 6.3, Fig. 6.4). They are only 0.15 log units apart. Higher differences of up to 0.4 log units are observed in solutions of sodium and potassium plumbites, $Pb(OH)_3^-$, and dicarbonato cadmates, $Cd(CO)_3^{2-}$ (Fig. 6.5, Fig. 6.6).

Fig. 6.3   Calculated activity coefficients for Na_2SeO_4 and K_2SeO_4 /HAG 12a/

Fig. 6.4   Calculated activity coefficients for Na_2CrO_4 and K_2CrO_4 /HAG 15a/

Fig. 6.5   Calculated activity coefficients for $Na_2[Cd(CO_3)_2]$ and $K_2[Cd(CO_3)_2]$ /HAG 12b/

Fig. 6.6   Calculated activity coefficients for Na[Pb(OH)$_3$] and K[Pb(OH)$_3$] /HAG 12b/

6.4   Estimation of β$^{(2)}$ for strongly associating ion pairs

In saline solutions, the parameter β$^{(2)}$ is usually irrelevant since the ionic strength de-pendent term $e^{-\alpha_2\sqrt{I}}$ approaches zero at low ionic strengths if the typical α_2 value 12 is chosen. It can be neglected under most circumstances. If an estimation is thought nec-essary, the following estimation method is a promising start /PIT 78/:

$$\beta^{(2)} = \frac{K}{2}$$

(6.6)

K   complex formation constant for the species MX(aq)

6.5   Reference values for Ion interaction coefficients based on their charge type

A simple approach to estimate unknown binary Pitzer ion interaction coefficients is based on the observation that the coefficients for certain charge types lie within defined band-widths. Thus, from the large number of meanwhile determined Pitzer parameters for "mean values" can be derived for the charge types 1-1, 1-2 and 2-1, and so on. A corre-sponding approach has been presented e.g. Plyasunov et al. and Humphreys et al. /PLY 98/, /NEC 11/, /HUM 22/.

/PLY 98/ /PLY 98/ pointed out that β$^{(1)}$ shows a typical range of values depending on the charge type:

- 1-1: 0.20 ± 0.20
- 2-1: 1.5 ± 0.6
- 3-1: 5.2 ± 1.2

In cases of poor data availability $\beta^{(1)}$ may be fixed at a typical value, and C/C^φ neglected, thus reducing the number of adjustable parameters to one. An extended set of fixed values was presented by Neck et al. /NEC 11/.

The purpose of this approach was to provide reasonably realistic values for the parameters $\beta^{(0)}$ and $\beta^{(1)}$ if the SIT interaction coefficient is zero. The approach was intended for moderate ionic strengths (< 1 mol/kg).

Humphreys et al. derived guide values for both $\beta^{(0)}$ and $\beta^{(1)}$ by averaging a large number of ion interaction coefficients. However, their approach was limited to charge types 1-1, 1-2 and 2-1, but a similar approach can easily be derived for 2-2 systems by averaging from tabulated Pitzer coefficients /KIM 88a/. In this case, the following reference values result (Tab. 6.2). The performance of this approach is given later.

Tab. 6.2 Reference values for ion interaction coefficients based on their charge type

Charge type	$\beta^{(0)}$	$\beta^{(1)}$	$\beta^{(2)}$	Source
1-1	0.0503	0.1951 $\alpha(1)=2$		1
1-2, 2-1	0.243	1.447 $\alpha(1)=2$		1
2-2	0.23	2.9 $\alpha(1)=1.4$	-40 $\alpha(2)=12$	2

1 /HUM 22/
2 This work based on /KIM 88a/

6.6 Correlation between physical properties of ions and ion interaction coefficients

Comparisons of a large number of experimentally determined Pitzer coefficients show that there is a correlation with the charge of the ions involved the ion radii and the chemical structure of the anion. Such relationships were evaluated by Kim as well as Simoes et al. /KIM 88b/, /SIM 16/, /SIM 17/.

A general function that applies to all ion types and sizes could not be found so far. Difficulties are posed by asymmetric ions (e.g., NO_3^- or $H_2PO_4^-$), ion combinations that tend to form complexes or ion pairs (if they are not explicitly considered in the chemical model), as well as certain combinations of ions with high and low charge density. According to Blandamer /BLA 70/ the room around an ion may be divided into three zones:

I.   the hydration shell, tightly bound to the ion by electrostatic forces
II. a structure broken layer with molecules that are not bound to the hydration shell but influenced by it so that they are more disoriented than in the bulk zone
III. the bulk water, unaffected by the coulombic force of the ion

Ions may be classified into structure breaking and structure forming ions:

a)   Structure breaking ions (chaotropes) are typically large ions with a low charge (low charge density, e.g., ClO_4^-) that interact weakly with water and form a rather weak hydration shell I. They cause a large zone II, increase the specific density and entropy.
b)   Structure making ions (kosmotropes) are small ions with a high charge (and high charge density) that strongly interact with water and facilitates its structuring (e.g., Mg^{2+}). The hydration sphere is prominent while zone II is rather small or missing. The impact of structure making ions on entropy and solution density is opposite to that of structure breaking ions.

Examples for both types are shown in Tab. 6.3. (taken from /SIM 16/). They may be classified based on the method described by Marcus /MAR 94/, which evaluates the Gibbs free energy connected with the binding and unbinding of water molecules in the vicinity of an ion. Combinations of the same type of ions typically lead to the formation of ion pairs and complexes, an effect that must be accounted for when ion interactions are quantified.

Tab. 6.3   Examples for structure making and structure breaking ions

Ion type	structure making/ kosmotrope	structure breaking/ chaotrope
cation	H^+, Li^+, Mg^{2+}, Ca^{2+}, Sr^{2+}, Ba^{2+}, Co^{2+}, Cu^{2+}, Fe^{2+}, Ni^{2+}, Zn^{2+}, Al^{3+}, Ce^{3+}	Ag^+, Cs^+, K^+, Na^+, NH_4^+, $Rb+$,
anion	F^-, OH^-, CH_3COO^-	Cl^-, Br^-, I^-, NO_3^-, ClO_3^-, ClO_4^-

A quantitative measure helping to assess the ion's affiliation to one or the other group is the relationship between charge and ionic radius, also called the ionic potential $p_i=z_i/r_i$. Another quantity is the coulombic term z^2/r. Wood et al. /WOO 84/ showed that there is a relationship between the activity coefficient and the ratio of ionic potentials p_{cation}/p_{anion}.

Kim et al. pointed out that ions with the same ionic potential may have different entropies because of differing electron configurations /KIM 88b/, /KIM 91/. Therefore, while z/r may be similar, the properties of ions also depend on their chemical type. The authors investigated the relationship between Pitzer coefficients and physical parameters such as ionic radii, ionic potential, and ionic entropy. In the first step, they correlated the standard state molar entropy and the coulombic term z^2/r with $\beta^{(0)}$.

For each type of 1-1 salts (alkali fluorides, chlorides, bromides, iodides, hydroxides, perchlorates, acetates, and nitrates) there was a linear relationship according to the following empirical function (Fig. 6.7).

$$\beta^{(0)} = a + b \, z_M^2/r_M \tag{6.7}$$

Fig. 6.7 Correlation between tabulated values for $\beta^{(0)}$ and the quotient of charge and ion radius of the cation /KIM 88b/

The properties of chlorides, bromides and iodides could be combined into one group when the values for $\beta^{(0)}$ were plotted against the potential ratio p_{cation}/p_{anion} (resulting in a straight line). For alkali sulphates (1-2 system) a quadratic function was needed to describe the relationship between $\beta^{(0)}$ ^{and} z^2/r with p_{cation}/p_{anion}.

The $\beta^{(0)}$ parameters for 2-1 systems such as earth alkali halides, chlorates and perchlorate show a good correlation with the standard entropy of the cation and the coulombic term. All these systems may be plotted in a narrow band. Interactions with nitrate belong to a different group.

As described by Pitzer and co-workers before, for all salts there was a simple relationship between $\beta^{(0)}$ and $\beta^{(1)}$:

1-1: $\beta^{(0)}/\beta^{(1)}=0.424$

1-2 and 2-1: $\beta^{(0)}/\beta^{(1)}=0.087$

For ternary systems $HX-MX_2-H_2O$ and $HX-MX-H_2O$ (x= Cl, Br, ClO_4) the parameter Ψ_{HMX} was considered unnecessary. The ternary interaction could be described by θ_{HM} alone. It was found that there is a correlation between θ_{HM} and the entropy of the cation, which

67

can be represented by a quadratic function for each of the two cation groups considered (IIA, IA and transition metals). However, omitting Ψ_{HMX} can lead to practical problems when other ternary systems with the same cation pair but different anions are to be modelled.

Sun et al. /SUN 92/ found for 1-1 electrolytes that $\beta^{(0)}$ and $\beta^{(1)}$ can be derived from the ionic radii of the cation and anion and another parameter that reflects the overlap of hydration shells when hydrated cations and anions approach each other in more concentrated solutions. This overlap coefficient had to be fitted based on osmotic coefficients – with the result that the empirical specific interaction parameters were replaced by another empirical parameter.

Li et al. /LI 04/ investigated the relationship between ionic radii, charge and rotational relaxation times and Pitzer ion interaction coefficients. They could demonstrate that the ion interaction coefficients $\beta^{(0)}$, $\beta^{(1)}$, and C for 1-1, 2-1, 3-1 and 1-2 pairs may be related to charge and ionic radio via the following expressions

$$\log \gamma_i = -z_i^2 A \frac{\sqrt{I}}{1 + b\sqrt{I}} + \sum_j \varepsilon_{i,j}\, m_j \tag{6.8}$$

$$\beta^{(0)} = 0.0561\frac{r_+}{r_-} - 0.0422\frac{r_+ + r_-}{z_+ z_-} + 0.2180\frac{z_+}{z_-} + 0.1771\frac{r_t}{r_l} - 0.2843 \tag{6.9}$$

$$\beta^{(1)} = 1.1513\frac{r_+}{r_-} - 0.9786\frac{r_+ + r_-}{z_+ z_-} + 1.3623\frac{z_+}{z_-} + 0.3328\frac{r_t}{r_l} + 0.5631 \tag{6.10}$$

$$10^3 C^\varphi = 1.8874\frac{r_+}{r_-} - 10.8250\frac{r_+ + r_-}{z_+ z_-} - 27.4160\frac{z_+}{z_-} + 22.1980\frac{r_t}{r_l} \\ + 35.4577 \tag{6.11}$$

The ratio r_t/r_l expresses the non-spherical shape of some ions, such as NO_3^-. Numerical values for ionic radii as well as the r_t/r_l ratio are not given in the paper. Reference to relevant literature is missing as well, so that it is not possible to reproduce the findings of the authors.

In a similar approach, Simoes et al. /SIM 16/ checked to which extend 1-1, 2-1, 3-1, 4-1, and 2-2 electrolytes could be treated on the basis of ionic radii. They reduced the original Pitzer equation by omitting $\beta^{(2)}$ and C which lead only to a minor reduction of fitting quality. Sets of parameters $\beta^{(0)}$ and $\beta^{(1)}$ were derived on the basis of osmotic coefficient data. In systems where ion pairing and complex formation is likely to be insignificant[11], $\beta^{(0)}$ and $\beta^{(1)}$ correlate reasonably well with expressions that include the ionic radii and the ionic charges:

$$\beta^{(0)} = 0.04432 z_M^{1.62} z_X^{-1.35} |r_M - 1.5 r_X| + 0.05758 \qquad (6.1)$$

$$\beta^{(1)} = 0.01001 z_X^{-0.4} \left[z_M^2 z_X^{0.6} \left(1 + |r_M - 1.2 r_X|^{0.2} \right) \right]^2 \qquad (6.2)$$
$$+ 0.12017 z_M^2 z_X^{0.2} \left(1 + |r_M - 1.2 r_X|^{0.2} \right) + 0.05226 z_X^{-0.4}$$

The authors excluded combinations of kosmotrope cations/ kosmotrope anions and chaotrope cations/ chaotrope anions as these tend to form complexes and ion pairs. Simoes et al. also provided a method for estimating ionic radii for complex ions /SIM 17/.

The presented correlation indeed shows a good general correlation (Fig. 6.8). However, especially at low function values (i.e., in the range of 1-1 and 1-2 / 2-1 salts), the scattering is considerable (Fig. 6.9). A systematic deviation between calculated and tabulated $\beta^{(0)}$ values is observed, not only in those cases where ion pair or complex formation is suspected.

---

[11] Systems with pairs of hard/ hard and soft/ soft ions as well as ion combinations where complex formation is well known

Fig. 6.8 Correlation between charge/ radii and $\beta^{(0)}$ und $\beta^{(1)}$ according to Simoes et al. /SIM 16/. Symbol ´+´: Suspected formation of ion pairs or complexes.

Fig. 6.9 Detailed analysis of the performance of the Simoes function at low values of $f(z_r)$

The approach did not work well for metal nitrates (1-1 and 1-2 systems) and salts with a bulky cation and fluoride (RbF, CsF). It can be applied at best for ion combinations with large size difference between cation and anion. 2:2 systems do not perform well, and the applicability is limited to small and medium concentrations.

Below are some examples for activity coefficients that have been calculated with Pitzer parameters developed from experimental data or estimated using the Simoes method. Fig. 6.10 shows the results for $Na[Pb(OH)_3]$. Experimentally based and estimated Pitzer coefficients result in similar activity coefficients. Up to 2 mol/kg the difference is lower than 0.1 log units, but at higher concentrations the gap increases considerably. This would be the region where the parameter C contributes considerably to the activity coefficients. The situation is different for the analogous potassium system (Fig. 6.11). The Simoes method produces interaction and activity coefficients that are similar to those of Na^+, but the experimentally based activity coefficients are considerably higher. A closer look to the source /HAG 12b/ shows that the binary interaction parameters for Na^+/ $Pb(OH)_3$ and K^+/$Pb(OH)_3$ were derived on the basis of solubility measurements in the ternary systems NaOH/ KOH-$Pb(OH)_2$-H_2O. No ternary interaction parameters could be calculated so that the binary interaction parameters $\beta^{(0)}$, $\beta^{(0)}$, and C^ϕ also contain contributions of θ and Ψ. The 'true' binary interaction parameters may be different.

Another example concerns the interaction of Na^+ with $Zr(OH)_6^{2-}$. Several authors have calculated SIT coefficients for this interaction, each time with quite different results (/ALT 08/: $\varepsilon=0.04$, /THO 14/: $\varepsilon=-0.1$, /RAI 18/: $\varepsilon=0.068$). Rai et al. /RAI 18/ also provided Pitzer coefficients. It should be expected that both parameters types (SIT and Pitzer) from /RAI 18/ lead to similar activity coefficients, at least at up to moderate concentration. Instead, a gap occurs already at 0.4 mol/kg that widens up quickly. The maximum difference is 0.5 log units raising doubts whether the same set of experimental data was used to derive both sets of parameters. Estimated parameters from a Simoes approximation led to differences up to 0.8 log units (Fig. 6.12). They are closer to the values calculated with the SIT parameters.

More examples are given in chapter 6.9. In summary, it can be said that the estimation procedure according to Simoes results in Pitzer coefficients that produce activity coefficients that may be close to experimental values. But there are too many cases of even simple salts of the types 1-1, 1-2 and 2-1 where it performs quite bad. The method cannot be used reliable for these salt types.

Nevertheless, there is potential to further develop the approaches of Kim et al. and Simoes et al. As Fig. 6.13 shows, other functions may be designed that allow a better representation of $\beta^{(0)}$ at least for certain subdomains of the anion/ cation space (here: chloride). This would be of interest for repositories in potentially suitable host rock

formations in Germany. If solutions of high ionic strength occur, most of these are expected to contain NaCl and/or MgCl$_2$ as the main component. So, focusing on the interactions with Na$^+$/Mg^{2+} and Cl$^-$ would allow to construct one or two simpler models that could describe the majority of relevant interactions.

Fig. 6.10   Calculated activity coefficients for Na[Pb(OH)$_3$] using experimentally based and estimated Pitzer coefficients

Fig. 6.11   Calculated activity coefficients for K[Pb(OH)$_3$] using experiment based and estimated Pitzer coefficients

Fig. 6.12 Calculated activity coefficients for $Na_2[Zr(OH)_6]$ using experiment based and estimated Pitzer coefficients

Fig. 6.13 Correlation of $\beta(0)$ values with the function $f(z_r)=z_M(r_M-2r_X)$ (chloride salts only)

6.7 Correlation between ion interaction parameters

If the focus is limited to solutions with moderate ionic strength (4 or 6 mol/kg), the influence of the ternary parameter C is low. In such cases the Pitzer model reduces to a two-

parameter function with $\beta^{(0)}$ and $\beta^{(1)}$. Pitzer and Mayorga /PIT 73/ demonstrated that in 1-1, 2-1 and 3-1 system there is a rather strong correlation between these two parameters. Some systems do not fit into the overall picture. Salts with large organic ions such as sulfonates or tetraalkylammonium show a remarkable scattering, Also, $KBrO_3$, $KClO_3$, Na_2HAsO_4 (but not K_2HAsO_4) and $RbNO_2$ (but not $CsNO_2$ or KNO_2) could be identified as outliers. Among 2-1 systems Na_2HAsO_4, Na_2HPO_4, $K_2Pt(CN)_4$ were outside the general band, among 3-1 systems $K_3P_3O_9$ stood out. Whether or not such behaviour may be caused by low quality experimental data cannot be assessed at the moment.

6.8   Ternary ion interaction parameters θ and Ψ

Rowland and May /ROW 12/ evaluated available literature on the ternary salt-water systems and found that in almost all cases Zdanovskii's rule applies /ZDA 38/: all mixtures of two binary salt solution with equal water activity have the same water activity as the pure binary solutions. If all mixtures with the same water activities (the isoactivity lines) are plotted on a m(salt1)/ m(salt 2) diagram the resulting points lie on a straight line that connects the pure salt solutions of the same water activity. Deviations from Zdanovskii's rule (recognized as curved isoactivity lines) are typically so small that they cannot be distinguished from experimental error.

Based on our own isopiestic measurements we could identify a number of systems where Zdanovskii's rule does not apply. These includes systems with $ZnCl_2$, $CdCl_2$, $HgCl_2$ or $CsCl$ (/HAG 12b/, /HAG 15a/, /BIS 16/). The first three salts include metal cations that are known to form chloro complexes. If the complex formation is ignored, the isoactivity plot leads to strongly curved lines – mainly because the total concentration of dissolved species is calculated incorrectly and thus the water activity. For CsCl, where chloro complex formation is typically not considered, the deviation from Zdanovskii's rule is an indication that ion pairing takes place to a significant extent.

For mixed $HgCl_2$-MCl_n systems /HAG 15a/ applied a simplified model that replaced the formally ternary system $HgCl_2$-MCl_n-H_2O by two complementary ternary systems MCl_n-$M_{2/n}HgCl_4$-H_2O and $HgCl_2$- $M_{2/n}HgCl_4$-H_2O that were calculated from the original solution data. Although the chemical model strongly simplifies the complex formation the resulting isoactivity lines were almost straight. This finding shows that in systems with strong complex formation the Zdanovskii's rule still applies, if the overall extend of complexation is

grossly accounted for and the most important occurring species are considered instead of the formal ones.

What are the consequences of Zdanovskii's rule for estimating Pitzer ion interaction co-efficients? In cases with little or no ion pairing/ complex formation the ternary interaction parameters may be calculated from artificial ternary data. One or more isoactivity lines are calculated from well-known binary solutions of the same water activity. In the next step, these artificial data are used to calculate θ and Ψ.

Such a calculation may also be done for ternary systems that do not exist in nature be-cause the involved complex species are always in equilibrium with a row of other com-plex species. An example would be the chloro complexes of lead. In chloride solutions the following five species exist: Pb^{2+}, $PbCl_2^-$, $PbCl_2(aq)$, $PbCl_3^-$, $PbCl_4^{2-}$. Or written as salts: $Pb(Cl)_2$, $(PbCl)Cl$, $(PbCl_2)$, $Na(PbCl_3)$, $Na_2(PbCl_4)$. A ternary system would be $NaCl$-Na_2PbCl_4-H_2O. If it is possible to derive binary interaction parameters for Na_2PbCl_4-H_2O, the ternary interaction parameters $\theta_{Cl,PbCl42-}$ and $\Psi_{Na,Cl,PbCl42-}$ could be determined by calculating a straight isoactivity line for the system $NaCl$-Na_2PbCl_4-H_2O.

Estimations of ternary interaction parameters were not performed in this study, because the uncertainty of estimated binary interaction coefficients was considered too high at the moment.

6.9   Comparison of the performance of different models and conclusion

To test the reliability of different approaches to estimating Pitzer coefficients, the activity coefficients of numerous systems were calculated with experimentally derived as well as estimated Pitzer parameters. In this analysis the reference values from Humphreys et al. are compared with estimated parameters using the Simoes model. For comparison, the Neck model assuming $\varepsilon(SIT)=0$ was applied as well as a null model where all ion inter-action coefficients were omitted.

Of the four tested methods for estimating the Pitzer ion interaction coefficients, none is clearly convincing. The model by Simoes et al., which on paper is the most advanced, shows a worse prediction quality than the other, simpler prediction models in almost all salt systems tested (Fig. 6.14 ff.). In part, the forecasts are even worse than the null models, in which either all interaction coefficients are zero or $\varepsilon(SIT)=0$. This is surprising,

especially since many very well-modelled systems are presented in the original publication., e.g., simple systems such as NaCl. For 1-1 systems, the Simoes parameters produce activity coefficients that are always clearly too high. For 1-2 and 2-1 systems they are sometimes too high, sometimes too low. On average, the reference values by Humphreys et al. perform much better. This is not the case for 2-2 systems, where the Simoes approach allows slightly better results.

Tab. 6.4 Maximum difference between calculated mean activity coefficients from experimentally derived and predicted ion exchange effect coefficients (bold: best model)

Charge type	Simoes et al. max $\Delta \log \gamma_\pm$	Humphreys et al. max $\Delta \log \gamma_\pm$
1-1	0.8	**0.4**
1-2, 2-1	1.7	**0.8**
2-2	**0.4**	0.5
1-3, 3-1	**0.5**	Not applicable
1-4, 4-1	**0.7**	Not applicable

For 1-3 and 1-4 systems, the prediction with the help of the Simoes model is sometimes surprisingly close to the literature values. I. However, since this class also includes rather difficult systems such as Na_3PO_4 and $K_4Fe(CN)_6$, higher deviations can occur in individual cases. The maximum deviations per model are listed in Tab. 6.4.

Based on this analysis, the following strategy was chosen for the estimation of unknown ion interaction coefficients:

1. Conversion from SIT parameters if these have been determined for sufficiently high ionic strengths
2. Estimation based on analogous structure and charge
3. 1-1, 1-2 and 2-1 systems: reference values according to Humphreys et al. (see Tab. 6.2)
4. 2-2, 3-1 and 4-1 systems: modelled values according to Simoes et al., except in cases where ionic radii cannot be calculated (only 2-2 systems: reference value from Tab. 6.2)

Fig. 6.14 Activity coefficients of 1-1 salt solutions calculated with experimentally derived and estimated Pitzer ion interaction coefficients

Fig. 6.15 Activity coefficients of 1-2 and 2-1 salt solutions calculated with experimentally derived and estimated Pitzer ion interaction coefficients

Fig. 6.16 Activity coefficients of 2-2 salt solutions calculated with experimentally derived and estimated Pitzer ion interaction coefficients

Fig. 6.17 Activity coefficients of 1-3, 3-1 and 1-4, and 4-1 salt solutions calculated with experimentally derived and estimated Pitzer ion interaction coefficients

7 Compilation of previously determined solubility limits for fission products in the near field of a repository

7.1 Overview

Solubility limits for radionuclides belong to the key chemical parameters in long-term safety assessments. Considerations about the identity and the properties of solubility limiting phases are therefore part of many studies on long-term safety of repositories. As the radionuclide inventory differs from project to project, the considered radionuclides vary. Tab. 7.1 provides an overview of studies from the past 40 years that were used to compile solubility limiting phases and calculated solubilities. The studies are not directly comparable to each other as the assumed geochemical conditions (pH, Redox, solution composition, temperature etc., waste types) are site-specific. Nevertheless, the overview is a good starting point to get a general impression of the solid phases that may be expected and the ranges of solubilities that are considered plausible. Details are given in the annex (A.2).

Most projects dealt with groundwaters with rather low mineralization. Values from these studies should be regarded with care as they cannot be easily transferred to saline conditions expected in salt or certain Lower Cretaceous clay formations. Among the foreign studies, those from Canada for the LLW/ ILW repository, Finland (variant a) and Sweden (variant b) are of special relevance for the German situation because they dealt with the solubility of radionuclides in concentrated salt solutions.

For a long time, German site-specific as well as generic radionuclide migration studies in saline media were based on solubility limits compiled by Tittel et al. (for solutions relevant for the Konrad mine: up to a salt concentration of about 3.5 mol/l) and Buhmann et al. (for solutions relevant for salt mines) /TIT 86/, /BUH 91/. They probably reflected the state of knowledge at the time of their creation but should no longer be considered reliable sources, because it is rather unclear how and on what experimental/ theoretical basis the solubilities were derived or for which solution composition they apply.

Tab. 7.1 Overview of studies that derived solubility limits

No.	Country	Waste type	Host hock/ solution	Database	Source
1	Belgium	HLW	Boom clay pore water I=0.0085 pH 8.36	MOLDATA (compilation of Thermochimie/ NAGRA/ PSI, LLNL)	/SAL 17/
2	Belgium	HLW	Cement pore water (3 corrosion states) pH 13.5 down to 10.5 I ≤ 0.08.	MOLDATA (compilation of Thermochimie/ NAGRA/ PSI, LLNL)	/WAN 13a/
3	Canada	LLW/ ILW	a) Argillaceous limestone model porewater (Guelph): Concentrated NaCl/CaCl$_2$ brine I=7.2 mol/kg pH 6.5 b) Argillaceous limestone model porewater (Cobourg 2): NaCl/KCl/CaCl$_2$ brine I=3.8 mol/kg pH 6.5 c) ditto, but equilibrated with cement pH 11.9	Databases from PHREEQC (Yucca Mountain Pitzer File R2), GEMS and SUPCRT92	/WAL 11/
4	Canada	HLW	a) Model groundwater for crystalline rock Na/Ca/Cl/SO$_4$ I=0.24 mol/l pH 7.1 (CR-10 eq) b) Model groundwater for crystalline rock equilibrated with bentonite and steel I=0.32 pH 8.7 (CR-10 NF) c) Brine from salt formation NaCl/CaCl$_2$ I=6.47 pH 5.8 (SR-270	Yucca Mountain Pitzer database, Thermochimie 7b (Some calculations were performed with the Yucca Mountain Pitzer database as well, but for most radionuclides considered in this study thermodynamic data	/DUR 10/

No.	Country	Waste type	Host hock/ solution	Database	Source
			eq)	were lacking)	
5	Finland	HLW	a) Altered groundwaters inside the canisters NaCl/ CaCl$_2$ I= 0.001 to 1.3 mol/l pH 7.33 to 10 b) Altered groundwaters at the bentonite/ host rock interface and inside the canisters (total 12) NaCl/CaCl$_2$ I= 0.001 to 1.3 mol/l pH 7 to 10 c) Bentonite porewater (six different) NaCl/CaCl$_2$ I=0.002 to 2.9, pH 7.23 to 10	Thermochimie 7b / Nagra/PSI 2002	/WER 14/
6	France	HLW: clay	a) Pore water in bentonite Buffer (unspecified) b) Pore water of cement-based materials (unspecified) c) Callovo-Oxfordian pore water NaCl/ CaCl$_2$ I=0.09-0.12 mol/l pH 6.9-7.6	Experimental data (partly unpublished) / Thermochimie v. 5	/AND 05b/
7a	Germany	LLW/ ILW	Unspecified solution expected to occur in the Konrad mine <pH12, possibly up to 3.3 mol/l Cl (NaCl/ CaCl$_2$/ MgCl$_2$)	Unpublished experimental sorption data combined with not documented literature data (/TIT 86/), /WEA 90/	based on /BRE 98/
7b	Germany	HLW	Unspecified brine under alkaline, neutral, and acidic conditions	Expert guesses, not specified	/BUH 91/
8	Germany	HLW	Solution in salt rock (spent fuel, HLW glass) (only Actinides, Tc, Zr and Sm)	Experimental data	/KIE 12/
9	Germany	HLW	Salt rock (waste from prototype and research reactors and other waste forms) (only Actinides, Tc, Zr and Sm	Experimental data	/KIE 13/

No.	Country	Waste type	Host hock/ solution	Database	Source
10	United Kingdom	HLW/ ILW	a) Granite water (Sweden) b) Cementitious system (not specified) c) Bentonite pore water (not specified)	cement system: not specified bentonite: database for Swedish SR97 study /AND 99/	/NUC 10/ taken from /NIR 03/, largely based on /NIR 97/
11	Japan	HLW	a) Bentonite porewater based on fresh groundwater Na_2CO_3 I=0.026 pH 8.4 b) Bentonite porewater based on saline groundwater NaCl/ Na_2CO_3 I=0.615 pH 7.8 c) Bentonite porewater based on fresh groundwater Na_2CO_3/ Na_2SO_4 I=0.211 pH 7.2 d) Bentonite porewater based on fresh groundwater Na_2CO_3 I=0.0083 pH 9.7 e) Bentonite porewater based on fresh groundwater, oxidizing Na_2CO_3 I=0.0223 pH 8.4	JNB database /YUI 99/	/AZU 99/, /JNC 00/
12	Sweden	HLW	a) Forsmark reference water (NaCl/ $CaCl_2$ I= 0.19 mol/l) b) Saline water (NaCl/ $CaCl_2$ I=1.86 mol/l) c) Ice-melting water (Na/Ca/Cl,HCO_3/F,Si I=0.0012 mol/l)	/DUR 06a/, /GRI 10a/	/BEN 14/ taken from /GRI 10a/ and /DUR 06b/
13	Switzerland	HLW	a) Cement/concrete system equilibrated with Opalinus clay porewater: NaCl/ $CaCl_2$ I=0.09 mol/kg	PSI/ Nagra database 12/07, Thermochimie 7b, CEMDATA07	/BER 14a/,

No.	Country	Waste type	Host hock/ solution	Database	Source
			pH12.5 b) Bentonite porewater system equilibrated with Opalinus clay porewater NaCl/ Na_2SO_4 I=0.239 mol/kg pH 7.79		

7.2 Databases for the modelling of fission product solubilities and previously determined solubility limits

7.2.1 Background ions and iron

The modelling of fission product solubilities in saline groundwaters requires a thermodynamic database that describes the properties of main constituents in relevant naturally occurring solutions (H^+, Fe^{2+}, Na^+, K^+, Mg^{2+}, Ca^{2+}, CO_3^{2-}, Cl^-, OH^-, SO_4) and is applicable to the high ionic strength conditions characteristics for many of these solutions. The THEREDA database provides a quality-assured set of thermodynamic parameters for the mentioned components. Date for iron was taken from Hageman et al. /HAG 14/.

The THEREDA database was complemented with a complex formation constant for $CaOH^+$ /BRO 16/.

$$CaOH^+ + H^+ \rightleftharpoons Ca^{2+} + H_2O; \qquad \log K = 12.57$$

The authors also provided interaction coefficients for an extended SIT model (Tab. 7.2)

Tab. 7.2 Ion interaction coefficients for $CaOH^+$

Ion pair	$\beta^{(0)}$	$\beta^{(1)}$	C^ϕ	Source/ method
$CaOH^+$, Cl^-	0.0116	-0.9797	0.01203	Calculated from ε_1=-0.29 and ε_2=0.5 /BRO 16/

7.2.2 Radionuclides

Only for lead and strontium comprehensive databases including stability constants and Pitzer ion interaction parameters were available at the beginning of the project (Pb: /HAG 99/, /HAG 12b/, Sr: THEREDA release 11). Databases for caesium and rubidium have been developed as well /SCH 12/, /SCH 13/, /WAN 10a/, /WAN 13b/, but in the solution systems considered these elements are not solubility limited.

For all other elements it was necessary to gather equilibrium constants and ion interaction coefficients from the literature or estimate data using analogies or correlation methods.

The sole purpose of the thermodynamic databases compiled in this study was to support the interpretation of the experimental results. It was not intended to develop new, internally consistent and quality assured sets of thermodynamic data for the elements and oxidation states covered in the following chapter. This is or will be the task of other projects. But we tried to use to the extent possible already developed databases and add information on species, interactions, and solid compounds where necessary and available. In principle, we proceeded in the following order:

1. Utilize consistent databases that are applicable to saline systems: Sr, Pb(II), Zr, Se(IV)
2. Utilize consistent databases that are applicable to low salinity systems and add available or estimate Pitzer ion interaction coefficients: Sn(II), Sn(IV), Ni(II)
3. Compile data from different sources to create a workable, but not necessarily consistent database: Mo(VI), Nb(V), Pd(II), Sm(III)

We are aware that data sources of categories 2 and 3 do not meet the quality requirements for reliable geochemical modelling because we could not ensure full consistency or verify whether the added interaction coefficients are applicable to saline systems and compatible with other thermodynamic data. On the other hand, the aspiration of the modelling efforts in this project differed a little from solubility calculation in purely thermodynamic studies. It was our objective to understand and, where possible support the experimental findings by confirming or supplementing the analytical data. Modelling is also a helpful tool to identify knowledge gaps or to develop assumptions about the presence or not-presence of certain complexes. Under such circumstances it is more important to confirm the general level of solubility, its pcH dependence and the observed solid phases than to achieve a perfect absolute agreement between experimental and calculated concentrations.

The efforts were limited to those minerals, complexes and binary interactions that would be most relevant for the systems studied. The derived database allowed us to generate a general understanding of the processes in the investigated solubility system and help to identify knowledge gaps that need to be addressed in future research.

We have imposed a safety margin of 0.5 log concentration units above the highest and below the lowest observed (or in certain cases calculated) concentrations. A calculated solubility that is within or near this margin is fully acceptable within this study. Moreover, it has to be taken into account that several fission products form disordered, amorphous solids with slowly decreasing solubilities (e.g., Sn(IV), Zr(IV)). The formation of colloids that cannot be fully separated from a homogeneous solution may cause significant over-estimations of concentrations and higher differences to calculated values. Many of the properties of variable solid phases cannot be predicted reliably if the precise conditions during the future development of a repository are not known and most probably won't be known. In such cases absolute precision in thermodynamic modelling has little value. Rather, research should concentrate on identification of the concentration bandwidths a certain chemical element could occupy under probable conditions.

This approach puts the focus on the key processes and interactions in a solution system:

- Identification of the solid phases that may form in the specific solution types considered relevant for site of a repository.
- Identify key aqueous complexes that would dominate the chemistry of an element in relevant solutions. There is no point in investigating minor species that do not make up at least 10 % in relevant pcH regions.
- Consider binary ion interactions. Ternary interaction coefficients are needed for fine-tuning ternary or higher systems. They could be omitted if the precision requirements are different. This approach drastically reduces the number of Pitzer coefficients. It also opens the possibility to use estimation methods based on ionic radii or other correlation methods. Although these methods often provide only rough guesses the calculated activity coefficients have a plausible order of magnitude.

7.2.3　　Caesium

Thermodynamic properties in aqueous systems/ oxidation states

Due to its very low oxidation potential, caesium only occurs in the oxidation state (+I) in aqueous systems. All solid compounds with chloride, sulphate, hydroxide, and carbonate are very soluble and do not constrain the solution concentration. A database containing

Pitzer coefficients was prepared by Scharge et al. /SCH 12/, /SCH 13/ and was later extended by Hagemann and Bischofer /HAG 24/ .

Previously considered solubility limiting solid phases and solubility limits

In all considered studies, the concentration of caesium was considered unlimited (Tab A. 2). There are reports that describe a strong retention of caesium in the zeolite mineral pollucite, but as far as known this mineral can only be synthesised at high temperatures /GAT 09/. Therefore, it is broadly assumed that the caesium concertation is not limited by solubility in any aqueous system.

7.2.4 Iodine

Thermodynamic properties in aqueous systems/ oxidation states

Under mildly reducing conditions, iodine only occurs in the oxidation state (-I). The free iodide ion is the only relevant species. In the presence of oxidizing agents, iodide may be converted into elemental iodine, I_2(s), which is in equilibrium with aqueous I_2(aq). If iodide is still present, the triiodide ion, I_3^- may form (Tab. 7.3). Other oxidation states (+I,+III,+V,+VII) require strongly oxidizing conditions that are not relevant for under-ground repositories.

A Pitzer database was developed by Hagemann et al. /HAG 12a/ that was later supplemented by Bischofer et al. /BIS 16/.

Tab. 7.3   Iodine redox equilibria

Equilibrium	log K	Reference
I_2(aq) + H_2(g)$^+$ $\rightleftharpoons$ 2 I^- + 2H^+	21.00	This work
I_3^- $\rightleftharpoons$ I_2(aq) + I^-	-2.844	1

1 /PAL 84/

Fig. 7.1 pH-f_{H2} diagram for iodine in 6 m NaCl solution ($c_{I,total}=1\cdot10^{-5}$ mol/kg)

Previously considered solubility limiting solid phases and solubility limits

Iodide does not form any poorly soluble solids with the major background ions. Iodide does form weakly soluble solids with some heavy metals such as silver (AgI, see 7.2.14) or lead (PbI$_2$, /CLE 80/). However, it must compete with chloride which is much more abundant and forms strong chloro complexes with these metals, so that the actual solubility in relevant solutions is much higher.

In almost all studies the solubility of iodine was assumed to be unlimited. Only /BER 14a/ considered the formation of silver iodide (AgI) which would strongly limit its concentration given that enough iodine is available to transfer all silver into a solid phase. In that case the solubility would be as low as 10^{-6} mol/kg. If the amount of silver is above that of iodine, silver would partially be bound in the soluble chlorargyrite (AgCl). In that case (only applicable to Opalinus clay with $c_{Cl}=0.161$ mol/kg) the solubility would be higher (10^{-5} mol/kg).

The solubility of solid iodine in water was reviewed by Ramette and Sandford /RAM 65/. They derived

$I_2(s) \rightleftharpoons I_2(aq)$

log K (25 °C) = -2.8812

The free enthalpy of formation of the iodide ion, I$^-$ is given as

90

$$\tfrac{1}{2}\ I_2(s) + \tfrac{1}{2}\ H_2(g)^+ \rightleftharpoons I^- + H^+$$

$$\Delta_f G = -51.724\ kJ/mol; \quad \log K = 9.06$$

Combination of both formula leads to

$$I_2(aq) + H_2(g)^+ \rightleftharpoons 2\ I^- + 2H^+; \qquad \log K = 21.00$$

The stability of the triiodide anion was determined by Palmer et al. /PAL 84/ :

$$I_3^- \rightleftharpoons I_2(aq) + I^-; \qquad \log K\ (25\ °C) = -2.844$$

Tab. 7.4   Ion interaction coefficients for iodine species

Ion pair	$\beta^{(0)}$	$\beta^{(1)}$	C^Φ	Source/ method
Na^+, I_3^-	0.0503	0.1951		Estimated (Humphreys)
K^+, I_3^-	0.0503	0.1951		Estimated (Humphreys)
Mg^{2+}, I_3^-	0.243	1.447		Estimated (Humphreys)
Ca^{2+}, I_3^-	0.243	1.447		Estimated (Humphreys)

7.2.5   Lead

Thermodynamic properties in aqueous systems/ oxidation states

Except under extremely oxidizing conditions, the chemistry of lead is dominated by the oxidation state (II) (Fig. 7.2). Lead in solution can be slowly reduced by metallic iron to metallic lead /RAG 98/. This process has not been taken into account by any study on near field solubilities so far. Similar to liquid mercury, the metal may have a solubility as well, but so far this has not been investigated /BER 14b/. In the presence of sulphide, PbS may form.

Fig. 7.2 pH-f_{H2} diagram for lead in 6 m NaCl solution ($c_{Pb,total}=1\cdot10^{-5}$ mol/kg), left: without solids, right: solids allowed

For the calculation of solid – liquid equilibria the thermodynamic database of Hagemann /HAG 99/ was used including the supplemented data in /HAG 23/for hydroxide and carbonate species and solid phases. Data on redox equilibria are summarized in Tab. 7.5.

Tab. 7.5 Lead redox equilibria

Equilibrium	log K	Reference
$Pb(s) + 2H^+ \rightleftharpoons Pb^{2+} + H_2(g)$	4.25	1
PbO_2 (plattnerite) $+ 2H^+ + H_2(g) \rightleftharpoons Pb^{2+} + 2H_2O$	49.09	2
Pb_3O_4 (minium) $+ 6H^+ + H_2(g) \rightleftharpoons 3Pb^{2+} + 4H_2O$	73.52	2

1 /GRE 92/
2 /ROB 95/

Some additional ion interaction coefficients were calculated using reference values by Humphreys et al. (Tab. 7.6).

The pH/ H_2 diagram shows that in the presence of halite saturated solutions and reducing conditions laurionite, blixite and metallic lead would be the most stable phases (Fig. 7.2). With the exemption of very alkaline solutions, Pb chloro complexes would prevail.

Tab. 7.6   Ion interaction coefficients for lead(II) species

Ion pair	$\beta^{(0)}$	$\beta^{(1)}$	C^ϕ	Source/ method
$PbOH^+$, Cl^-	0.0503	0.1951		Estimated (Humphreys)
$PbOH^+$, SO_4^{2-}	0.243	1.447		Estimated (Humphreys)
Ca^{2+}, $Pb(OH)_3^-$	0.243	1.447		Estimated (Humphreys)

Previously considered solubility limiting solid phases and solubility limits

As the studies listed in Tab A. 6 reflect, the solubility of lead in natural solutions strongly depends on the presence of complexing and solid forming anions. If carbonate is present in considerable amounts $PbCO_3$ (cerussite) or $Pb_3(CO_3)_2(OH)_2$ (hydrocerussite) may form. In alkaline solutions, an oxide (PbO) or the hydroxide $Pb(OH)_2$ is expected. Other solids that may occur are galena (PbS), anglesite ($PbSO_4$) or a phosphate. In saline solutions either laurionite, PbClOH is assumed to form or no solubility limiting solid is considered at all. The latter assumption is wrong but may have been caused by inappropriate databases.

7.2.6   Molybdenum

Thermodynamic properties in aqueous systems/ oxidation states

The speciation of molybdenum in aqueous systems is quite complex. It includes the metallic phase as well as the oxidation states +III, +IV, +V, and +VI. In addition, oligomeric species with mixed oxidation states exist. The oxidation state of radioactive molybdenum (the activation product Mo-93 or the fission product Mo-99, a precursor of Tc-99) depends on the primary chemical state of molybdenum in the waste matrix.

Mo-93 is generated by neutron activation of non-radioactive molybdenum present in steel. It is considered to be present as molybdate /LID 17/, MoO_4^{2-} but no evidence is provided why in a reducing metallic environment consisting mainly of elemental iron and free of oxygen elemental molybdenum should change to the highest oxidation state. Instead, it may be assumed that molybdenum stays in its original elemental form and is mobilized only in the course of the corrosion of the steel matrix.

The fission product Mo-99 in vitrified glass is present mainly or completely as Mo(VI) /SHO 02/, /KON 16/. In spent fuel, molybdenum either occurs in a solid solution with uranium $(U,Mo)O_2$ or as a metallic precipitate /HA 11/.

Corrosion of metallic molybdenum in anaerobic solutions first leads to a Mo(III) phase, Mo_2O_3 and then to a mixture of MoO_2 and $MoO(OH)_2$ /LU 89/. On the other hand, reduction of Mo(VI) under acidic conditions by a strong agent such as metallic zinc/ hydrogen gas or Cr(II) does not lead to the formation of metallic molybdenum but of aqueous Mo(III). On the other hand, reduction with Fe(II) or Sn(II) only leads to Mo(V) /HÖL 41/. The molybdate ion, MoO_4^{2-} as well as its monoprotonated variant species $HMoO_4^-$ is considered not reducible. Reduction takes place in the presence of strong acids, if poly-molybdate ions have been formed or in the presence of certain organic acids that form complexes with molybdate /TYT 87/, /GME 89/. Several bacteria were identified that can reduce molybdate to mixed Mo(V,VI) complexes /SHU 09/, /LIM 12/ or to MoS_2 /BIS 09/. To what extend metallic iron is capable of reducing Mo(VI) remains to be examined.

In general, the data situation regarding Mo species is still quite patchy and contradictory. In summary, it can be said that under relevant redox conditions, molybdenum in solution can occur in oxidation states III, IV, V and VI. The redox state +II has also been described in aqueous solutions but it seems that the synthesis of Mo(II) ions requires the hydrolysis of metalorganic compounds not expected to occur outside laboratories /RIC 13/.

All oxidation states form solid phases and oligonuclear oxo complexes with mixed oxidation states. Furthermore, it cannot be excluded that metallic molybdenum is deposited under high hydrogen pressures or at the contact surface with metallic iron. Thermodynamic data are only known for a few species and solid phases below oxidation state VI.

The calculated pH/ H_2 diagram for Mo is shown in Fig. 7.3 for a solution saturated with halite. Under strongly reducing, alkaline conditions Mo(III) and Mo(IV) would be the dominating species. Slightly less reducing conditions would favour the formation of Mo(VI). Tugarinovite, MoO_2, is the least soluble solid phase over most of the pH range.

Data on the main redox equilibria are summarized in Tab. 7.7.

Tab. 7.7   Molybdenum redox equilibria

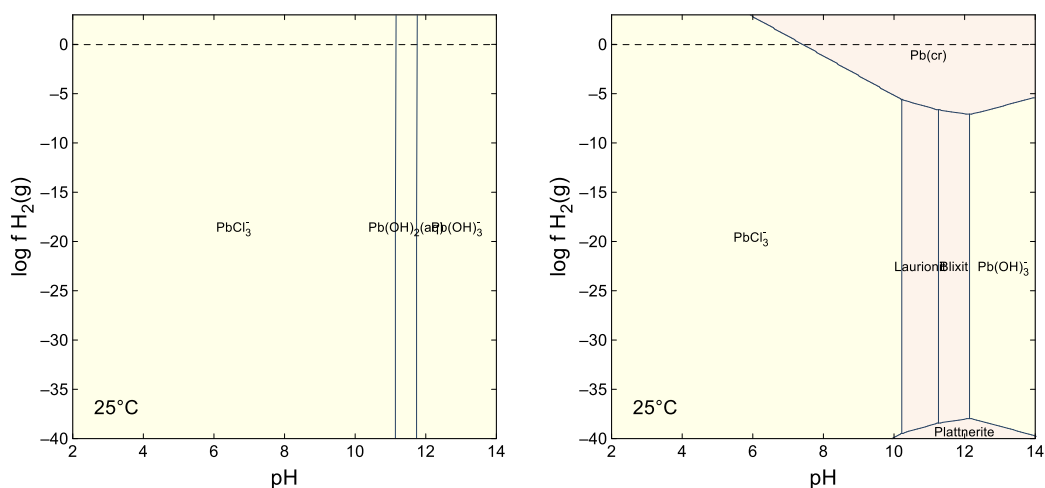| Equilibrium	log K	Source
$Mo(s) + H_2O + 1.5O_2(aq) \rightleftharpoons MoO_4^{2-} + 2H^+$	109.725	1
$Mo^{3+} + 2.5H_2O + 0.75O_2(aq) \rightleftharpoons MoO_4^{2-} + 5H^+$	35.112	1
$Mo(OH)_4(aq) + 0.5O_2(aq) \rightleftharpoons MoO_4^{2-} + 2H^+ + H_2O$	22.622	Calculated by combining the redox equilibrium constant for $MoO_2(cr)$ (see below) and the estimated equilibrium between $MoO_2 \rightleftharpoons Mo(OH)_4(aq)$ (see text)
$MoO_2(cr) + 0.5O_2(aq) + H_2O \rightleftharpoons MoO_4^{2-} + 2H^+$	13.432	1
$MoO_2^+ + 0.25O_2(aq) + 1.5H_2O \rightleftharpoons MoO_4^{2-} + 3H^+$	1.641	Based on 2

1 /KIT 10a/
2 /VLE 77/

Fig. 7.3   pH-f_{H2} diagram for molybdenum in 6 m NaCl solution ($c_{Mo,total}=1\cdot10^{-5}$ mol/kg), left: without solids, right: solids allowed

Mo(III) species and solid phases

More recent investigations revealed that the previously ignored aqueous chemistry of Mo(III) is dominated by chloro and hydroxo complexes. It is possible to establish an equilibrium between Mo(III), hydrogen gas and solid MoO_2 under strongly reducing conditions (Wang et al. /WAN 10b/). The experiments were conducted at 80 °C and cannot be extrapolated to 25 °C without a considerable degree of uncertainty. According to these

investigations, Mo(III) does not have a stability field in dilute NaCl solutions. The hydroxo complexes are always metastable with respect to molybdenum metal and MoO_2, except at the lowest pH values (< 2).

Very few other thermodynamic investigations of Mo(III) systems exist. The only other study on hydrolysis of Mo(III) /MIT 78/ was not considered reliable enough by Brown and Ekberg /BRO 16/ to be taken into account in their overview study. However, they updated the model of Brown and Sylva /BRO 87a/ for the prediction of hydrolysis constants of metal cations and calculated the stability constants for $Mo(OH)_x^{3-x}$ (x=1-3) species. Using the same approach, the stability constant of $Mo(OH)_4^-$ was estimated in this study (Tab. 7.8). Molybdenum(III) also forms oligomeric cationic hydroxo complexes /RIC 13/. Whether or not these play a significant role in near neutral to alkaline solutions is unclear. At least one mixed chloro hydroxo complex, $[Mo_2Cl_4(OH_2)_4]^{2+}$ has been described /RIC 13/, but no information of its stability is given.

Tab. 7.8 Stability constants for Mo(III) hydroxide complexes

Equilibrium	log β	Source
$MoOH^{2+} + H^+ \rightleftharpoons Mo^{3+} + H_2O$	2.41	1
$Mo(OH)^+ + 2H^+ \rightleftharpoons Mo^{3+} + 2H_2O$	5.89	1
$Mo(OH)_3(aq) + 3H^+ \rightleftharpoons Mo^{3+} + 3H_2O$	11.13	1
$Mo(OH)_4^- + 4H^+ \rightleftharpoons Mo^{3+} + 4H_2O$	17.68	Estimated using the method described in 1 for $M(OH)_4$ complexes

1 /BRO 16/

No thermodynamic data could be found for solid Mo(III) compounds such as Molybdenum hydroxide, $Mo(OH)_3$ /TYT 87/. Brown and Ekberg /BRO 16/ presented a method to predict the solubility of solid hydroxides based on the equilibrium between $M(OH)_3(aq)$ and $M(OH)_3(s)$. Applied to $Mo(OH)_3$, the equilibrium

$$Mo(OH)_3(s) + 2Mo^{3+} \rightleftharpoons 3MoOH^{2+}$$

could be expressed by the formula

$$\beta_1^{*(-0.94z)} K_S^* = K$$

With $K = 10^{-0.94}$ for many highly charged cations such as Cr(III), Fe(III) or Bi(III). The resulting equilibrium constant would be log $K_S = 5.86$ for the reaction

$$Mo(OH)_3(s) + 3H^+ \rightleftharpoons Mo^{3+} + 3H_2O$$

The calculated solubility constant lies between the values for $Cr(OH)_3$ (9.41) and $Fe(OH)_3$ (2.5-5.4). Estimated Pitzer ion interaction coefficients are summarized in Tab. 7.10.

Mo(IV) species and solid phases

The chemistry of aqueous Mo^{IV} has long been neglected, but the existence of a couple of species has now been established. In highly acidic solutions the dimeric ion $Mo_2O_4(H_2O)_6^{2+}$ and the trimeric $Mo_3O_4(H_2O)_9^{4+}$ could be identified. In solutions of hydrogen chloride oxychloro complexes such as $MoOCl^+$ exist /SOU 70/, /TYT 87/. Souchay et al. also described a molybdite ion MoO_3^{2-} in strongly alkaline solutions.

If metallic molybdenum is oxidized electrochemically at ambient temperature or if aqueous Mo(IV) is precipitated by NaOH a brown hydrated compound $MoO_2 \cdot xH_2O$ is produced /TYT 87/. No solubility data could be found for this phase, but it may be considerably more soluble than $MoO_2(cr)$ that was postulated as the solubility limiting phase in many studies (Tab A. 9). In alkaline solutions weakly soluble alkali metal (Na, K) molybdites $MMoO_2(OH)$ occur /SOU 70/.

Thermodynamic stability data for MoO_2 and MoS_2 (molybdenite) are available from several sources. These were derived either thermochemically or from reductive or oxidative dissolution experiments (e.g. /WAN 10b/). No data is available for amorphous MoS_2 (jordisite).

Due to the lack of experimental data, the stabilities of known or predicted solutions species and solid phases had to be estimated.

Data for the equilibria

$$MoO_2(cr)/ MO_2(am)/ MO_2 \cdot xH_2O + 2H_2O \rightleftharpoons Mo(OH)_4(aq)$$

are available for Zr^{IV}, Sn^{IV}, Tc^{IV}, and Re^{IV} analogues (Tab. 7.9). The constants are quite similar for Zr^{IV}, Sn^{IV}, whereas the Tc^{IV} oxide and the oxide hydrate are much less soluble

than $ZrO_2 \cdot xH_2O$. Rhenium dioxide has a higher solubility but may not be comparable since it is from the third row of transition metals.

For the time being, it was assumed that crystalline zirconium dioxide, $ZrO_2(cr)$ would provide a viable orientation. In the same way the stability difference between $ZrO_2(am)$ and $ZrO_2(cr)$ and $ZrO_2(am)$ and $ZrO_2(cr)$ between was used to calculate the solubility constant of $MoO_2(am)$ and $MoO_2 \cdot xH_2O$ respectively (Tab. 7.9).

In accordance with Zr^{IV}, Hf^{IV}, and Sn^{IV}, a complex $Mo(OH)_6^{2-}$ was assumed to exist (a hydrated variant of the molybdite ion, MoO_3^{2-} Souchay et al described). The equilibrium constant for the reaction

$$Mo(OH)_6^{2-} + 2H^+ \rightleftharpoons Mo(OH)_4(aq) + 2H_2O$$

was estimated from the analogue reaction for Zr^{IV} (log K = 26.81). For this species coefficients for the interaction with Na^+ were estimated (Tab. 7.10). However, under alkaline conditions, it is predicted that Mo(IV) reacts with water to Mo(VI) and H_2 so that $Mo(OH)_6^{2-}$ has no stability field.

Tab. 7.9 Stability of $M(OH)_4(aq)$ complexes and M(IV) phases

Ele-ment	log β $MO_2(cr)$ $+2H_2O \rightleftharpoons$ $M(OH)_4(aq)$	log β $MO_2(am)$ $+2H_2O \rightleftharpoons$ $M(OH)_4(aq)$	log β $MO_2 \cdot xH_2O(am)$ $+(2-x)H_2O \rightleftharpoons$ $M(OH)_4(aq)$	Source
Zr^{IV}	-9.19	-6.49	-5.43	1
Sn^{IV}	-8.02	-7.22		2
Tc^{IV}	-12.39 *		-8.8 (x=0.6) -8.4 (x=1.6)	3 * calculated from $\Delta_f G$=401.8 kJ/mol (4)
Re^{IV}	-6.1			5
Mo^{IV}	-9.2	-6.5	-5.4	Estimated based on Zr^{IV} oxides

1 /THO 14/
2 /GAM 12/
3 /YAL 16/
4 /GUI 03/
5 /KIM 03/

Tab. 7.10 Ion interaction coefficients for molybdenum(III) and molybdenum(IV) species

Ion pair	$\beta^{(0)}$ / θ / Ψ	$\beta^{(1)}$	Source/ method
$MoOH^{2+}$, Cl^-	0.243	1.447	Estimated (Humphreys)
$MoOH^{2+}$, SO_4^{2-}	0.1854	2.3709	Calculated using the Simoes method (ionic radius 1.43 Å)
$Mo(OH)_2^+$, Cl^-	0.0503	0.1951	Estimated (Humphreys)
$Mo(OH)_2^+$, SO_4^{2-}	0.243	1.447	Estimated (Humphreys)
Na^+, $Mo(OH)_4^-$	0.0454	0.398	Analogue to $Al(OH)_4^-$ /REA 90/
K^+, $Mo(OH)_4^-$	-0.0003	0.1735	ditto
Cl^-, $Mo(OH)_4^-$	0.14		ditto
Na^+, Cl^-, $Mo(OH)_4^-$	-0.0048		ditto
Na^+, $Mo(OH)_4^-$, SO_4^{2-}	-0.0094		ditto
K^+, $Mo(OH)_4^-$, SO_4^{2-}	-0.0677		ditto
Mg^{2+}, $Mo(OH)_4^-$, SO_4^{2-}	-0.0425		ditto
Na^+, $Mo(OH)_6^{2-}$	0.243	1.447	Estimated (Humphreys)
K^+, $Mo(OH)_6^{2-}$	0.243	1.447	Estimated (Humphreys)

Mo(V) species

In slightly acidic solutions Mo(V) occurs in form of the species MoO_2^+. Increase of the pH leads to the formation of a neutral complex $MoO_2OH(aq)$ in equilibrium with the solid hydroxide $MoO_2OH \cdot xH_2O$ /NAB 84/. In other sources, the solid was identified as $MoO(OH)_3$ /GME 89/. Depending on the molybdenum concentration, the ion undergoes dimerization into $Mo_2O_4^{2+}$. /GME 89/.

At pH values above 6.5 Mo(V) ion is easily oxidized to MoO_4^{2-}. Nabivanets and Gorina /NAB 84/ investigated the equilibrium between MoO_2^+, $MoO_2OH(aq)$ and $MoO_2OH \cdot xH_2O$ and found log K_c=10.6 for the reaction

$$MoO_2^+ + OH^- \rightleftharpoons MoO_2(OH)(aq)$$

At 0.1 M (H,Na)ClO$_4$ assuming an activity coefficient of 0.77 for both ions at this ionic strength the equilibrium constant log K would be 10.4.

The solubility constant was given as log K_c=-14.2 for the reaction

$$MoO_2(OH) \cdot xH_2O(s) \rightleftharpoons MoO_2^+ + OH^-$$

This would lead to log K_c=-14.4.

Little information exists about anionic Mo(V) species. Two instable complexes were reported: $MoO(OH)_5^{2-}$, $Mo_7O_{19}^{3-}$, that occur during the reduction molybdate(VI) /GME 89/. No thermodynamic data could be found on these species.

Many mixed polymetalate complexes containing Mo(V) and Mo(VI) are known, many of whom are deep blue (molybdenum blue). Due to the scarcity of data for Mo(V) species they are omitted in the thermodynamic calculations and not discussed here.

Mo(VI) species

The solution chemistry of Mo(VI) in weakly acidic to alkaline systems is dominated by the molybdate ion MoO_4^{2-}. In acidic solutions the MoO_4^{2-} ion hydrolyses to $HMoO_4^-$ and $H_2MoO_4(aq)$ /TAU 02/. According to the JAEA Database (version 190329g0), their stabilities are as follows:

$$HMoO_4^- \rightleftharpoons MoO_4^{2-} + H^+; \qquad \log K = -6.7$$

$$H_2MoO_4(aq) \rightleftharpoons MoO_4^{2-} + 2H^+; \qquad \log K = -4.1$$

There is no significant complex formation between MoO_4 and chloride except under extremely acidic solutions /BOR 12/. In the presence of sulphide a thiomolybdate may be formed /COU 98/. Complex formation between molybdate and calcium or magnesium is described in the literature /ESS 92/.

$$Mg^{2+} + MoO_4^{2-} \rightleftharpoons MgMoO_4(aq); \qquad \log K = 3.03 \pm 0.13$$

$$Ca^{2+} + MoO_4^{2-} \rightleftharpoons CaMoO_4(aq); \qquad \log K = 2.57 \pm 0.08$$

Ion interaction parameters for the pair Na^+/ MoO_4^{2-} were taken from /NIN 16/. No coefficients were available for the interaction between K^+ and MoO_4^{2-}. In a rough guess, it was assumed that they are similar to K^+/ SeO_4^{2-} /HAG 12a/.

To model magnesium containing solutions interaction parameters for the ion pair Mg^{2+}, MoO_4^{2-} were needed. Such data were determined by Grambow et al. /GRA 92/ on the basis of undocumented isopiestic measurements in the quaternary system $MgCl_2$-Na_2MoO_4-H_2O. As their interaction coefficients for Na_2MoO_4 already caused incorrect solubilities of powellite in NaCl solutions (see Fig. 8.4), the interactions coefficients for Mg^{2+}, MoO_4^{2-} were not used in this study. Instead, interaction coefficients for Mg^{2+}, SeO_4^{2-} were employed /HAG 12a/. In our view, this is a reasonable approach as the ionic radii of MoO_4^{2-} (2.31 Å) and SeO_4^{2-} (2.43 Å) are similar.

Complex formation constants for $MgMoO_4(aq)$ and $CaMoO_4(aq)$ or a $\beta^{(2)}$ could not be used because they would be incompatible with interaction parameters for Mg^{2+}/ SeO_4^{2-} and Ca^{2+}/ SO_4^{2-} that were derived without assuming ion pairing or complex formation.

For the solubility constant of $CaMoO_4$, the value of Felmy et al. was used (log K = -7.93 /FEL 92/), who also provided an estimated interaction coefficient for the ion pair Ca^{2+}/ MoO_4^{2-}(assumed to be the same as Ca^{2+}/ SO_4^{2-}). The authors considered to explicitly include the complex $CaMoO_4(aq)$ but concluded that a model without this species performed better in explaining the experimental results. According to them, ternary interaction parameters for Cl^-/ MoO_4^{2-} are not necessary.

Solubility constants for $MgMoO_4 \cdot 5H_2O$ and $MgMoO_4 \cdot 2H_2O$ were calculated on the basis of the investigations by /RIC 51/.

log K ($MgMoO_4 \cdot 5H_2O$) = -2.16

log K ($MgMoO_4 \cdot 2H_2O$) = -1.52

The latter one was calculated after the ternary data for solutions in equilibrium with $MgMoO_4 \cdot 5H_2O$ were exploited to determine ternary interaction coefficients for the ion pairs MoO_4^{2-}/ Cl^- and Mg^{2+}/ Cl^-/ MoO_4^{2-} (Tab. 7.11).

These two solubility constants should be considered as preliminary as only estimated binary interaction parameters for the MoO_4^{2-} ion were used. Up to about 3 mol/kg the calculated solubility of $MgMoO_4 \cdot 5H_2O$ agreed well with the data from /RIC 51/. At the highest $MgCl_2$ concentrations experimental and predicted concentrations differed by a factor of two (not shown). The error is still acceptable for the purpose of the calculations done in this work.

Interaction parameters for $HMoO_4^-$ were assumed to be similar to those of HSO_4^-. These data were taken from the THEREDA database.

Tab. 7.11 Ion interaction coefficients for MoO_4^{2-} used in this study

Ion pair	$\alpha^{(1)}/$ $\alpha^{(2)}$	$\beta^{(0)}$	$\beta^{(1)}$	$\beta^{(2)}$	C^Φ	Source
Na^+, MoO_4^{2-}	2	0.1671	0.2285		-0.002592	1
K^+, MoO_4^{2-}	2	0.1671	0.2285		-0.002592	1 for Na^+/ MoO_4^-
Mg^{2+}, MoO_4^{2-}	1.4	0.32761	3.90403		0.008943	2 for Mg^{2+}, SeO_4^{2-}
Ca^{2+}, MoO_4^{2-}	1.4 / 12	0.2	3.1973	-54.24	-	3 for Ca^{2+}/ SO_4^{2-}
Na^+, $HMoO_4^-$	2	0.1058	0.0208		-0.005834	4 Analogue to M/ HSO_4^{2-}
K^+, $HMoO_4^-$	2	-0.0003	0.0120		0.000538	4 Analogue to M/ HSO_4^{2-}
Mg^{2+}, $HMoO_4^-$	2	0.5192	1.7290		-0.012029	4 Analogue to M/ HSO_4^{2-}
Ca^{2+}, $HMoO_4^-$	2	0.2986	2.3636		0	4 Analogue to M/ HSO_4^{2-}
		θ	Ψ			
Mg^{2+}, Cl^-, MoO_4^{2-}		0.0463	-0.0315			This work

1 /NIN 16/
2 /HAG 12a/
3 /FEL 92/
4 THEREDA database

Previously considered solubility limiting solid phases and solubility limits

Molybdenum-93 is produced by neutron activation of the stable molybdenum-92, a component of many steels. It is considered to be released as molybdate /LID 17/. However, no arguments were given, why molybdenum should be oxidized from the metallic state (0) to the state +VI, when at the same time the redox level within the steel is still strongly reducing.

In studies concerning the solubility of molybdenum under repository conditions, only the oxidation states VI and IV were considered (Tab A. 9). /WER 14/ observed that under the conditions of a repository in Finland at pH values up to 8.6 MoO_2 (tugarinovite) would

be the solubility limiting phase. At higher alkalinities and/ or redox potentials, $CaMoO_4$ (powellite) would prevail /DUR 10/. In the presence of sulphide, the very weakly soluble MoS_2 (molybdenite) may occur (as predicted for Boom Clay pore water, /SAL 17/). Predicted solubilities range from log c = -13 (MoS_2) to unlimited values ($CaMoO_4$).

The nature of the solubility determining solid under reducing conditions remains unclear. If $MoO_2(cr)$ is considered, very low concentrations would have to be expected (see e.g. /DUR 10/ for a saline water: 10^{-9} to 10^{-15} mol/kg). However, even at higher temperatures solutions a hydrous oxide precipitates first ($MoO_2 \cdot xH_2O$), which is considerably more reactive /TYT 86/ and probably also more soluble. For this reason, the calculations of /DUR 10/ should be treated with caution.

In corrosion experiments with vitrified glass, molybdenum was found to form to be present in powellite, $CaMoO_4$ but also in the oxidation state +IV in spherules of CeO_2 (cerianite) /GRA 99/. Its concentration was in the order of 10^{-4} mol/l.

7.2.7   Nickel

Thermodynamic properties in aqueous systems/ oxidation states

In aqueous solutions, nickel only occurs in the oxidations state +II. Under moderately reducing conditions ($p_{H2} > 10^{-5}$ bar) and slightly acidic to slightly alkaline conditions, aqueous Ni^{2+} may be reduced to the metal which is insoluble in water. The equilibrium constant for the reaction

$$Ni(s) + 2H^+ \rightleftharpoons Ni^{2+} + H_2(g)$$

$$\Delta_r G = -45.77 \text{ kJ/mol or log K} = 8.02$$

is taken from the NEA Review /GAM 05/. Reactions with metallic iron would be sufficient to accomplish this reaction. Strongly oxidizing conditions may lead to the formation of solid phases containing the Ni(III) or even Ni(IV), but these are not considered relevant here.

In a repository, radioactive nickel may occur as the activation products Ni-59 and Ni-63 /LIN 07/:

- Ni-59 produced by irradiation with thermal neutrons from Ni-58 or by fast neutrons from Ni-60.

- Ni-63 is produced by irrigation with thermal neutrons from Ni-62 and from Zn-66 and Cu-63 by fast neutrons. The half-life of Ni-63 is only 96 years so that is not important in the long-term

Nickel occurs in stainless steel but also as an impurity in Zircaloy and reactor fuel. In steel, it may be assumed that it remains in the elemental form until it is released during the corrosion of the steel matrix.

Fig. 7.4   pH-f_{H2} diagram for nickel in 6 m NaCl solution ($c_{Ni,total}$=1·10^{-5} mol/kg) , left: without solids, right: solids allowed

Speciation

According to recent reviews of nickel hydroxide complexation, up to pH 13 only the complex Ni(OH)$_2$ has a significant stability field. The stability constants proposed in the NEA database /GAM 05/ suggest a too high stability of the anionic species Ni(OH)$_3^-$ which would lead to increasing solubility at high pH. This evaluation was based on results of a single literature source /GAY 49/ which could not be confirmed in later studies /FEL 16a/, /GON 18/, /PAL 04/. The reasons were probably of experimental (very long equilibration times, insufficient exclusion of CO$_2$) and analytical nature (measurements close to detection limits). At least until pH 13, there is no sound evidence for a complex Ni(OH)$_3^-$. The complex formation constant for Ni(OH)$_2$(aq) has been taken from the recent work by /GON 18/.

$$Ni(OH)_2(aq) + 2H^+ \rightleftharpoons Ni^{2+} + 2H_2O; \quad \log \beta_2 = 19.7 \pm 0.7$$

At extreme NaOH concentrations (> 61 w.- %) solid phases may be synthesised such as $NaNi(OH)_4$ or $BaNi(OH)_6$ /SCH 62/ that suggest that higher complexes are relevant at least under more extreme conditions.

Data on carbonate complexes were reviewed by /GAM 05/. Only the first complex was considered relevant:

$$NiCO_3(aq) \rightleftharpoons Ni^{2+} + CO_3^{2-}; \quad \log \beta_{1n} = -4.2$$

Solid phases

In combination with the solubility constant for β-$Ni(OH)_2$

$$\beta\text{-}Ni(OH)_2 \text{ (theophrastite) } +2H^+ \rightleftharpoons Ni^{2+} + 2H_2O; \log K = -12.10 \pm 0.11$$

solubilities at a broad range of pH values could be calculated. In contrast to these data, the values from the NEA TDB lead to solubilities that are too low, because only data for well crystallized $Ni(OH)_2$ and metastable NiO were taken into account. González-Siso et al. did not consider a complex $NiOH^+$ /GON 18/. It was not needed to explain their experiments. For completeness, in our database we included the stability constant from /GAM 05/:

$$NiOH^+ + H^+ \rightleftharpoons Ni^{2+} + H_2O; \quad \log K = 9.54$$

Ion interaction coefficients for this complex were calculated using reference values (Tab. 7.12). It became apparent that the complex also does not play a role in the solution systems we have investigated.

/MAK 69/ observed the formation of $Ni_2(OH)_3Cl$ in diluted NaCl solutions. In the chosen pH range (7 to 9.5) the fresh precipitate converted into $Ni(OH)_2$. They found the following stabilities:

$$Ni_2(OH)_3Cl(fresh) \rightleftharpoons 2Ni^{2+} + 3OH^- + Cl^-; \quad \log K = -22.76 \pm 0.14$$

$Ni_2(OH)_3Cl(aged) \rightleftharpoons 2Ni^{2+} + 3OH^- + Cl^-$;   log K= -23.08 ± 0.14

The compounds seem to be stable if prepared from moderately concentrated (>0.5 mol/kg) $NiCl_2$ solutions /BET 17/. Other nickel hydroxy chlorides that initially form during hydrolysis are not thermodynamically stable (such as NiClOH, $Ni_3Cl_{2+x}(OH)_{4-x}\cdot4H_2O$). However, they are converted only very slowly into more stable compounds /FEI 36/, /BET 17/.

Thermodynamic data for nickel carbonates were taken from the NEA database /GAM 05/. $NiCO_3$ (gaspéite) may be the thermodynamically more stable phase if carbonate is present, but hydrated $NiCO_3 = NiCO_3\cdot5.5H_2O$ is the primarily forming phase under ambient conditions. The existence of the hydrate as a naturally occurring mineral (hellyerite, /ISA 63/) shows that transformation into gaspéite maybe very slow if taking place at all at ambient temperatures. In that case, it must be assumed that hellyerite would be the solubility limiting phase and the solubility of Ni could be five to six orders of magnitude higher if no other nickel phases were allowed /GAM 01/.The solubility constant for this phase was taken from /GAM 05/ but taking into account the water content (5.5 instead of 6) as described by /BET 16/.

Numerous basic nickel carbonates have been described in the literature, including the minerals nullaginite, $Ni_2(CO_3)(OH)_2$ (Nickel and Berry 1981), otwayite , $Ni_2(CO_3)(OH)_2\cdot H_2O$ /NIC 77/, paraotwayite, $Ni(OH)_{2-x}(SO_4,CO_3)_{0.5x}$ /NIC 87/, kambaldaite, $Na_2Ni_8(CO_3)_6(OH)_6\ 6H_2O$ /NIC 85/, zaratite (doubtful), $Ni_3(CO_3)(OH)_4\cdot4H_2O$, and widgiemoolthalite, $Ni_5(CO_3)_4(OH)_2\cdot4\text{-}5\ H_2O$ /NIC 93/. Another basic nickel carbonate, $Ni_{12}(CO_3)_8(OH)_8\cdot(x\text{-}1)H_2O$, was characterized by /RIN 15/. For none of this solids, thermodynamic data could be found. As the chemistry of nickel(II) and iron(II) is quite similar, it was assumed that the equilibrium constant for the reaction

$2M(OH)_2(s) + HCO_3^- + H^+ = M_2(CO_3)(OH)_2(s) + 2H_2O$

is the same for nickel and iron(II). The calculation was performed with the stability data for $Fe(OH)_2$(aged) /HAG 14/. In that case the equilibrium constant for nullaginite would as follows:

$Ni_2(CO_3)(OH)_2(s) + 2H^+ \rightleftharpoons 2Ni^{2+} + CO_3^{2-} + 2H_2O$;   log K = -0.24.

For Ni^{2+}, a set of Pitzer ion interaction coefficients has been derived by Hagemann et al. /HAG 15a/. The solubility of $Ni(OH)_2$ seems to depend on the concentration of NaCl between 0.5 and 3 M NaCl, according to the data presented by /GON 18/. However, there are only very few experimental data at different ionic strengths in the pcH region where $Ni(OH)_2(aq)$ dominates (pcH >10). Only at pcH 10 a comparison could be done. At that point, the solubility in 3 M NaCl (about 3.19 mol/kg) is about one order of magnitude higher than in 0.5 M NaCl. Experimental data are not given but can be derived from the diagram. In combination with our findings a linear dependence between NaCl concentration and Ni solubility could be established for pcH >10. As a first guess it could be formulated as

$$\log m_{Ni(OH)2(aq)} = -7.6 + 0.26\, m_{NaCl}$$

This relationship can be translated into a Pitzer ion interaction coefficient of about

$$\lambda(Ni(OH)_2(aq),\ Na^+) = -0.3 = -0.26 * \ln(10)/2$$

Tab. 7.12   Ion interaction coefficients for nickel species estimated in this study

Ion pair	$\alpha^{(1)}/$ $\alpha^{(2)}$	$\beta^{(0)} / \lambda$	$\beta^{(1)}$	Source
$NiOH^+$, Cl^-	2	0.0503	0.1951	1
$NiOH^+$, SO_4^{2-}	2	0.243	1.447	1
Na^+, $Ni(OH)_2(aq)$		-0.3		2

1 Estimated (Humphreys)
2 This study

<u>Previously considered solubility limiting solid phases and solubility limits</u>

At pH values of about 7 and higher, most often aqueous $Ni(OH)_2$ is assumed to be the solubility limiting phase in weakly mineralized waters. In the presence of surplus hydrogen sulphide Nickel could precipitate as sulphides such as $FeNi_2S_4$. $NiCO_3$ was suggested by /BER 14b/ in Opalinus clay water system. In highly alkaline cement pore water, a layered nickel aluminium double hydroxide (an LDH) was assumed to form. Predicted solubilities were in the range of 10^{-9} M to unlimited.

In glass corrosion experiments at 90 °C nickel was found to be incorporated in complex manganese(III,IV) oxides, such as birnessite $(Na,Ca,K)_{0.6}(Mn^{4+},Mn^{3+})_2O_4 \cdot 1.5H_2O)$ or in the secondary clay mineral saponite, serpentine and smectite /ABR 90/.

7.2.8   Niobium

Thermodynamic properties in aqueous systems/ oxidation states

In the presence of water only the oxidation state V+ of niobium is stable. Oxides of lower valence states such as NbO_2 and NbO react with water to hydrogen gas and Nb_2O_5 /LOT 99/.

Jehng and Wachs reported spectroscopic evidence that in aqueous solutions above pH 7 hexaniobate ions of the type $[H_xNb_6O_{19}]^{(8-x)-}$ (x=0-3) prevail /JEH 91/. The findings were confirmed by Antonio et al. and Deblonde et al. /ANT 09/, /DEB 15/. At lower pH values mononuclear species such as $Nb(OH)^{4+}$, $Nb(OH)_5(aq)$ and $Nb(OH)_6^-$ are postulated /FIL 20/. Their relative stability in relation to the various Nb_6O_{19} species is not clear.

The octavalent hexaniobate ions may bind up to ten alkali cations, resulting in contact ion pairs such as $K_4[Nb_6O_{19}]^{4-}$, $K_4[Nb_6O_{19}](aq)$,or $K_{10}[Nb_6O_{19}]^{2+}$ /ANT 09/. On the other hand, Deblonde et al. stated that such ion pairs are not necessary to describe observed equilibria. The number of sodium cations per unit cell is variable (and then compensated by additional hydroxide anions). Only in very alkaline solutions (pH>14), hexaniobate ions degrade into tetrameric and monomeric species.

The formation of niobium carbonate complexes is assumed to be likely in alkaline solutions but so far, no investigations have been made. Berner et al. introduced carbonate complexes on a purely theoretical basis and concluded that they may lead to a moderate increase of niobium solution concentrations /BER 14a/.

If niobium is precipitated from aqueous solution a hydrous oxide $Nb_2O_5 \cdot nH_2O$ occurs /DEB 15/. Its water content varies depending on the precipitation conditions /NIK 12/. The solubility of the hydrous oxide is much higher than the anhydrous Nb_2O_5, typically assumed as the solubility limiting phase.

The solubility limiting phase in natural groundwaters could be sodium, calcium or mixed sodium calcium niobates, some of which belong to the pyrochlore supergroups and have been identified as naturally occurring minerals /ATE 10/. For example, Deblonde et al. found that in solutions containing sodium chloride (0.02 to 0.12 mol/l) $Na_7HNb_6O_{19}\cdot15$ H_2O is the solubility limiting phase between pH 8 and 12 and not $Nb_2O_5\cdot xH_2O$ /DEB 15/. A slightly other composition was found by Peiffert et al. who observed $Na_8Nb_6O_{19}\cdot13H_2O$ at pH > 9 /PEI 10/. In the mineralogical literature, the mineral franconite $NaNb_2O_5(OH)\cdot3H_2O = Na_3Nb_6O_{15}(OH)_3\cdot9H_2O$ is described /JAM 84/, /HAR 14/.

The calcium mineral hochelagaite, $CaNb_4O_{11}\cdot8H_2O$, was detected in experiments that investigated the solubility of niobium in cement equilibrated solutions /TAL 04/. One example for mixed sodium calcium niobates is pyrochlore with the formula $(Na,Ca)_2Nb_2O_6(OH,F).xH_2O$ (x=1 to 1.75). The pure sodium end member does not exist, while a pure calcium pyrochlore has been observed. Many natural samples show Na/ Ca at or around 1 /ATE 10/. Potassium also forms niobates as well mixed compounds with calcium /DEB 16/. Presence of potassium leads to the formation of ion pairs (or complexes) that enhance the solubility of other niobates /DEB 15/.

Niobium also forms compounds with iron(II). A resulting mineral is columbite, $(Fe, Mn)Nb_2O_6$. Natural samples always contain manganese, but a pure iron endmember can be assumed /TAR 05/.

Currently, modelling of niobate speciation and solubility is not possible due to the lack of reliable thermodynamic parameters especially for the liquid phase /FIL 20/. Although a solubility constant for $Na_7HNb_6O_{19}\cdot15 H_2O$ has been derived /DEB 15/, /FIL 20/, the activity coefficients for the highly charged ions $HNb_6O_{19}^{7-}$ and $Nb_6O_{19}^{8-}$ that are thought to be dominating species in solution /ANT 09/, /DEB 15/ cannot be modelled without having at least a rough idea of specific ion interactions in concentrated NaCl solutions. None of the methods described above (chapter 1) has been tested or intended for such highly charged ions.

Talerico et al. developed an empirical model that links the observed niobium concentration to the calcium content and pH of a solution /TAL 04/:

$$c_{Nb} = 1.4643e^{-1.3402pH}\frac{c_{Ca}^{-0.8922}}{10^{2.6766}}$$

This model was applied to our system replacing pH by pcH and using a relationship between calcium concentration and pcH as it was observed in the equilibrium solutions:

$$c_{Ca} = 0.0459 - 0.000958 \, pcH$$

Previously considered solubility limiting solid phases and solubility limits

In most cases, Nb_2O_5 is taken as the solubility limiting phase (Tab A. 14). /DUR 10/ noted that data on possibly even less soluble calcium niobates were missing. An empirically derived pH - solubility relationship is used by /WAN 13a/ because it has been shown that under alkaline conditions the niobium concentration is dependent on the calcium content of the solution /TAL 04/. These authors concluded that $CaNb_4O_{11} \cdot 8H_2O$ (hochelagaite) is the most likely phase to control the solubility in cementitious systems. Predicted solubilities ranged from 10^{-12} to 10^{-2} M (and in one instance unlimited).

7.2.9 Palladium

Thermodynamic properties in aqueous systems/ oxidation states

Under normal conditions, palladium occurs only in the oxidation states 0 and +II. Only at high O_2 pressures, palladium(IV) species are stable /COL 08/. The equilibrium between Pd(s) and Pd^{2+} was given as

$$Pd^{2+} + 2e^- \rightleftharpoons Pd(s);$$

$$\log K = 30.93$$

Which translates into

$$Pd(s) + \tfrac{1}{2} O_2(aq) + 2H^+ \rightleftharpoons Pd^{2+} + H_2O;$$

$$\log K = 12.11$$

Fig. 7.5 pH-f_{H2} diagram for palladium in 6 m NaCl solution ($c_{Pd,total}=1\cdot10^{-5}$ mol/kg) , left: without solids, right: solids allowed

A model was constructed to calculate the solubility of palladium(II). It consists of the complex formation constants and solubilities from Rai et al. and includes the following species: $PdCl^+$, $PdCl_2(aq)$, $PdCl_3^-$, $PdCl_4^{2-}$, $PdOH^+$, $Pd(OH)_2(aq)$ and $Pd(OH)_3^-$ as well as the mixed complex $Pb(OH)Cl_3^{2-}$ /RAI 12/. According to Rai et al., no other species, such as $Pd(OH)_2Cl_2^2$ were necessary to explain the results in diluted as well in moderately concentrated NaCl and NaOH solutions. In oversaturated solutions, the complex $Pb(OH)Cl_3^{2-}$ may undergo condensation to chain-like molecules with three to seven palladium atoms that finally results in the precipitation of $Pd(OH)_{1.72}Cl_{0.28}$ /BOI 07/.

The existence of $Pd(OH)_4^{2-}$ is well established, e.g. in solid compounds such as $Na_2Pd(OH)_4$, $CaPd(OH)_4$ or $BaPd(OH)_4$ /IVA 84/, /ZAI 91/ but the complex seems to occur only in very alkaline solutions /IVA 85/. For very highly concentrated NaOH solutions, even a $Pd(OH)_6^{4-}$ complex was postulated /IVA 85/.

A stability constant for $Pd(OH)_4^{2-}$ was provided by Duro et al. /DUR 06a/. They also estimated stabilities for palladium carbonato and sulphato complexes.

In neutral and alkaline solutions, the solubility of Pd(II) is governed by the following solid phases /RAI 12/

$$Pd(OH)_2(am) + 2H^+ \rightleftharpoons Pd^{2+} + 2H_2O; \qquad \log K = -3.58$$

$Pd(OH)_2(colloidal) + 2H^+ \rightleftharpoons Pd^{2+} + 2H_2O;$

$\log K = -2.41$

Byrne and Yao found that hydrolysis of Pd(II) in chloride rich solutions (0.5 M NaCl) does not lead to pure $Pd(OH)_2$ but a mixed chloride hydroxide $PdCl_{0.27}(OH)_{1.73}$ /BYR 00/. These findings were later confirmed by /BOI 07/. Rai et al. /RAI 12/ derived

$Pd(OH)_{1.72}Cl_{0.28} + 1.72H^+ \rightleftharpoons Pd^{2+} + 1.72H_2O + 0.28Cl^-;$ $\log K = -3.99$

Tab. 7.13   Stability of Pd species and solid phases[-]

Reaction	log K	Source
$PdOH^+ + H^+ \rightleftharpoons Pd^{2+} + H_2O$	7.23	1
$Pd(OH)_2(aq) + 2H^+ \rightleftharpoons Pd^{2+} + 2H_2O$	3.49*	2
$Pd(OH)_3^- + 3H^+ \rightleftharpoons Pd^{2+} + 3H_2O$	15.48	2
$Pd(OH)_4^{2-} + 4H^+ \rightleftharpoons Pd^{2+} + 4H_2O$	29.36	3
$PdCl^+ \rightleftharpoons Pd^{2+} + Cl^-$	-5.00	2
$PdCl_2(aq) \rightleftharpoons Pd^{2+} + 3Cl^-$	-8.42	2
$PdCl_3^- \rightleftharpoons Pd^{2+} + 3Cl^-$	-10.93	2
$PdCl_4^{2-} \rightleftharpoons Pd^{2+} + 4Cl^-$	-13.05	2
$PdCl_3(OH)^{2-} + Cl^- + H^+ \rightleftharpoons PdCl_4^{2-} + H_2O$	9.28	2
$PdCO_3(aq) \rightleftharpoons Pd^{2-} + CO_3^{2-}$	-6.83	3
$Pd(CO_3)^{2-} \rightleftharpoons Pd^{2-} + 2CO_3^{2-}$	-12.53	3
$PdSO_4(aq) \rightleftharpoons Pd^{2+} + SO_4^{2-}$	-2.91	3
$Pd(SO_4)_2^{2-}(aq) \rightleftharpoons Pd^{2+} + 2SO_4^{2-}$	-4.17	3
$Pd(OH)_2(am) + 2H^+ \rightleftharpoons Pd^{2+} + 2H_2O$	-3.58	2
$Pd(OH)_2(colloidal) + 2H^+ \rightleftharpoons Pd^{2+} + 2H_2O$	-2.41	2

* considered as lower limit in 2, most likely to be <-5.42
1 /KIT 10b/
2 /RAI 12/
3 /DUR 06a/

To apply this model to saturated NaCl solutions, Pitzer parameters were estimated using the methods of Humphreys et al or Simoes et al. It is obvious that these parameters are not fully consistent with the derived complex formation constants from /RAI 12/, but their model was derived from measurements with an ionic strength up to 1 M only. The results are shown in Tab. 7.14 and Tab. 7.15.

Tab. 7.14 Ion interaction coefficients for Pd species calculated from SIT coefficients in /RAI 12/, $\alpha_1 = 2$

Ion pair	ε	$\beta^{(0)}$	$\beta^{(1)}$
Na^+, $PdCl_3^-$	0.03	0.0614	0.4067
Na^+, $PdCl_4^{2-}$	-0.044	0.0146	2.7027
Na^+, $Pd(OH)Cl_3^{2-}$	-0.044	0.0146	2.7027
Na^+, $Pd(OH)_3^-$	0.11	0.1535	0.4067
K^+, $PdCl_4^{2-}$	0	-0.0038	2.7027
K^+, $PdCl_3^-$	-0.06	0.0269	0.4067
K^+, $Pd(OH)Cl_3^{2-}$	-0.06	-0.0038	2.7027

Tab. 7.15 Ion interaction coefficients for Pd species

Ion pair	Ionic radius (Pd species) [Å]	α_1	$\beta^{(0)}$	$\beta^{(1)}$	Source
$PdCl^+$, Cl^-		2	0.0503	0.1951	1
$PdOH^+$, Cl^-		2	0.0503	0.1951	1
Na^+, $PdCl_3^-$		2	0.0503	0.1951	1
Na^+, $PdCl_4^{2-}$		2	0.243	1.447	1
Na^+, $PdCl_3(OH)^{2-}$		2	0.243	1.447	1
Na^+, $Pd(OH)_3^-$		2	0.0503	0.1951	1
Mg^{2+}, $PdCl_3^-$		2	0.243	1.447	1
Mg^{2+}, $PdCl_4^{2-}$	2.79	1.4	0.2946	2.6269	2
Mg^{2+}, $PdCl_3(OH)^{2-}$	2.73	1.4	0.2872	2.6148	2
K^+, $PdCl_3^-$		2	0.0503	0.1951	1
K^+, $PdCl_4^{2-}$		2	0.243	1.447	1
K^+, $PdCl_3(OH)^{2-}$		2	0.243	1.447	1
K^+, $Pd(OH)_3^-$		2	0.0503	0.1951	1
Ca^{2+}, $PdCl_3^-$		2	0.243	1.447	1
Ca^{2+}, $PdCl_4^{2-}$	2.79	1.4	0.2718	2.5788	2
Ca^{2+}, $PdCl_3(OH)^{2-}$	2.73	1.4	0.2645	2.5656	2
Ca^{2+}, $Pd(OH)_3^-$		2	0.243	1.447	1
Na^+, $Pd(OH)_4^{2-}$		2	0.243	1.447	1
K^+, $Pd(OH)_4^{2-}$		2	0.243	1.447	1
Na^+, $Pd(CO_3)_2^{2-}$		2	0.243	1.447	1
K^+, $Pd(CO_3)_2^{2-}$		2	0.243	1.447	1
Na^+, $Pd(SO_4)_2^{2-}$		2	0.243	1.447	1
K^+, $Pd(SO_4)_2^{2-}$		2	0.243	1.447	1
Mg^{2+}, $Pd(SO_4)_2^{2-}$	2.87	1.4	0.3048	2.6430	2

1 Estimated (Humphreys)
2 Estimated (Simoes)

Previously considered solubility limiting solid phases and solubility limits

Under reducing conditions metallic palladium may be the least soluble solid phase (Tab A. 18) with solution concentrations around 10^{-9} mol/l. However, its formation may be inhibited due to slow kinetics /WER 14/. In that case $Pd(OH)_2$ is assumed to be the solubility limiting phase. Expected solubilities for this phase were around 10^{-7} to 10^{-5} M.
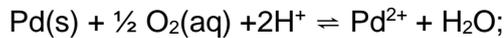
7.2.10   Radium

Thermodynamic properties in aqueous systems/ oxidation states

Under relevant conditions, radium only occurs in the oxidation state (+II). It forms a weakly soluble salt with sulphate ($RaSO_4$). Under real conditions with very low radium concentration it is more likely that radium would be incorporated into other sulphate minerals such as baryte /ROS 14/. Pitzer ion interaction coefficients for $RaCl_2$ have been estimated by Rosenberg et al. /ROS 11/.

Previously considered solubility limiting solid phases and solubility limits

In most studies, either radium carbonate or radium sulphate was considered the least soluble radium mineral (Tab A. 22). But due to the low quantities of radium occurring in nuclear waste, it is highly probable that radium does not form pure substances but is incorporated in other earth alkali sulphates such as anhydrite, celestite or barite. Depending on sulphate or carbonate levels, predicted solubilities were in the range of 10^{-12} to 10^{-4} mol/l.

7.2.11   Rubidium

Thermodynamic properties in aqueous systems/ oxidation states

Similar to caesium, rubidium only occurs in the oxidation state (+I) in aqueous systems. All solid compounds with chloride, sulphate, hydroxide, and carbonate are very soluble and do not constrain the solution concentration. A database containing Pitzer coefficients was prepared as part of the THEREDA project /ALT 11/.

Previously considered solubility limiting solid phases and solubility limits

Rubidium was addressed only in one study, where it was assumed that the solubility is unlimited (Tab A. 26).

7.2.12   Samarium

Thermodynamic properties in aqueous systems/ oxidation state

In aqueous systems, samarium only occurs as Sm(III). The oxidation state +II is not stable and occurs only in high temperature solids. In contact with water, samarium metal reacts to Sm(III).

Fig. 7.6   pH-f_{H2} diagram for samarium in 6 m NaCl solution ($c_{Sm,total}=1\cdot10^{-5}$ mol/kg) , left: without solids, right: solids allowed
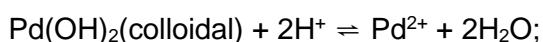
Model

The behaviour of Sm(III) in NaCl solutions was modelled using the thermodynamic data of Neck at al. for the chemically very similar Nd(III) /NEC 09/. For hydroxo complexes as well as ternary calcium samarium complexes it was assumed that the relative stabilities in relation to LnOH$^+$ are the same for Nd^{3+} and Sm^{3+} (Tab. 7.16 f.). Another more recent set of complex formation constants was tested /BEN 04/ but lead to samarium concentrations many orders of magnitude too high.

The solubility constant for of Sm(OH)$_3$ was taken from /RAI 99/, the original source is /BAE 76/. In analogy to the findings by /NEC 09/ an amorphous Sm(OH)$_3$(am) with a 1.2 log unit higher solubility constant was defined. Samarium also forms a basic chloride, Sm(OH)$_2$Cl. For this phase, a solubility constant was published by /RAI 99/ on the basis of experimental data by /AKS 60/.

Complex formation and solubility constants were compiled by /RAI 99/

$Sm^{3+} + CO_3^{2-} \rightleftharpoons SmCO_3^+$;

log K = 7.3 (original source: /MIL 92/)

$Sm^{3+} + 2CO_3^{2-} \rightleftharpoons Sm(CO_3)_2^-$;

log K = 12.11 (original source: /MIL 92/)

$Sm(OH)CO_3 \cdot 0.5H_2O \rightleftharpoons Sm^{3+} + OH^- + CO_3^{2-} + 0.5H_2O$;

log K = -21 (original source: /MER 96/)

$Sm_2(CO_3)_3 \rightleftharpoons 2Sm^{3+} + 3CO_3^{2-}$;

log K = -32.5 (original source: /JOR 66/)

/VOI 16/ determined the solubility of hydroxylbastnäsite-Nd and kozoite-Nd.

$Nd(OH)CO_3$ (hydroxylbastnäsite-Nd) $\rightleftharpoons Nd^{3+} + OH^- + CO_3^{2-}$;

log K = -23.8 ± 0.1

$Nd(OH)CO_3$ (kozoite-Nd) $\rightleftharpoons Nd^{3+} + OH^- + CO_3^{2-}$,

log K = -22.3 ± 0.1

They used the complex formations from /OHT 00/ that are about one order of magnitude higher than reported by other sources (e.g. /LIU 98/). Both minerals were prepared at a high temperature (165 °C) so that they may not represent properties to be expected at room temperature. As a first guess, it was assumed that the data for these neodymium solids are applicable to samarium analogues as well.

The mineral kozoite is the end point of a series of solid solutions with the composition $(REE)_x(Ca,Sr)_{2-x}(CO_3)_2(OH)_x \cdot (2-x)H_2O$. It is known as the mineral ancylite /DAL 75/. So far, no thermodynamic data could be found for this solid phase.

Tab. 7.16 Stability of Sm species and solid phases

Reaction	log K	Source
$Sm^{3+} + H_2O \rightleftharpoons SmOH^{2+} + H^+$	-7.84	1
$Sm^{3+} + 2H_2O \rightleftharpoons Sm(OH)_2^+ + 2H^+$	-16.14	Adapted from 2 (Nd^{3+})
$Sm^{3+} + 3H_2O \rightleftharpoons Sm(OH)_3(aq) + 3H^+$	-26.64	Adapted from 2 (Nd^{3+})
$Sm^{3+} + 4H_2O \rightleftharpoons Sm(OH)_4^- + 4H^+$	-41.14	Adapted from 2 (Nd^{3+})
$Ca^{2+} + Sm^{3+} + 3H_2O \rightleftharpoons CaSm(OH)_6^{2+} + 3H^+$	-26.74	Adapted from 2 (Nd^{3+})
$2\,Ca^{2+} + Sm^{3+} + 4H_2O \rightleftharpoons Ca_2Sm(OH)_4^{3+} + 4\,H^+$	-37.64	Adapted from 2 (Nd^{3+})
$3\,Ca^{2+} + Sm^{3+} + 6H_2O \rightleftharpoons Ca_3Sm(OH)_6^{3+} + 6H^+$	-61.14	Adapted from 2 (Nd^{3+})
$Sm(OH)_3(cr) + 3H^+ \rightleftharpoons Sm^{3+} + 2H_2O$	16.5	3
$Sm(OH)_3(am) + 3H^+ \rightleftharpoons Sm^{3+} + 2H_2O$	17.7	Adapted from 2 (Nd^{3+})
$Sm(OH)_2Cl + 2H^+ \rightleftharpoons Sm^{3+} + Cl^- + 2H_2O$	10.70	3

1 /KLU 00/
2 /NEC 09/
3 /RAI 99/

Tab. 7.17   Ion interaction coefficients for samarium species in NaCl solutions

Ion pair	$\beta^{(0)}/\lambda/\theta$	$\beta^{(1)}$	C^{ϕ}	Source
Sm^{3+}, Cl^-	0.5978	5.279	-0.01992	1
$SmOH^{2+}$, Cl^-	0.055	1.81	0	2 (Nd)
$Sm(OH)_2^+$, Cl^-	-0.13	0	0	2 (Nd)
$Sm(OH)_3(aq)$, Na^+	-0.2	0	0	2 (Nd)
Na^+, $Sm(OH)_4^-$	0	0	0	2 (Nd)
K^+, $Sm(OH)_4^-$	0	0	0	2 (Nd)
Ca^+, $Sm(OH)_4^-$	0	0	0	2 (Nd)
$CaSm(OH)_3^{2+}$, Cl^-	0.21	1.6	0	2 (Nd)
$Ca_2Sm(OH)_4^{3+}$, Cl^-	0.70	4.3	0	2 (Nd)
$Ca_3Sm(OH)_6^{3+}$, Cl^-	0.37	4.3	0	2 (Nd)
Sm^{3+}, Na^+	0.1			2 (Nd)
$SmCO_3^+$, Cl^-	0.0503	0.1951		3
Na^+, $Sm(CO_3)_2^-$	0.0503	0.1951		3

1 /MAY 11/
2 /NEC 09/
3 Estimated (Humphreys)

Previously considered solubility limiting solid phases and solubility limits

In the presence of carbonate, crystalline $Sm(OH)CO_3$ or the more amorphous $Sm(OH)CO_3 \cdot 0.5H_2O$ were often considered the solubility limiting solid phase (Tab A. 27). However, incorporation of Sm (and other lanthanides) into Ca bearing phases (e.g., calcium phosphates, calcite, portlandite) or formation of $SmPO_4$ were two other options mentioned in previous studies.

Predicted solubilities were in the range of 10^{-12} to 10^{-4} mol/l, whereby Sm incorporated in Calcium minerals lead to the lowest concentrations and $Sm(OH)CO_3 \cdot 0.5H_2O$/ $Sm(OH)_3$ to the highest.

In corrosion experiments with vitrified glass, lanthanides were found to occur in powellite, $CaMoO_4$ as a host phase /GRA 99/.

7.2.13   Selenium

Thermodynamic properties in aqueous systems/ oxidation states

Selenium may occur in the oxidation states -II, 0, IV and VI. In addition, polyselenides Se_x^{2-} and mixed polyselenosulfides $(Se_xS_y)^{2-}$ with a formal oxidation state between -2 and 0 may form. Data on the redox equilibria originate from the NEA database /OLI 05/ as presented in the JAEA database 190329g9. A pH/ H_2 stability diagram for Se in saturated halite solution is shown in Fig. 7.7. It shows that under reducing anaerobic conditions HSe^-, $Se_8(aq)$, and Se_4^{2-} are the dominating species.

Some doubts remain whether oxidized selenium species, especially selenate are reduced completely by iron(II) and metallic iron surface. While Se(-II) species would be the thermodynamically most stable oxidation state under such circumstances, several investigations showed that the reaction may stop at Se(0), more specifically red amorphous selenium /SCH 03/, /BÖR 18/. It seems that under certain conditions even this reduction does not take place and insoluble selenites such as $Ca_2(OH)_2SeO_3 \cdot 2H_2O$ are formed /FEL 16b/. Recent experiments in salt solutions showed that in the presence of metallic iron and/ or iron hydroxide compounds selenite is expected to be reduced almost completely to iron selenide, while selenate is only partially reduced. Only in one batch elemental selenium was detected /HAG 24/.

Due to its volatility at high temperatures, the fission product selenium (Se-79) is sometimes not found in vitrified waste. Instead, it is trapped in the scrubber of the reprocessing plant. Fractions of oxidized selenium forms may remain in the glass, but so far, there is little evidence /CAN 10/. However, Bingham et al. could show that selenium was present in a glass sample as selenite with minor levels of Se^0 and Se^{VI} /BIN 11/. According to Curti et al. selenium in spent fuel occurs as selenide, where it replaces oxygen, O^{2-}, in the UO_2 lattice /CUR 15/.

Tab. 7.18 Selenium redox equilibria at 25 °C (Source: /OLI 05/ as presented in the JAEA database)

Equilibrium	log K	Source
$HSe^- + 2O_2(aq) \rightleftharpoons SeO_4^{2-} + H^+$	90.437	1
$Se_2^{2-} + H_2O + 3.5O_2(aq) \rightleftharpoons 2SeO_4^{2-} + 2H^+$	142.38	1
$Se_3^{2-} + 2H_2O + 5O_2(aq) \rightleftharpoons 3SeO_4^{2-} + 4H^+$	180.083	1
$Se_4^{2-} + 3H_2O + 6.5O_2(aq) \rightleftharpoons 4SeO_4^{2-} + 6H^+$	218.947	1
$Se(aq) + H_2O + 1.5O_2(aq) \rightleftharpoons SeO_4^{2-} + 2H^+$	47.14	2

1 /OLI 05/ as presented in the JAEA database,
2 this work (see text)

Fig. 7.7 pH-f_{H2} diagram for selenium in 6 m NaCl solution ($c_{Se,total}=1\cdot10^{-5}$ mol/kg) , left: without solids, right: solids allowed

Fig. 7.8 pH-f_{H2} diagram for selenium in halite/ anhydrite saturated water in presence of ferrihydrite ($c_{Se,total}$=0.001 mol/kg)

Se(0)

Elemental selenium may occur in ten allotropic forms, seven crystalline (trigonal, α-mon-oclinic, β-monoclinic, α-cubic, β-cubic, rhombohedral, and ortho-rhombic) and three amorphous (red, black, vitreous) states /MIN 05/. If precipitated from solution, e.g. through abiotic or biotic reduction of selenite, amorphous red selenium is found /SCH 08/. At temperatures above 30 °C, it transforms slowly to black amorphous sele-nium and finally to grey trigonal selenium /KES 99/. Red amorphous as well as the mon-oclinic allotropes consist mainly of Se_8 rings, whereas the grey trigonal form consists of Se_n chains /MIN 05/.

So far, thermodynamic databases (NEA, Thermochimie, JAEA) did not include an aque-ous Se(0) species, so that extremely low total selenium concentrations are calculated under anaerobic conditions. Experimental evidence and comparison with the chemical analogue sulphur led to the conclusion that soluble Se(0) species exist and need to be included in order not to seriously underestimate the solubility of selenium.

For sulphur (rhombohedral α-S containing S_8 rings) solubilities of $1.9 \cdot 10^{-8}$ and $3 \cdot 10^{-8}$ mol S_8/ kg water were determined /BOU 78/, /KAM 09/ and linked to the following equilibrium

$$8 \text{ α-S}_{(s)} \rightleftharpoons S_8(aq); \qquad\qquad K = 2.6 \cdot 10^{-8}$$

Berner /BER 14c/ assumed that a similar reaction would take place for crystalline selenium. The author referred to a 'modification with a (distorted) structure similar to that of rhombohedral $S_8(\alpha)$ and expected a solubility around 10^{-7} to 10^{-6} mol/l. Whether or not rhombohedral selenium is meant, we assume that α-sulphur at least from a chemical point of view is closer to monoclinic selenium (α-Se or β-Se) as both contain rings of eight atoms, whereas rhombohedral Se contains Se_6 rings and the most stable modification, trigonal Se contains chains.

Based on the discussion above, we assume as a first rough guess that the intrinsic solubility of solid selenium (monoclinic) is similar to solid α-sulphur so that

$$C_{sat,Se} \approx c_{sat,S} = 8 \cdot 2.6 \cdot 10^{-8} \text{ mol/kg} = 2.08 \cdot 10^{-7} \text{ mol/kg}^{12}$$

The order of magnitude is supported by experiments by Kim et al. /KIM 12/ who measured the solubility of red (monoclinic, red Se_8) and "black"[13] selenium in an hydrazine solution. In both cases, the solubility was at $8 \cdot 10^{-8}$ mol/l which is about 2.5 times smaller than for sulphur. The identity of the aqueous species in equilibrium with solid selenium was not analysed but assumed to be selenide. However, as long as solid selenium is present, the equilibrium between a neutral aqueous selenium species and solid selenium

$$Se(\text{monoclinic}) \rightleftharpoons \text{ 'Se (aq)'}$$

would not be affected by the presence of a strongly reducing agent. The chemical properties of hydrated $Se_8(aq)$ in relation to $S_8(aq)$ are unknown. It is noted that the solubility of noble gases increases with atomic weight /POT 78/. It was expected that the solubility of neutral $Se_8(aq)$ would also be larger than that of $S_8(aq)$ for a solid of similar crystal structure. However, the intermolecular forces between Se_n and S_n may not follow the same trend as monoatomic noble gases.

The nature of solvated Se(0) is unknown, so far. It may be $Se_8(aq)$ similar to $S_8(aq)$. For the time being, Se(aq) shall stand for this neutral species of unknown constitution.

---

[12] The solubility of S_8 (eight atoms per molecule) is multiplied by 8 to represent the solubility of hypothetical monomolecular selenium.

[13] The black selenium was described as 'metallic', which would be the grey allotrope provided by Sigma Aldrich (the basis for the experiments by Kim et al.)

Based on the discussion above, we assume that K = 8·10^{-8} applies to the following equilibrium

Se(monoclinic) $\rightleftharpoons$ Se (aq)

Iida et al. /IID 10/ determined the solubility for monoclinic and two other selenium allotropes under reducing conditions

Se(am) + H_2O $\rightleftharpoons$ HSe$^-$ + H$^+$ + 0.5O_2(aq);   log K = -49.572

Se(monoclinic) + H_2O $\rightleftharpoons$ HSe$^-$ + H$^+$ + 0.5O_2(aq);   log K = -50.393

Se(trigonal) + H_2O $\rightleftharpoons$ HSe$^-$ + H$^+$ + 0.5O_2(aq);   log K = -50.618

In combination with the redox equilibrium for HSe$^-$ in Tab. 7.18 the equilibria for Se(aq) in Tab. 7.18 and the three selenium allotropes in Tab. 7.19 could be derived.

Tab. 7.19   Solubility of selenium allotropes

Equilibrium	log K
Se(am) $\rightleftharpoons$ Se (aq)	-6.3
Se(monoclinic) $\rightleftharpoons$ Se (aq)	-7.1
Se(trigonal) $\rightleftharpoons$ Se (aq)	-7.3

Se(-II)

Equilibrium data for HSe$^-$ hydrolysis and stability of polyselenide species (Se_2^{2-}, Se_3^{2-}, Se_4^{2-}) were taken from the JAEA database (version 190329g0.tdb) that is based on Doi et al. /DOI 09/ and in great part on the NEA database /OLI 05/.

However, it must be said that the existence of the free ion Se^{2-} that is included in JAEA and in the NEA databases, is rather doubtful. The analogue sulphide ion, S^{2-} has been postulated throughout the modern history of chemistry, but May et al. provided evidence that this species does not exist even in concentrated NaOH brines /MAY 18/. For the time being, Se^{2-} is kept in our database, but it would form only at extreme pcH values (>>14) and is of no relevance.

The polysulfide ions Se_2^{2-}, Se_3^{2-}, Se_4^{2-} are expected to hydrolyse in acidic solutions as do their polysulfide counterparts /KAM 04/. So far, there has been only one determination of polyselenide hydrolysis equilibria. It dealt with the diselenide species /SCH 69/

$$H_2Se_2(aq) \rightleftharpoons HSe_2^- + H^+; \qquad \log K = -1.7$$

$$HSe_2^- \rightleftharpoons Se_2^{2-} + H^+; \qquad \log K = -9.3$$

These data were not included by the NEA review in the set of recommended data but a comparison with sulphide and polysulphide equilibria shows that at least the difference between the first dissociation constants K_1 of $H_2Se_2(aq)$ /SCH 69/ and H_2S /LEM 20/ and the K_1 for $H_2S_2(aq)$ as $H_2Se_2(aq)$ is similar (3.14 and 3.41). It is a reasonable assumption that this difference (mean value 3.3) is applicable to $H_2Se_3(aq)$ and $H_2Se_4(aq)$ as well:

$$K(H_2Se_n(aq)) = K(H_2S_n(aq)) + 3.3$$

In the same manner, the observed dissociation constant for HSe_2^- was used as a basis to estimate the dissociation constants of HSe_3^- and HSe_4^- by assuming that the difference in K for H_2Se^- and $H_2S_2^-$ (0.7) is applicable for $H_2Se_3^-$ and HSe_4^- as well so that

$$K(HSe_n^-) = K(HS_n^-) + 0.73$$

Tab. 7.20 First dissociation constant of polysulphanes and polyselanes for the reaction $H_2S_n(aq)/ H_2Se_n(aq) \rightarrow HS_n^-/ HSe_n^- + H^+$

n	1	2	3	4	Source
$H_2S_n(aq)$	-6.99	-5.11	-4.31	-3.91	/KAM 04/
$H_2Se_n(aq)$	-3.85	-1.7	*-1.0*	*-0.6*	/SCH 69/ *estimated (italics)*
$\log K_1$ $(H_2Se_n(aq))$ $- \log K_1$ $(H_2S_n(aq))$	3.14	3.41	*(3.3)*	*(3.3)*	

Tab. 7.21 Second dissociation constant for polysulphanes and polyselanes for the reaction $HS_n^-/ HSe_n^- \rightarrow S_n^-/ Se_n^- + H^+$

n	1	2	3	4	Source
HS_n^-	-	-10.03	-7.83	-6.63	/KAM 04/
HSe_n^-	-	-9.3	*-7.1*	*-5.9*	/SCH 69/ *estimated (italics)*
$K_2(H_2Se_n(aq))-$ $K_2(H_2S_n(aq))$	-	0.73	*0.73*	0.73	

Interaction coefficients for Na^+/ HSe^- as well as for other Na^+/ Se_n^{2-} and Na^+/ HSe_n^- pairs were calculated using the reference values from Humphreys et al. (Tab. 7.24). The calculated stability field suggest that the species HSe_n^- and $H_2Se_n(aq)$ are not relevant at near neutral to alkaline conditions. They are expected to dominate under strongly reducing acidic conditions only (not shown).

In the presence of iron, solid iron selenides are among those phases that could control the solubility selenium. Stability data were taken from the NEA database (Tab. 7.22) /LEM 20/.

Tab. 7.22 Solubility iron selenides

Reaction	log K	Reference
β-$Fe_{1.042}Se + 1.084H^+ \rightleftharpoons 1.042Fe^{2+} + HSe^- + 0.042H_2(g)$	-4.24	1
γ-Fe_3Se_4 (greigite) + $4H^+ \rightleftharpoons Fe^{2+} + 2Fe^{3+} + 4HSe^-$	-41.14	1
α-$Fe_7Se_8 + 6H^+ + H_2(g) \rightleftharpoons 7Fe^{2+} + 8HSe^-$	-45.52	1
$FeSe_2$(ferroselite) + $H_2(g) \rightleftharpoons Fe^{2+} + 2HSe^-$	-18.91	1

1 /LEM 20/

Selenide also forms very insoluble solid phases with other waste components such as USe_3, Ag_2Se, $CoSe_2$, or $PbSe$.

Se(IV)

Data for the dissociation of selenic acid, $H_2SeO_3(aq)$ were taken from the NEA review. Stability data for two selenite complexes was presented by Seby et al. and Duro et al. /SÉB 01/, /DUR 06a/ (Tab. 7.23).

Tab. 7.23 Stability of selenite species

Reaction	log K	Source
$H_2SeO_3(aq) \rightleftharpoons HSeO_3^- + H^+$	-2.64	1
$HSeO_3^- \rightleftharpoons SeO_3^{2-} + H^+$	-8.36	1
$CaSeO_3(aq) \rightleftharpoons Ca^{2+} + SeO_3^{2-}$	-3.17	2
$MgSeO_3(aq) \rightleftharpoons Mg^{2+} + SeO_3^{2-}$	-2.87	2

1 /OLI 05/,

2 /DUR 06a// /SÉB 01/

Ion interaction coefficients for SeO_3^{2-} were determined by Hagemann et al. and then updated by Bischofer et al. /HAG 12a/, /BIS 16/. So far, no Pitzer interaction coefficients were developed for the pair Mg^{2+}/ $HSeO_3^-$. As an analogue, the interaction coefficients for HSO_4^- were used for hydrogen selenite. Their structures differ considerably, but they have comparable molecular weights and a OH group in common. In the same way, an interaction coefficient was derived for Mg^{2+}/ SeO_3^{2-} on the basis of the known interaction for Mg^{2+}/ SO_4^{2-}. These data are summarized in Tab. 7.24.

Tab. 7.24 Ion interaction coefficients for HSe^-, SeO_3^{2-} and $HSeO_3^-$ used in this study

Ion pair	$\beta^{(0)}$	$\beta^{(1)}$	$\beta^{(2)}$	$C\phi$	Source/ estimation method
K^+, HSe^-	0.1656	0		-0.0253	1 (Analogue to K^+, HS^-)
Na^+, HSe^-	0.1386	0		-0.0104	1 (Analogue to Na^+, HS^-)
Ca^{2+}, HSe^-	0.243	1.447			2
Mg^{2+}, HSe^-	0.243	1.447			2
K^+, HSe_n^- (n=2…4)	0.0503	0.1951			2
Na^+, HSe_n^- (n=2…4)	0.0503	0.1951			2
Ca^{2+}, HSe_n^-	0.243	1.447			2
Mg^{2+}, HSe_n^-	0.243	1.447			2
Na^+, Se_n^{2-} (n=2…4)	0.243	1.447			2
K^+, Se_n^{2-} (n=2…4)	0.243	1.447			2
Ca^{2+}, Se_n^{2-} (n=2…4)	0.23	2.9	-40		3
Mg^{2+}, Se_n^{2-} (n=2…4)	0.23	2.9	-40		3
Mg^{2+}, $HSeO_3^-$	0.51924	1.72898		-0.012029	4 (value for Mg^{2+}, HSO_4^-)
Mg^{2+}, SeO_3^{2-}	0.22088	3.34290		0.025001	4 (value for Mg^{2+}, SO_4^{2-}, α_1=1.4)

1 /HAG 15b/
2 Estimated (Humphreys)
3 Estimated (This work)
4 THEREDA database

Selenite forms sparingly solids compounds with many cations, including Mg^{2+}, Ca^{2+}, Fe^{2+} and Fe^{3+}. Data on the solubility of nestolaite, $CaSeO_3 \cdot H_2O$ is given in /BIS 16/ (log K = -6.61). The solubility constant for $MgSeO_3.6H_2O$ (log K = -5.82) was taken from the NEA review (Olin et al. 2004).

At least under certain conditions selenite may be precipitated by iron(II) resulting in the formation of $FeSeO_3 \cdot xH_2O$. The hydrate content of this compounds is unknown. Probably, the composition is $FeSeO_3 \cdot 2H_2O$, analogous to the Mn^{II}, Ni^{II}, $Zn^{II,}$ Cu^{II} and Co^{II} salts /KRI 11/. For the anhydrous phase Essington /ESS 88/ estimated a solubility constant of

-9.99, but this value should be considered with care as many of the underlying thermodynamic data for other M^{II} selenites in his model are rather uncertain (see /OLI 05/). For $CoSeO_3 \cdot 2H_2O$ (cobaltomenite) a solubility constant of -6.83 was found /CHA 14/, /CHA 17/. Since the ionic radius of Co^{2+} (0.745 Å) is close to the value of Fe^{2+} (0.79 Å) /MAR 88/ it may be assumed that the solubility constant of $FeSeO_3 \cdot 2H_2O$ is similar to $CoSeO_3 \cdot 2H_2O$. We define

$$FeSeO_3 \cdot 2H_2O \rightleftharpoons Fe^{2+} + SeO_3^{2-} + 2H_2O; \qquad \log K = -6.8^{[14]}$$

The predominance field of this compound would be rather small. Even small concentrations of Ca^{2+} lead to the precipitation of calcium selenite (nestolaite). If calcium is removed from the system, iron(II) selenite becomes stable at pH>10 at moderate H_2 pressures (Fig. 7.9). Fe(III) also forms selenites according to the formula $Fe_2(SeO_3) \cdot nH_2O$. Several values for n are reported in the literature (1.3.4.5.6) /RAI 95/, /LEL 18/, /HOL 18/, /GIE 96a/.

Kitamura et al. provided a solubility constant for the compound $Fe_2(SeO_3)_3 \cdot 6H_2O$ /KIT 12/. It is based on /RAI 95/, but /GIE 96a/ could show that the real composition must have been $Fe_2(SeO_3)_3 \cdot 3H_2O$ if the preparation method of /RAI 88/ is applied. Holzheid et al. carefully synthesized several hydrates and concluded that the mineral mandarinoite that was reported to contain six water molecules, probably has the formula $Fe_2(SeO_3)_3 \cdot 5H_2O$ /HOL 18/. Synthesis at higher temperatures or careful dehydration leads to $Fe_2(SeO_3)_3 \cdot 3H_2O$, $Fe_2(SeO_3)_3 \cdot H_2O$ and finally $Fe_2(SeO_3)_3$. The stability of $Fe_2(SeO_3)_3 \cdot 5H_2O$ (mandarinoite) was determined by Lelet et al. /LEL 18/

$$Fe_2(SeO_3)_3 \cdot 5H_2O \rightleftharpoons 2Fe^{3+} + 3SeO_3^{2-} + 5H_2O; \qquad \log K = -51.9$$

Some other Fe(III) selenites are reported in the literature such as $KFe(SeO_3)_2$, $Fe_6Ca_2(SeO_3)_9Cl_4$, $Ca_3Fe_2(SeO_3)_6$, $Fe_2O(SeO_3)_2$ /GIE 93/, /HU 13/, /GIE 96b/, /GIE 96c/ but no thermodynamic data could be found so that their relevance remains unclear.

According to Felipe-Soleto et al., the selenite solubility in anoxic cementitious systems may be controlled either by $CaSeO_3 \cdot 2H_2O$ or under more alkaline conditions (pH>12.5)

---

[14] For comparison, the solubility constant for the Ni^{II} (0.69 Å) and Mn^{II} (0.83 Å) analogues are -7.5 /CHA 17/ and -7.6 /OLI 05/.

by a mixed hydroxide selenite compound $Ca_2(OH)_2SeO_3 \cdot 2H_2O$ /FEL 16b/. Its solubility constant was calculated based on the experimental data of Nishimura and Hata /NIS 07/ using the Ion interaction parameters for Ca^{2+}/ OH^- from the THEREDA database (no other interactions were considered). This resulted in the following equilibrium

$$Ca_2(OH)_2SeO_3 \cdot 2H_2O \rightleftharpoons 2Ca^{2+} + SeO_3^{2-} + 2OH^- + 2H_2O; \quad \log K = -12.6$$

This compound has also been found as the solubility limiting phase during the contact of selenite with metallic iron instead of expected iron selenide or elemental selenium /FEL 16b/. Even in the presence of iron no significant reduction of selenite to Se(0) or FeSe occurred. Instead, iron may have provided nucleation sites for the precipitation of $Ca_2(OH)_2SeO_3 \cdot 2H_2O$. Only if the Eh was lowered to values well below -300 mV (e.g., by addition of $Na_2S_2O_4$) selenite was reduced. The existence of an analogue Fe(II) compound is likely (see the similar chukanovite, $Fe_2(OH)_2CO_3$).

Fig. 7.9   Stability field of iron selenites in a calcium-free saturated NaCl solution

Se(VI)

Ion interaction coefficients and solubilities were taken from the THEREDA database, which is based on /BIS 16/. For selenate, the two following solubility constants were added

$$CaSeO_4 \cdot 2H_2O \rightleftharpoons Ca^{2+} + SeO_4^{2-} + 2H_2O; \qquad \log K = -2.601 \text{ /BIS 16/}$$

$$Ca_2(OH)_2SeO_4 + 2H^+ \rightleftharpoons 2Ca^{2+} + SeO_4^{2-} + 2H_2O; \qquad \log K = 22.3. \text{ /NIS 07/}$$

Previously considered solubility limiting solid phases and solubility limits

In most studies it was assumed that under reducing conditions, selenium occurs in the oxidation states -II or 0 (Tab A. 30). It would be bound in an iron or cobalt selenide ($Fe_{1.04}Se$, $FeSe_2$, $CoSe_2$), incorporated into pyrite, FeS_2, or occurs as elemental selenium. Only in few instances, the formation of calcium selenite, $CaSeO_3$ was considered (in cement pore waters). In those cases, the maximum Se concentration was predicted to be in the order of 10^{-5} M or higher, whereas the solubility of iron or cobalt selenides as well as solid solution with sulphides would lead to concentrations of 10^{-14} to 10^{-9} mol/l and elemental selenium to levels in between (10^{-7} to 10^{-6} mol/l).

7.2.14   Silver

Thermodynamic properties in aqueous systems/ oxidation states

In aqueous solutions, silver may occur in the oxidation state +I. Higher states up to +V are known, but mainly in solids /LEV 87/. In aqueous media special ligands are necessary to stabilize the silver ion against reduction. Beside +I, other oxidation states are of no relevance for the conditions in a repository. As a noble metal, silver has a strong tendency to be reduced to the elemental form. Under reducing conditions silver may be expected to be completely reduced and the concentration of its solution would be close to zero. What has been neglected for a long time is that elemental silver has probably a solubility of its own by being in equilibrium with zero-valent aqueous silver, Ag(aq). While this species behaviour has not been investigated directly, so far, available solubility experiments may be interpreted very well if a species Ag(aq) is included /BER 14d/. Complex formation, especially with chloride extends the stability field of Ag(I). The stability diagram in Fig. 7.10 was calculated using the Thermochimie database (version 10a), being fully aware that this database was not designed to work in concentrated salt solutions.

131

Fig. 7.10 pH-f_{H2} diagram for silver in 6 m NaCl solution ($c_{Ag,total}=1\cdot10^{-5}$ mol/kg) , left: without solids, right: solids allowed

Ag(0)

Based on solubility data from Dobrovolski and Oglaza /DOB 63/ as well as Kozlov and Khodakovskii /KOZ 83/ who investigated the solubility of metallic silver in chloride solutions, Berner et al. /BER 13/ concluded that there is enough evidence to assume an equilibrium

$$Ag(s) \rightleftharpoons Ag(aq)$$

with an equilibrium constant near K = 10^{-7}. However, Zotov /ZOT 95/ tried to determine the solubility in the absence of complexing ligands and found that the solubility is very low. Kopeikin /KOP 20/ summarized the available data and pointed out that Zotov did not rule out the existence of an zero-valent aqueous silver, but that its equilibrium concentration must be very low (<10^{-7} mol/l). For the time being, we include the suggested solubility of elemental silver by Berner et al. /BER 13/ in order not to underestimate the silver concentration under reducing conditions.

Ag(I)

Brown and Ekberg /BRO 16/ summarized the available literature on the hydrolysis of the Ag$^+$ ion. They concluded that two hydroxo species exist, AgOH(aq) and Ag(OH)$_2^-$ for which they recommended stability constants (Tab. 7.25). Silver forms strong complexes with halides. Their stability increases in the order F<Cl<Br<I. In the case of chloride, the complexes AgCl(aq), AgCl$_2^-$, AgCl$_3^{2-}$, and possibly AgCl$_4^{3-}$ have been identified at 25°C.

Up to $AgCl_3^{2-}$, there is broad consensus about their stability, but regarding $AgCl_4^{3-}$ quite different opinions exist. Proposed constants differ by three orders of magnitude /FRI 85/. On the other hand, Gammons et al. /GAM 97/ in accordance with Zotov et al. /ZOT 95/ considered the existence of $AgCl_4^{3-}$ as doubtful and unnecessary to describe experimental observations of AgCl solubility even in concentrated chloride solutions.

As this species may or may not be the predominating species in saturated solutions, calculated solubilities of AgCl may turn up much too high if inadequate values for complex formation constants are chosen. The reason may be, as Fritz (l.c.) pointed out, inappropriate assumptions about the activity constant of the bulky, triple-charged $AgCl_4^{3-}$. Fritz (l.c.) developed a Pitzer model to describe the speciation and solubility of silver in NaCl and KCl solutions. But closer examination showed that his model did not include the full Pitzer model as it excluded the higher order electrostatic terms, necessary to describe binary interactions between ions of the same sign. Moreover, test calculations failed to represent experimental AgCl solubilities in concentrated NaCl. The results were too high by many orders of magnitude. Replacing the Fritz`s Pitzer coefficients by Simoes estimates didn't improve the situation, indicating that the complex formation constant for $AgCl_4^{3-}$ proposed by Fritz (l.c.) is still too high even though it was two orders of magnitude lower than all previously published values.

Removing $AgCl_4^{3-}$ from the database still leads to predicted solubilities about six times higher than observed. This discrepancy could principally be lowered by adjusting the Pitzer ion interaction parameters for $AgCl_3^{2-}$, the dominating species at concentrations above 1 mol/kg chloride. As shown later, the predicted solubility of AgCl in $MgCl_2$ solutions is about three orders of magnitude higher than observed solubilities in $CaCl_2$ solutions. Such a discrepancy cannot be explained by ion interaction parameters alone. Obviously, there is still a need to re-examine the formation of chloro complexes at ambient temperatures. There is still an astonishing lack of spectroscopic data on halogeno complexes at ambient temperature. Concluding on the current state of knowledge, the solubility of silver(I) cannot be reliably modelled in salt solutions at the moment. The thermodynamic data in the following tables are for information only. They were not used to calculate the solubility of silver solids.

Tab. 7.25   Stability of Ag species

Reaction	log K	Source
$Ag^+ + H_2O \rightleftharpoons Ag(OH)(aq) + H^+$	-11.75	1
$Ag^+ + 2H_2O \rightleftharpoons Ag(OH)_2^- + 2H^+$	-24.34	1
$Ag^+ + Cl^- \rightleftharpoons AgCl(aq)$	3.23	2
$Ag^+ + 2Cl^- \rightleftharpoons AgCl_2^-$	5.21	2
$Ag^+ + 3Cl^- \rightleftharpoons AgCl_3^{2-}$	5.1	2
$Ag^+ + Br^- \rightleftharpoons AgBr(aq)$	4.54	2
$Ag^+ + 2Br^- \rightleftharpoons AgBr_2^-$	7.48	2
$Ag^+ + 3Br^- \rightleftharpoons AgBr_3^{2-}$	8.86	2
$Ag^+ + I^- \rightleftharpoons AgI(aq)$	6.41	2
$Ag^+ + 2I^- \rightleftharpoons AgI_2^-$	11.54	2
$Ag^+ + 3I^- \rightleftharpoons AgI_3^{2-}$	13.36	2
$Ag^+ + CO_3^{2-} \rightleftharpoons AgCO_3^-$	2.69	3
$Ag^+ + 2CO_3^{2-} \rightleftharpoons Ag(CO_3)_2^{3-}$	2.16	3
$Ag^+ + HS^- \rightleftharpoons AgHS(aq)$	14.05	3
$Ag^+ + 2HS^- \rightleftharpoons Ag(HS)_2^-$	18.45	3

1: /BRO 16/; 2: /GAM 97/; 3: /DUR 06b/

Solid phases

Under alkaline conditions, silver is precipitated as silver oxide, Ag_2O. Amorphous and crystalline forms are documented, for which Brown and Ekberg /BRO 16/ reviewed and selected solubility constants.

In chloride-containing systems AgCl, the mineral chlorargyrite may be the solubility limiting solid. The solubility of this halogenide as well of the iodide and bromide is given by Gammons et al. /GAM 97/. Further important poorly soluble solids include Ag_2CO_3, Ag_2SO_4 and Ag_2S (acanthite) as well as Ag_2Se (naumannite). Stability constants were taken from Duro et al. /DUR 06b/.

Tab. 7.26 Stability of silver-containing solid phases[-]

Reaction	log K	Source
$Ag_2O(cr) + 2H^+ \rightleftharpoons Ag^+ + H_2O$	5.99	1
$Ag_2O(am) + 2H^+ \rightleftharpoons Ag^+ + H_2O$	6.27	1
$AgCl$ (chlorargyrite) $\rightleftharpoons Ag^+ + Cl^-$	-9.76	2
$AgBr$ (bromargyrite) $\rightleftharpoons Ag^+ + Br^-$	-12.31	2
AgI (oodargyrite) $\rightleftharpoons Ag^+ + I^-$	-16.09	2
$Ag_2CO_3 \rightleftharpoons 2Ag^+ + CO_3^{2-}$	-11.05	3
Ag_2S (acanthite) $+ H^+ \rightleftharpoons 2Ag^+ + HS^-$	-36.07	3
$Ag_2SO_4 \rightleftharpoons 2Ag^+ + SO_4^{2-}$	-5.01	3

1 /BRO 16/
2 /GAM 97/
3 /DUR 06b/

<u>Previously considered solubility limiting solid phases and solubility limits</u>

So far, silver was either assumed to be not solubility limited or limited by the formation of AgI (Tab A. 34) if iodine is present in the system. For that case, /BER 14b/ estimated a solubility limit of about 1.8 to $9.0 \cdot 10^{-7}$ mol/l in a cement/ concrete system equilibrated with Opalinus clay porewater.

7.2.15 Strontium

Thermodynamic properties in aqueous systems/ oxidation states

Under relevant conditions, strontium only occurs in the oxidation state +II. Data describing the solubility of strontium in marine waters are part of the THEREDA database (release 11).

Previously considered solubility limiting solid phases and solubility limits

Depending on the carbonate/ sulphate ration either $SrSO_4$ (strontianite) or $SrCO_3$ (celestite) are expected to be the solubility limiting phases (Tab A. 36). Depending on carbonate and sulphate levels, the solubilities were expected to be between 10^{-6} to 10^{-2} M.

In glass corrosion studies, strontium was found to be incorporated in baryte, $BaSO_4$ with concentration in the order of 10^{-4} to 10^{-2} mol/l /GRA 99/.

7.2.16 Tin

Thermodynamic properties in aqueous systems/ oxidation states

A consistent database for tin was developed as part of the NEA TDB program /GAM 12/. All data were taken from this source if not stated otherwise. In aqueous systems tin occurs in the oxidation states +II and +IV (Tab. 7.27).

Tab. 7.27 Redox equilibria for tin

Reaction	$\Delta_f G$ [kJ/mol]	log K	Reference
$\beta\text{-Sn(s)} + 4H_2O \rightleftharpoons Sn(OH)_4(aq) + 2H_2(g)$	3.65	-0.64	1
$Sn^{2+} + 4H_2O \rightleftharpoons Sn(OH)_4(aq) + H_2(g) + 2H^+$	31.04	-5.44	1

1 /GAM 12/

As the pH/ H_2 diagram shows, Sn(II) has almost no stability field and solid Sn(cr) is expected to be in equilibrium with Sn(IV) oxide or other Sn(IV) compounds such as $Sn(OH)_4(am)$ or burtite, $CaSn(OH)_6$. This would suggest that tin(II) phases are almost always irrelevant. However, on ancient tin artefacts that were buried in anoxic marine sediments for over 2000 years tin corrosion products included only Sn(II) compounds (SnS, herzenbergite, $Sn_{21}Cl_{16}(OH)_{14}O_6$, abhurite, SnO, romarchite, $2SnO \cdot 5H_2O$, hydromarchite, /DUN 03/, /DUN 04/). This is consistent with the findings by Séby et al. that under strongly reducing conditions Sn(II) becomes stable /SÉB 01/. The existence of Sn(II) compounds in the near field would be important, because the solubility of Sn(II) compounds is considerably higher than those of Sn(IV) phases.

Eventually, it was found that tin(II) oxide disproportionates into Sn(IV) and metallic tin only at high temperatures (> 500K) so that this process plays no relevant role under moderate conditions in a repository (<100 °C). Direct reduction of Sn(II) with hydrogen to metallic tin would require hydrogen pressures and/ or temperatures that are also not likely to occur.

Corrosion of metallic tin in water is slow. Even though the process is enhanced by the presence of chloride, tin objects may survive centuries or millennia in contact with seawater /DUN 03/, /BER 19/.

Fig. 7.11 pH-f_{H2} diagram for tin in 6 m NaCl solution ($c_{Sn,total}=1\cdot10^{-5}$ mol/kg) , left: without solids, right: solids allowed

Tin - Sn(II)

Data on the stability of tin(II) hydroxo, chloro, carbonato, and sulphato complexes were taken from /GAM 12/. The model includes the species $SnOH^+$, $Sn(OH)_2(aq)$, $Sn(OH)_3^-$, $Sn_3(OH)_4^{2+}$, $SnCl^+$, $SnCl_2(aq)$, $SnCl_3^-$, $SnCl_4^{2-}$, $SnSO_4(aq)$, $SnCO_3(aq)$, $Sn(OH)CO_3^-$.

Pettine et al. reported on the formation of ternary $MSn(OH)_3^+$ complexes, where M is a mixture of Ca, Mg, Sr /PET 81/. Only few measurements were conducted, but a rough assessment showed that at metal concentrations of 0.065 the ternary complex dominated at pH>10 in seawater.

Only one mixed chloro hydroxo complex is described for Sn(II), SnOHCl(aq). No stability constant was accepted by /GAM 12/ because the only source reported high uncertainties. But Hummel et al. /HUM 02/ included the species in their database and found its way in the Thermochimie database as well

$$Sn^{2+} + H_2O + Cl^- \rightleftharpoons SnOHCl(aq) + H^+; \qquad \log K = -3.1 \pm 0.2$$

Cigala et al. /CIG 12/ estimated the stability of this mixed complex based on the statistical method of Beck and Nagypal /BEC 90/ and derived log K = - 1.5 ± 0.1. The data in /HUM 02/ is preferred because it is based on experimental work. Moreover, it is

137

reasonable to assume that mixed complexes with three or four ligands also exist as has been found for the similar Pd(II), but experimental data are missing so far.

There has been only one determination of the formation constants of Sn(II) carbonato complexes /CIG 12/. Their value for the reaction

$$Sn^{2+} + CO_3^{2-} \rightleftharpoons SnCO_3(aq); \qquad \log K = 16.25 \pm 0.25$$

is very high in comparison to other M^{2+} carbonato complexes. It would cause $SnCO_3(aq)$ to be the dominating species at all relevant pcH levels, even in the presence of up to 10 mol/kg chloride and low carbonate concentration. Using a correlation method, Brown and Wanner /BRO 87b/ estimated $\log K = 9.72$. In that case, $SnCO_3(aq)$ would have a negligible impact on the solubility. The data from /CIG 12/ for $SnCO_3(aq)$ and $Sn(OH)CO_3^-$ were not used.

Several mixed hydroxo chlorides for Sn(II) were described. One is often referred to as '$Sn(OH)Cl \cdot H_2O$', but the correct formula is probably $Sn_{21}Cl_{16}(OH)_{14}O_6$ (abhurite) /SCH 81/, /EDW 92/ for many experimental findings. The following solubility constant was used /GAM 12/

$$Sn_{21}Cl_{16}(OH)_{14}O_6 + 26\ H^+ \rightleftharpoons 21\ Sn^{2+} + 20\ H_2O + 16\ Cl^-; \quad \log K = -34.02$$

Thermodynamic data for the important tin(II) hydroxide $Sn_3O_2(OH)_2$, the mineral hydroromarchite is still lacking. It was found on ancient corroding tin metal items where it occurs together with romarchite, SnO and other minerals such as abhurite or cassiterite /DUN 03/, /DUB 22/. A solubility constant is reported for amorphous "$Sn(OH)_2$", but obviously the real composition was not determined /CIG 12/. It may well be close to the composition of hydroromarchite, but the reported value is taken for $Sn(OH)_2(am)$

$$Sn(OH)_2(am) + 2H^+ \rightleftharpoons Sn^{2+} + 2H_2O; \qquad \log K = 1.74 \pm 0.08$$

Furthermore, the solubility constant for basic tin(II) sulphate, $Sn_3(OH)_2OSO_4$ from Edwards et al. /EDW 96/ was added.

$$Sn_3(OH)_2OSO_4 + 4H^+ \rightleftharpoons 3Sn^{2+} + 3H_2O + SO_4^{2-} \quad \log K = -5.01$$

It was not selected by /GAM 12/. Pitzer coefficients for Sn(II) species were estimated using the estimation methods described above (Tab. 7.28).

Tab. 7.28   Ion interaction coefficients for Sn species

Ion pair	α_1	$\beta^{(0)}$	$\beta^{(1)}$	Source
$SnCl^+$, Cl^-	2	0.0503	0.1951	1
$SnOH^+$, Cl^-	2	0.0503	0.1951	1
$SnOH^+$, SO_4^-	2	0.243	1.447	1
$Sn_3(OH)_4^{2+}$, Cl^-	2	0.243	1.447	1
Na^+, $SnCl_3^-$	2	0.0503	0.1951	1
Na^+, $SnCl_4^{2-}$	2	0.243	1.447	1
Na^+, $Sn(OH)_3^-$	2	0.0503	0.1951	1
K^+, $SnCl_3^-$	2	0.0503	0.1951	1
K^+, $SnCl_4^{2-}$	2	0.243	1.447	1
K^+, $Sn(OH)_3^-$	2	0.0503	0.1951	1
Mg^{2+}, $SnCl_3^-$	2	0.243	1.447	1
Mg^{2+}, $SnCl_4^{2-}$	1.4	0.2978	2.6320	2 (2.81Å)
Ca^{2+}, $SnCl_3^-$	2	0.243	1.447	1
Ca^{2+}, $SnCl_4^{2-}$	1.4	0.2750	2.5843	2 (2.81Å)
Ca^{2+}, $Sn(OH)_3^-$	2	0.243	1.447	1

1 Estimated (Humphreys)
2 Estimated (Simoes)

Tin - Sn(IV)

Tin(IV) undergoes strong hydrolysis even in very acidic solutions. To suppress the formation of hydroxo complexes, high acid concentrations such as 5M $HClO_4$ are required /FAT 78/.

Already at 1 M HCl, the most important Sn(IV) are mixed hydroxo chloro complexes /GAM 12/. It is therefore highly improbable that neutral tin(IV) chloro complexes play any role in near neutral to alkaline saline solutions. However, the formation of mixed hydroxo chloro complexes with a high OH/ Cl ratio cannot be fully excluded under slightly acidic conditions, but a concise thermodynamic treatment of these species is still lacking.

The stability constants for the two complexes $Sn(OH)_5^-$ and $Sn(OH)_6^{2-}$ were taken from the NEA database /GAM 12/

$Sn(OH)_5^- + H^+ \rightleftharpoons Sn(OH)_4(aq) + H_2O;$ log K = 8.6

$Sn(OH)_6^{2-} + 2H^+ \rightleftharpoons Sn(OH)_4(aq) + 2H_2O;$ log K = 18.67

For the two solid phases $SnO_2(am)$ and $SnO_2(cr)$ the stability was assumed to be as follows:

$SnO_2(am) + 2H_2O \rightleftharpoons Sn(OH)_4(aq);$ log K = -7.22

$SnO_2(cr)$ (cassiterite) $+ 2H_2O \rightleftharpoons Sn(OH)_4(aq);$ log K = -8.02

The database was supplemented by a solubility constant for burtite, $CaSn(OH)_6$, which Lothenbach et al. /LOT 00/ determined in alkaline cement systems:

$CaSn(OH)_6(fresh) + 2H^+ \rightleftharpoons Ca^{2+} + Sn(OH)_4(aq) + 2H_2O;$ log K = 8.82

$CaSn(OH)_6(cr) + 2H^+ \rightleftharpoons Ca^{2+} + Sn(OH)_4(aq) + 2H_2O;$ log K = 7.74

Potassium stannate is very soluble in water (about 87 wt.- %, /ROS 68/) and would pre-cipitate only in concentrated KOH media. A magnesium stannate $MgSn(OH)_6$, known as the mineral schoenfliesite /FAU 71/ can be synthesized by grinding a 1:1 mixture of $MgCl_2 \cdot 6H_2O$ and $Na_2Sn(OH)_6$ at room temperature /KRA 10/. The solid is only slightly soluble as it can be used to prepare coatings. It was also found in contact with seawater in ancient shipwrecks /BAS 98/. The stability of several stannates was recently deter-mined calorimetrically by Haase et al /HAA 21/. They found

$CaSn(OH)_6$ (burtite)$+ 2H^+ \rightleftharpoons Ca^{2+} + Sn(OH)_4(aq) + 2H_2O;$ log K = 15.2

The log K value is seven orders of magnitude higher than that reported by Lothenbach et al. Using this constant, tin solubilities would increase tremendously at higher pcH value. Therefore, it must be assumed that the calculation of Haase et al. contains a se-rious error. That may also apply to the analogue Mg and Fe(III) stannates:

$MgSn(OH)_6$ (schoenfliesite) $+ 2H^+ \rightleftharpoons Mg^{2+} + Sn(OH)_4(aq) + 2H_2O$

$\Delta_f G = -1812.4$ kJ/mol; log K = 10.9

$$FeSnO(OH)_5 \text{ (jeanbandyite)} + 3H^+ \rightleftharpoons Fe^{3+} + Sn(OH)_4(aq) + 2H_2O$$

$$\Delta_f G = -1425.4 \text{ kJ/mol; } \log K = 1.8$$

Because of the problems with burtite, the solubilities of schoenfliesite and jeanbandyite are considered unreliable and were not included in the calculations.

Rai et al. /RAI 11b/ observed that the solubility of $SnO_2(cr)$ remains constant up to pH> 11.7 (log c_{Sn} about -9). They concluded that in sodium containing solutions, sodium stannate, $Na_2Sn(OH)_6$ was the solubility limiting phase and assumed that from pH 11.7 onwards a species of $Na_2Sn(OH)_6(aq)$ abruptly predominates, whereas previously $Sn(OH)_6^{2-}$ occurred almost exclusively. Although the solid $Na_2Sn(OH)_6$ is known from the literature, the authors did not prove it by XRD or chemical analysis. Their experimental results are in sharp contradiction to literature that report a very high solubility of $Na_2Sn(OH)_6$ (> 30 % wt.- %, /ZOC 20/, /REI 39/, /UZA 59/).

Mixed oxychlorides are known for tin(IV), such as $Sn(OH)Cl_3 \cdot 3H_2O, Sn(OH)_2Cl_2$ and $Sn(OH)_3Cl \cdot H_2O$, but reliable thermodynamic data are lacking /GAM 12/.

Pitzer ion interaction coefficients are required to create a database for saline solutions. They are not available for tin(IV) hydroxo species. Two methods were tested and compared. In the first attempt, the ion interaction parameters for $Na^+/ Zr(OH)_6^{2-}$ were used. $Zr(OH)_6^{2-}$ and $Sn(OH)_6^{2-}$ have similar ionic radii (calculation with the method of /SIM 17/ gave 2.53 Å for both). A second set of parameters was estimated using the methods described by Simoes et al. and Humphreys et al. The two sets of Pitzer interaction parameters lead to similar results when the solubility is calculated. Due to the typically weak performance of SIT at higher ionic strength, the estimated coefficients were given priority.

Tab. 7.29 Ion interaction coefficients for tin(IV) species

Ion pair	$\beta^{(0)}$	$\beta^{(1)}$ ($\alpha_1=2$)	C^ϕ	Source/ method
Na$^+$, Sn(OH)$_5^-$	0.0503	0.1951		1
K$^+$, Sn(OH)$_5^-$	0.0503	0.1951		1
Ca^{2+}, Sn(OH)$_5^-$	0.243	1.447		1
Na$^+$, Sn(OH)$_6^{2-}$	0.243	1.447		1
K$^+$, Sn(OH)$_6^{2-}$	0.243	1.447		1
Ca^{2+}, Sn(OH)$_6^{2-}$	0.2841	2.6001 $\alpha_1=1.4$	-	5 (2.89 Å)
Na$^+$, Sn(OH)$_5^-$	*-0.0652**	*0.4067**		*2 Calculated from ε-0.08*
Na$^+$, Sn(OH)$_6^{2-}$	*0.0122**	*1.9000**	*-0.00940**	*3 Calculated from SIT for Na$^+$, Zr(OH)$_6^{2-}$*
Na$^+$, Sn(OH)$_6^{2-}$	*-0.0787**	*2.7027**		*2 Calculated from ε-0.125*
K$^+$, Sn(OH)$_6^{2-}$	*0.0122**	*1.9000**	*-0.00940**	*Estimated, based on the observation that SIT ion interaction coefficients for Na$^+$ and K$^+$ are similar for 2:1 salts (4)*

1 Estimated (Humphreys)
2 (Rai et al. 2011)
3 /THO 14/
4 /GAM 12/
5 /SIM 16/
* values in italics were not used in the final modellings

Previously considered solubility limiting solid phases and solubility limits

In all considered studies, Sn(IV) war assumed to be the predominant oxidation state. It would occur as cassiterite, SnO$_2$(cr), SnO$_2$(am) or burtite, CaSn(OH)$_6$ (Tab A. 39). Solubilities were predicted to be in the order of 10^{-12} to 10^{-5} mol/l. If sulphides are present tin sulphides may form /DUR 10/, but so far, this was not considered relevant.

7.2.17 Zirconium

Thermodynamic properties in aqueous systems/ oxidation states

In aqueous systems, zirconium occurs only in the oxidation state (IV). Lower valencies (I,II,III) are known from solid compounds, but these decompose when in contact with

water. Elemental zirconium cannot be formed from aqueous solution. On the other hand, corrosion of zirconium in water is often very slow.

Fig. 7.12   pH-f_{H2} diagram for zirconium in 6 m NaCl solution ($c_{Zr,total}$=1·10^{-5} mol/kg), left: without solids, right: solids allowed

Model

In moderately acidic to alkaline solution the speciation of Zr(IV) is dominated by hydroxo complexes of the type $Zr(OH)_x^{4-x}$ (x = 1-6). Around pH 0 to 2 polynuclear cationic complexes occur that may also include chloride ions /SAS 10/. They are not relevant or not needed to describe moderately acidic to alkaline conditions /SAS 08/, /RAI 18/. Only in extremely acidic systems, the free Zr^{4+} ion may occur. At high pH values, the presence of calcium leads to the formation of ternary complexes of the type $Ca_xZr(OH)_6^{2-2x}$ (x= 1-3) that cause a strong increase of the overall zirconium solubility /BRE 07/, /ALT 08/. It was assumed that these bulky complexes sorb at the surface of solid phases in the near field /KIE 13/.

If no ultrafiltration is performed, colloids, especially in weakly concentrated solutions of medium pH, may contribute strongly to the observed total concentration of zirconium. That is why many early solubility experiments suggested $Zr(OH)_4$ solubilities in the order of 10^{-4} mol/kg and were attributed to $Zr(OH)_4$(aq). /ALT 08/ observed log c Zr in the order of -8.5 to -7 but even that may have been not realistic (see comment in /RAI 18/). Instead, a comparison with the careful investigation of Rai et al. /RAI 01/ on the solubility of $Hf(OH)_4$(am) shows that $Zr(OH)_4$(am) could have a similar solubility and then would be in the order of 10^{-10} mol/kg /RAI 18/.

The most recent thermodynamic model to describe zirconium solubility depending on pcH and ionic strength has been developed by Rai et al. /RAI 18/, mainly but not exclusively by re-evaluating the results by Altmaier et al. /ALT 08/. Another set of date was prepared by Thoenen et al. /THO 14/. All three publications provided stabilities and SIT coefficients for some species, only /RAI 18/ presented Pitzer coefficients, but only for a limited range of species and interactions. Each model covers an individual field of species that does not fully overlap with the other two models.

In order to prepare a complete set of stability constants, the following procedure was used: The model of Rai et al. /RAI 18/ was taken as a basis. A stability constant for $Zr(OH)_4$(aq) was included that was purposely omitted by Rai et al. (2018) because it was thought to be inaccurate. In neutral solutions, Altmaier et al. observed a constant solubility of log c = -7.8 for $ZrO_2 \cdot xH_2O$ (am, aged) (= $Zr(OH)_4$ (am, aged) in this study). If this solid is in equilibrium with $Zr(OH)_4$(aq)

$$Zr(OH)_4 \text{ (am, aged)} \rightleftharpoons Zr(OH)_4\text{(aq)}; \qquad \log K = -7.8$$

the stability constant for the complex may be easily derived by combining the intrinsic solubility with the solubility constant of the solid phase

$$Zr(OH)_4 \text{ (am, aged)} + 4H^+ \rightleftharpoons Zr^{4+} + 4H_2O; \qquad \log K = -0.19 \text{ (Rai et al.)}$$

which leads to

$$Zr(OH)_4\text{(aq)} + 4H^+ \rightleftharpoons Zr^{4+} + 4H_2O; \qquad \log K = 7.6$$

The reason for omitting this value in Rai et al. was the assumption that the solubilities measured by Altmaier et al. were still too high (see above). However, there is no indication that the study of this group and the measures taken to prevent colloid contamination in the samples were inaccurate. It is noted that previous estimations of the stability of $Zr(OH)_4$(aq) were much higher (-2.2 in /ALT 08/ and /THO 14/). This depends, among other things on the activity coefficient calculated for Zr^{4+} in extremely acidic solutions. In future models, this problem may be solved by using $Zr(OH)_4$(aq) or $Zr(OH)_6^{2-}$ as a basis species and reference point.

The stabilities of $Ca_2Zr(OH)_6^{2+}$ and $CaZr(OH)_6(aq)$ where derived by combining the stability for $Ca_3Zr(OH)_6^{4+}$ (Rai et al.)

$$3Ca^{2+} + Zr^{4+} + 6H_2O \rightleftharpoons Ca_3Zr(OH)_6^{4+} + 6H^+; \quad \log K = -26.54$$

with the data from Thoenen et al. (that was based on Altmaier et al.)

$$Ca^{2+} + Ca_2Zr(OH)_6^{2+} \rightleftharpoons Ca_3Zr(OH)_6^{4+}; \qquad \log K_3 = -0.6$$

$$Ca^{2+} + CaZr(OH)_6(aq) \rightleftharpoons Ca_2Zr(OH)_6^{2+}; \qquad \log K_2 = 2.0$$

This procedure leads to a set of stability constants that is compatible with Rai et al. :

$$Ca^{2+} + Zr^{4+} + 6H_2O \rightleftharpoons CaZr(OH)_6(aq) + 6 H^+; \quad \log K = -28.9$$

$$2Ca^{2+} + Zr^{4+} + 6H_2O \rightleftharpoons Ca_2Zr(OH)_6^{2+} + 6 H^+; \quad \log K = -26.9$$

The solubilities of $Zr(OH)_4$(am,fresh) and ZrO_2(baddeleyite) were derived by considering the relative stabilities of these solids in relation to $Zr(OH)_4$(am,aged) in Thoenen et al.

$$\Delta_1 = \log K (Zn(OH)_4)(am,fresh,Thoenen) - \log K (Zn(OH)_4)(am,aged,Thoenen)$$
$$= -3.24 - (-4.3) = 1.06$$

$$\Delta_2 = \log K (ZnO_2(cr),Thoenen) - \log K (Zn(OH)_4)(am,aged,Thoenen)$$
$$= -7 - (-4.3) = -2.7$$

This leads to the following solubility constants

$$\log K (Zn(OH)_4)(am,fresh) = \log K (Zn(OH)_4)(am,aged,Rai) + \Delta_1 = 0.9$$

$$\log K (ZnO_2(cr)) = \log K (Zn(OH)_4)(am,aged,Rai) + \Delta_2 = -2.9$$
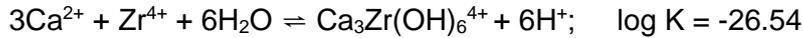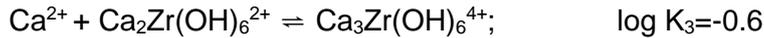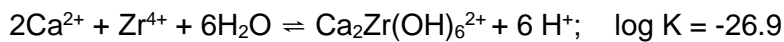
Stability constants for carbonate complexes were taken from the study of Kobayashi and Sasaki /KOB 17/ (Tab. 7.33). However, if these complexes were included in the model calculations very high zirconium concentrations were observed because of extremely low ion activity coefficients. In the presence of Ca^{2+} it may be assumed that they form

ternary complexes with even higher stability but probably lower charge (such as described for Zr(IV) hydroxides, /BRE 07/ or uranyl(VI) carbonates /KEL 07b/. In the end, the highly charged zirconium carbonate complexes had to be excluded from the calculations.

Like titanium, zirconium forms a mineral with calcium that has perovskite structure, $CaZrO_3$ (lakargiite). However, it has only been observed in high temperature experiments /GAL 08/. An analogue of burtite, $CaSn(OH)_6$, is not yet known. In solubility experiments in $CaCl_2$ solution, a corresponding compound with Zr did not occur even after 198 days /ALT 08/.

Rai et al. provided Pitzer interaction coefficients for only three zirconium species. These are probably the most relevant ones, but to cover all possible conditions, further Pitzer coefficients were estimated (Tab. 7.32).

Tab. 7.30 Stability of Zr species and solid phases⁻

Reaction	Altmaier et al. (1)	Thoenen et al. (2)	Rai et al. (3)	This work
$Zr^{4+} + H_2O \rightleftharpoons ZrOH^{3+} + H^+$	0.32	0.32	0.32	0.32
$Zr^{4+} + 2H_2O \rightleftharpoons Zr(OH)_2^{2+} + 2H^+$	0.98	0.98	≤-2.7	0.98
$Zr^{4+} + 4H_2O \rightleftharpoons Zr(OH)_4(aq) + 4H^+$	-2.2	-2.19	<-10.11	-7.6
$Zr^{4+} + 5H_2O \rightleftharpoons Zr(OH)_5^-(aq) + 5H^+$		-	-19.66	-19.66
$Zr^{4+} + 6H_2O \rightleftharpoons Zr(OH)_6^{2-} + 6H^+$	-29.2	-29.0	-33.06	-33.06
$Ca^{2+} + Zr^{4+} + 6H_2O \rightleftharpoons CaZr(OH)_6(aq) + 6H^+$		-24.6	-	-28.9
$2\,Ca^{2+} + Zr^{4+} + 6H_2O \rightleftharpoons Ca_2Zr(OH)_6^{2+} + 6H^+$	-22.6	-22.6	-	-26.9
$3\,Ca^{2+} + Zr^{4+} + 6H_2O \rightleftharpoons Ca_3Zr(OH)_6^{4+} + 6H^+$	-23.2	-23.2	-26.54	-26.54
ZrO_2 (baddeleyite) $+ 4H+ \rightleftharpoons Zr^{4+} + 2H_2O$		-7.0	-	-2.9
$Zr(OH)_4$ (am, fresh) $+ 4H+ \rightleftharpoons Zr^{4+} + 4H_2O$	-3.2	-3.24		0.9
$Zr(OH)_4$ (am, aged) $+ 4H+ \rightleftharpoons Zr^{4+} + 4H_2O$	-4.3		-0.19	-0.19

1 /ALT 08/
2 /THO 14/
3 /RAI 18/

Tab. 7.31 Stability of Zr carbonate complexes /KOB 17/

Reaction	log K
$Zr^{4+} + 5CO_3^{2-} \rightleftharpoons Zr(CO_3)_5^{6-}$	41.6
$Zr^{4+} + 4CO_3^{2-} \rightleftharpoons Zr(CO_3)_4^{4-}$	42.4
$Zr^{4+} + 2OH^- + 2CO_3^{2-} \rightleftharpoons Zr(CO_3)_4^{4-}$	46.9

Tab. 7.32 Ion interaction coefficients for zirconium species

Ion pair	$\beta^{(0)}$	$\beta^{(1)}$	C^ϕ	Source/ method
Zr^{4+}, Cl^-	1.664	15.5	0.0995	1 (from Hf^{4+}, Cl^-)
$ZrOH^{3+}$, Cl^-	0.464	7.85	0	1
$Zr(OH)_2^{2+}$, Cl^-	0.243	1.447	0	Estimated (Humphreys)
$Zr(OH)_2^{2+}$, SO_4^{2-}	0.1684	2.3058	0	Estimated (Simoes) r_i= 1.61
Na^+, $Zr(OH)_5^-$	0.0503	0.1951	0	Estimated (Humphreys)
K^+, $Zr(OH)_5^-$	0.0503	0.1951	0	Estimated (Humphreys)
Ca^{2+}, $Zr(OH)_5^-$	0.243	1.447	0	Estimated (Humphreys)
Na^+, $Zr(OH)_6^{2-}$	0.44	0.70	-0.0318	1 (from Na^+, $Hf(OH)_6^{2-}$)
K^+, $Zr(OH)_6^{2-}$	0.243	1.447	0	Estimated (Humphreys)
Ca^{2+}, $Zr(OH)_6^{2-}$	0.2844	2.6006 α_1=1.4	0	Estimated (Simoes) r_i= 2.78
$Ca_2Zr(OH)_6^{2+}$, Cl^-	0.1804	2.7027	0	Calculated from ε=0.1 in 2
$Ca_3Zr(OH)_6^{4+}$, Cl^-	1.0633	15.5	0.0995	1

1 /RAI 18/
2 /THO 14/

Tab. 7.33 Ion interaction coefficients for Zr carbonate complexes calculated from SIT coefficients in Kobayashi and Sasaki /KOB 17/, α_1=2

Ion pair	ε	$\beta^{(0)}$	$\beta^{(1)}$
Na^+/ $Zr(CO_3)_4^{4-}$	0.64	0.8865	23.6822
Na^+/ $Zr(CO_3)_5^{6-}$	0.95	1.3375	88.2404
Na^+/ $Zr(OH)_2(CO_3)_2^{2-}$	-0.01	0.0537	2.7027

Previously considered solubility limiting solid phases and solubility limits

In all studies, either baddeleyite, ZrO_2(cr) or amorphous ZrO_2/ $Zr(OH)_4$ was considered the least soluble phase (Tab A. 43). Predicted solubilities ranged from 10^{-11} to 10^{-4} M.

In corrosion experiments with vitrified glass, zirconium was present as zirconia, $ZrSiO_4$ or as a mixed oxide phase with Ce^{IV}, but could not be detected in solution /GRA 99/.

8 Solubility of selected fission and activation products in saline groundwaters

8.1 Selection of elements and oxidation states for laboratory experiments

Within the scope of the project, the solubility of the following elements was investigated:

Mo, Sr, Zr, Ni, Sm, Pd, Se, Pb, Ag, Nb, Sn

Under relevant redox conditions, some radionuclides occur in several oxidation states. It is not always possible to identify a priori which state will prevail in the long-term, since the reduction kinetics under the actual boundary conditions of a repository are not known. Mo, Se, and Sn may occur in aqueous solutions in two or more stable oxidation states. For Mo the states (IV) and (VI) were selected. The oxidation state +III is not easy to synthesise and was omitted in this study. For Se the states -II (selenide) and +IV (selenate) were selected. The oxidation state +VI is not solubility limited as far as can be said. For Sn the oxidation states +II and +IV were investigated separately. At this stage, the solubility of the potentially occurring elemental forms (Ni, Pd, Se, Pb, Ag) was not determined. This should be done first in water or simple salt solutions.

The three elements caesium, rubidium and iodine were not covered experimentally, because they are not solubility limited according to current knowledge.

8.2 Selection of aqueous solutions to be used as a matrix and range of geo-chemical conditions

The following solution types were used as a background medium for solubility experiments:

- Halite/ anhydrite-saturated salt solution ("Hal/ Anh"). A type E solution[15]

- IP9 solution (NaCl/ $MgCl_2$/ $MgSO_4$ solution formed from water and polyhalitic rock salt) and the Mg depleted solution after pH increase ("IP9" and "IP9 Reak"). It's a representative of solution type D (see above). For some selected systems, IP9 solution in contact with Sorel cement was investigated

---

[15] Categories of salt solutions are described in chapter 2.3.1

- IP21 solution (MgCl$_2$-rich equilibrium solution in contact with potash rocks) (a type B solution) and the Mg-depleted solution after pH increase ("IP21" and "IP21-Reak")

- Saline model pore water of a Lower Cretaceous clay formation (unsaturated NaCl/ CaCl$_2$ dominated solution) ("UK"). For some selected systems, UK water in contact with portlandite was investigated (as a component of a cementitious building material used in the near field) ("UK-Po")

The range of possible solutions is much wider. These four solutions were selected to reflect the range at least to some extent.

8.3   Preparation of starting solutions

The selected solutions were prepared by adding appropriate amounts of salts (chlorides and sulphates of Na, K, Mg and Ca) to water to achieve solution concentrations close to the theoretical values. To obtain saturated solutions certain amounts of equilibrium minerals were added and the mixtures stirred for several weeks in a temperature-controlled room (T = 25±1 °C).

For this purpose, several minerals that were not commercially available had to be synthesized in pure form:

- Polyhalite
- Syngenite
- Glauberite
- Carnallite
- Kainite

Details on the preparation method for the individual salts as for the equilibrium solutions may be found in annex A.4.

Equilibrium was achieved quite quickly in the case of halite/ anhydrite solutions. On the other hand, several months were needed to stabilise the concentrations in IP9 and IP21 solutions. The laboratory compositions were close to the values calculated using the THEREDA and the HMW database /HAR 84/ (Tab. 8.2, Tab. 8.3).

The IP9 and IP21 solutions contain considerable amounts of $MgCl_2$. Adjusting the pcH to higher values would require the precipitation of high quantities of Mg hydroxides around pH8. Instead, 'reacted solutions" were calculated that would result after an almost complete precipitation of Mg from IP21 or IP9 but where the original equilibrium minerals are still present. The theoretical composition was calculated with the THEREDA database. The final experimental compositions of the equilibrium solutions are summarized in Tab. 8.1. The actual starting solutions were 95 % dilutions to avoid precipitation of salts due to small temperature changes or oversaturation. The equilibrium concentration of Ca in these solutions is low. It cannot be excluded that the solubility limiting phase of the radionuclides contains Ca. The supply from the starting solution is very low and may become depleted before the total amount of oversaturated radionuclide could be precipitated. To maintain a constant supply of Ca the equilibrium Ca minerals (e.g., anhydrite in case of a halite/ anhydrite saturated solution) were added in excess in each experiment.

Tab. 8.1   Composition of equilibrium solutions [mol/kg]

Com-ponent	HalAnh	IP9	IP9 Reak	IP21	IP21 Reak	UK
Na	6.20	4.49	5.79	0.461	5.56	2.47
K	-	0.889	0.983	0.524	1.162	0.0119
Mg	-	1.15	0.00394	4.21	-	0.0767
Ca	0.043	<3e-6	0.00638	0.00134	0.00319	0.188
Cl	6.20	6.83	6.50	8.92	6.47	3.08
SO_4	0.043	0.420	0.284	0.287	0.320	0.0202
Density	1.2010	1.24	1.2313	1.2908	1.2369	1.10

A comparison of the manufactured solution concentrations of IP9 and IP21 solution and modelling results calculated with the HMW and THEREDA data base are given in Tab. 8.2 and Tab. 8.3. It is noted that the calculated composition of IP9 solution differs between HMW and Thereda. The main reason is probably the introduction of the mineral pentasalt that was not part of the HMW database. The synthetic IP9 solution is closer to the HMW value in the case of magnesium, but higher in chloride than in both calculations.

The sodium concentrations is in the middle between HMW and Thereda values. Possibly, there were still some minerals not in full equilibrium with each other. On the other hand, neither the point IP9 nor IP21 has been experimentally determined so far, so it could also be that the 'real' composition is somewhere else than calculated.

For IP21, the differences between the two calculated sets of concentrations and the synthetic solution is rather small.

Tab. 8.2 Composition of IP9 solution [mol/kg]

Component	Analysis	Calculated (HMW)	Calculated (THEREDA)
Na	4.49	4.178	4.959
K	0.889	0.9185	0.9268
Mg	1.15	1.040	0.6356
Ca	<3e-6	0.005891	0.00422
Cl	6.83	6.391	6.364
SO_4	0.420	0.3985	0.4015
Equilibrium phases		Glauberite, halite, syngenite, polyhalite, syngenite, anhydrite	Glauberite, halite, polyhalite, pentasalt

Tab. 8.3 Composition of IP21 solution [mol/kg]

Component	Analysis	Calculated (HMW)	Calculated (THEREDA)
Na	0.461	0.479	0.508
K	0.524	0.567	0.592
Mg	4.21	4.211	4.185
Ca	0.00134	0.000636	0.000653
Cl	8.92	8.839	8.85
SO_4	0.287	0.315	0.311

8.4 Description of the experimental procedure

8.4.1 Overview

The general approach of the experiments was to start with a near neutral equilibrium solution to which a compound of an individual radionuclide was given. The pH was then adjusted to cover the desired pcH range (between 6 to 12, the difference between pH and pcH was calculate beforehand). This was done either by preparing a large batch (e.g., 200 ml) for which the pH was adjusted. A certain amount of the slurry (containing about 20-25 ml liquid and solids) was removed when the desired pH was achieved. A different strategy was to change the pH of individual small batches (25 ml). After individual batches were prepared, The pH was checked some days after the start of the experiment to make sure that it remained close to the desired value. After not less than four weeks later and then another four weeks the pH was checked again. If the pH remained stable between these measurements, a sample was taken. If a change was too large, the pH was adjusted again. However, slow precipitation/ solution processes sometimes lead to shifts over the period of months. In such cases no further adjustment was made because it would have prolonged the experiments beyond the limits of the project. If a pH was considered stable, a first sample was taken, a second sample was taken not earlier than one month later. The sample was analysed with ICP-OES for the main ions and by ICP-MS for trace ions. Chloride was determined only in the last sample by titrimetry. Apparent pH values were measured using a Ross electrode and later recalculated into pcH values using the method and the parameters described in /HAG 14/.

8.4.2 Detailed description

At first, starting solutions were prepared by diluting the equilibrium solutions (Tab. 8.1) to 95 % with water. This was done to prevent precipitation of main salts during the experiments. For the adjustment of pH values, acidic and alkaline solutions were prepared from the 100 % stock solutions by adding concentrated HCl or carbonate-free NaOH solutions (e.g., producing 0.1 HCl or NaOH). For experiments with IP9 and IP21 the IP9Reak and IP21Reak solutions were used as a basis for the preparation of alkaline solutions.

Solubility experiments were carried out either by

a) adjusting the pH of a larger volume (e.g., 200 ml) from which a sample (20 ml slurry containing liquid and solid) was taken once the desired pH was reached

b) adjusting the pH of a smaller batch (e.g., 25 ml)

For version a) about 200 ml of the solution were filled in a 250 ml screw-capped bottle, after which calcium minerals were added that are in equilibrium with the respective starting solution (Tab. 8.4). Then, the element to be investigated was added in the form of a mineral phase that is likely the solubility limiting phase in the specific solution and in the desired pH range. Typically 5 g the solid starting material were added to 200 ml of solution. Such solids were either obtained from commercial sources or prepared in advance (sources and methods are described in A.5). In some cases, a soluble compound (a chloride or oxychloride) was chosen instead, because the preparation of the starting solid was rather difficult ($Nb_2O_5 \cdot xH_2O$, $Pd(OH)_2$, $Sm(OH)_3$) or did not lead to a solid phase that was stable in the initial solution (Sn: abhurite). This would lead to the formation of a hydroxide or oxide when brought into contact with neutral solutions. The pH of the mixture was then adjusted to the first intended pH value by adding acidic or alkaline salt solutions (see above). About 20 ml of the constantly stirred slurry (liquid and solids) was removed from the slurry and transferred to a 20 ml screw-capped bottle. The next pH (in distances of about 0.5 pH units) was prepared with the large batch in the same way. In some cases, it was necessary to add concentrated HCl or NaOH to overcome the strong buffering behaviour of the mixture. This procedure was intended to cover a pcH range of approx. 6 to 12 but sometimes because of slow transformation processes either the lower or the higher end could not be reached or there occurred larger gaps within this range.

Experiments following variant b) started with about 20 ml of a salt solutions in a 25 ml screw capped bottle to which about 0.5 g of the solid mineral were added. The following steps were the same. In some cases the added amount of mineral was smaller because of the expensiveness of the substance (palladium and silver).

Some experiments were carried out in the glovebox to avoid oxidation or the formation of strong carbonate complexes by absorption of atmospheric CO_2. This was the case for Ag(I), Mo(IV), Pd(II), Se(-II), Se(IV), Sm and Sn(II). For experiments with Ag(I) all operations were done under red light to avoid photoreduction of AgCl.

The bottles were shaken overhead in a climatic chamber at 25 °C. Bottles in the glove box had to be shaken manually several times a week.

154

After several weeks, the pH value was checked and, if it deviated too much from the target value, it was corrected by adding acidic or basic solution. In some cases, if no permanent adjustment of the pH could be achieved even after several corrections, further corrections were not undertaken for reasons of practicability. For this reason, some experimental series did not completely cover the desired pH range.

Sampling and measurement of the pH value followed after one month at the earliest and then after another month. All samples were filtered through 0.2 µm syringe filters.

By analysis with ICP-MS, it was checked whether the fission product concentration was stable. If so, the other elements (in this case Na, Ca, and Cl) were also measured. If the concentrations differed too much and showed a consistent tendency over at least part of the pH range, another sample was taken not earlier than four weeks later and analysed again.

For some other elements, the concentrations were below the limit of determination of the measuring instrument (ICP-MS). As a more powerful triple quadrupole ICP-MS (Agilent 8900) became available at the end of the project, all samples for which the values were below the limit of quantification were measured again. In many cases, this allowed the solution concentrations to be quantified.

The measured apparent pH values were converted into hydrogen ion concentrations (pcH) using the method described in /HAG 14/. Often, the solid phases could not be identified by X-ray diffractometry, probably because they were amorphous, or the amount of the phase was too low. A chemical analysis was not undertaken, because of the ubiquitous presence of calcium minerals. More dedicated work will be necessary to identify the phases and prepare them in pure form.

The experimental results are described in chapter 8.6 to 8.10. Detailed analytical results may be found in annex A.6. Tab. 8.5 contains an overview of all experiments. The results are listed in A.6.

Tab. 8.4 Minerals added to each solubility experiment (beside radionuclide compound)

Solution type	Added minerals
Hal/ Anh	anhydrite
IP9	anhydrite syngenite polyhalite glauberite
IP9Reak	brucite syngenite glauberite
IP21	polyhalite glauberite syngenite
IP21 Reak	brucite syngenite glauberite
UK	gypsum calcite

Tab. 8.5 Overview of the solubility tests performed (X: under air; G glovebox: N_2 atmosphere, O_2 and CO_2 free)

Element	Hal/ Anh	IP9/ IP9Reak	IP21/ IP21 Reak	UK	UK Po	UK So
Ag/ I	G	G	G	G		
Mo(IV)	G					
Mo(VI)	X	X	X	X	X	X
Nb	X		X	X		
Ni	X	X	X	X	X	X
Pb	X	X	X	X	X	X
Pd(II)	G		G	G		
Se(-II)	G					
Se(IV)	G		G	G		
Sm	G		G	X		
Sn(II)	G		G	G		
Sn(IV)	X	X	X	X	X	X
Sr	X	X	X	X		
Zr	G		G	X		

8.5 Method for the derivation of solubility limits

A solubility limit is understood as the maximum concentration a radionuclide can reach in dissolved form in aqueous solution under defined boundary conditions (temperature, pressure, redox level, pcH, solution composition). The conditions, especially the solution composition and the pcH depend on local characteristics of a site. As long as the site has not been selected, neither the properties of the host rock nor the disposal concept are determined. Many variables remain that prevent the development of a single set of solubility limits. To allow the use of up-to date solubility limits in generic performance assessment studies und varying conditions, several sets were developed that cover three ranges of pcH (6-8, 8-10, 10-12(12.5)) and four solution compositions. Higher pcH values can only occur in direct contact with ordinary Portland cement (OPC). Based on the current repository concept this could only occur in clay stone where OPC may be used for shotcrete to stabilize drifts or as closure of boreholes, but not in direct contact

with HLW waste containers[16]. OPC is expected to alter clay in host rock or backfill, but only within a narrow zone of few cm /SAV 18/. Tests in this study with mixtures of model clay water, brucite and Portland cement produced pcH values at 12.5 and lower. Therefore, it is reasonable to limit the maximum pcH in this study to 12.5 for clay pore water and 12 in HalAnh, IP9 and IP21 solutions.

In this study, solubility limits were derived mainly on the basis of experimental results but supported by calculated solubilities, if needed. They are given in form of ranges. The minimum value corresponds to the minimal concentration of the specific fission product in solution in the given pcH range minus 0.5 log units as an uncertainty margin. The maximum value is calculated from the highest found concentration plus 0.5 log units. If in a certain pcH range the maximum concentration of a fission product could be above 0.1 mol/kg the solubility is considered unlimited. In that case the upper concentration limit is given as 0 (log units) even if the highest concentration achievable is higher.

The solubilities found and predicted for the halite/ anhydrite saturated system are compared to the solubility limits given in Buhmann et al. /BUH 91/. This source provides ranges of solubility limits for three pH regions "acidic, neutral, alkaline" in saline solutions. The pH regions where not further defined nor was it clear which pH scale was used. Moreover, the nature of the saline solutions was nowhere defined. At one point of the publication, the density of the solution was given as 1.2 kg/l which would indicate a saturated NaCl solution. It could also be that the solubility limits were defined for saline solutions in general. For the purpose of comparison, the pH ranges in /BUH 91/ are assumed to represent

- Acidid: pcH <6
- Neutral: pcH 6-8
- Alkaline: pcH >8

Solubility limits are marked with an asterisk (*) if the experimental pcH range did not cover the full range, but modelling allowed an extrapolation. If the modelling did not allow an extrapolation because the results deviated too much from the observed values,

---

[16] In currently developed disposal concepts for Germany, heat generating radioactive waste (spent fuel and vitrified waste from reprocessing) is not planned to be disposed in cemented form. However, cementation has been performed for other waste types (low and medium level waste) which are not considered here.

experimental results, if applicable, were used to determine the solubilities at the limits of the respective pcH range. Such values are indicated with two asterisks (**).

8.6   Solubility of fission products in halite/ anhydrite saturated brines

8.6.1   Solubility of lead in halite/ anhydrite-saturated solution

Laurionite, PbClOH was used as the initial lead-containing solid[17]. It was also found by XRD at the end of the experiments. The solubility of lead decreased linearly from log c - 3.1 to 4.3 in the pcH range 9.4 to 10.7. The results at lower and higher pcH (7.4 and 12.4) deviate slightly from this trend (Fig. 8.1).

In accordance with the analytical findings, laurionite was the solubility limiting phase in the models at most pcH values. Only above pcH 12, the formation on blixite. $3PbO.PbCl_2.H_2O$ was predicted. A possible analogue of blixite was found to have slightly less water than shown in this formula: $3PbO \cdot PbCl_2 \cdot \frac{1}{2}H_2O$ or $Pb_8O_5(OH)_2Cl_4$ /KRI 06/. Using the latter composition would not change the predicted solubilities significantly.

Experimental and calculated values agreed well over the pcH range, but the observed concentrations were slightly lower in the pcH range 9 to 11. It is probable that under these conditions mixed chloro/ hydroxo complexes occur. The existence of such species has been shown by Lébl /LÉB 66/ and Becht /BEC 94/, but so far no reliable thermody-namic data is available that would allow an implementation in our model.

At pcH 7.4, the predicted solubility was about 1.5 concentration units higher. Unfortu-nately, there is a gap in the experimental values between pcH 7.4 and 9.2 after 239 days, so that it cannot be evaluated whether this discrepancy is a single experimental outlier or a systematic deviation. The slope of the other measurements as well as another point after 37 days at pcH 11.4 indicates that there is a continuous trend in this pcH region. For the time being, we assume that the modelled solubility is more accurate in this pcH region.

---

[17] Laurionite was prepared according to the method described in A.5.1
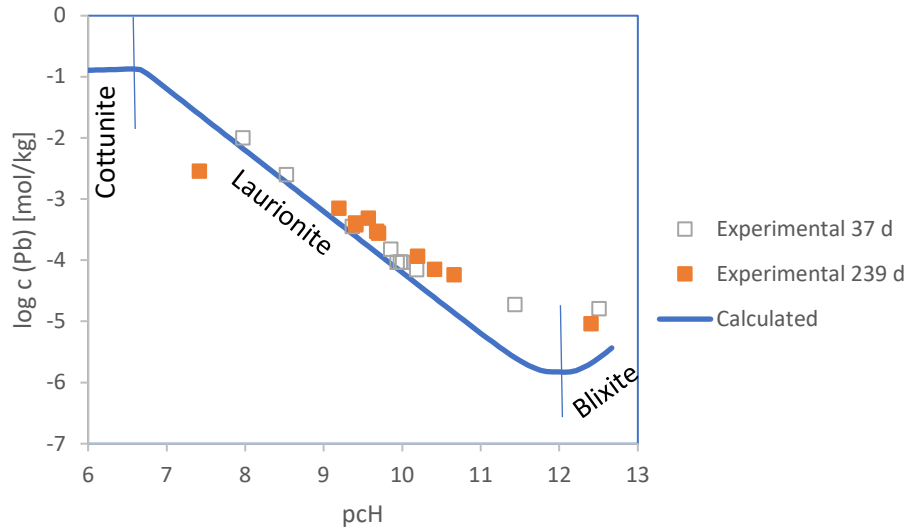
Fig. 8.1 Solubility of lead in halite/ anhydrite-saturated solution

The following solubility limits are proposed:

pcH 6-8: -3.5 to -0.5

pcH 8-10: -4.5 to -2.0

pcH 10-12: -5.5 to -3.0

Some further work is needed to support the assumptions made in this study:

- Extend the solubility measurements to the pcH range below 9.2 and for the range 10.8 to 12.3
- Verify the identity of the solubility limiting phase above 10.7
- Redetermine the solubility constant of blixite and other lead hydroxy chlorides (very few experimental data exist)
- Identify the nature of mixed complexes in alkaline solutions of chloride salts

8.6.2 Solubility of molybdenum (IV) in halite/ anhydrite-saturated solution

Molybdenum dioxide (MoO_2) and anhydrite were mixed with halite/ anhydrite-saturated solution in screw capped flasks. To reduce trace amounts of oxidized Mo species and to maintain strongly reducing conditions iron powder was added to the system as well. It

remained in the flasks for 99 days until it was removed magnetically (except in one batch to serve as a reference point). Only then the pH was adjusted to the desired values. At the end of the experiments, the solids in all batches uniformly showed the colour of the starting material (Fig. 8.2).

Fig. 8.2   Experimental batches of molybdenum(IV) in halite/ anhydrite-saturated solution

The resulting Mo concentrations were constant in the pcH range 7.5 to 11 (log c = -5.1± 0.1). Only at pcH 6.1 the solubility was a little bit lower (log c = -6.0). The batch with added metallic iron had a pcH of 10.5 and didn't differ significantly from other experiments.

if only Mo(IV) species are allowed in the modelling, and amorphous MoO_2(am) is considered the solubility limiting phase, the predicted Mo concentration would be in the order of log c = -6.7 throughout all pH values (Fig. 8.3). Allowing crystalline MoO_2(cr),the total Mo concentrations would be in the order of log c = -9.4 (not shown).

If the other oxidations states are included (III and VI), aqueous Mo(IV) species may react with water to form Mo(VI). The resulting total Mo concentrations depend on the hydrogen pressure. Two boundary conditions were tested $p_{H2}=10^{-10}$ and $p_{H2}=100$ bar. At the lower pressure, oxidation to Mo(VI) starts early (pcH <5). If MoO_2(cr) is suppressed, the solubility of $CaMoO_4$ is reached (log $c_{Mo} \approx -5.3$) at pcH 6. This calculation very well corresponds with the experimental results, where the hydrogen pressure was not controlled and was probably very low. If MoO_2(cr) is allowed, saturation of $CaMoO_4$ is achieved only at pcH 7.5. Maintaining a H_2 pressure of 100 bar supresses the formation of Mo(VI). Instead, M(III) species dominate at pcH >8 leading to a continuous solubility increase up to pcH 12. The solubility limiting phase, however, would still be MoO_2(am), if MoO_2(cr) is supressed.

Based on these findings, it is very likely that the solubility of Mo was controlled by Ca-MoO$_4$ in most of the experiments. It may have been formed during the experiment by oxidation of MoO$_2$(s) to more soluble MoO$_4^{2-}$ or it was still present after the addition of iron. The experiment with added metallic iron showed the same concentration level. But the pcH of this experiment is exactly at the point where the calculated solubilities of MoO$_2$(am) and CaMoO$_4$ cross. So, it cannot be decided whether the presence of iron still had an impact.

Many of the thermodynamic data used for modelling this system are based on assumptions so that the results delivered by our calculation should be considered with care. The confidence interval is unknown but may well be in the order of 2 log units or more. More experimental data are needed to verify at least some key assumptions such as the existence and stability of MoO$_2$(am), Mo(OH)$_3$(am), Mo(OH)$_6^{2-}$ and Mo(OH)$_4^-$.

The experimental results alone are not sufficient to derive reliable solubility limits because the hydrogen pressure was not controlled. However, they provide an upper limit, as more oxidizing conditions would have led to the same dominating Mo(VI) species. It cannot be excluded that under strongly reducing conditions a reduction to Mo(III) takes place. In that case, the species Mo(OH)$_4^-$ may become dominant and lead to increased total molybdenum concentrations. The upper solubility limit was based on the modelling results, but a confidence interval of 2 log units was added because of numerous uncertainties in the model. The lower solubility limit is assumed to be within two orders of magnitude of the calculated solubility of MoO$_2$(am).

pcH 6-8: -8.7 to -4.5

pcH 8-10: -8.7 to -3.5

pcH 10-12: -8.7 to -1.7 (max. exp. pcH 11)

Several knowledge gaps were identified:

- Experimental solubility at defined H$_2$ pressure and at pcH >11
- Identity of the solubility limiting phase
- Dominating aqueous species in equilibrium with MoO$_2$
- Solubility of hydrous molybdenum oxide MoO$_2$.xH$_2$O and amorphous MoS$_2$ (jordisite).

- Solubility of Mo(OH)$_3$(am) and stability of Mo(OH)$_4^-$

- Reduction/ oxidation processes of Mo(IV) under saline conditions
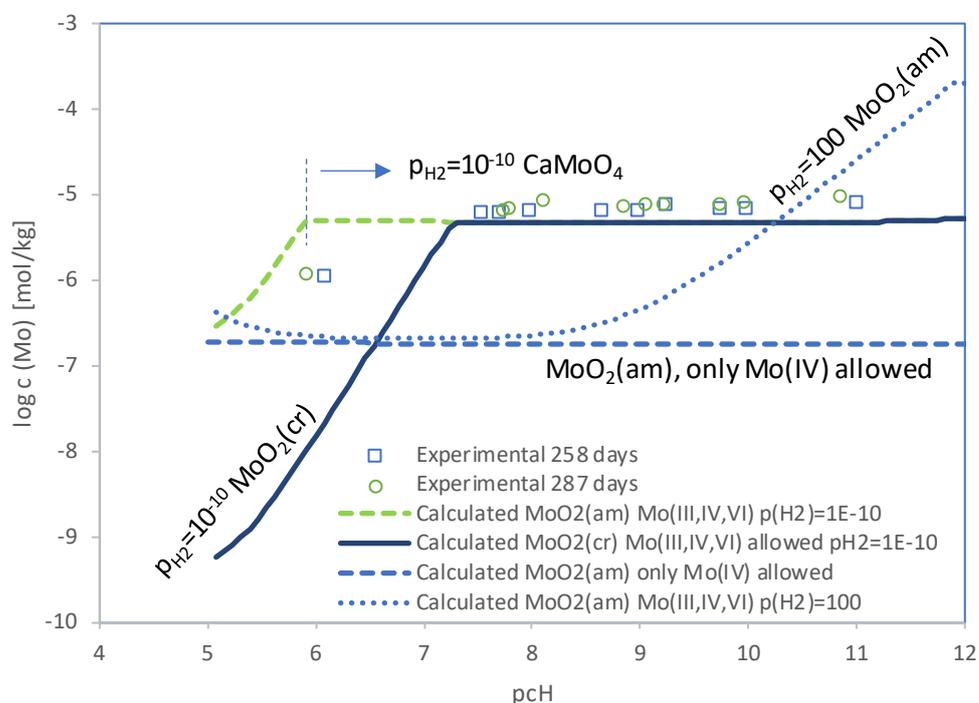
Fig. 8.3 Solubility of Mo(IV) in halite/ anhydrite-saturated solution

8.6.3 Solubility of molybdenum (VI) in halite/ anhydrite-saturated solution

The starting material in these experiments was calcium molybdate, CaMoO$_4$ (powellite). It could also be found as the final solid phase by XRD. After the first sampling (43 d), the molybdenum concentrations were at log c = -4.98 ± 0.03 at all pcH values (5.3 to 11.2). After 224 days, the concentration of molybdenum was still constant but slightly lower (log c = -5.2 ± 0.2) except for one batch with a lower value (log c = -5.6). (Fig. 8.4).

The calculated solubility of CaMoO$_4$ is constant over the entire pcH range (log c = -5.36). The results are very close to the measured values after 43 days (log c = -4.98) and after 273 days (log c = -5.2). In contrast to that, the data set of Grambow et al. /GRA 92/ produced powellite solubilities about an order of magnitude lower (Fig. 8.4).

This allows us to define the solubility limit for Mo(VI) at log c = -5.9 to -4.5 at a pcH range of 6 to 11.

The former solubility limit of /BUH 91/ did not specify the oxidation state of molybdenum. If Mo(VI) were the dominating state, the upper solubility limit could be reduced by 3.5 orders of magnitude.
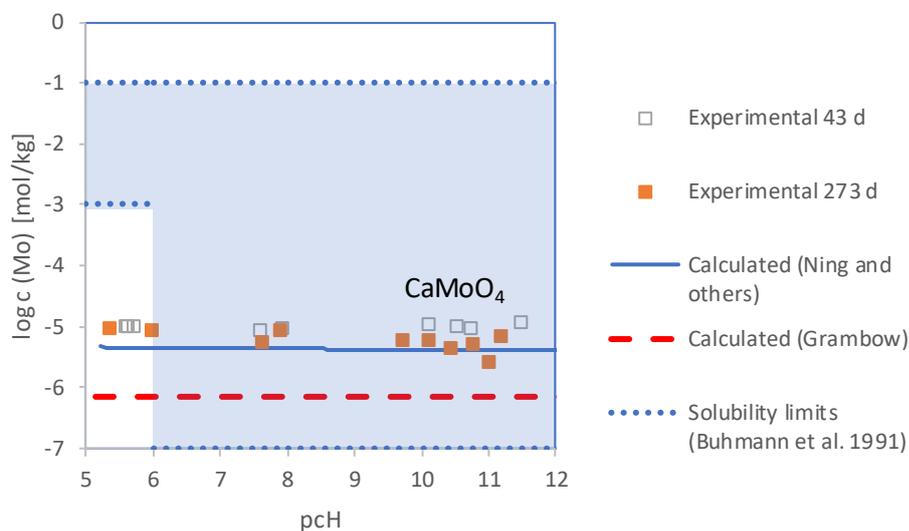
Fig. 8.4   Solubility of molybdenum(VI) in halite/ anhydrite-saturated solution

8.6.4   Solubility of nickel in halite/ anhydrite-saturated solution

Nickel hydroxide, $Ni(OH)_2$, was used as the starting material. It also appeared as a solid phase after completion of the experiments. In accordance with results by González-Siso et al. /GON 18/ no trace of chloride compounds such as $Ni(OH)_3Cl$ (Ni-Hibbingite) was found. The solubility of nickel is strongly pH dependent. While it is about 10^{-3} mol/kg at pcH 8.35, it drops to about 10^{-6} mol/kg at pcH 10. It remains at this level until pcH 10.5, the highest pcH value reached (Fig. 8.5).

The calculated solubility for Ni in Hal/ Anh solution fits very well with the experimental data. The solubility limit could be set as follows:

pcH 6-8: -2.9* to 0* (no exp.)

pcH 8-10: -6.6 to -2.0:

pcH 10-12: -6.7* to -5.5* (max. exp. pcH 10.4)

The solubility limiting phase is Ni(OH)$_2$ at all pcH. Further work could improve the modelling by:

- Extending the measurements to pcH> 10.4
- Further analyse the impact of NaCl concentrations on the solubility of Ni(OH)$_2$
- Check the long-term stability of the Ni(OH)$_2$ phase (very different solubilities are reported in the literature for solids prepared by different methods)
- Check the stability of Ni$_2$(OH)Cl$_3$, the analogue to hibbingite, (Fe,Mg)$_2$(OH)$_3$Cl and the fate of nickel if Fe(II) corrosion phases such as Fe-hibbingite or chukanovite are present in the near field (e.g., by formation of solid solutions).
- Evaluate the impact of trace carbonate on the Ni(OH)$_2$ solubility (in our experiments CO$_2$ was not rigorously excluded and its potential impact could not be quantified)
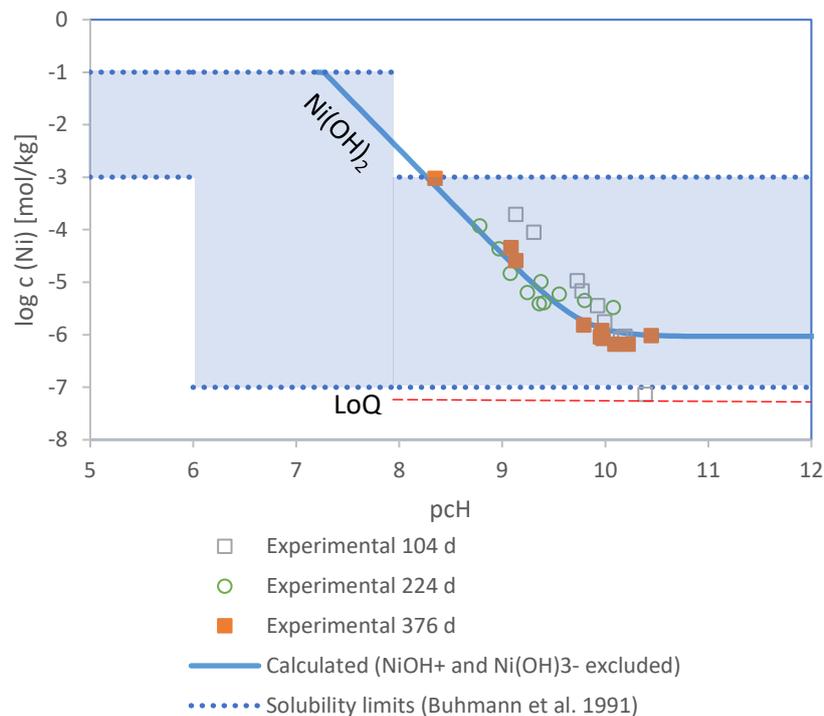
Fig. 8.5 Solubility of nickel in halite/ anhydrite-saturated solution

8.6.5   Solubility of niobium in halite/ anhydrite-saturated solution

Amorphous niobium oxide hydrate[18] was used as the initial lead-containing solid. Neither the starting material nor any of the solid phases at the end of the experiments gave an identifiable signal in XRD measurements. All niobium concentrations were in the corridor of -6.5 to 7.5 (log c). Between pcH 8.7 and 10.3 the values increase from -7.7 to 6.5. At higher pcH the solubilities decrease again to -7.2 (Fig. 8.6).

The formation of a calcium niobate is supported by the significantly lower calcium to sulphate ratios in our solutions. Normally, the value is very close to 1 due to the dissolution of anhydrite. In solutions containing niobium, the ratio scattered around 0.6 to 0.8.

Although the formula of Talerico et al. /TAL 04/ does not account for ionic strength in general nor considers specific interactions between medium ions and niobium, the calculated niobium concentrations are roughly in the order of the experimental values. The maximum deviation occurs at low pcH and amounts to 1.7 log units.

Based on the experimental findings the solubility limits have the following borders:

pcH 6-8: -8.2 to -7 (minimum exp. pcH 7.7)

pcH 8-10: -8.2 to -6

pcH 10-12: -7.7** to -6** (max. exp. pcH 11.5)

At least in the experimental range (pcH 7.7 to 11.5) the previous solubility limit may be reduced by five orders of magnitude.

Further work is needed to

- understand the nature of the niobium containing solids in concentrated NaCl brines with Ca present or absent.
- Further validate the empirical model of Talerico et al (2004) at high ionic strength

---

[18] This solid was prepared according to the method described in A.5.4

- Investigate the composition and stability of the principal niobium species between pcH 6 and 12

- Develop a model that describes the activity coefficients of the main niobium species
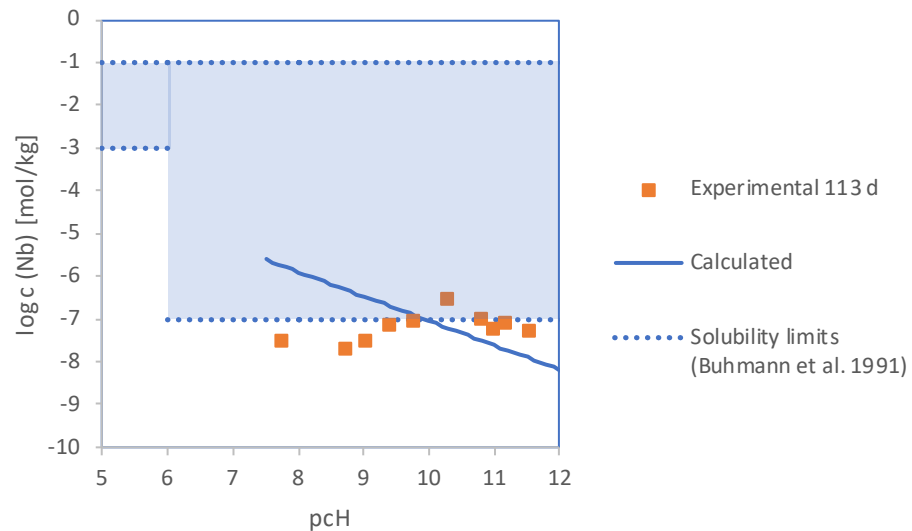
Fig. 8.6   Solubility of niobium in halite/ anhydrite-saturated solution

8.6.6   Solubility of palladium(II) in halite/ anhydrite-saturated solution

Soluble palladium chloride was added to the initial halite saturated solution. Due to the expensiveness of the material, only a small amount could be used (0.2 g per 20 ml batch). Consequently, the amount of the solids at the end of the experiments was too small for an XRD analysis.

Fig. 8.7   Experimental batches of palladium(II) in halite/ anhydrite-saturated solution

At the lowest pcH values (6.8 to 8.44) the palladium concentrations were constant at about 0.013 mol/kg (see batches 2, 3, and 4 in Fig. 8.7 with no or almost no solids at the bottom of the glasses but reddish-brown solutions). These values correspond to the initial

concentration at the beginning of the experiments. At pcH values higher than 8.44 the solubility decreased linearly up to at least pcH 9. At the same time the colour of the experimental batches turned into dark brown.

No data was obtained up to pcH 10.9. Between pcH 10.9 and 11.9 the Pd concentrations rose again, but slowly from log c = -5.9 to -5.6 (Fig. 8.8). Starting with pcH 8 the calcium to sulphate ratio decreased to 0.8 and lower. This indicates that calcium was probably partly bound in a palladium containing solid, such as $CaPd(OH)_4$ or mixed sodium calcium hydroxide palladates (II). So far, only structural but no thermodynamic data are available for such compounds /ZAI 91/, /BUG 13/.

According to Rai et al. /RAI 12/ and Boily et al. /BOI 07/, the solubility limiting solid in alkaline NaCl solutions is either $Pd(OH)_2$ or $Pd(OH)_{1.72}Cl_{0.28}$. The latter is probably only a metastable phase. However, earlier experiments reached only to 0.6 m NaCl and 1 m KCl, so that it cannot be excluded that the solid in our experiments had a different composition.
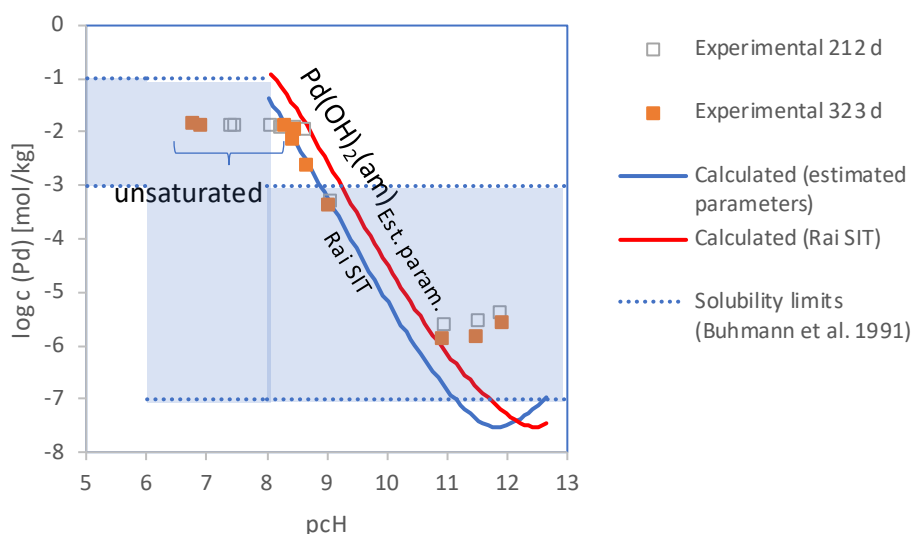
Fig. 8.8   Solubility of palladium(II) in halite/ anhydrite-saturated solution

Despite the rather rough assumptions regarding the activity coefficients of Pd species, the experimental solubilities could be well described up to about pcH 11 either if estimated parameters (Humphrey et al.) or recalculated SIT parameters were used. However, the increase of solubilities above pcH 11 was not observed in the modelling and indicates the formation of a complex more stable than the assumed hydroxo complexes $Pd(OH)Cl_3^{2-}$ and $Pd(OH)_3^-$. Further work will be necessary to:

- close the experimental gap in halite/ anhydrite solutions that occurred between pcH 9 and 11

- investigate the solubility and speciation of Pd at high chloride solutions at high pcH

- establish an activity model for the main Pd species in concentrated NaCl solutions: $PdCl_4^{2-}$ and $Pd(OH)_3^-$ It is assumed that the activity coefficients of mixed hydroxide chloride complexes lie somewhere in between the pure hydroxide and chloride complexes

The following solubility limits are proposed:

pcH 6-8: 0 (unlimited)

pcH 8-10: -6.4** to 0*

pcH 10-12: -6.4 to -5.0** (max. exp. pcH 11.9)

The upper solubility limit of palladium in acidic, neutral, and mildly alkaline solutions is higher than previously assumed /BUH 91/.

8.6.7   Solubility of samarium in halite/ anhydrite-saturated solution

This experiment was started with $Sm(OH)_3$ as the initial phase. Due to slow drifting, it was not possible to achieve solubility data for the whole intended pcH range. After 333 and 225 days, the observed Sm solubilities did not show a clear pcH dependence. With ± 0.7 log units, the scattering is quite large. At pcH 9 the concentrations started at $10^{-6.4}$ mol/kg and then tend to increase slightly (Fig. 8.9). In the solid residues sometimes $Sm(OH)_3$, and sometimes no Sm-solid phase was found. Apparently, the phase is either amorphous or present in too small amounts. It was found that the solubilities at higher pcH increased with time. The reason for this unusual behaviour could not be identified. Neither ternary Ca-Sm-OH complexes nor Sm carbonato complexes (tested with at 0.01 mol/kg CO_3^{2-}) are expected to contribute significantly to the overall speciation.

The calculation predicts the formation of $Sm(OH)_2Cl$ between pcH 7 and 8.5. At higher pcH $Sm(OH)_3$(am) or $Sm(OH)_3$(cr) are the solubility limiting phases. A solubility minimum is observed around pcH 12.5 followed by an increase of samarium concentrations

caused by the formation of ternary calcium samarium hydroxo complexes (not shown). The calculated solubilities are lower than those observed in our experiments after 225 and 333 days. The scattering of our results may be an indication of insufficient filtering (Fig. 8.9).

The following solubility limits may be derived from the results:

pcH 6-8: unlimited

pcH 8-10: -8.1 to -2.9* (min. pcH 9.0)

pcH 10-12: -9.3 to -5.2 (min. pcH 9.0)

The results show that:

- Another experiment is needed to understand the contradictory samarium concentrations after 225 and 333 days and to check whether the deviation between observed and calculated solubilities can be reduced by ultrafiltration or ultracentrifugation.
- Additional experiments are needed to cover the pcH range below pcH 9
- The nature of the solubility limiting solids needs a closer look
- The stability of ternary calcium samarium hydroxide complexes needs to be determined (or confirmation that data for analogous neodymium complexes are valid)
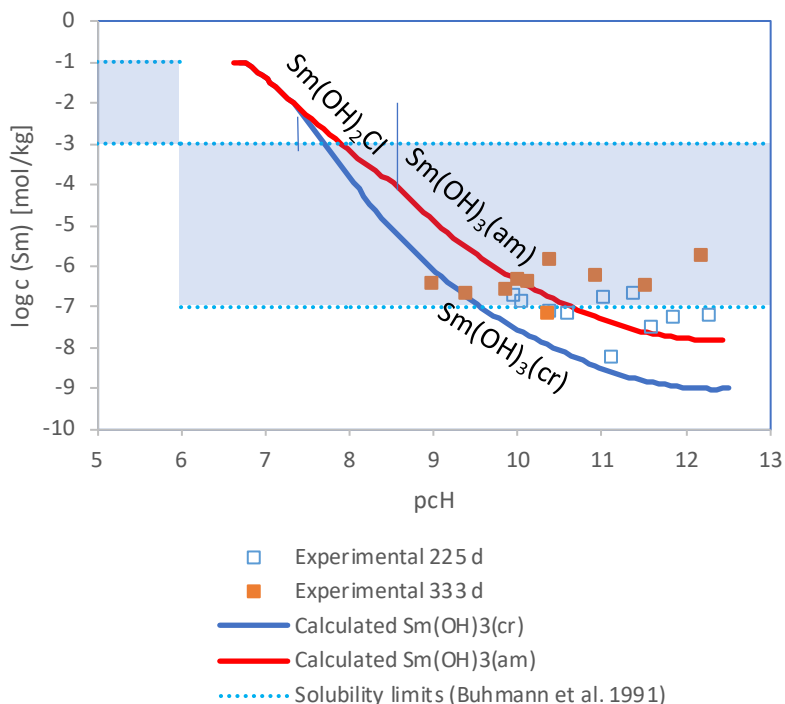
Fig. 8.9   Solubility of samarium in halite/ anhydrite-saturated solution

8.6.8   Solubility of selenium(-II) in halite/ anhydrite-saturated solution

Iron selenide (FeSe) and anhydrite were mixed with halite/ anhydrite-saturated solution in screw capped flasks. To reduce trace amounts of oxidized Se species and to maintain strongly reducing conditions iron powder was added to the system as well. It remained in the flasks for 99 days until it was removed magnetically. Only then the pH was adjusted to the desired values.

After 258 and 287 days the aqueous solutions were sampled. No significant difference between the concentrations was found. Batches 2 to 10 contained a dark brown solid that was indistinguishable from the added "FeSe". In batch 1 that had the lowest pcH at 5.7, a grey precipitate was present. This could be a hint to the formation to other iron(II) selenides such as the polymorphs ferroselite and dzharkenite that may have a steel grey color.

Fig. 8.10   Experimental batches of FeSe in halite/ anhydrite-saturated solution

Starting from pcH 5.7 the concentration of Se decreased from log c -4.8 to -7.0 at pcH 7.5. At higher pcH values, the Se concentration increased to -4.6 at pcH 9.6 where it remained constant up to the highest experimental pcH (10.6). The iron concentrations on the other hand were significantly higher and reached log -2.3 at pcH 5.7, increased to -log 1.8 at pcH 6.9 and the fell to log c -5.0 at pcH 9.6, not far away from the Se value. The identity of the final solid phase was not determined.

Thermodynamic modelling was performed under the assumption of strongly reducing conditions. These were maintained by fixing the hydrogen pressure at 1 bar. If all iron(II) selenides in the database are allowed to form, the calculated solubility line above pcH 6.5 follows closely the experimental values, but at a level approximately 0.2 to 1 log units lower. The key features of the observed results are represented well: a minimum around pcH 7, rising concentrations up to pcH 10 followed by a plateau. According to this calculation, three solid phases are formed subsequently: $FeSe_2$, Fe_3S_4 and finally $Fe_{1.04}Se$. The solubility at pcH at 5.8 is not represented well by the model. The predicted iron concentrations in solutions are about 1.5 to 2.8 log units lower than observed in the experiments, especially in the region above pcH 9. But below pcH 9 the calculation explains well the gap between iron and selenium concentrations that is caused by a disproportionation of $FeSe_{1.04}$ into aqueous Fe^{2+} and selenium rich Fe_3Se4 or $FeSe_2$.

If all Iron(II) selenides except $Fe_{1.04}Se$ are suppressed the depression in Se concentrations around pcH7 is not found. On the other hand, if it is assumed that in the initial phase of the experiment the addition of metallic iron led to the formation of significant amounts of Fe-hibbingite, $Fe_2(OH)_3Cl$, the iron concentrations would be much higher so that the concentrations of selenide would be lower.

Although the initial thermodynamic modelling performed well, it must be noted that the course of the reaction is quite sensible to changes of the initial conditions such as the hydrogen pressure or added metallic iron at the beginning of the reaction. They

determine the pcH range where $FeSe_{1.04}$ and $Fe_{3}Se_{4}$ are in equilibrium. More experiments under stricter defined conditions are needed to allow a better comparison of observed and calculated solubilities.

The following solubility limits were derived. They reflect the uncertainty regarding the transformation of the carious iron selenides. The upper limit represents the calculated solubility of unaltered $FeSe_{1.04}$ while the lower limit was estimated based on the observed solubilities.

pcH 6-8: -7.5 to -4.2

pcH 8-10: -7.0 to -4.1

pcH 10-12: -5.3 to -4.1 (max. pcH 10.6)

These limits apply only for the specific conditions chosen for the solubility experiments in this study. As discussed above, they may not be valid for other circumstances, e.g., if Fe-hibbingite is present. But we assume that they represent a maximum.

Because of this, these solubility limits are not considered to be generally applicable for NaCl media.

The results show that:

- The solubility limiting phases need to be identified
- Ion interaction coefficients for HSe- should be determined experimentally to confirm the estimated values
- The impact of Fe-hibbingite on the solubility of selenide needs to be investigated separately
- More experiments are needed under better defined redox conditions
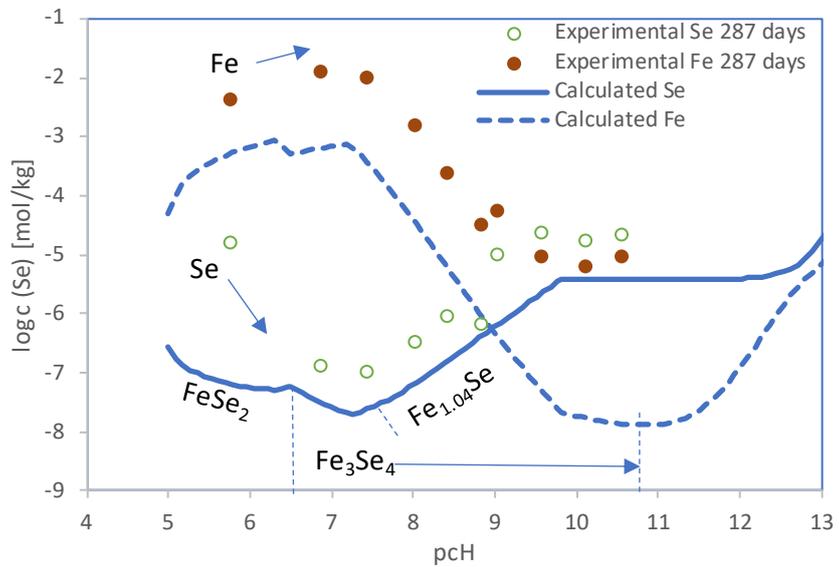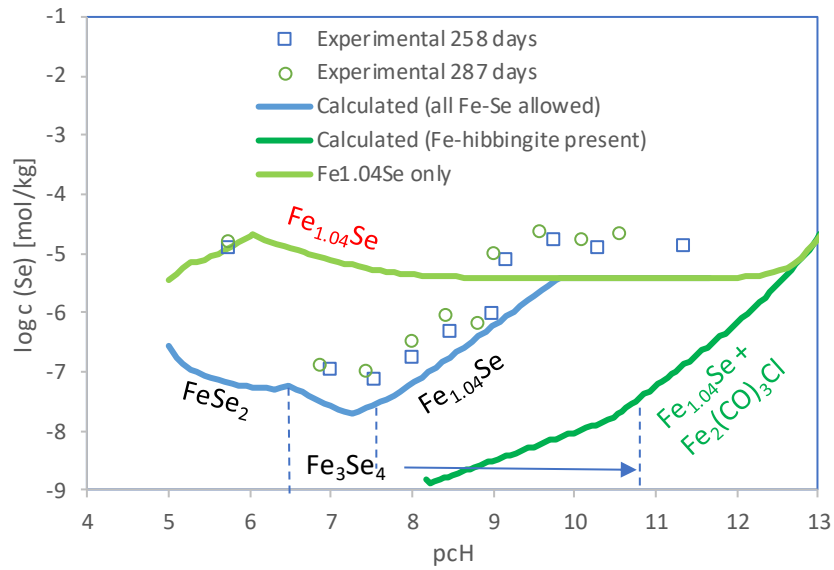
Fig. 8.11   Solubility of FeSe in halite/ anhydrite-saturated solution

8.6.9   Solubility of selenium(IV) in halite/ anhydrite-saturated solution

In this series of experiments, calcium selenite was used as the selenium source. The same compound was found at the end of the experiments. The observed concentration of selenium decreased from $c = 10^{-3.2}$ mol/kg at pcH 7.8 to $c = 10^{-3.8}$ mol/kg at pcH 9.4. At higher pcH values the solubility remained constant.

The results of the modelling show a very good agreement between calculated and ex-perimental solubilities. This also applies to the pcH range below pcH 8.5. The assump-tions regarding the interactions of $HSeO_3^-$ seems to be appropriate.
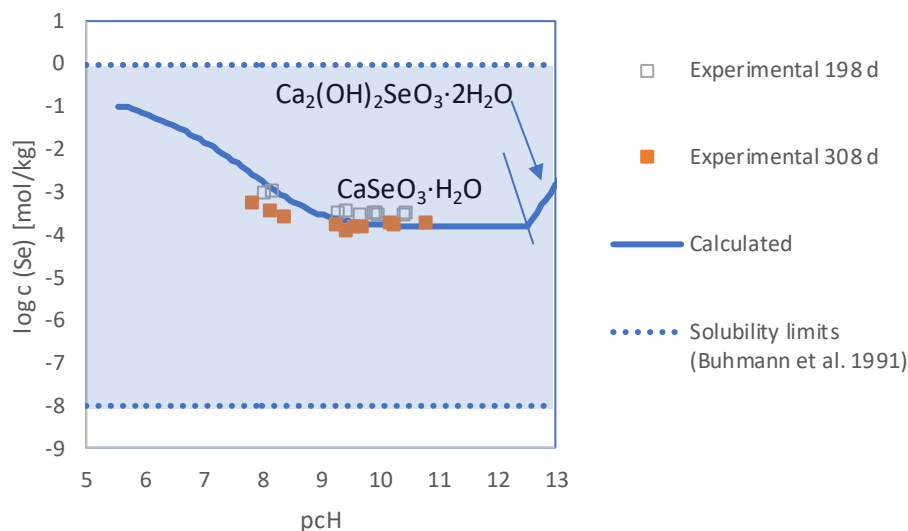
Fig. 8.12   Solubility of selenium(IV) in halite/ anhydrite-saturated solution

The solubility limits in /BUH 91/ only to refer to selenium as an element. This could also include Se(VI), Se(0), and Se(-II). If selenite is considered the dominating selenium oxi-dation state, the following solubility limits are proposed:

pcH 6-8: -3.9 to -2.7 (min exp. pcH 7.8)

pcH 8-10: -4.3 to -2.7

pcH 10-12: -4.3* to -2.7* (max. exp. pcH 10.8)

Some additional experiments are needed to cover solutions with pcH >10.8. Ion interac-tion coefficients for $HSeO_3^-$ or a closer analogue should be determined experimentally as well.

8.6.10   Solubility of silver in halite/ anhydrite-saturated solution

The experiments were conducted by adding silver iodide (AgI) to HalAnh solution and adjusting the pH value. Due to the expensiveness of AgI, only three batches were

prepared that ranged from about pcH 8 to pcH 11. After 358 days equilibrium time the observed concentrations were in a narrow range at around $10^{-3.91\pm0.02}$. The results fit well with the findings of Coetzee et al. /COE 84/ who measured the solubility of AgI in saturated NaCl solution (1.6-1.7$\cdot10^{-4}$ mol/l). Due to a lack of reliable thermodynamic data, no geochemical modelling could be undertaken.

From these data, the following solubility limits are derived:

pcH 6-8: -4.4** to -3.4** (min exp. pcH 7.95)

pcH 8-10: -4.4 to -3.4

pcH 10-12: -4.4** to -3.4** (max. exp. pcH 10.8)

If the concentration of iodide is not sufficient to completely bind silver in AgI, the higher solubility of AgCl needs to be considered. Extrapolating tabulated solubility data for NaCl solutions at 25 °C /FRI 85/ to the concentration of a saturated solution (5.4 mol/l) and converting the calculated AgCl solubility from molality to molarity (using a density of 1.20 kg/l) results in a maximum concentration of AgCl of 0.01 mol/kg. The solubility limit would be:

pcH 6-12: -2.5** to -1.5**

There is a need to further investigate the complex equilibria of silver in concentrated chloride solution and to derive a thermodynamic model to describe them.
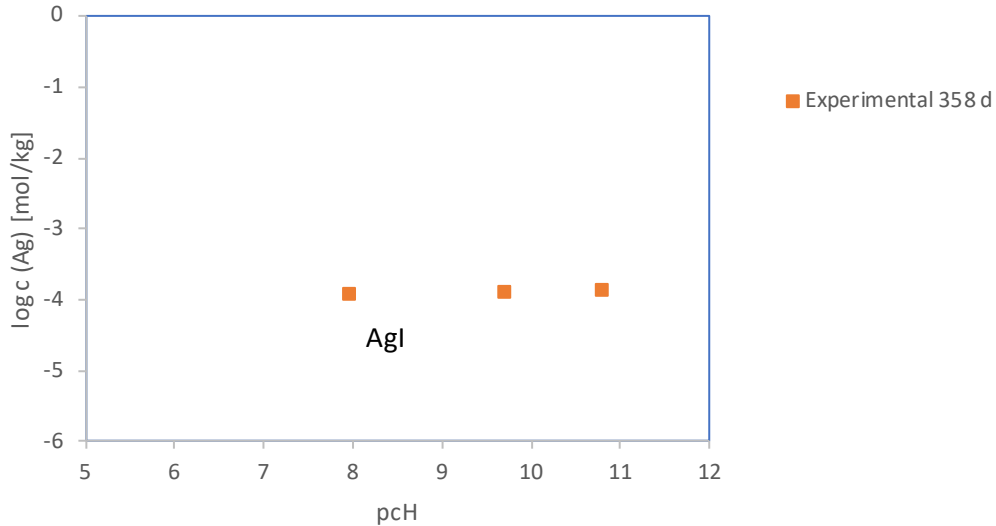
Fig. 8.13   Solubility of silver iodide in halite/ anhydrite-saturated solution

8.6.11   Solubility of strontium in halite/ anhydrite-saturated solution

The starting material in these experiments was strontium sulphate, $SrSO_4$ (celestine). It could also be found as the final solid phase by XRD. The concentration of strontium was constant at all pcH values (7.4 to 12.9) after 42 and 272 days. It amounted to log c = -3.40 ± 0.05 (Fig. 8.14).

In the thermodynamic modelling, also a constant solubility was found, however at levels about 0.5 log units higher. At pcH > 12.5 the calculated solubility decreased because Ca was removed from the solution due to the precipitation of portlandite. The sulphate concentration increased.

It is not clear why the observed solubility is lower than in the modelling. A possible cause would be the formation of a more stable solid solution with anhydrite (Ca, Sr)SO_4 with up to 15 % Ca or 35 % Sr /BUS 88/.

Based on the findings the following solubility limit of strontium is proposed:

pcH 6-12: -3.9 to -2.8 (min exp. pcH 7.4)
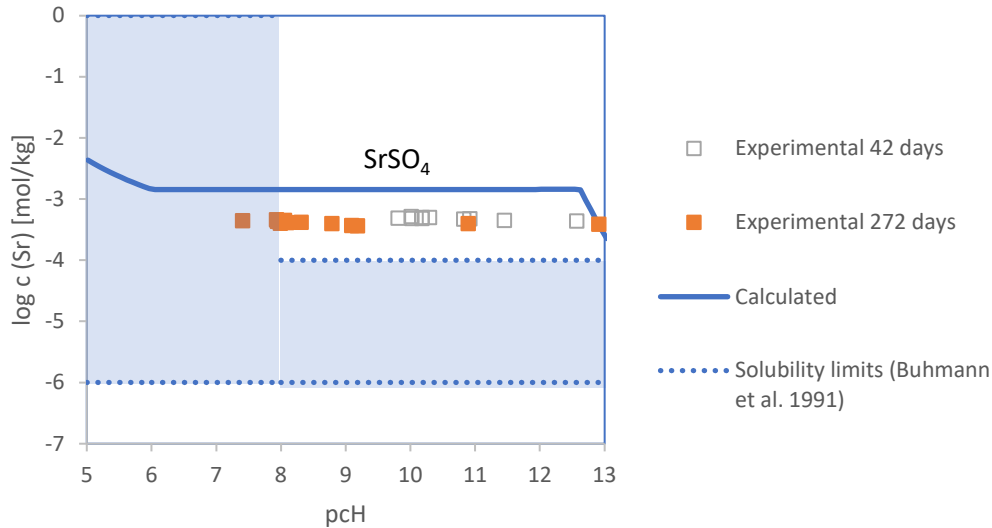
Fig. 8.14   Solubility of strontium in halite/ anhydrite-saturated solution

8.6.12   Solubility of tin(II) in halite/ anhydrite-saturated solution

The experiment was started with abhurite, specifically prepared for this study (see A.5.8). However, addition of alkali resulted in complete transformation of the white abhurite into a dark brown to black precipitate (Fig. 8.15). The same process was also observed if a water/ abhurite mixture or pure but wet abhurite was left standing for some months. The process shows that abhurite is not stable under mildly acidic conditions. Slow H^+ consuming processes prevented pcH levels of lower than 7.

Fig. 8.15   Experimental batches of tin(II) in halite/ anhydrite-saturated solution

Between pcH 7.4 and 8.0 the solubility of Sn(II) decreased from -4.8 to -6.0 (log units). The following experiments from pcH 8 and higher showed an increase again. At the highest pcH value (11.5) the solubility reached -3.7. The equilibrium solid was not determined, but the brown colour in the bottles indicated the presence of tin(II) oxide probably in mixture with other Sn(II) or Sn(IV) compounds. If all tin were converted to tin(IV) white

178

precipitates would be expected such as $SnO_2 \cdot xH_2O$ or $CaSn(OH)_6$ or grey mixtures of the same solids with elemental tin.

Up to pcH 8 the calculated tin solubility corresponds well with the experimental data. The result at pcH 5 probably belongs to a solution that was not saturated with respect to tin. Up to pcH 5.7, abhurite is predicted as the solubility limiting phase. At higher alkalinities romarchite, SnO, is identified as the most stable phase.

At higher pcH values the calculated curve shows an extended flat minimum at pcH 8 after which the concentrations rise again. The experimental values are up to one log units higher and with little scattering. The calculated and the experimental lines run mostly in parallel which may hint at a higher solubility of the SnO used in this study than the SnO considered in /GAM 12/. Another possibility would be the formation of a complex that is more stable than the predicted $Sn(OH)_2(aq)$ and $Sn(OH)_3^-$. A similar observation was made in the palladium system, but only at higher pcH values (around 12). Mixed calcium tin(II) hydroxide complexes, such as $CaSn(OH)_3^+$ would be reasonable candidates that could explain the behaviour of tin(II) in calcium containing NaCl solutions. An alternative explanation that cannot be proven now would be the formation of ternary calcium tin(IV) hydroxo complexes of the same type as have been found for zirconium.

If the formation of Sn(IV) is allowed the solubility of tin would be controlled at a much lower level by calcium stannate(IV). The presence of a brown precipitate in the batches indicates that at least not all tin(II) was oxidised or disproportionated to tin(IV) and the solubility is still controlled by tin(II).
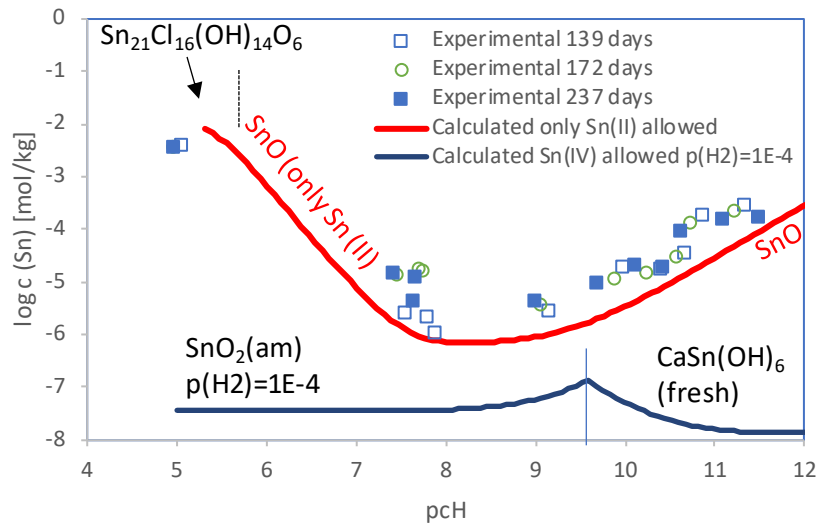
Fig. 8.16　Solubility of tin(II) in halite/ anhydrite-saturated solution

Based on the experimental findings the solubility limits have the following borders:

pcH 6-8: -6.6 to -2* (min. exp. pcH 7.6)

pcH 8-10: -6.7 to -4.1

pcH 10-12: -5.2 to -2.0** (max. exp. pcH 11.5)

Several open points need to be addressed in the future:

- Solubility of tin(II) at pcH <7.4
- Speciation of tin(II) at pcH >8
- Nature of the equilibrium solids at all pcH values
- Ion interaction of tin(II) species with Na^+ and Cl^-

8.6.13　　Solubility of tin(IV) in halite/ anhydrite-saturated solution

To carry out the experiment, freshly prepared tin oxide hydrate, $SnO_2 \cdot xH_2O$ was employed as a starting material (see A.5.9). For tin(IV), concentrations between $1 \cdot 10^{-11}$ to $2 \cdot 10^{-10}$ mol/kg were observed over the entire pcH range (7.5 to 10.5). No clear tendency was identified (Fig. 8.17).

The results of the modelling are shown in Fig. 8.17. The first observation is that the experimental solubilities are in the same order of magnitude as calculated for $SnO_2 \cdot xH_2O(am)$. Presence of cassiterite, $SnO_2(cr)$ would lead to considerably lower concentrations.

There is no visible increase of the solubility at pcH values above 9, that would be expected if $SnO_2 \cdot xH_2O(am)$ was the solubility limiting phase. Although burtite, $CaSn(OH)_6$, was not found in XRD, its formation in the experiments is supported by the fact that in solutions with a pcH greater than 10.2 the calcium concentration is significantly lower and the sulphate concentration higher. Such an observation would be caused by a reaction of SnO_2 and anhydrite that sets free additional sulphate and reduces the solubility of calcium.

$$CaSO_4(s) + SnO_2 \cdot xH_2O(s) + 2H_2O + 2OH^- \rightleftharpoons CaSn(OH)_6 + SO_4^{2-}$$

Modelled Sn concentrations are at the lower end of the scattered experimental values when pcH exceeds 9.5. Here, burtite is expected to form. The deviation may be due to analytical reasons (insufficient filtration of colloidal Sn causing higher concentrations in the samples or caused by inappropriate thermodynamic data (predicted activity coefficients of $Sn(OH)_5^-$/ $Sn(OH)_6^{2-}$ too high, solubility constant of burtite too low). Another option would be that the precipitate in the samples is still closer to "fresh" than to "crystalline" burtite. A calculation with $CaSn(OH)_6(cr)$ is shown in Fig. 8.5. It shows calculated Sn solubilities that are considerably lower than found in the experiment. The actual solid phase may have properties that are somehow in the middle between "fresh" and "crystalline".

To make the discussion even more complicated, modelling with the Zr interaction coefficients from Rai et al. lead to sharply decreasing Sn concentrations above pcH 8 that are much lower than in the experiment (not shown). However, if "fresh" burtite is used, the deviation is much smaller.

Finally, it must be mentioned, that it cannot be excluded that $Sn(OH)_6^{2-}$ forms one or more complexes with Ca^{2+} as it has been shown for $Zr(OH)_6^{2-}$. This would lead to increasing Sn concentrations at higher pcH. The measurements in UK water with its higher Ca concentrations exactly show such a behaviour (Fig. 8.55).

181

The experimental values are at or below the lower estimates of Sn solubility limits (log c -7 to 0) in /BUH 91/.
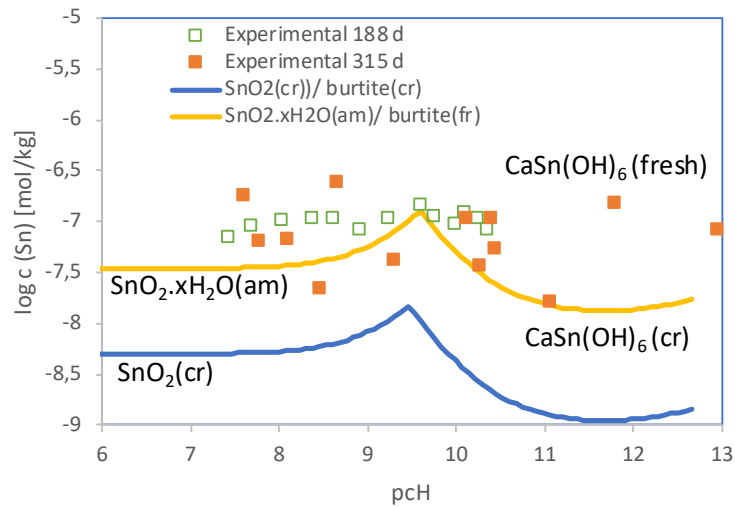
Fig. 8.17   Solubility of Sn(IV) in halite/ anhydrite-saturated solution

Based on these findings, the solubility limit (log c) for Sn(IV) has the following borders:

pcH 6-8: -8.2* to -6.2* (min. exp. pcH 7.6)

pcH 8-10: -8.2 to -6.1

pcH 10-12: -8.3** to -6.3**

Further work will be necessary to

- check for the relevance of mixed chloride hydroxide complexes at low pcH
- confirm the identity of the solid phases. This would require specific measurements without the addition of anhydrite to facilitate chemical analysis
- determine the stability of the solid phase in concentrated NaCl solutions. This is best done by varying the concentration of NaCl and NaOH
- quantify the interaction of tin (IV) species with Na^+. As $Na_2Sn(OH)_6$ is quite soluble this could be done in pure homogeneous solutions using established methods (e.g., isopiestic).
- determine the solubility below 7.6.
- evaluate the formation of calcium stannate complexes at pcH >8

8.6.14 Solubility of zirconium in halite/ anhydrite-saturated solution

As a starting material zirconium oxide hydrate, $ZrO_2 \cdot xH_2O$ was used. In NaCl solutions, the solubility of Zr was constant over the entire pcH range (7.75 to 10.62). It amounted to log c = -6.7 ± 0.2 mol/kg, indicating a single dominating species in equilibrium with the solid phase (Fig. 8.18).

The evaluation of solubility experiments with $Zr(OH)_4$ is complicated by the formation of Zr colloids (see discussion above). In our experiments the solutions were only filtered through 0.2 µm syringe filters. That is not sufficient to effectively exclude colloids. The observed Zr concentrations are at the upper limit of the experimental bandwidth reported by Altmaier et al. /ALT 08/ in 1 and 3 mol/l NaCl solutions.

The calculated zirconium concentrations are about one order of magnitude lower if aged amorphous $ZrO_2 \cdot xH_2O$ is considered to be the relevant solid phase. On the other hand, fresh amorphous $ZrO_2 \cdot xH_2O$ would have the same solubility as we have found in our experiments. Part of the difference could also be explained by a decreasing activity co-efficient of $Zr(OH)_4(aq)$. So far, there are no data available for the interaction of this complex with medium ions.

Previously, the upper solubility limit of zirconium in saturated NaCl solutions was esti-mated at log c = -6 mol/kg /KIE 12/. This assumption was valid only in the absence of Ca^{2+}.

From the experimental data and the modelling several important conclusions could be drawn:

- The stability constants of the neutral complex $Zr(OH)_4(aq)$ and amorphous $Zr(OH)_4(am)$ is still a matter of debate and needs to be looked into further.
- The solubility limiting phase is $ZrO_2 \cdot xH_2O(am)$ and not $ZrO_2(cr)$ which would lead to solubilities about three orders of magnitudes lower.
- The formation of colloids needs to be considered further as there are doubts whether previous experimental data at acidic to moderately alkaline conditions really represent aqueous zirconium species.
- The formation of ternary complexes between calcium, zirconium and hydroxides requires more attention in future work. The existence of such species is well

established, but questions remain regarding their constitution and stability in con-
centrated brines.

- More information is needed on the activity coefficient of the neutral complex
  $Zr(OH)_4(aq)$

Based on the information discussed above the following solubility limits are proposed:

pcH 6-8: -7.2 to -6 (min exp. pcH 7.7)

pcH 8-10: -7.2 to -6

pcH 10-12: -7.2* to –4.8* (max. exp. pcH 10.8)
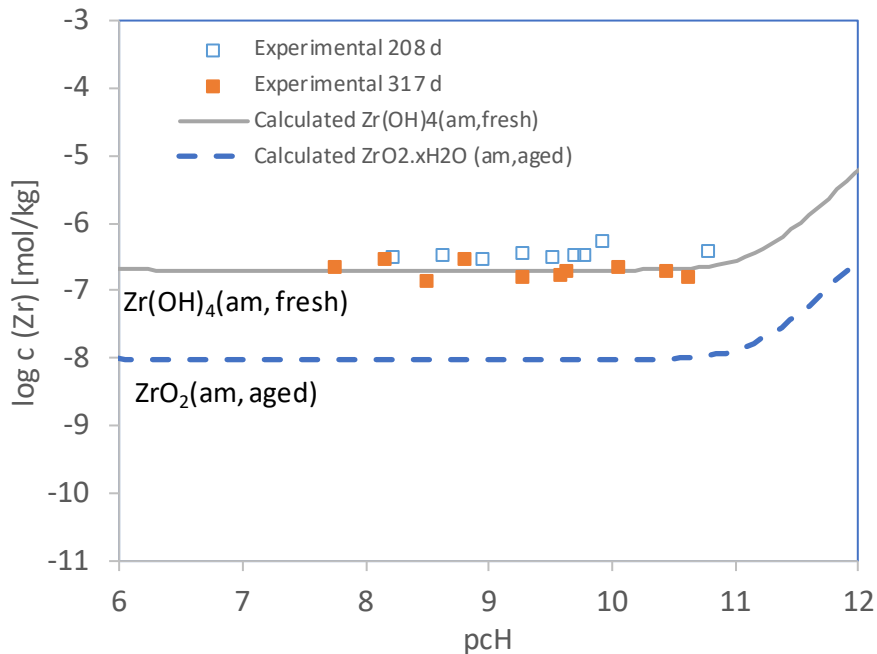
Fig. 8.18   Solubility of zirconium in halite/ anhydrite-saturated solution

8.7   Solubility in halite/ anhydrite solutions in the presence of metallic iron or Fe(II) containing corrosion phases

The previously described series of experiments were performed with specific oxidation
states to understand their behaviour in a halite/ anhydrite saturated environment. Many
of the considered elements exhibit a redox sensitive speciation that could not be fully
covered by the experiments. The near-field of a nuclear repository necessarily contains

corroding iron containing materials. It is reasonable to assume that the release of radio-nuclides from the containers takes place at a time when a large part of the metallic content of the containers is still present. If it is further assumed that the radionuclides get into contact with uncorroded metallic surfaces or Fe(II) containing corrosion phases a redox reaction between metallic iron and the radionuclides may happen. It is well known that such a reaction may not be complete or does not take place at all (see the example of Mo^{VI}), but it is interesting to study the effect such a reduction would have on the solubility. For this purpose, the same modelling calculations as in chapter 8.6 were performed, but a certain amount of metallic iron was added as well. In a second set of calculations, only solid $Fe(OH)_2$ was added. This configuration simulates a situation where released radionuclides only come in contact with iron(II) containing corrosion phases and do not react with elemental hydrogen that has been produced by steel corrosion. The formation of pure iron(III) oxides such as hematite, lepidocrocite and maghemite has been suppressed, as there is no solid evidence that they would form under strongly anoxic conditions - at least at moderate temperatures that are expected after the end of the thermal phase of a repository.

8.7.1   Silver

In the presence of metallic iron or $Fe(OH)_2$, silver is expected to be reduced to the metallic state. In that case a maximum silver concentration of 10^{-7} mol/kg may occur due to the formation of Ag(aq).

8.7.2   Lead

Addition of metallic iron leads to the precipitation (cementation) of metallic lead from the solution (Fig. 8.19). The solubility of lead is drastically reduced and is lower by more than eight ten orders of magnitude in the alkaline region. According to the calculation, chloro complexes are the dominating species throughout the entire pcH range. Only near pcH 12 hydroxo complexes start to play a more important role.

If $Fe(OH)_2$ is added, the formation of elemental lead starts later, only at about pcH 8. It also leads to a steep decrease of total lead concentration but does not achieve the same low level as found when iron was added.

185
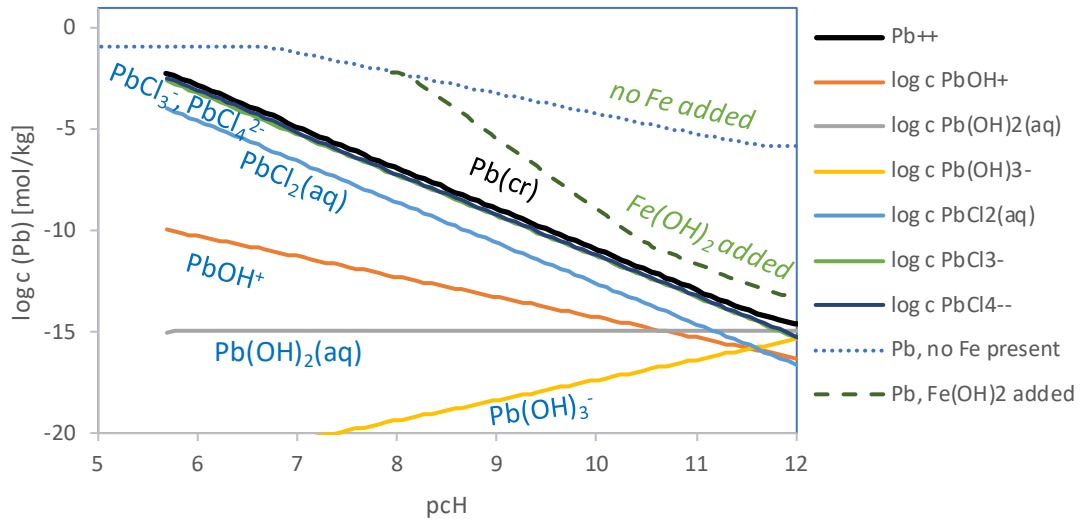
Fig. 8.19 Solubility of lead in halite/ anhydrite-saturated solution with added metallic iron or Fe(OH)$_2$

8.7.3 Molybdenum

In the case of molybdenum, the presence of iron largely prevents the oxidation/ dispro-portionation of Mo(IV) to Mo(VI). The Mo concentration remains constant at log c =-6.7 up to pcH 8.5. MoO$_2$(am) is the solubility limiting solid and Mo(OH)$_4$(aq) the dominating species. Above pcH 8.5 Mo(IV) is reduced by Fe or Fe(OH)$_2$ to Mo(III), which mainly occurs as Mo(OH)$_4^-$. The total Mo concentration increases linearly to log c = -3.6 at pcH 12. Adding Fe(s) or Fe(OH)$_2$ leads to similar results (Fig. 8.20). If no iron is added and at a fixed hydrogen pressure of 10^{-10} bar, the solubility becomes controlled by powellite around pcH 7.4 resulting in constant Mo concentrations above this value. However, due to the lack of reliable data for Mo(IV) species and solids these deliberations remain ten-tative.
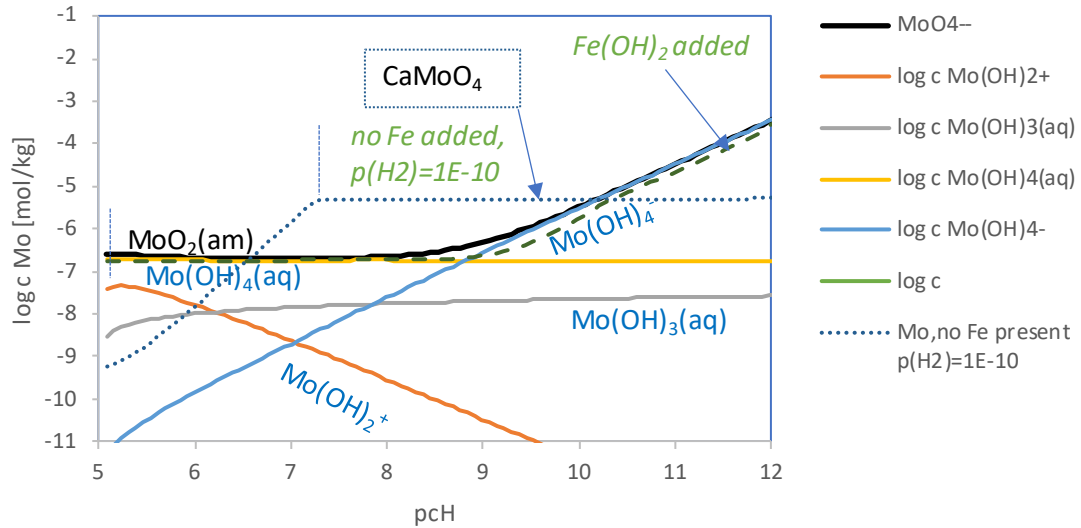
Fig. 8.20 Solubility of molybdenum in halite/ anhydrite-saturated solution with added metallic iron or Fe(OH)$_2$

8.7.4 Nickel

Nickel behaves similar to lead. After addition of iron, nickel is precipitated in elemental form leading to a drop of nickel concentrations by about six orders of magnitude (see Fig. 8.21). Addition of Fe(OH)$_2$ causes the same effect at pcH levels above 7. Whether or not nickel can be reduced by metallic iron in practice, needs to be confirmed.
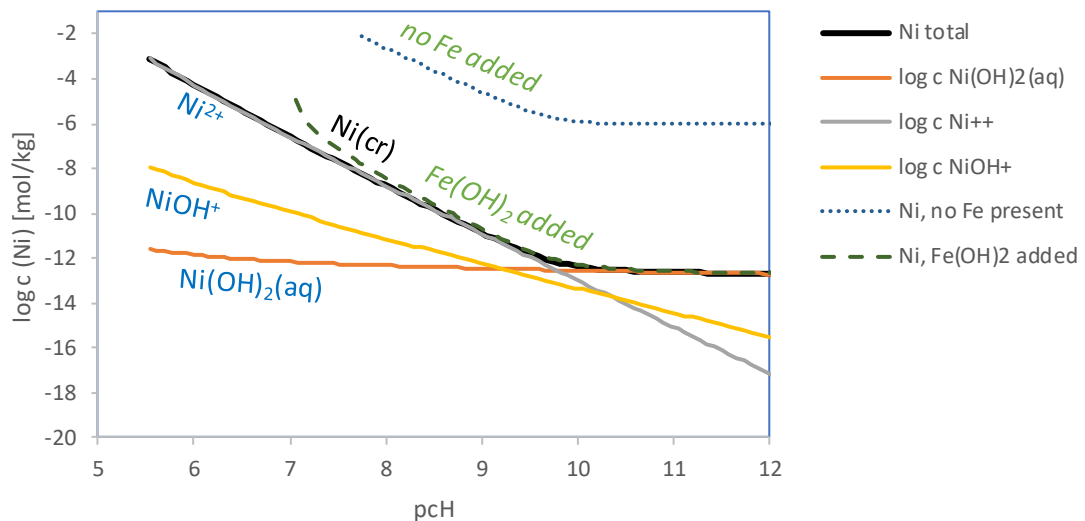
Fig. 8.21 Solubility of nickel in halite/ anhydrite-saturated solution with added metallic iron or Fe(OH)$_2$

8.7.5   Palladium

Among all elements considered in this study, palladium is the most noble one. If iron is present in the system, palladium is expected to precipitate in metallic form. Palladium concentrations would decrease to levels below log c = -25 mol/kg (Fig. 8.22). The slightly higher redox level determined by addition of $Fe(OH)_2$ leads to enhanced palladium concentrations that are some orders of magnitude higher (log c = -15 mol/kg).
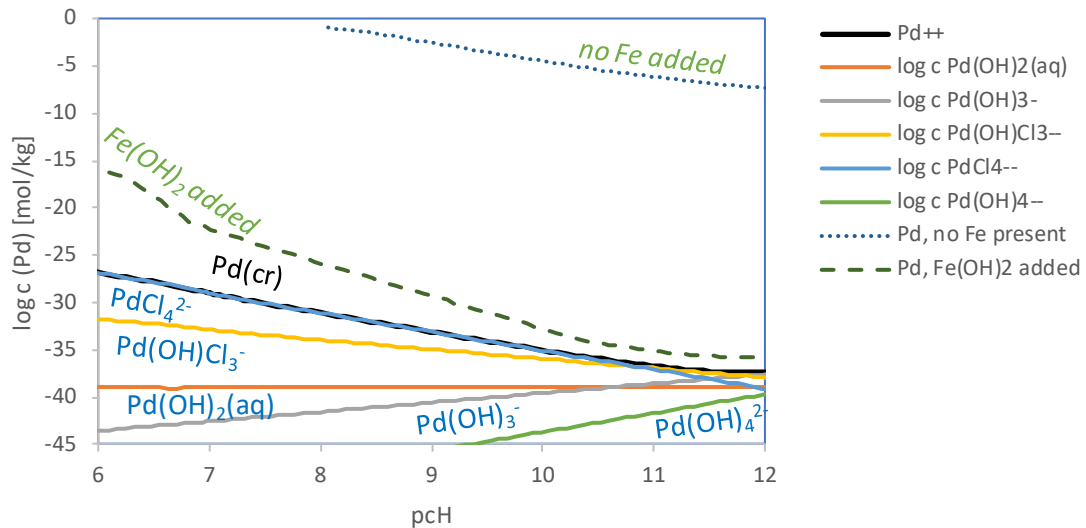
Fig. 8.22   Solubility of palladium in halite/ anhydrite-saturated solution with added metallic iron or $Fe(OH)_2$

8.7.6   Selenium

The presence of iron forces all selenium into the $Fe_{1.04}Se$ phase (at least above pcH 5.5) thus preventing the formation of other, slightly better soluble iron(II) selenides (Fig. 8.23). In the presence of $Fe(OH)_2$ slightly different concentrations are computed up to pcH 8, but the solubility of Se is the same at higher pcH values. At nearly all pcH values, HSe^- is the only relevant selenium species. The calculated solubility of $Fe_{1.04}Se$ (see section 8.6.8) cannot be directly compared to these results because the amount of iron(II) corrosion phases in the batches is not exactly known.

If oxidation states below zero are supressed, all selenite and selenate would be reduced to amorphous selenium in equilibrium with Se(aq).
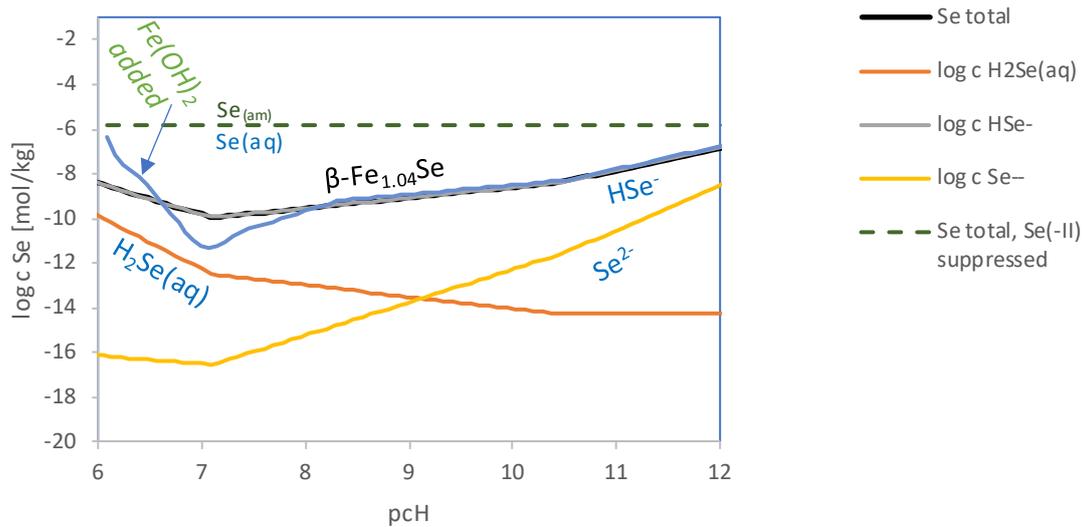
Fig. 8.23 Solubility of selenium in halite/ anhydrite-saturated solution with added metallic iron

8.7.7 Tin

Concerning tin, addition of iron or $Fe(OH)_2$ only has an effect at the lowest pcH values (pcH <6). $SnO_2(am)$ governs the solubility up to pcH 9.5, after that burtite(am) is the stable solid phase. Up to pcH 9 $Sn(OH)_4(aq)$ is the dominating aqueous species. It is then replaced by the anionic complexes $Sn(OH)_5^-$ and $Sn(OH)_6^{2-}$. However, as we have seen in the experiments, oxidation to Sn(IV) may to not take place or at least only partially as long appropriate redox partners are absent. If tin is released as Sn(II), this oxidation state may prevail for a certain time. In that case the tin concentration may be higher, because solid tin(IV) phases do not from and the better soluble SnO controls the solubility (Fig. 8.24). In the alkaline region, the total tin concentration increases again because of the formation of tin(II) hydroxo complexes.
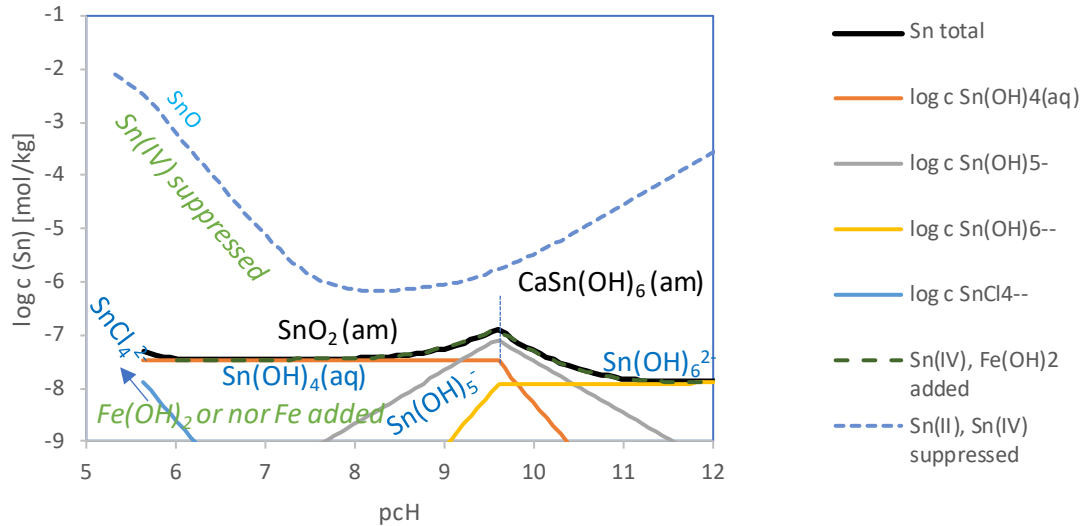
Fig. 8.24 Solubility of tin in halite/ anhydrite-saturated solution with added metallic iron or Fe(OH)$_2$

8.8 Solubility of fission products in IP9 brine

8.8.1 Change of solution composition during increase of pcH

The pcH of an IP9 solution may be increased without a change of the solution composition until pcH 9.2 (Fig. 8.25). At this point magnesium is precipitated as oxychloride, Mg$_2$Cl(OH)$_3$·4H$_2$O. But already at pcH 9.5 this solid becomes unstable with respect to brucite, Mg(OH)$_2$. The decrease of magnesium concentration is compensated by an increase of sodium and, to a lesser extent of potassium. All other concentrations (Ca, Cl, SO$_4$) remain nearly constant. At pcH 13.5, portlandite, Ca(OH)$_2$, becomes saturated so that the calcium concentration is reduced as well.
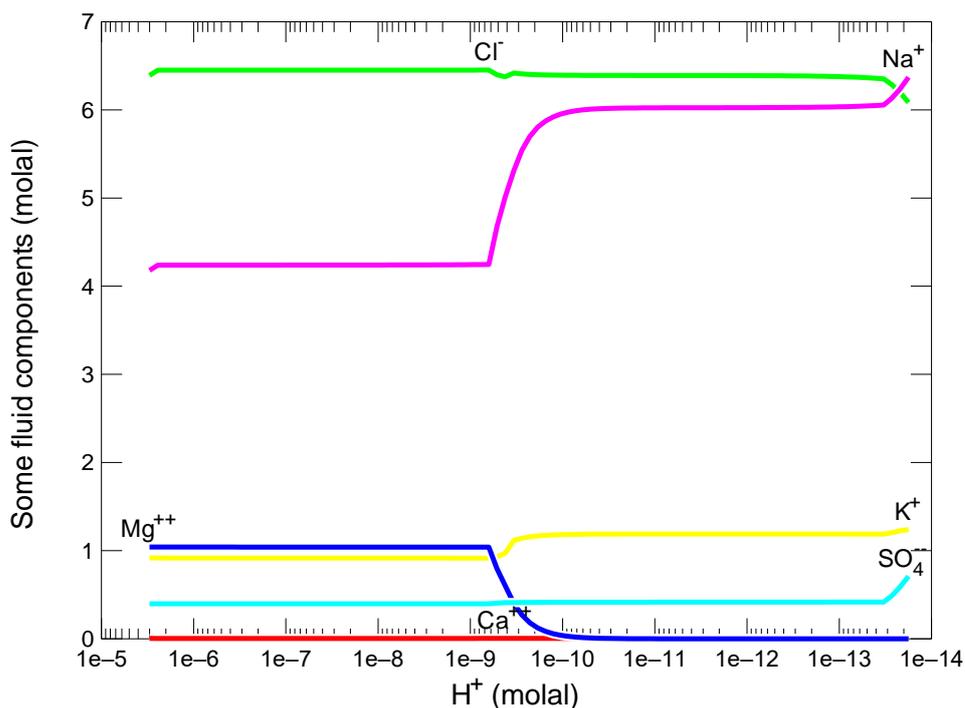
Fig. 8.25   Development of IP9 composition after addition of hydroxide

8.8.2   Solubility of lead in IP9/ IP9 Reak solutions

In these experiments, laurionite, PbClOH was added as a source of lead. In the batches with IP9 solutions the mineral challacolloite, KPb_2Cl_5 and symesite, $Pb_{10}(SO_4)O_7Cl_4 \cdot H_2O$ were detected. In the experiments with IP9Reak the original laurionite was retained. The solubility of lead decreased linearly with the pcH in the range of 8.5 to 11.6 (Fig. 8.26).

For symesite, no thermodynamic data could be found. In the calculation, the occurrence of challacolloite could not be confirmed. At all experimental pcH levels laurionite was the solubility limiting phase. In slightly neutral to acidic solutions the formation of palmierite, $K_2SO_4 \cdot PbSO_4$, at more alkaline solution of blixite was predicted. Modelled and experimental lead solubilities are in close vicinity.

The results allowed us to propose the following solubility limits:

pcH 6-8: -2.3* to -1.0* to (no exp. Data)

pcH 8-10: -4.8 to -1.3* (min pcH 8.5)

pcH 10-12: -6.1* to -4.1 (max pcH 11.6)

Further work is needed to:

- Determine the stability of symesite and other possibly occurring lead hydroxysulphate salts such as sundiusite and $Pb_4(Cl,SO_4)_2O_3$
- Extend the experiments to low pcH areas
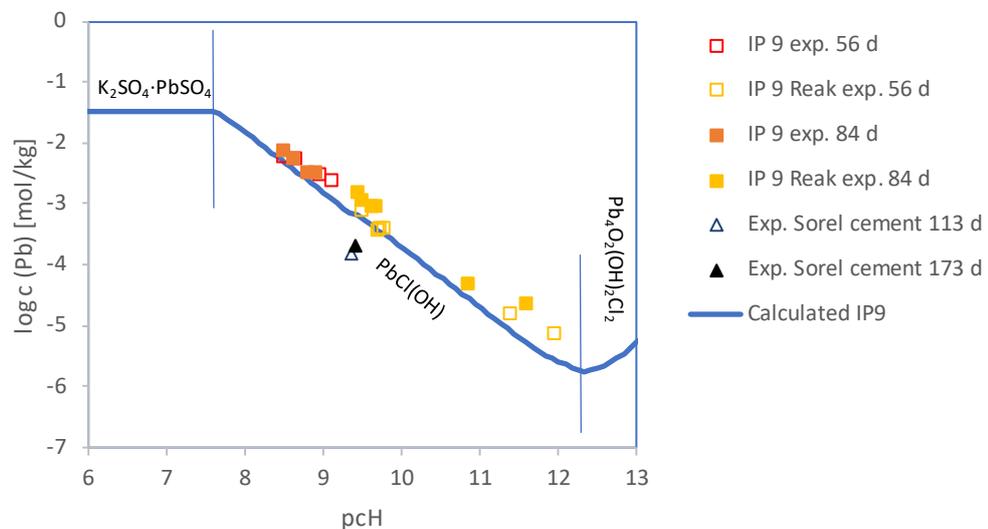
Fig. 8.26   Solubility of lead in IP9/ IP9 Reak solutions

8.8.3   Solubility of molybdenum(VI) in IP9/ IP9 Reak solutions

Calcium molybdate was used as a starting material, it was also found at the end of the experiments. The solubility of molybdenum(VI) was quite constant. In IP9 solutions between pcH 6.8 and 9.5 it amounted to log c = -4.15 ± 0.05. In IP Reak solutions it was a little bit lower: log c = -4.60 ± 0.05 (Fig. 8.27). The reason for this behaviour is not obvious.

The calculated solubility of molybdate in IP9 solutions was almost constant at all pcH levels and very similar to the experimental values. The experimental result in IP9 Reak solutions were a little bit lower so that a difference of 0.4 log units occurred (Fig. 8.27).
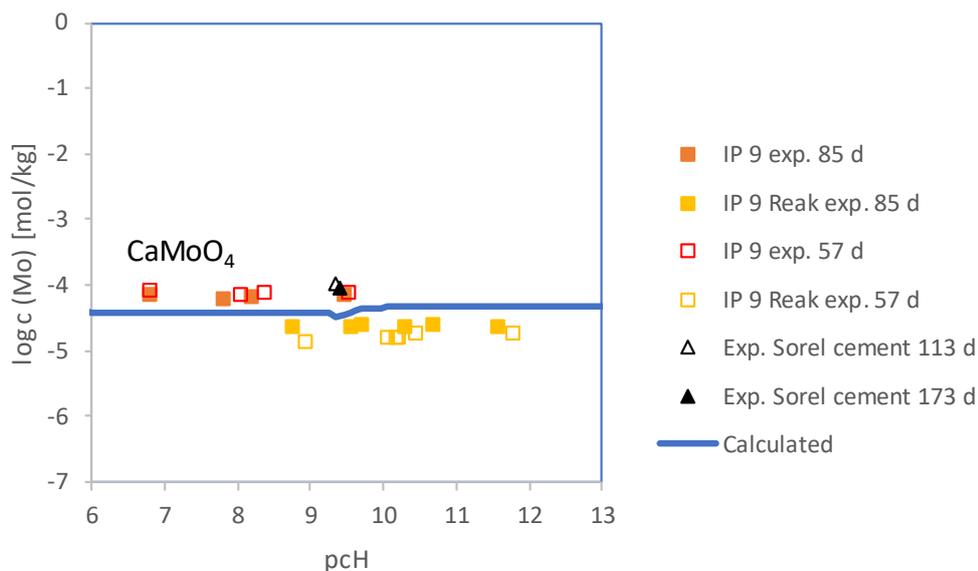
Fig. 8.27   Solubility of molybdenum(VI) in IP9/ IP9 Reak solutions

Based on these results the following solubility limits are proposed:

pcH 6-8: -4.7* to -3.5* (min exp. pcH 6.8)

pcH 8-10: -5.1 to -3.5

pcH 10-12: -5.1 to -4.1 (max. exp. pcH 11.6)

Additional efforts are necessary to

- understand the difference of molybdate solubilities in IP9 and IP9Reak solutions
- determine ion interaction coefficients for K_2MoO_4 and $MgMoO_4$

8.8.4   Solubility of nickel in IP9/ IP9 Reak solutions

In these experiments, nickel hydroxide was employed at the start of the experiments. It was also the only nickel bearing phases that could be detected by XRD. The solubility of nickel decreased linearly with the pcH in the range of 8.0 to 10.3 and then remained at the same level at pcH 11.8 (Fig. 8.28). The observed constant concentration level at higher pcH is about one order of magnitude lower than in halite/ anhydrite saturated solutions.

The calculated solubility of Ni(OH)$_2$ agrees very well with the experimental values up to pcH 10 (Fig. 8.28). At higher pcH the analytical nickel concentration decreases to about log c = -7 whereas a solubility of log c = -6 was calculated. IP9Reak and HalAnh solution mainly differ in potassium and sulphate concentration that have presumably little impact on the activity coefficients of the prevailing Ni(OH)$_2$(aq) species or the properties of the Ni(OH)$_2$ phase. The observed difference cannot be explained at the moment.

Based on these findings and conservatively assuming that the calculated, higher Ni(OH)$_2$ solubility at high pcH is correct we derived the following solubility limits:

pcH 6-8: -2.6 to 0 (min pcH 8)

pcH 8-10: -6.5 to -1.5

pcH 10-12: -7.4 to -4.9

The following open points should be addressed in later research

- Difference between Ni(OH)$_2$ solubility at pcH > 10 in HalAnh and IP9 solutions
- Specific impact of K^+, Mg^{2+}, Na^+ and SO_4^{2-} on the activity coefficient of the complex Ni(OH)$_2$(aq).
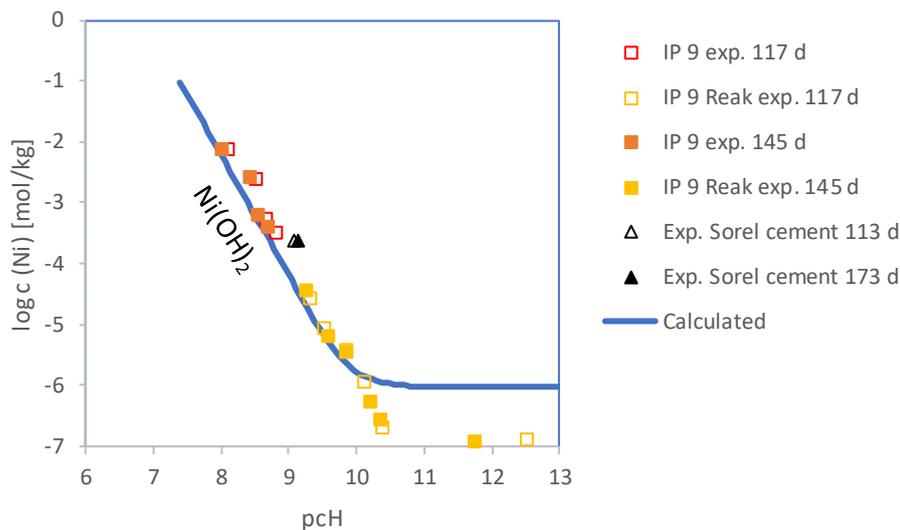
Fig. 8.28   Solubility of nickel in IP9/ IP9 Reak solutions

8.8.5 Solubility of silver in IP9/ IP9 Reak solutions

Two datapoints were experimentally determined to characterize the solubility of AgI in IP9 solutions. Both gave similar results: $10^{-3.8}$ mol/kg at pcH 8.4 and 10.1 (Fig. 8.29).

pcH 6-8: -4.3** to -3.3**

pcH 8-10: -4.3 to -3.3 (min pcH 8.4)

pcH 10-12: -4.3** to -3.3** (max pcH 10.1)

If the concentration of iodide is not sufficient to completely bind silver in AgI, the higher solubility of AgCl needs to be considered. Taking into account the difference between AgI and AgCl solubilities in saturated NaCl solutions (1.9 log units), it may be concluded that solubility of AgCl in IP21 solutions would be higher by the same amount, since the difference is mainly caused by the difference in the solubility constants of AgCl and AgI:

pcH 6-12: -2.4** to -1.4**
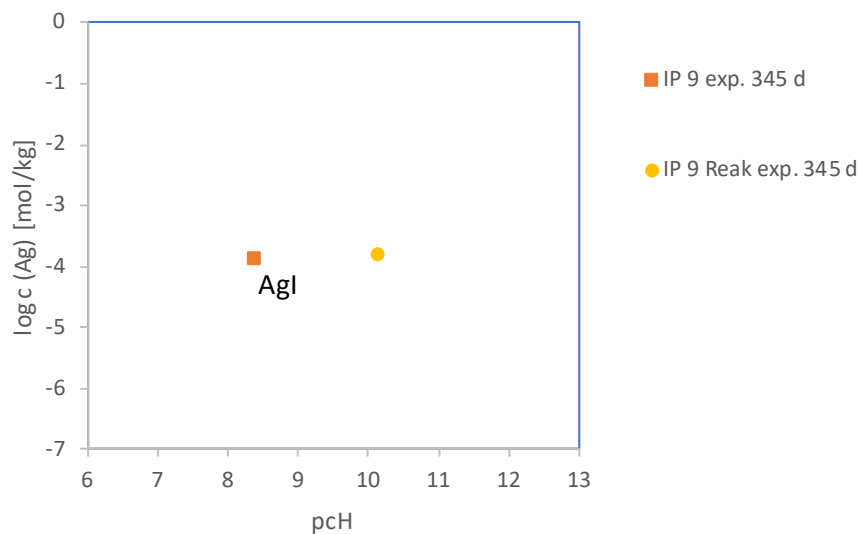
Fig. 8.29   Solubility of silver in IP9/ IP9 Reak solutions

8.8.6 Solubility of strontium in IP9/ IP9 Reak solutions

Strontium sulphate, SrSO$_4$ (celestine) was used as the starting solid. It was also detected at the end of the experiments. All strontium solubilities were comparable and centred around log c = 4.1±0.1 (Fig. 8.30) .

Modelling of the system lead to very similar results (Fig. 8.30). Only at the highest pcH a decline of Sr concentrations is predicted due to an increase of the sulphate concentration.

For all pcH levels (6-12), a solubility limit of log c = -5.1 to -3.5 is proposed (min. exp. pcH 7.3).
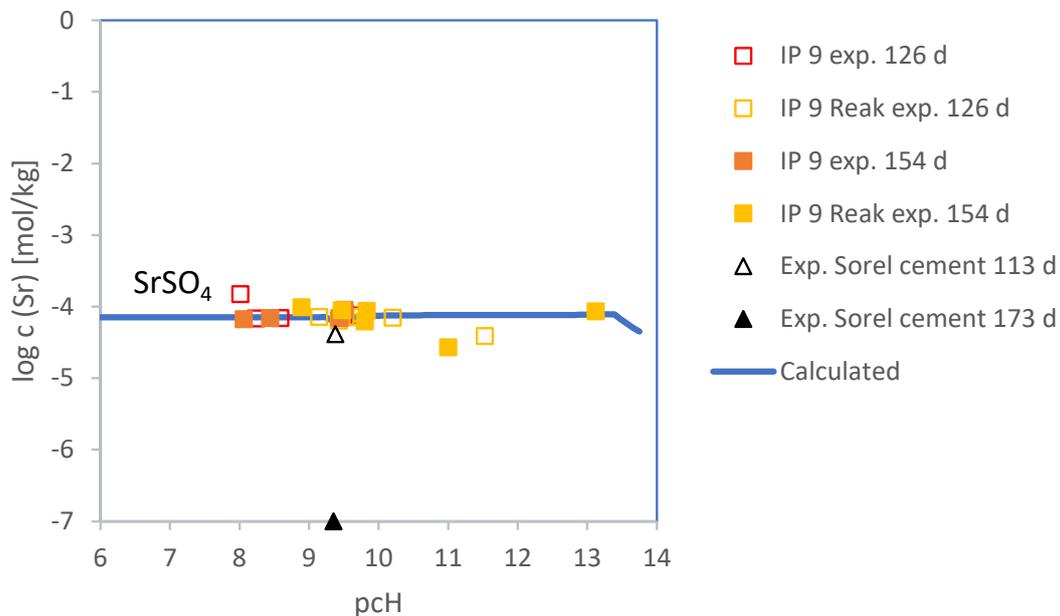
Fig. 8.30   Solubility of strontium in IP9/ IP9 Reak solutions

8.8.7 Solubility of tin(IV) in IP9/ IP9 Reak solutions

Tin(VI) oxide hydrate was the initial solid phase in the mixtures. It was not possible to detect any tin containing solid phase in the experiments. However, the synthesized SnO$_2$·xH$_2$O did not show any identifiable reflections either.

In the IP9 solutions the solubility shows no clear tendency, but it seemed that the concentrations rose between pcH 7.3 and 8.6. In IP9 Reak solutions, the tin concentrations

were quite constant (log c = 6.4 ± 0.3) (Fig. 7.3). One point at pcH 8.04 with log c = -3.8 is considered an outlier.

The calculated tin concentrations are similar at pcH >10 if fresh burtite is assumed as the solubility limiting phase. At lower pcH values, the experimental tin concentrations are higher by about 1.5 to 2 orders of magnitude (log c = -6 to -5, neglecting one outlier). In comparison with the results in halite/ anhydrite saturated solutions the concentrations are one order of magnitude higher. Obviously, Mg, that is only present in relevant amounts in IP9 not in IP9Reak solutions has an impact on the solubility of $SnO_2 \cdot xH_2O$.

So far, ternary magnesium tin(IV) hydroxide complexes of the type $Mg_xSn(OH)_{4+y}^{2x-y-}$ that could be a cause of higher tin concentrations are not known but cannot be excluded. Another explanation would be the formation of mixed colloids between $Mg(OH)_2$ and $Sn(OH)_4$ or sorption of Sn(IV) on $Mg(OH)_2$ or $Mg_2(OH)_3Cl$ colloid particles. Such a process has been observed in solubility experiments with $Th(OH)_4$ in $MgCl_2$ media /ALT 04/. They may cause an increase of observed Th concentrations by two orders of magnitude, if filtered through ordinary (0.2 μm) filters but not submitted to ultrafiltration. The same concentration difference is observed in our experiments in NaCl saturated and IP21 solutions. The important difference is that we also observed this increase at pcH levels where we do not expect the formation of $Mg(OH)_2$ colloids (pcH <7.5).

Although we cannot exclude that our tin concentrations are increased by the presence of colloids, we will base our proposal on the present analytical values:

pcH 6-8: -6.4** to -4.7** (min. exp. pcH 7.3)

pcH 8-10: -6.9 to -4.7

pcH 10-12: -7.2* to -5.7* (max exp. pcH 11.5)
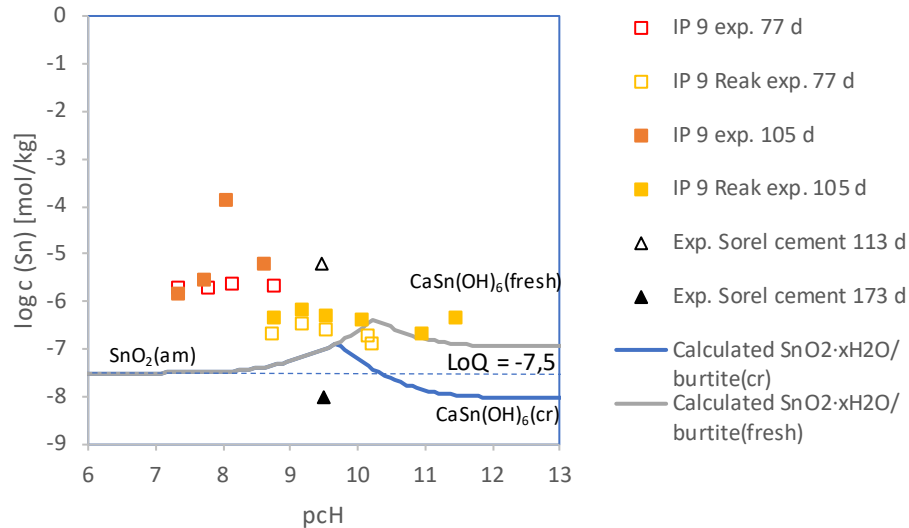
Fig. 8.31 Solubility of tin(IV) in IP9/ IP9 Reak solutions

An improved understanding of tin(IV) solubility could be achieved by

- an investigation of the influence of $MgCl_2$ concentration on the solubility of $SnO_2 \cdot xH_2O$
- identification of the solid phase formed at pcH >10
- determination of the solubility of $MgSn(OH)_6$
- conduct experiments with a more rigid control of potential colloid formation

8.9 Solubility of fission products in IP21 brine

8.9.1 Solubility of lead in IP21 solution

For the experiments in IP21 solutions, a combination of lead chloride and potassium chloride were added to allow the formation of $KCl \cdot 2PbCl_2$ that should be the solubility limiting lead phase in this system. For the investigations in IP21 Reak solution, laurionite was used.

In IP21 solutions, the concentration of lead remained constant at 0.0245 ± 0.015 mol/kg up to pcH 9.0. This concentration is well below the initial concentration of lead that was approximately 0.06 mol/kg (Fig. 8.32). In IP21 Reak solutions the solubility of lead was about one log unit lower at pcH 8.2 to 9.3 and decreased further when the pcH rose to

9.8. In accordance to expectations in batch 3 KCl·2PbCl$_2$ was found by XRD, while in batch 10 there was laurionite.

According to the modelling at pcH <9 the double salt KCl·2PbCl$_2$ forms. Its solubility is close to the observed levels. At higher pcH the precipitate is transformed into laurionite, PbClOH. Here the experimental data is a little bit scattered, but the maximum values are again close to the calculated line.

The following solubility limits were derived:

pcH 6-8: -2.1* to -1.0* (min. exp. pcH 6.3)

pcH 8-10: -4.4* to -1.1 (max pcH 9.8)

pcH 10-12: -6.3* to -2.7* (no experiments)

Some further work is necessary to:

- Extend the experiments to pcH 12
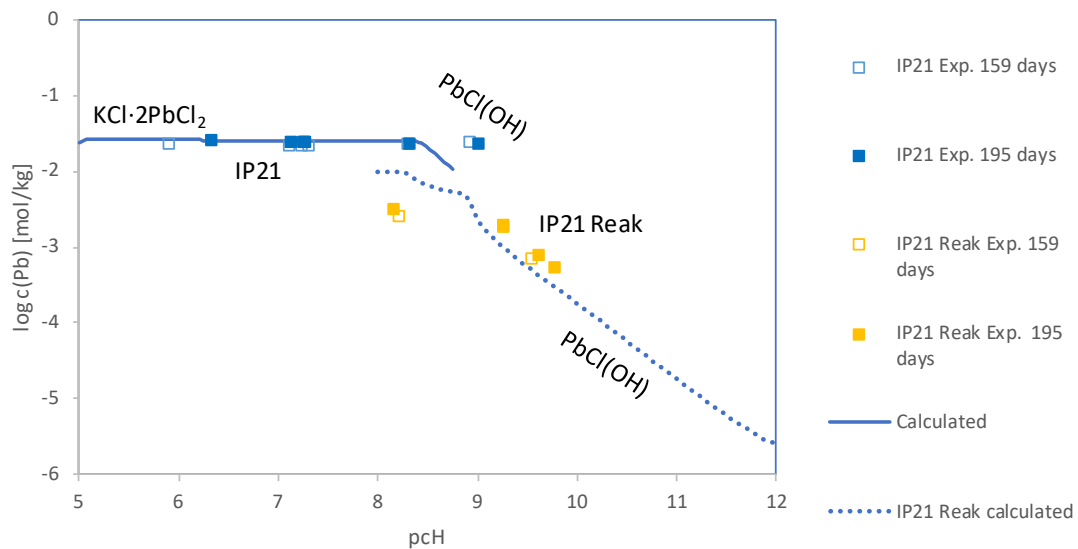
Fig. 8.32   Solubility of Pb in IP21 solution

8.9.2 Solubility of molybdenum(VI) in IP21 solution

Powellite, $CaMoO_4$ was employed in this set of experiments. The solubility of molybdenum in IP21 solutions increased slightly from $2.9 \cdot 10^{-4}$ to $3.9 \cdot 10^{-4}$ mol/kg between pcH 5.5 and 9. In the IP21Reak solutions the Mo concentrations were significantly lower, probably due to the higher Ca concentrations. Here, they amounted to log c = 4.3 ± 0.1 with no clear pcH tendency. (Fig. 8.33). Powellite was found by XRD in batches with the lowest and highest pcH.

The calculated solubility of molybdate in IP21 solutions is shown in Fig. 8.33. At all pcH powellite is the solubility limiting phase. Magnesium molybdate hydrates are not saturated. The difference between modelled and experimental data is 0.9 log units at maximum. However, if the complex $MgMoO_4(aq)$ is allowed to form, the solubility would lead to an increase of the solubility by several orders of magnitude higher than the observed value.
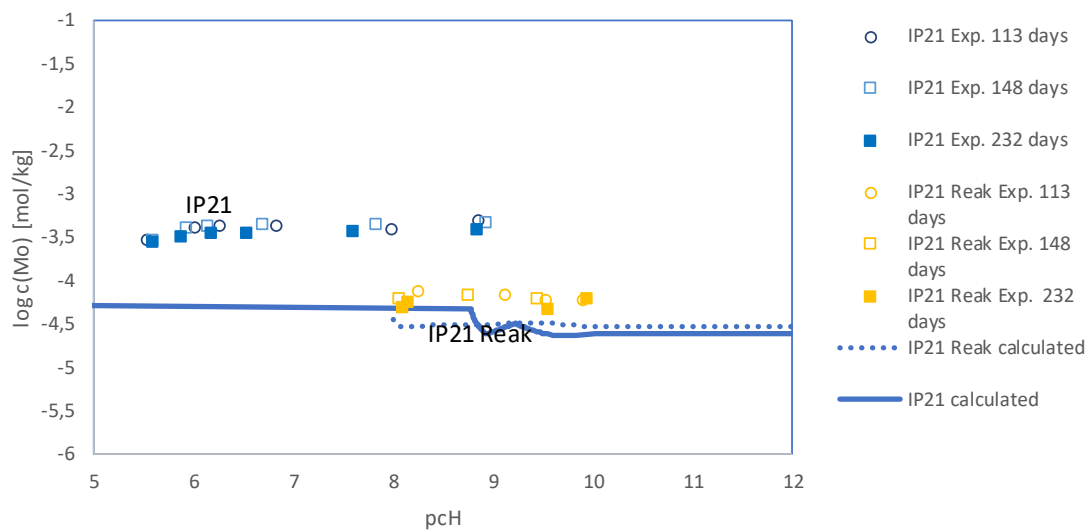
Fig. 8.33 Solubility of Mo(VI) in IP21 solution

For Mo(VI) the following solubility limits were derived:

pcH 6-8: -4.1 to -2.9

pcH 8-10: -4.9 to -2.9 (max pcH 9.9)

pcH 10-12: -4.9* to -3.7* (no experiments)

Some additional work is needed to:

- Confirm the predicted solubility at pcH >10
- Derive a model to calculate the solubility of magnesium molybdates more precisely
- Redetermine the complex formation constants of $MgMoO_4(aq)$ and $CaMoO_4(aq)$ and include them in the model

8.9.3 Solubility of nickel in IP21 solution

In these experiments, $Ni(OH)_2$ acted as the starting material. The observed Ni concentrations dropped sharply with pcH value in IP21 solutions. The slope is even steeper in IP21 Reak solutions. It is not entirely clear whether the solubility curve flattens above pcH 9.5 as the results from the samplings after 118 and 153 days differ from those after 237 days (Fig. 8.34). In batch 3 a mixed $(Ni,Mg)(OH)_2$ phase was found by XRD, whereas pure $Ni(OH)_2$ could be excluded. Batch 10 showed $Ni(OH)_2$.
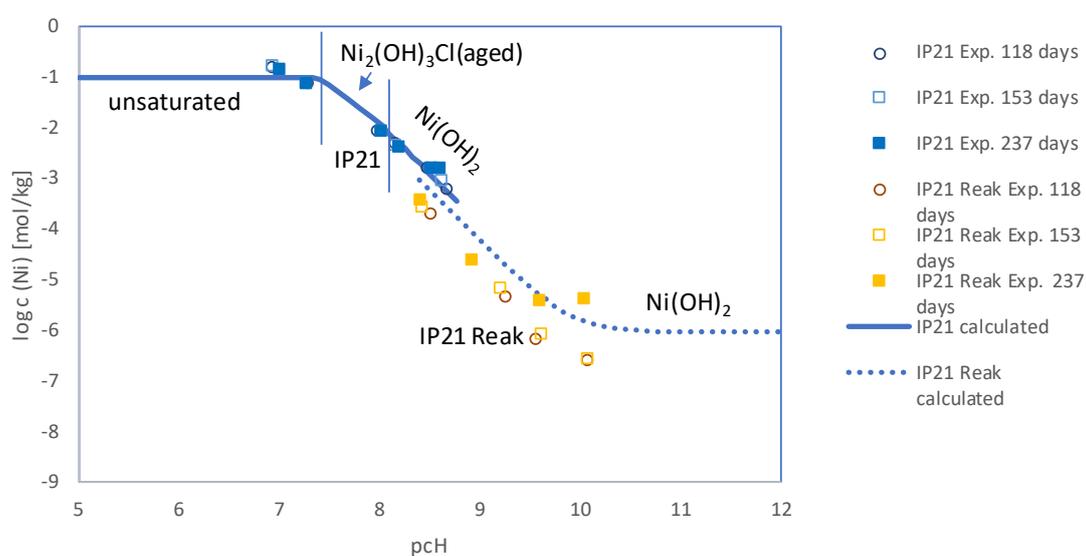
Fig. 8.34   Solubility of Ni in IP21 solution

Calculated and experimental nickel solubilities agree well in IP21 solutions. The difference is below one order of magnitude at all pcH. Basic nickel chloride, $Ni_2(OH)_3Cl(aged)$ was predicted to form between pcH 7.4 and 8, but the calculated solubility of $Ni(OH)_2$ is almost the same in this region (not shown).

Although the maximum experimental pcH is close to 10 it is reasonable to assume that the solubility of Ni(OH)$_2$ remains constant at higher values as it has been observed in IP9 solutions and as it is predicted in the models.

The following solubility limits were derived:

pcH 6-8: -2.6 to 0* (min pcH 7)

pcH 8-10: -7.1 to -1.5

pcH 10-12: -7.1* to -4.8* (max exp. pcH 10)

In the future, the solubility of nickel in solutions above pcH 10 needs to be further investigated.

8.9.4   Solubility of niobium in IP21 solution

Amorphous niobium oxide hydrate was used as the initial lead-containing solid. Adjustment of the pH was quite difficult especially at higher pcH values. A hydroxide consuming reaction caused a slow decrease of the pcH. In the end it was not possible to achieve values above pcH 9.3. This is accordance with findings from XRD measurements that showed the presence of various niobates (K$_2$NbO$_3$ and CaNbO$_3$ in batch 1; Ca$_3$Nb$_2$O$_8$ and Nb$_2$O$_5$ in batch 1).

At pcH values below 7.3 the niobium concentrations slipped below the limit of detection (log c = -7.3). Above this limit the niobium solubility increased from about log c = -7 to -5. The nature of the solubility limiting phase was not determined, but the slow pcH shifting process that apparently consumed some Ca hints to the dissolution of some calcium sulphate solid and the precipitation of a calcium niobate. The empirical model of Talerico et al. /TAL 04/ that could be applied to halite saturated solutions (see 8.6.5) cannot be used to predict the solubility in IP21 solutions.
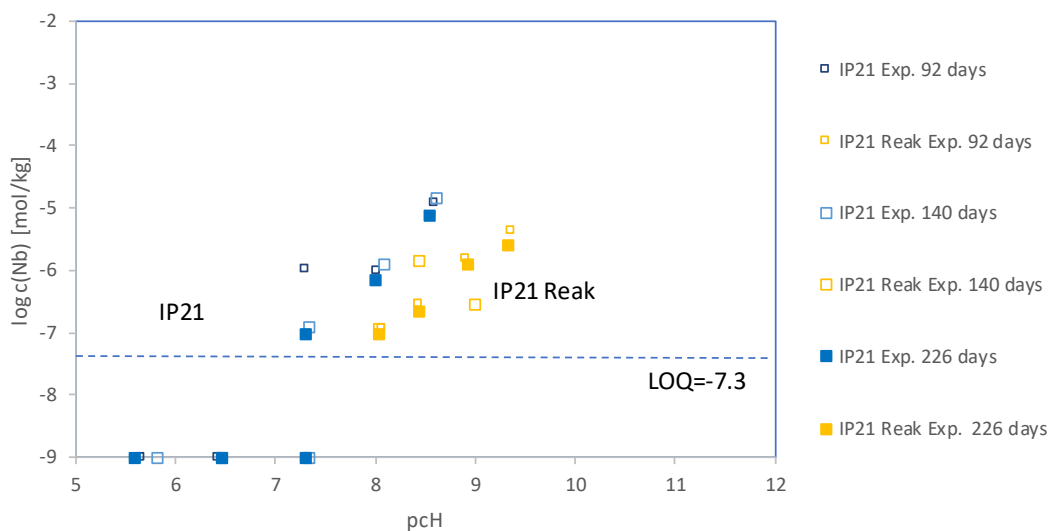
Fig. 8.35   Solubility of Nb in IP21 solution

The following solubility limits were derived:

pcH 6-8: ≤-7.9 to -5.6

pcH 8-10: -7.6 to -4.3 (max pcH 9.3)

pcH 10-12: -6.1** to -1.5** (no exp.) (upper limit extrapolated from linear trend pcH 8 and 9.3)

In the future, further efforts are necessary to:

- Extend the experiments to pcH >9.3
- Identify the dominating solutions species of niobium and the nature of the solid phase in the relevant pcH range
- Determine the stability of these species and phases

8.9.5   Solubility of palladium(II) in IP21 solution

In the experiments with Pd(II) in IP21 solutions, $PdCl_2$ was used as the starting material. The first six batches at low pcH values showed a brown-red solution with a white solid (probably anhydrite). The last four batches contained almost colourless solutions with a brown precipitate (Fig. 8.36).

Fig. 8.36 Experimental batches of palladium(II) in IP21 solution

Slow drifting processes caused the pcH to remain within narrow ranges (3.5 to 6.8 and 8.8 to 9.6). At pcH up to 6.8 no precipitation of phases occurred. Between pcH 8.8 to 9.6 the palladium concentration decreased linearly.

The calculated solubility was controlled by $Pd(OH)_2$(am) at pcH >9. It was about one log unit higher than observed in the experiment at pcH 8.8 to 9.6. A similar but smaller gap was also observed in HalAnh solution. This is an indication that either the solid phase contains structural chloride and has a lower solubility or the interaction coefficients for Pd species need significant change. So far, a magnesium hydroxo palladate, $MgPd(OH)_4$ has not been described in the literature. Analogue compounds exist for the heavier earth alkali elements /ZAI 91/. It should be checked whether $MgPd(OH)_4$ could play a relevant role in IP21 solutions.

The following solubility limits are proposed for Pd in IP21 solutions

pcH 6-8: 0

pcH 8-10: -6.8** to -2.0** (estimated from slope in exp. Range pcH 8.8 – 9.6)

pcH 10-12: not determined (no experiments)

In the future, additional work is needed to clarify these open points:

- Identity of the solid phase at pcH >9.3
- Solubility of Pd at pcH >9.6 and between 6.8 and 8.8
- Existence, stability, and relevance of magnesium hydroxo palladate(II)
- Ion interaction between dominant Pd species and K^+ and Mg^{2+} (probably $PdCl_4^{2-}$, $Pd(OH)Cl_3^{2-}$, $Pd(OH)_2Cl_2^{2-}$, $Pd(OH)_3^-$)
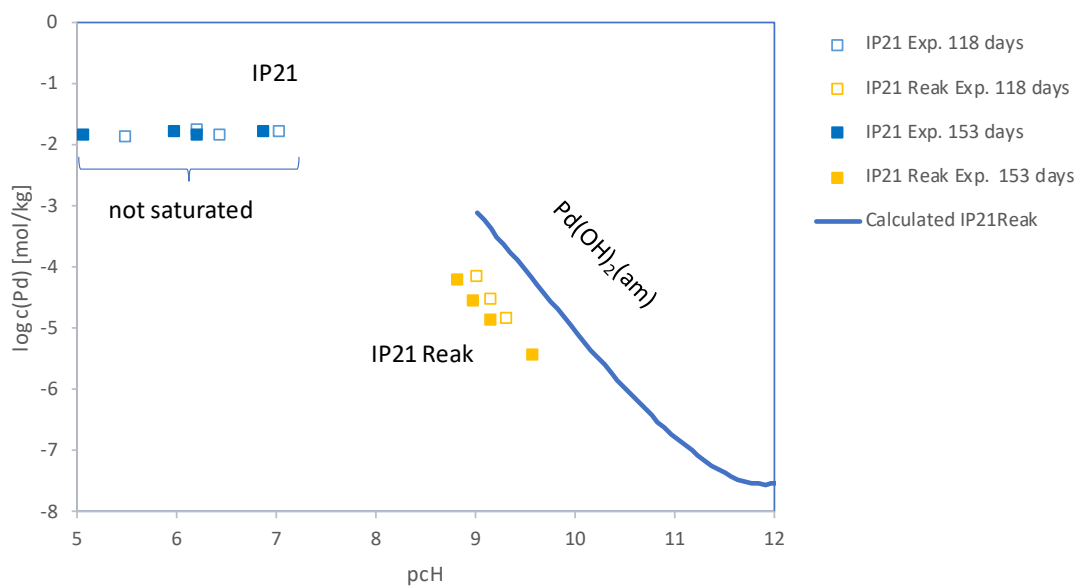
Fig. 8.37 Solubility of palladium(II) in IP21 water

8.9.6 Solubility of selenium(IV) in IP21 solution

In the experiments with Se(IV), $CaSeO_3$ was added as starting material in all batches. In IP21 solutions, the solubility of selenite decreases from 0.066 mol/kg at pcH 6.0 to 0.005 at pcH 8.7, In IP21Reak solutions the concentration of Se(IV) is constant at 0.0013 mol/kg between pcH 9.4 to 10.6.

As long as significant magnesium concentrations are present, precipitation of $MgSeO_3.6H_2O$ is predicted. However, using the thermodynamic data listed above, the calculated solubilities are about two orders of magnitude lower than found in the experiments. Several reasons could lead to this observation: strong complex formation between Mg^{2+} and SeO_3^-, inadequate Pitzer ion interaction coefficients or slow transformation of $CaSeO_3 \cdot H_2O$ to $MgSeO_3 \cdot 6H_2O$. An alternative calculation with suppressed $MgSeO_3 \cdot 6H_2O$ suggests the latter process as the gap between calculated and experimental data is closed to less than 0.3 log units (Fig. 8.38). In the realm of IP21 Reak the model agrees very well with the analytical data.

The following solubility limits are derived from the combined experimental and calculated results:

pcH 6-8: -2.8 to 0

pcH 8-10: -3.4 to -1.7

pcH 10-12: -3.5 to -2.3 (max. exp pcH 11.1)

In the future, additional work is needed to clarify these open points:

- Identity of the solid phase at pcH <9
- Redetermination of the solubility constant of $MgSeO_3 \cdot 6H_2O$
- Ion interaction coefficients for $MgSeO_3$
- Complex formation between Mg^{2+} and SeO_3^{2-}
- Transformation of $CaSeO_3 \cdot H_2O$ into $MgSeO_3 \cdot 5H_2O$
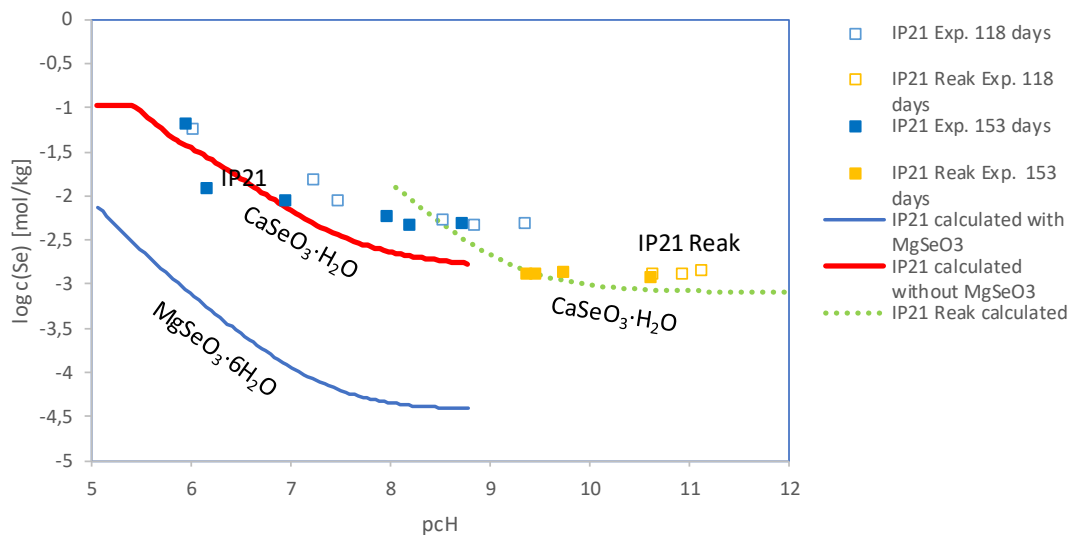
Fig. 8.38   Solubility of selenium(IV) in IP21 water

8.9.7   Solubility of silver in IP21 solution

Three datapoints were experimentally determined to characterize the solubility of AgI in IP21 solutions. All three gave similar results: log c = -3.73±0.04. mol/kg between pcH 7.4 and 10.3 (Fig. 8.39).

pcH 6-8: -4.2** to -3.2** (min pcH 7.4)

pcH 8-10: -4.2 to -3.2

pcH 10-12: -4.2** to -3.2** (max pcH 10.3)

In the literature, there are no solubility data for AgCl in MgCl$_2$ solutions that would allow a direct comparison. However, taking into account the difference between AgI and AgCl solubilities in saturated NaCl solutions (1.9 log units), it may be concluded that solubility of AgCl in IP21 solutions would be higher by comparison to AgI by the same amount, since the difference is mainly caused be the difference in the solubility constants of AgCl and AgI:

pcH 6-12: -2.3** to -1.3**
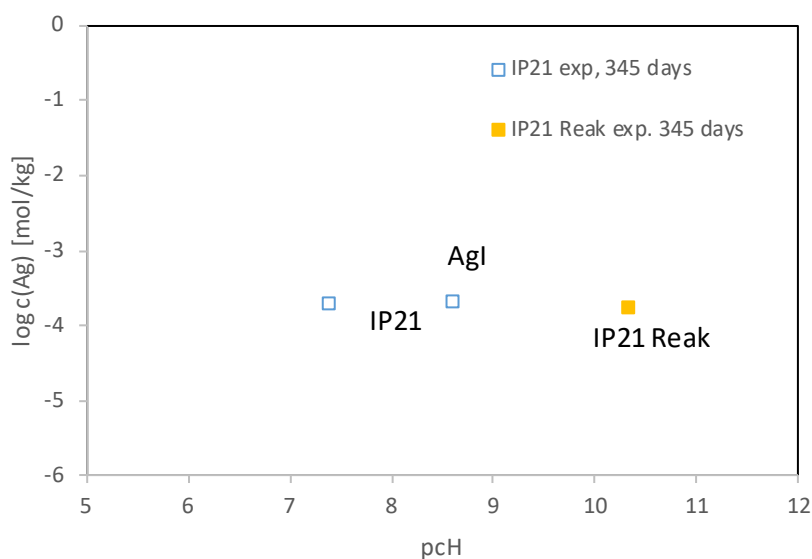
Fig. 8.39   Solubility of silver in IP21 solution

8.9.8   Solubility of strontium in IP21 solution

In the case of strontium, synthesized produced strontium sulphate was used as the starting substance. The results of the investigations are summarised in Fig. 8.40. In all IP21 solutions, a concentration of about $2.4 \cdot 10^{-5}$ mol/kg was observed. Celestine was identified at the end of the experiments. This is in very good agreement with the modelling performed with the THEREDA database (Release 11) for the IP21 solution..

Due to slow pcH shift all but one solution ended up around pcH 8, a region that is also covered by magnesium-rich IP21 solutions However, the equilibrium activity of sulphate is lower, allowing the strontium concentration to increase to higher levels. Celestine was again found at the end of the experiments, but the evidence was rather weak in the last experiment. More prominent XRD signals were found for kalistrontite, K$_2$Sr(SO$_4$)$_2$. At the

same time, the strontium concentration at pcH 9.5 was significantly lower than around pcH 8. The formation of kalistrontite may explain such a behaviour, but it is not clear why such a reaction should not take place at pcH 8 as well. A stability constant for kalistrontite is not available, so that the solubility of this phase cannot be calculated. The solubility at pcH 8 is predicted correctly by thermodynamic modelling, but not at pcH 9.5..

We propose the following solubility limits:

pcH 6-8: -5.2* to -4.1* (min exp. pcH 6.5)

pcH 8-10: -5.3 to -3.4 (max pcH 9.6)

pcH 10-12: -4.9** to -3.2* (no exp.)

Some additional experiments are needed to confirm the calculated solubility at pcH >9.6
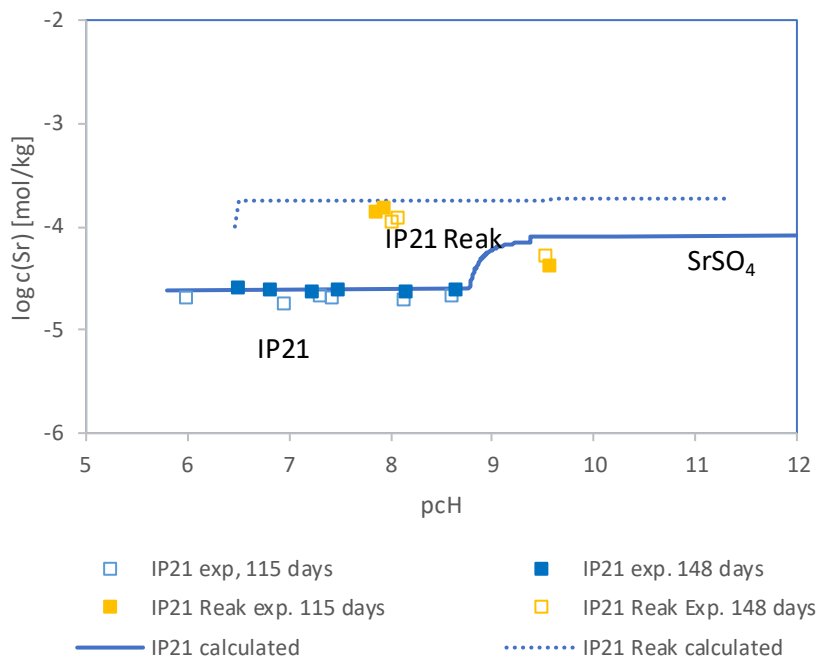
Fig. 8.40   Solubility of Sr in IP21 solution

Compared to the solubility ranges considered by Buhmann et al. /BUH 91/, the experimental concentrations in IP21 solutions of all pcH are higher (log c > -5) than the lower limit assumed so far (log c = -6). On the other hand, in alkaline solutions, if magnesium

is absent, the upper limit of the range (log c = -4) is too optimistic. It should be lifted to log c = -3.5.

8.9.9 Solubility of tin(II) in IP21 solution

For this experiment solid tin(II) chloride hydrate was used as a starting material. After the end of the experiments batch 1 showed a light grey precipitate, from batch 2 to on the solid was brown starting with grey brown in batch 2 and the getting darker until batch 5. From batch 6 on, the amount of precipitate increased. At the same time the solid became greyer again, obviously less crystalline, and more voluminous (Fig. 8.41).

Fig. 8.41   Experimental batches of tin(II) in IP21 solution

The solubility shows distinct features. In IP21 solutions the concentrations at the lowest pcH 6.7 equals log c= 2.6. It decreases to log c = -4.2 at pcH 7.7 and increases again to log c = -3.4 at pcH 8.7. In the IP21 Reak solutions falls from log c = -4.7 at pcH 9 to log c = -5.1 at pcH 9.6. the next experimental point is at pcH 10.5 and shows the same concentration level. The nature of the solid phase was not determined, but during the experiments the initially white suspension turned black when alkali was added. The results suggest that at least two different Sn(II) solids are present. The solubility of both minerals depends on the pcH.

Modelling of the two solubility series in IP21 and IP21 Reak solutions lead to tin concentrations that are only roughly in the same order of magnitude (formation of Sn(IV) was supressed). The main features of the solubility curves are not predicted correctly. Up to pcH 7.7 the calculated solubilities are too high by up to two orders of magnitude. The fall and rise of tin(II) concentrations between pcH 6.5 and 8.5 is not represented at all.

The decrease of the solubility between pcH 8 and 9.5 is shown but at a level approximately 1.5 log units too low. Several reasons may lead to this disparity: At lower pcH a

mixed solid of unknown composition may have formed (probably including magnesium). The solid compound at higher pcH could be romarchite, SnO, but the difference between experimental and calculated solubilities needs to be further investigated. Allowing Sn(IV) in the calculations (but supressing crystalline SnO_2 and $CaSn(OH)_6$ and a fixed p_{H2} of 10^{-10} bar) causes even lower concentrations
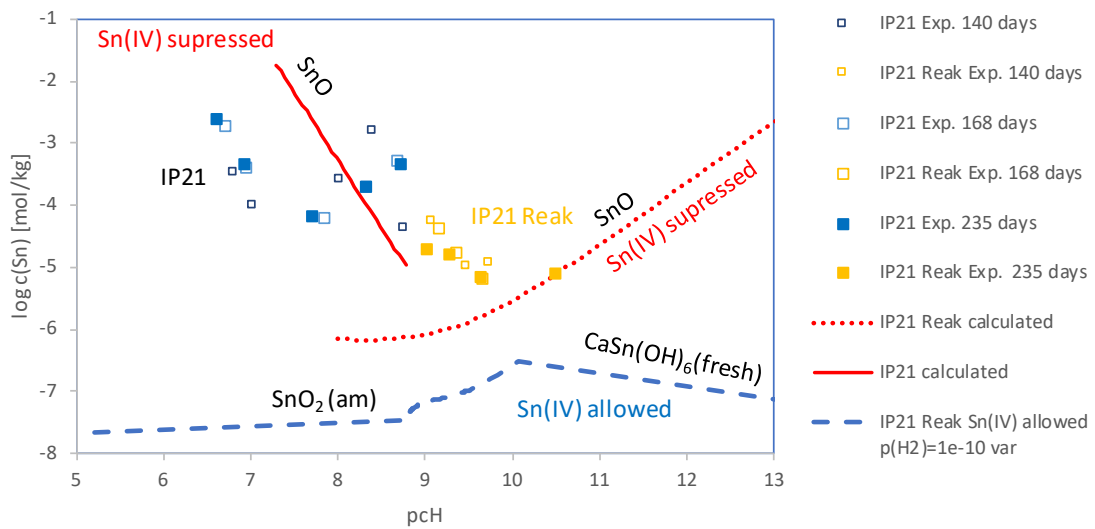
Fig. 8.42 Solubility of Sn(II) in IP21 solution

Based on the analytical findings the following solubility limits are proposed:

pcH 6-8: --4.7 to 0* (min exp. pcH 6.6)

pcH 8-10: -5.7 to -2.8

pcH 10-12: -5.7 to -3* (max. pcH 10.5)

Further research is needed to:

- Determine the solubility of Sn(II) at pcH <6.5 and >10.5
- Identify the solubility limiting solids in the full pcH range
- Determine the dominating Sn(II) species
- Check the importance of mixed halide hydroxide complexes at medium pcH

8.9.10 Solubility of tin(IV) in IP21 solution

For the experiments with tin (IV) amorphous $SnO_2 \cdot xH_2O$ was used as a starting material. In IP21 solutions up to pcH 8.2 the solubility of tin(IV) was constant in the range log c = -5.1±0.3. No clear pcH dependence could be observed. In IP21 Reak solutions, all tin concentrations were below the detection limit log c = -8.8 (Fig. 8.43). XRD of the solid residues at the end of the experiments did not reveal a clear picture of the present Sn phases. There were weak indications of SnO_2 and $CaSn(OH)_6$. There were no hints to schoenfliesite, $MgSn(OH)_6$.

The calculated solubility of tin in IP21 and IP21 Reak solutions differ considerably from the experimental values. In IP21 solutions with pcH <9 the experimental value are about 2.5 log units higher (around log c = -5). This is one log unit higher than in IP9 and two log units higher than in halite/ anhydrite saturated solutions. Obviously, magnesium has an impact on the tin(IV) solubility from slightly neutral to moderately alkaline solutions, even though only the uncharged $Sn(OH)_4(aq)$ is calculated to be the dominating species. The formation of colloids or ternary complexes may explain this behaviour (see discussion under IP9 solution).

At higher pcH values, an increase of the solubility is predicted whereas in IP21 Reak solutions tin could not be detected. Formation of insoluble magnesium hydroxo stannate(IV), $MgSn(OH)_6$ could be an explanation but would need further analytical confirmation.

Based on the analytical findings the following solubility limits are proposed:

pcH 6-8: -5.8 to -4.3 (min exp. pcH 6.5)

pcH 8-10: -9.3 to -4.5 (lower limit based on limit of quantification -8.8)

pcH 10-10.2: -9.3 to -8.3(no exp., limits based on limit of quantification -8.8)

Further research is needed to:

- Determine the solubility limiting phase at pcH >8.5
- Determine the Sn concentration at pcH >8.5
- Determine the solubility constant of schoenfliesite
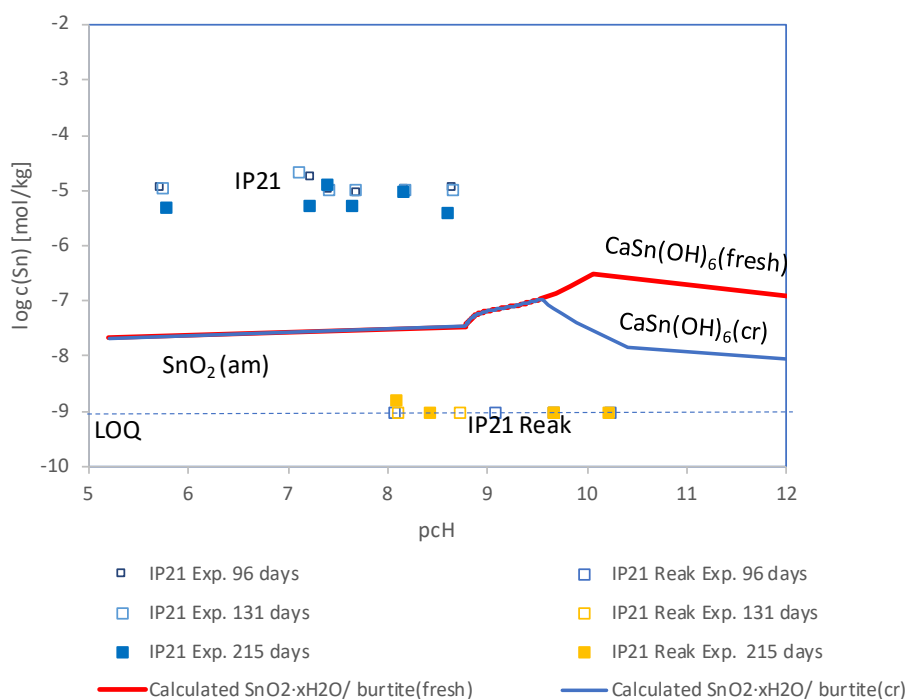
Fig. 8.43 Solubility of Sn(IV) in IP21 solution

8.9.11 Solubility of zirconium in IP21 solution

The experiments were conducted with amorphous $ZrO_2 \cdot H_2O$. At all pcH values (6.9 to 10.4) the zirconium concentration scattered around log c = – 6.1±0.3. Only after the first of three samplings some Zr concentration were below the limit of quantification. The equilibrium phase was not determined but it may be assumed that it was the same uni-dentified phase that also occurred in other salt systems, probably $ZrO_2 \cdot xH_2O$.

The calculated solubility curve predicted a zirconium concentration of about log c = -8 (aged $ZrO_2 \cdot xH_2O$) or to log c = -6.7 log units (fresh $Zr(OH)_4$). Only at the highest pcH values the concentration may increase a little bit due to the formation of ternary Ca com-plexes.
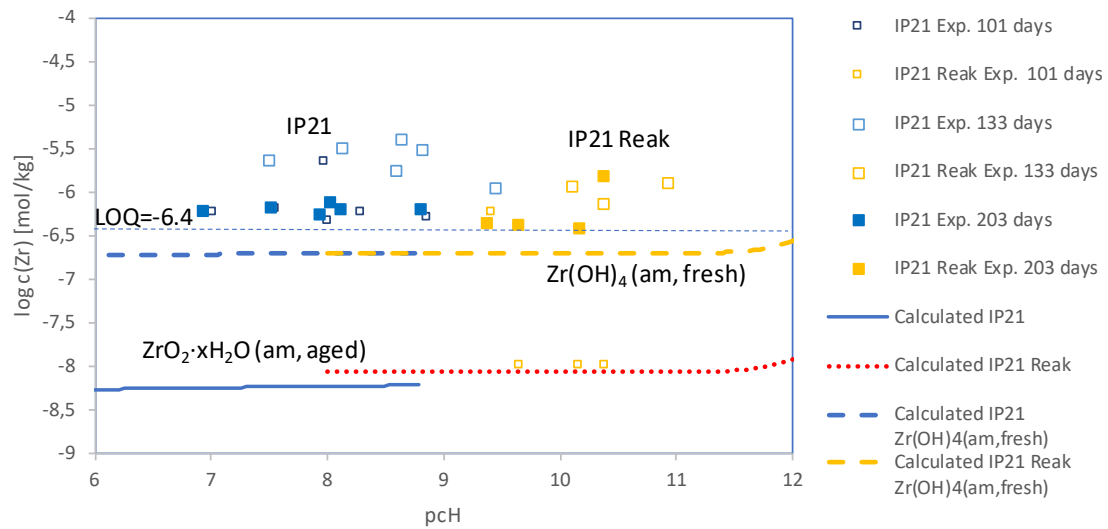
Fig. 8.44   Solubility of Zr in IP21 solution

Based on the analytical findings the following solubility limits are proposed:

pcH 6-8: -6.8** to -5.6** (min exp. pcH 6.96)

pcH 8-10: -6.8 to -5.6

pcH 10-12: -7.0** to -5.3** (max pcH 10.4)

Some questions should be answered by future research:

- Solubility of zirconium at pcH >10.4
- Identity of the solid phase
- Impact of ultrafiltration on the analytical Zr concentration

8.10 Solubility of fission products in model pore water in Lower Cretaceous clay pore water (UK water)

8.10.1 Solubility of lead in UK water

The starting material was laurionite, PbClOH. It was not found in the solid residue after the end of the experiments. Instead, the XRD analysis indicated $PbCl_2$ (cotunnite), KPb_2Cl_3 (challacolloite) and hydrocerussite ($Pb_3(CO_3)_2(OH)_2$). Only in the experiment with portlandite, laurionite was identified at pcH near 12. The solubility of lead decreased between pcH 7.4 and 9.8. At higher pcH values an increase could be observed.

According to geochemical modelling, the three minerals phosgenite $PbCl_2(CO_3)_2$, laurionite, $PbCl(OH)$ and blixite, $3PbO \cdot PbCl_2 \cdot H_2O$ are the solubility limiting phases in this system. None of the three phases found in XRD are even close to saturation at any pcH.

The solubility curve resembles the characteristics of the experimental data but exceeds the analytical values by about 0.5 log units up to pcH 9.5. At higher pcH values, especially between pcH 10 and 12 the difference increases to about 1-2 log units (Fig. 8.45). Several reasons may lead to this behaviour. The solubility of blixite has been investigated only a few times and has resulted in quite scattered data, so that the solubility branch at higher pcH may be higher (or lower). Another effect not accounted for is the impact of the considerable Ca^{2+} concentration on the complex $Pb(OH)_3^-$ that dominates above pcH 11. Ion interaction between the two species may be relevant but a far more serious effect would be caused by the formation of a ternary complex, e.g. $CaPb(OH)_3^+$. So far, such species have not been described, but the existence of ternary calcium complexes with trivalent actinides (Am(III), Cm(III), /NEC 09/) and neodymium may be an indication that analogue complexes with lead also exist. Suppression of blixite in the modelling leads only to a small increase of Pb concentrations at high pcH (not shown) and cannot explain the gap alone.

The increased lead concentration at moderately alkaline pcH is found in all solution types but is most prominent in UK water. According to the simplified model used in the calculations, the dominating species $PbCl_3^-$ and $PbCl_4^{2-}$ are replaced by $PbOH^+$ and $Pb(OH)_2$ at pcH 10 and higher. A more plausible explanation would be that mixed chlorohydroxo complexes are formed by stepwise substitution of chloride ions:

214

Sufficient evidence exists that support the existence of such mixed complexes, but so far, derived stability constants were not reliable enough /HAG 12/. Some tests were performed by including the mixed hydroxochloro complexes PbCl(OH)(aq), $PbCl_2(OH)_2^{2-}$ and $PbCl(OH)_2^{-}$. Stability constants were derived using the statistical method of Fedorov et al. (1979) /FED 79/ and by applying the Pitzer ion interaction coefficients for $PbCl_3^{-}$ and $Pb(OH)_3^{-}$ to $PbCl_2(OH)_2^{2-}$ and $Pb(OH)_3^{-}$, respectively. While the total lead concentration increased slightly in the region pcH 9 to pcH 11, the test model could not explain the much higher gap at lower and higher pcH values (not shown in Fig. 8.45).
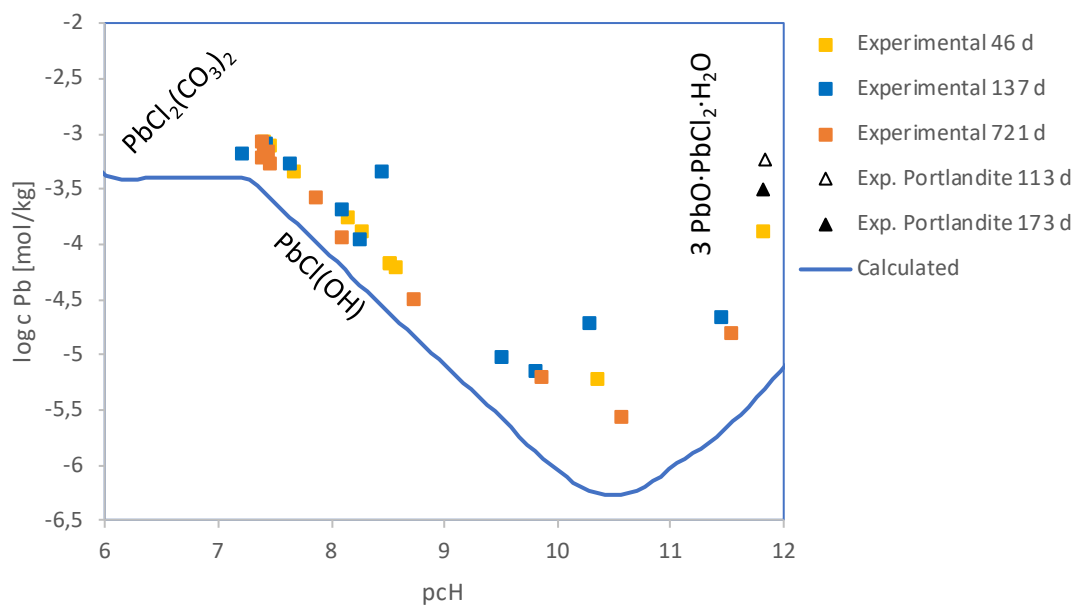
Fig. 8.45 Solubility of lead in UK water

Based on the experimental data we derived the following solubility limits:

pcH 6-8: -4.5 to -2.6* (min. exp. pcH 7.5)

pcH 8-10: -5.7 to -3.1

pcH 10-12: -6.1 to -2.7 (max pcH 11.8)

Further work will be necessary to

- Identify the solid lead phases in equilibrium with UK water

- Check whether ternary calcium lead hydroxide complexes contribute to higher lead solubilities at pcH >10
- Investigate the relevance of mixed chloro hydroxo complexes and verify the applicability of models (e.g. /FED 79/) to estimate their stability

8.10.2 Solubility of molybdenum(VI) in UK water

For the experiments with molybdenum(VI) $CaMoO_4$ was used as the starting substance. During the tests in the GRS laboratory, two samples were initially taken after 46 and 140 days. It turned out that the molybdenum concentration was not yet stable. Therefore, the experiments were continued, and another sample was taken after 482 days. These yielded slightly lower values (Fig. 8.46). The molybdenum concentrations decreased from sample to sample by about 30-40 %. Whether the last measured values (1.6 to 4 10^{-5} mol/kg) describe a lower limit cannot be said. Powellite was found as solid phase in each case.

In all measurements, a weak relationship between solubility and pcH was observed, at least at values pcH <9. In log units, it amounts to a maximum of 0.07 log c/ pcH and is too small to justify the presence of OH$^-$ or H$^+$ in the reaction equation. The dependence decreases with increasing ageing of the samples. The speed of ageing may depend on the pH value.
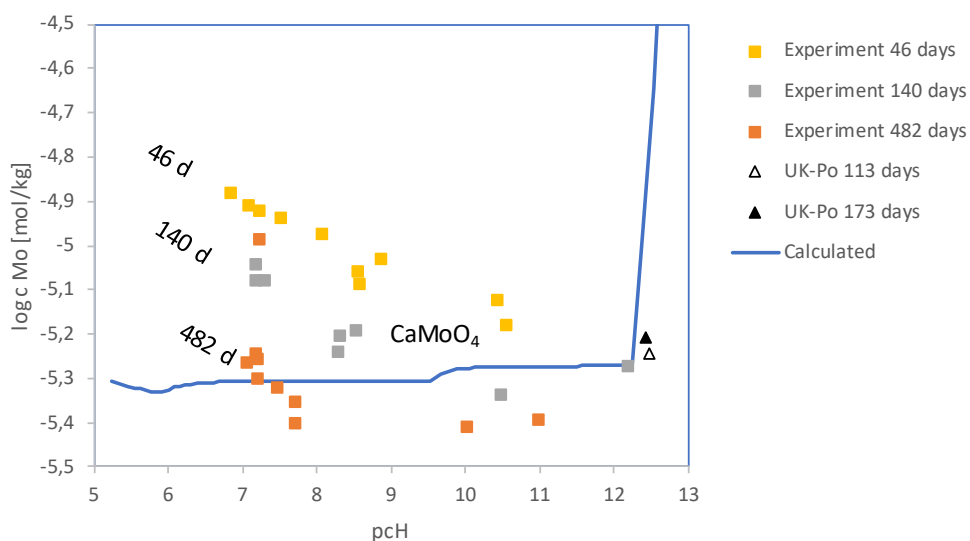
Fig. 8.46 Solubility of molybdenum (VI) in UK water

In the whole pcH range between 6.8 and 11.1, the calculated solubility is very close to the observed values. A closer look shows that Felmy et al. /FEL 92/used freshly prepared $CaMoO_4$ and the experiments lasted a maximum of 36 days. The establishment of equilibrium in our samples took considerably longer. This shows that aged samples have a slightly lower solubility constant than assumed by Felmy et al..

The following solubility limits were derived:

pcH 6-8: -5.9** to -4.3** (min pcH 7.0, upper limit constructed from measurements after 46 days, lower limit from measurements after 482 days)

pcH 8-10: -6.0 to -4.6

pcH 10-12: -6.0 to -4.6 (max pcH 11.0)

The illustrations show that there are still some open questions regarding molybdenum:

- Solubility of powellite after long equilibration periods (> 1.5 years)

8.10.3   Solubility of nickel in UK water

The starting material was nickel hydroxide, $Ni(OH)_2$. It could also be detected in the sample by XRD. Between pcH 7.3 and 8.9 the solubility of nickel decreased with a linear trend from log c = -0.1 to 4.6 mol/kg. A higher pcH values the solubility increased again and reached log c= -3.6 at pcH 11.5. (Fig. 8.47).
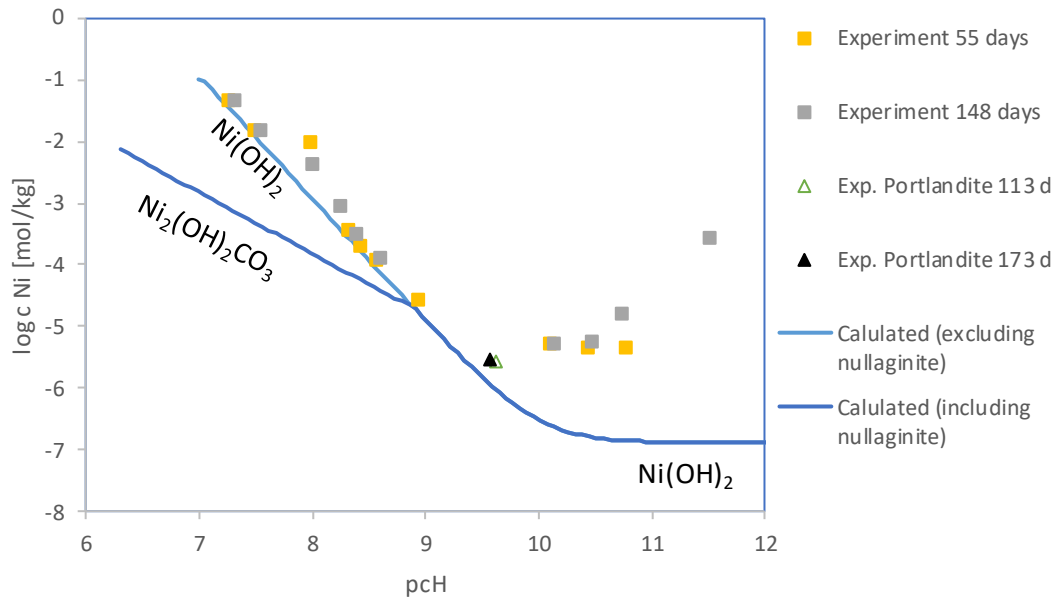
Fig. 8.47   Solubility of nickel in UK water

The modelling showed that the experimental data up to pcH 9.5 are best represented if Ni(OH)$_2$ is assumed as the only relevant solid phase (Fig. 8.47). A calculated solubility line with nullaginite would have the wrong pcH dependence (slope about -1 instead of -2). Either the nullaginite solubility is different, or the mineral does not form out of kinetical reasons.

At pcH 10 and higher the predicted solubility is constant whereas in the experiment it increases strongly with a slope +1. The reason for that behaviour is not clear. Higher hydroxo (Ni(OH)$_3^-$) or carbonato (NiCO$_3$(aq)) complexes are not relevant in this pcH range. An explanation could be ternary complexes between nickel, calcium, and hydroxide.

Based on the experimental results we derived the following solubility limits:

pcH 6-8: -3.5 to 0* (min pcH 7.3)

pcH 8-10: -6.1 to -1.5

pcH 10-12: -6.1 to -2.2** (max pcH 11.5)

More information is needed on the following issues:

- Solubility of nullaginite and other nickel carbonates
- Composition of the dominating nickel species at pcH >9

8.10.4   Solubility of niobium in UK water

Amorphous niobium oxide hydrate was used as starting material. Slow processes prevented the establishment of equilibrium solutions beyond pcH 10.5. After 229 days the observed niobium solubility was only slightly lower than after 104 days. No niobium could be quantified in batches with a pcH below 8.5. Above this value the solubility of Nb increased slightly up to pcH 9.5 (from about -7 to -6.5 log units). After that point a small decrease could be observed (Fig. 8.48). The nature of the solid has not been determined.

The model of Talerico et al. /TAL 04/roughly describes the solution behaviour of niobium in UK water. The predicted solubilities are up to one log unit too low, especially at higher pcH values.
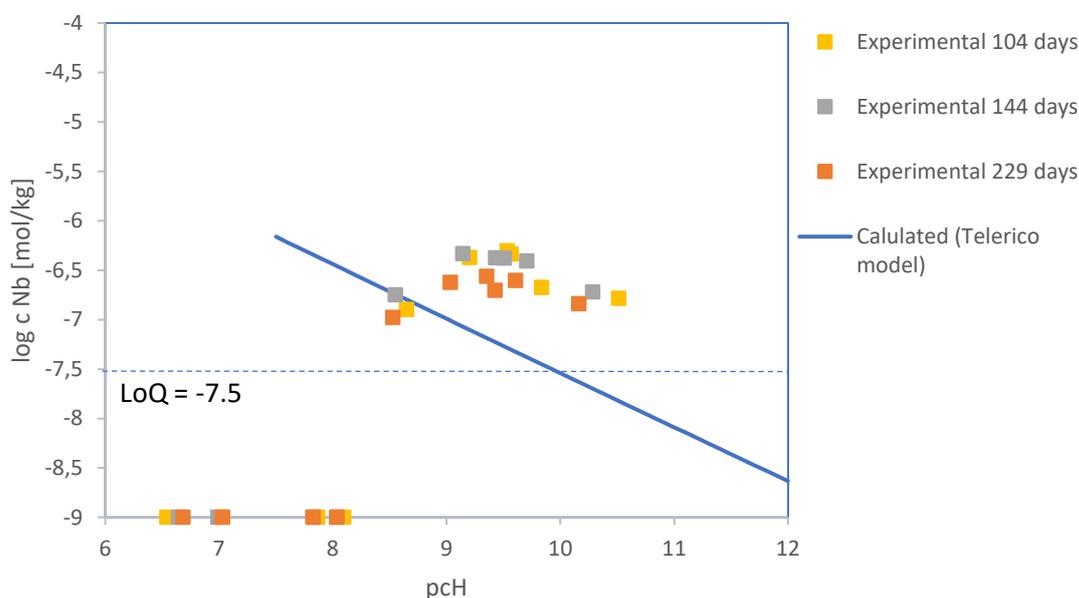
Fig. 8.48   Solubility of niobium in UK water

Based on the experimental results we derived the following solubility limits:

pcH 6-8: -8** to -7** (min pcH 6.5, based on limit of quantification at -7.5)

pcH 8-10: -8 to -5.8

pcH 10-10.2: -7.4** to -6.2** (max pcH 10.5)

More information is needed on the following issues:

- Solubility of niobium at pcH >10.5 and below pcH 7
- Identity of the solubility limiting phase in the relevant pcH range
- Complex formation and solubility of niobium species and phases

8.10.5   Solubility of palladium (II) in UK water

The experiments in this system were started by dissolving $PdCl_2$ in UK water. No palladium phases were saturated up to pcH 7.1. At higher pcH the solubilities are ordered in a 'V' curve with a minimum of log c = -6 around pcH 10 followed by a rise of concentrations.

The calculated solubilities were in very good agreement with the experimental data up to pcH 9.5. At this point the observed solubility curve flattens and soon rises again while the modelled values still decrease and find a minimum near pcH 10.9. The gap between both lines amounts to nearly three log units, an effect that cannot be explained by activity coefficients alone. A similar but weaker gap was observed in HalAnh solutions. In IP21 solutions the experiments didn't stretch far enough into the alkaline region. It seems plausible that complex formation led to the high increase of Pd concentration above pcH 10, similar to the effect found in the analogue Ni system. However, strong carbonate complexes (binary or ternary) cannot be excluded either, but so far, no data on the stability of Pd(II) carbonate complexes could be found that would allow an evaluation of this effect.

Based on the experimental results and the modelling we derived the following solubility limits:

pcH 6-8: -3.8 to 0*

pcH 8-10: -6.5 to -2.9

pcH 10-11.3: -6.5 to -2.5** (max pcH 11.3)

The following open points need to be addressed by future research:

- Solubility of palladium hydroxide at pcH >10 in the presence of calcium and potassium chloride
- Stability of Pd(II) carbonate complexes
- Solubility of CaPd(OH)$_4$
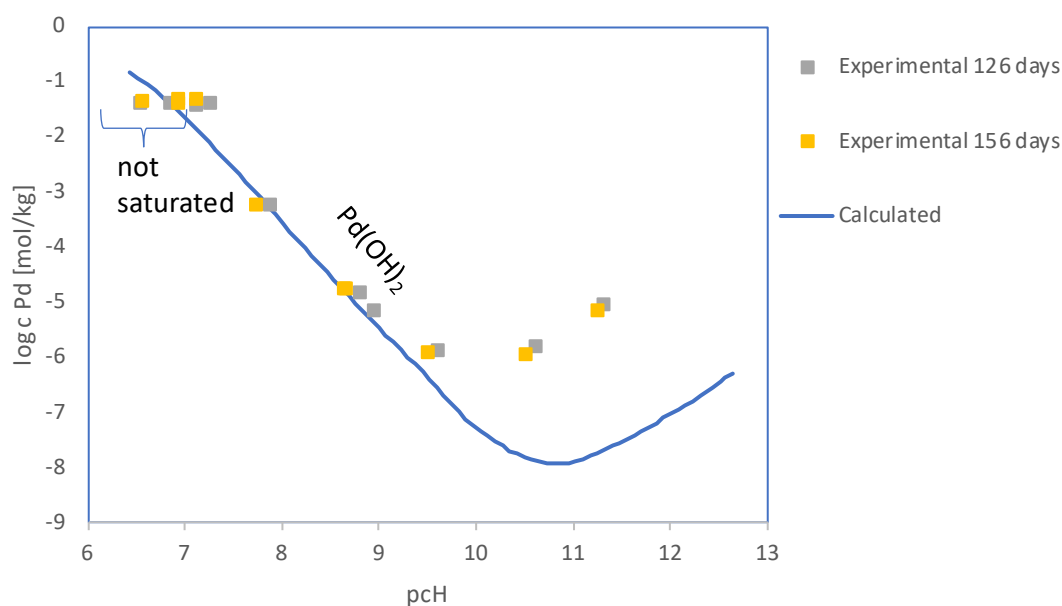
Fig. 8.49   Solubility of palladium(II) in UK water

8.10.6   Solubility of samarium in UK water

This experiment was started with Sm(OH)$_3$. The samarium concentrations decreased continuously from about log c = -6 at pcH 6.5 to log c = -8 at pcH 9.5. At higher pcH values the Sm concentration dropped below the limit of quantification (-8.8). The composition of the solid phase was not determined.

Modelling the solubility of samarium in UK water led to a very similar concentration curve. Until about pcH 8.5 Sm(OH)CO$_3 \cdot 0.5 H_2O$ is the solubility determining phase, after that Sm(OH)$_3$. The calculated concentrations correspond very well with the observed values.

221

If the minerals hydroxylbastnäsite-Sm and kozoite-Sm are permitted, the solubility of Sm would be about 1.8 log units lower than observed in the experiment. It needs to be clarified which of the three phases Sm(OH)CO$_3$·0.5H$_2$O, kozoite-Sm, hydroxylbastnäsite-Sm are stable in the long term and which stability they have.
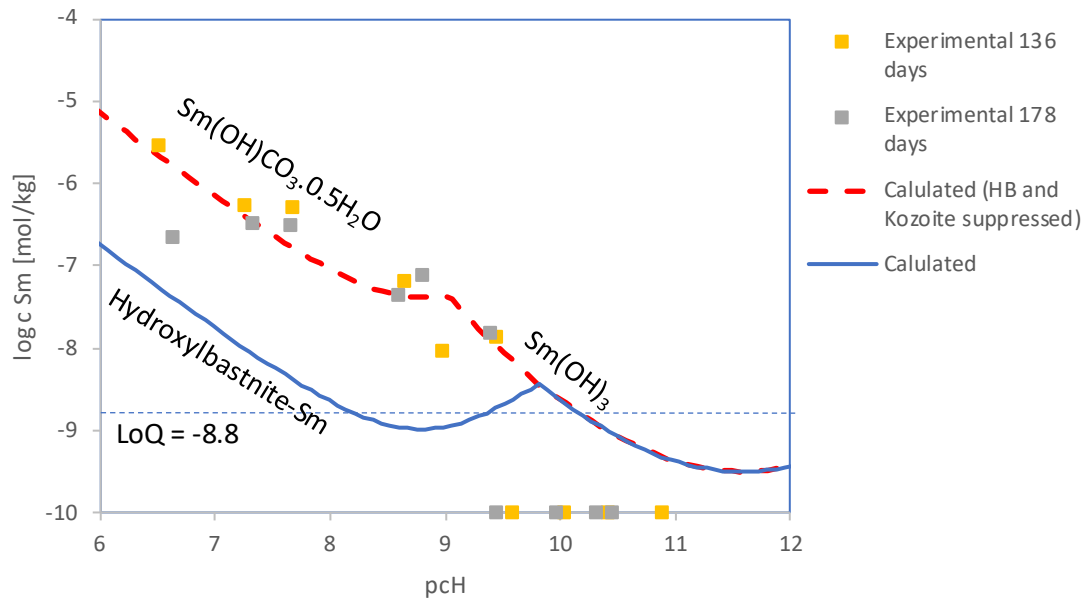
Fig. 8.50   Solubility of samarium in UK water

Based on the experimental results and the modelling we derived the following solubility limits:

pcH 6-8: -7.5 to -4.5** (min. exp. pcH 6.5)

pcH 8-10: ≤-8.8 to -6.3

pcH 10-12: ≤-8.8 to -8.0 (max. exp. pcH 10.9)

The following open points need to be addressed by future research:

- Identity of the solubility limiting Sm phase in the relevant pcH range
- Solubility constant of Sm(OH)CO$_3$·0.5H$_2$O, kozoite-Sm and hydroxylbastnäsite-Sm
- Solubility of Sm at pcH >9.4

222

8.10.7 Solubility of selenium(IV) in UK water

The experiments were started with $CaSeO_3$. The solubility decreased continuously from log c -2.2 to -3.7 between pcH 6 and 9. At higher pcH values the concentration of selenium remained constant. The modelled solubility line agrees perfectly with the data from our experiments (Fig. 8.51) but predicts a decline above pcH 12 when $Ca_2SeO_3(OH)_2 \cdot 2H_2O$ becomes saturated.

The derived solubility limits are

pcH 6-8: -4.2 to -1.7

pcH 8-10: -4.4 to -3.1

pcH 10-12: -4.5* to -3.3* (max pcH 10.7)

Some additional work needs to be done:

- Extension of the experimental investigation to pcH >10.7
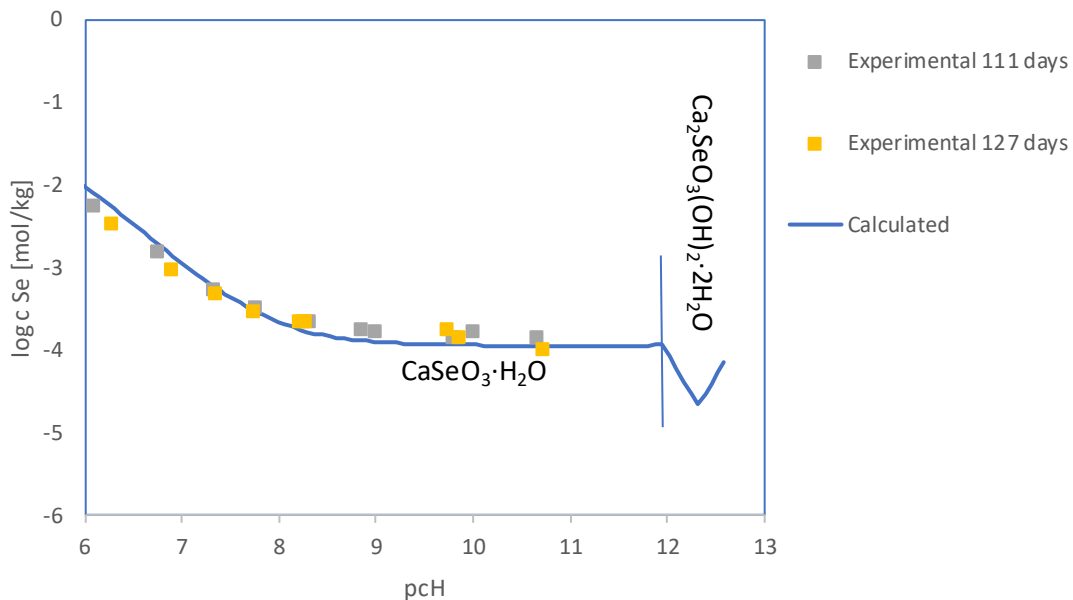
Fig. 8.51 Solubility of selenium(IV) in UK water

8.10.8 Solubility of silver in UK water

Two datapoints were experimentally determined to characterize the solubility of AgI in IP9 solutions. Both gave similar results: log c = -5.38±0.03 at pcH 7.9 and 9.5 (Fig. 8.52) and led to the following solubility limits:

pcH 6-8: -5.9** to -4.9** (min pcH 7.9)

pcH 8-10: -5.9** to -4.9** (max pcH 9.5)

pcH 10-12: -5.9** to -4.9** (no exp.)

If the concentration of iodide is not sufficient to completely fixate silver in AgI, the higher solubility of AgCl needs to be considered. If UK water is simplified to a 3.08 m NaCl solution (based on its chloride content using the same approximation method as for the HalAnh solution), the solubility of AgCl would be approximately log c = -2.8. The solubility limit would then be:

pcH 6-12: -3.3** to -2.3**
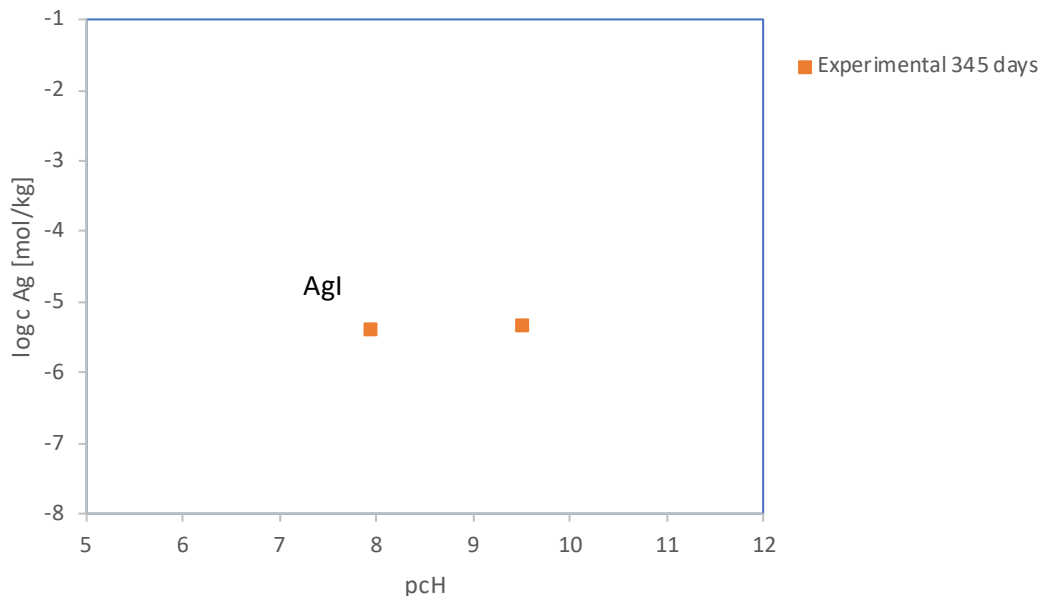
Fig. 8.52 Solubility of silver in UK water

224

8.10.9   Solubility of strontium in UK water

The starting material in this series was celestine, $SrSO_4$. It was also found throughout at all pcH values. The solubility of strontium remained constant at log c -2.7 ± 0.1. Only in the experiment with portlandite the value was lsightly higher (Fig. 8.53).

The calculated solubility of Sr corresponds with the laboratory values at all pcH. The solubility limit would be

pcH 6-8: -3.2 to -2.0* (min pcH 7.0)

pcH 8-10: -3.2 to -2.2

pcH 10-12: -3.8 to -2.2 (max pcH 11.8)
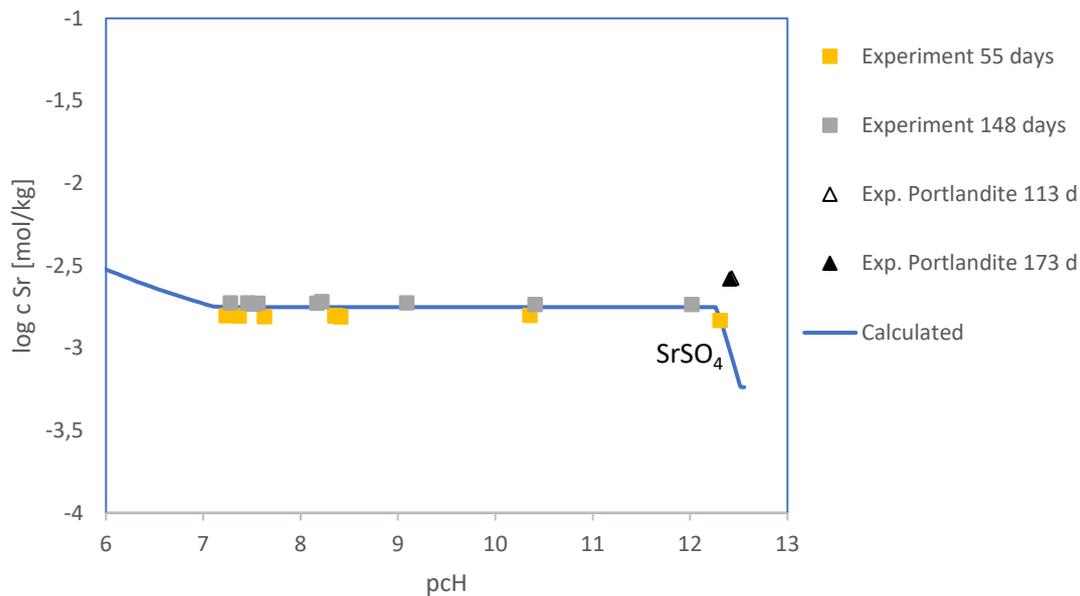
Fig. 8.53   Solubility of strontium in UK water

8.10.10   Solubility of tin(II) in UK water

The experiment was started with UK Water with added $SnCl_2 \cdot 2H_2O$. In all batches, slow processes lead to a shift of the equilibrium pcH. The effect was especially visible in the alkaline region where a OH^- consuming reaction caused a change of pcH of one unit and

more. Frequent adjustment of the pcH could not stop the process so that the final pcH range was limited from pcH 5.9 to 9.6.

In the acidic region, from pcH 5.9 to 7.2 the solubility of tin(II) was reduced from log c = -6.7 to -7.2. From here on the concentrations of tin increased almost linearly to log c = -6.2 at pcH 9.6. Measurements of earlier samples extended the range to pcH 10.6. They show the same linear trend.

The modelling of the system (only Sn(II) was allowed) shows, in principle, the same feature: decrease of solubility up to pcH 7, increase at higher values. Romarchite would be the equilibrium mineral at all relevant pcH levels. But the predicted tin concentration is considerably lower up to pcH 8 (up to 1.5 log units). In this region, $Sn(OH)_2$(aq) is calculated as the dominating species. Most probably, mixed chloro hydroxo complex occur instead as has been shown for Pd^{2+}. But even then, the tabulated stability of this neutral complex is probably too high because an extended solubility plateau as shown in the modelling cannot be seen in the experiment.

It is interesting to see that the modelling results were much closer to the experimental results if Sn(IV) was allowed to form, at least in the neutral to slightly alkaline region. In that case, also the slight bend in the solubility line at about pcH -8.7 was reflected in the calculated concentrations (change from SnO_2(am) to $CaSn(OH)_6$(fresh)). This might be coincidence especially because at higher pcH values there is no calculated increase of Sn solubilities.

The solubility limits would be:

pcH 6-8: -7.8 to -6.2 (min pcH 7.0)

pcH 8-10: -7.7 to -5.6

pcH 10-12: -6.6 to -3.0** (max. pcH 10.7)

Further work is necessary to:

- Determine the solubility of tin(II) at pcH >9.6
- Check the relevance of mixed tin(II) chloro hydroxide complexes
- Identify the solubility controlling solid phases
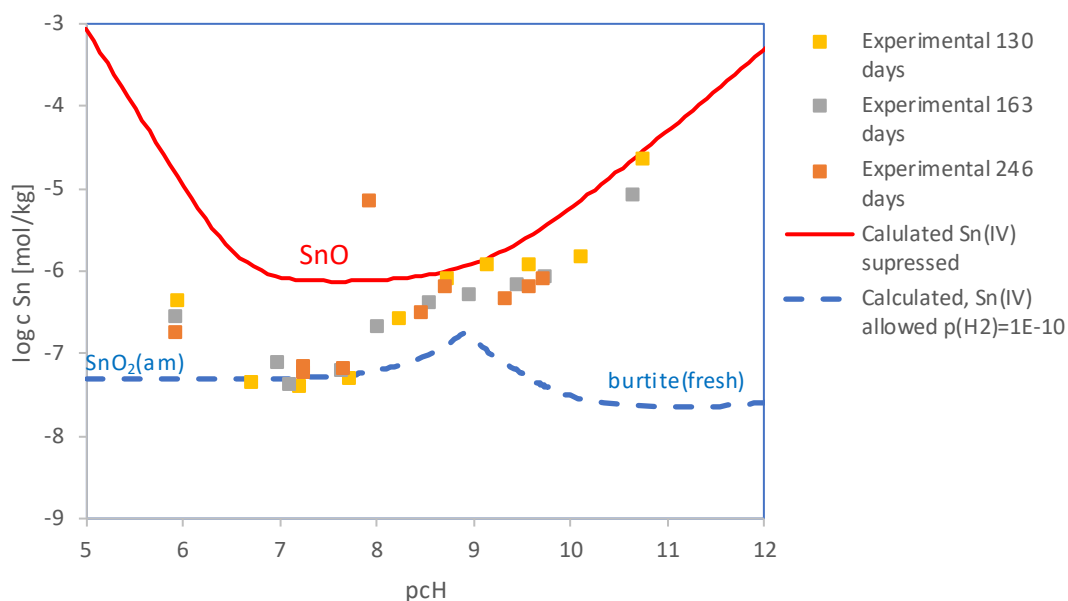
Fig. 8.54   Solubility of tin(II) in UK water

8.10.11   Solubility of tin(IV) in UK water

The starting material in this series was tin hydroxide, $Sn(OH)_4$. Due to its amorphous structure, it is not detectable in XRD. Instead, burtite, a calcium stannate with the formula $CaSn(OH)_6$ was identified. In the UK-Portlandite experiment no tin phase could be found. In three samples around pcH 7 the tin concentration was below the limit of quantification (10^{-7} mol/kg). Between pcH 7.5 and 9.7 the solubility rose to about $2 \cdot 10^{-6}$ mol/kg, but in the same pcH range (9.3 to 9.9) another solubility branch became visible that suggests a decreasing solubility. The scattering of data was quite strong, so that it is not clear whether this is an arbitrary or systematic effect (Fig. 8.55).

The calculated solubility of tin is about 1 to 2 of units below the experimental results if fresh burtite is assumed to be present and up to 3 if aged burtite is allowed to precipitate. A strong increase of tin solubility is calculated for pcH >12 because the precipitation of portlandite reduces the aqueous calcium concentration. Obviously, there is an impact of the calcium concentration on the tin solubility (see discussion above) that cannot be accounted for with the current model. The incomplete separation of colloids from the solution may have impacted the experimental results.

The following solubility limits are proposed for tin(IV):

pcH 7.1-8: ≤-7.5 to -5.9 (min. exp. pcH 7.1)

pcH 8-10: -7.2 to -5.1

pcH 10-12: -7.2 to -5.5

Additional efforts are needed to:

- Identify the tin(IV) species that lead to an increase of the total tin concentration at all pcH values
- Close the experimental gaps between pcH 10 and 12
- Identify the solubility limiting phase in experiments with pcH >10
- Check whether stannate(IV) also forms aqueous complexes with Ca^{2+}, analogously to Zr(IV). Th(IV) and Pu(IV).
- Perform ultrafiltration to exclude colloids
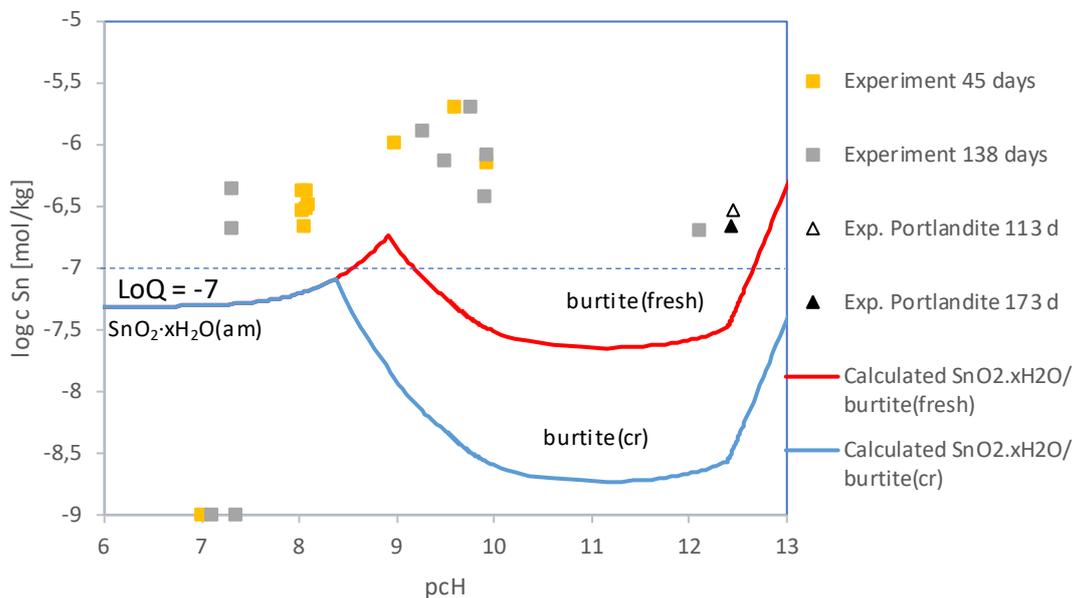
Fig. 8.55 Solubility of tin(IV) in UK water

8.10.12   Solubility of zirconium (IV) in UK water

The observed solubility of zirconium in UK water was nearly constant at all pcH (7.0 to 11.2). After 143 days it amounted to log c = -6.1 ± 0.1.

The experimental Zr concentrations were above the calculated solubilities of $ZrO_2 \cdot xH_2O$(am, aged) and $ZrO_2 \cdot xH_2O$(am, fresh), at least in the range pcH 7 to 10. At higher OH^- concentrations the zirconium solubilities are expected to increase due to the formation of ternary calcium complexes. However, such a development was not observed in the experiments up to pcH 11.2. There is no obvious effect of the low carbonate concentrations ($<10^{-4}$ molal at pcH >8) on the solubility or Zr. The situation may be different in the pcH region not experimentally covered. At pcH below 7, formation of the mixed hydroxo carbonate complex $Zr(OH)_2CO_3^{2-}$ contributed strongly to the total zirconium solubility. Unfortunately, no experimental data point covered this area.

Based on the experimental results and the predictions we derived the following solubility limits:

pcH 6-8: -6.8** to -5.4** (min pcH 7.0)

pcH 8-10: -6.8 to -5.4

pcH 10-12: -6.8 to -3.8* (max pcH 11.2)

The calculated solubility of $ZrO_2 \cdot xH_2O$(am, fresh) was chosen as the upper limit.

Some questions should be answered by future research:

- Solubility of zirconium at pcH >11.2
- Relevance of binary and ternary zirconium carbonate complexes in UK water
- Relevance and stability of zirconium carbonato complexes in saline waters
- Identity of the solid phase
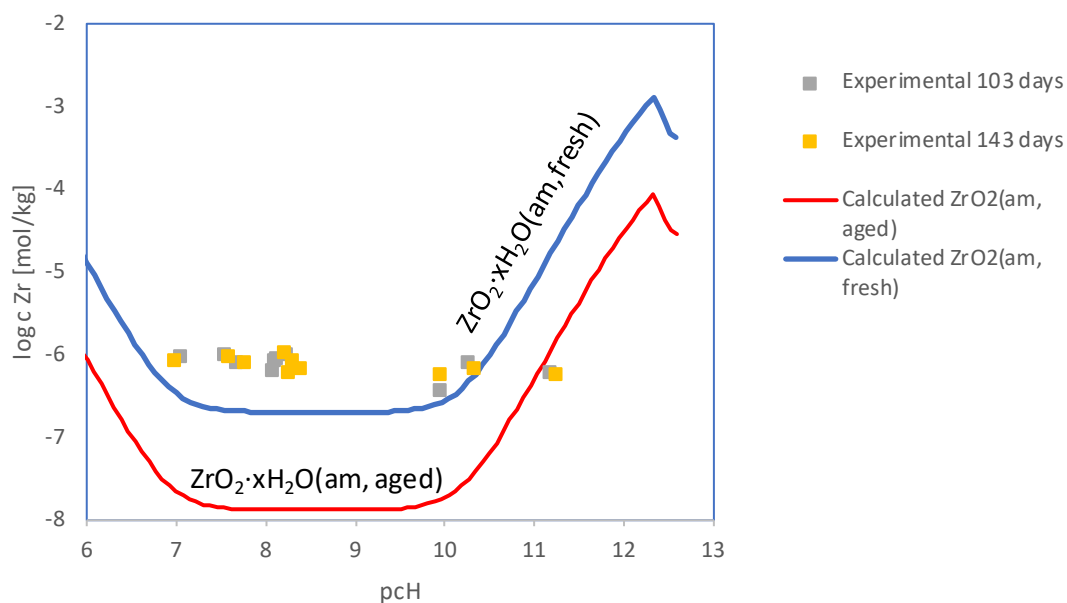
Fig. 8.56 Solubility of zirconium in UK water

8.11 Summary of solubility limits

8.11.1 Solubility limits determined in this study

Based on the experimental findings, solubility limits were derived for slightly acidic to strongly alkaline pcH ranges in UK water, and halite/ anhydrite, IP9, and IP21 solutions (Tab. 8.6 to Tab. 8.9). A safety margin of 0.5 log units was added to all analytically found concentration maxima and minima to take account of analytical uncertainties or lack of equilibrium. If a pcH range was not covered by the experiments, it was marked as 'no exp.' (no experiments). In some cases, the solid phase in equilibrium with the solution could not be identified. These are marked as 'n.i.' (not identified). Solubility limits are marked with an asterisk (*) if the experimental pcH range did not cover the full range, but modelling allowed an extrapolation. If the modelling did not allow an extrapolation be-cause the results deviated too much from the observed values, experimental results, if applicable, were used to determine the solubilities at the limits of the respective pcH range. Such values are indicated with two asterisks (**). If no extrapolation could be done because modelling was not trustworthy in the pcH region and experimental results gave no clear picture, the applicable pcH range is expressed explicitly.

Abbreviations used in the tables

- 0: no solubility limit
- min. pcH: minimal experimental pcH
- max. pcH: maximal experimental pcH
- no exp.: no experimental data in this pcH range
- n.i.: solid phase not identified
- * modelled solubilities are used to extrapolate the solubility to the limits of the respective pcH range
- ** experimental solubilities are extrapolated to determine the solubility limit

Tab. 8.6   Solubility limits in halite/ anhydrite saturated brine

Element	log c [mol/kg] pcH 6-8	log c [mol/kg] pcH 8-10	log c [mol/kg] pcH 10-12	Solubility limiting phase
Ag(I)	AgI: -4.4** to -3.4** (min pcH 7.95) AgCl: -2.5** to -1.5** (no exp.)	AgI: -4.4 to -3.4 AgCl: -2.5** to -1.5** (no exp.)	AgI: -4.4** to -3.4** (max pcH 10.8) AgCl: -2.5** to -1.5** (no exp.)	AgI (if $n_I \geq n_{Ag}$) AgCl (if $n_I < n_{Ag}$)
Cs(I)	0	0	0	none
Mo(IV)	-8.7 to -4.5	-8.7 to -4.5	-8.7 to -1.7 (max pcH 11)	MoO_2?
Mo(VI)	-5.9 to -4.5	-5.9 to -4.5	-5.9 to – 4.5* (max pcH 11.2)	$CaMoO_4$
Ni(II)	-2.9* to 0*	-6.6 to -2.0	-6.7* to -5.5* (max. pcH 10.4)	$Ni(OH)_2$
Nb(V)	-8.2 to -6 (min pcH 7.7)	-8.2 to -6	-7.7** to -6** (max. pcH 11.5)	$CaNb_4O_{11} \cdot 8H_2O$?
Pb(II)	-3.5 to -0.5	-4.5 to -2.0	-5.5 to -3.0	PbClOH
Pd(II)	0	-6.4** to 0*	-6.4 to -5.0** (max pcH 11.9)	$Pd(OH)_2$?
Rb(I)	0	0	0	none
Se(-II)	-7.5 to -4.2	-7.0 to -4.1	-5.3 to -4.1 (max. pcH 10.6)	$FeSe_{1.04}$?
Se (IV)	-3.9 to -2.7 (min pcH 7.81)	-4.3 to -2.7	-4.3* to -2.7* (max. pcH 10.8)	$CaSeO_3$
Sm(III)	0	-8.1 to -2.9* (min. pcH 9.0)	-9.3 to -5.2	$Sm(OH)_2Cl$, $Sm(OH)_3$?
Sn(II)	-6.6 to -2* (min. pcH 7.6)	-6.7 to -4.1	-5.2 to -2.0** (max. pcH 11.5)	$Sn_{21}Cl_{16}(OH)_{14}O_6$, SnO?
Sn(IV)	-8.2* to -6.2* (min pcH 7.6)	-8.2 to -6.1	-8.3** to -6.3**	$Sn(OH)_4$? $CaSn(OH)_6$?
Sr(II)	-3.9* to -2.8* (min pcH 7.4)	-3.9 to -2.8	-3.9 to -2.8	$SrSO_4$
Zr(IV)	-7.2 to – 6.0 (min pcH 7.7)	-7.2 to – 6.0	-7.2* to -4.8*	$ZrO_2 \cdot xH_2O$ (am, aged) ?

Tab. 8.7   Minimum solubility in halite/ anhydrite saturated brine in the presence metallic iron or $Fe(OH)_2$

Element	log c [mol/kg] pcH 6-8	log c [mol/kg] pcH 8-10	log c [mol/kg] pcH 10-12	Expected solubility limiting phase
Ag	-7	-7	-7	Ag(cr)
Cs	0	0	0	none
Mo	-7.2	-7.2	-6.3	MoO_2(am)
Ni	-9.2	-12.9	-13.2	Ni(cr)
Nb	-8.2	-8.2	-7.7	$CaNb_4O_{11} \cdot 8H_2O$?
Pb	-7.3	-11.4	-15	Pb(cr)
Pd	-31.6	-35.7	-37.9	Pd(cr)
Rb	0	0	0	none
Se	-11.8	-10.2	-9	$FeSe_{1.04}$
Sm	0	-8.1	-9.3	$Sm(OH)_2Cl/$ $Sm(OH)_3$
Sn	-8.2	-8.2	-8.3	SnO_2(am)
Sr	-3.9	-3.9	-3.9	$SrSO_4$
Zr	-7.2	-7.2	-7.2	$ZrO_2 \cdot xH_2O$ (am, aged)

Tab. 8.8   Solubility limits in IP9 solution

Ele-ment	log c [mol/kg] pcH 6-8	log c [mol/kg] pcH 8-10	log c [mol/kg] pcH 10-12	Solubility limiting phase
Ag(I)	AgI: -4.3** to -3.3** (no exp.) AgCl: -2.4** to -1.4** (no exp.)	AgI: -4.3 to -3.3 (min pcH 8.4) AgCl: -2.4** to -1.4** (no exp.)	AgI: -4.3** to -3.3** (max pcH 10.1) AgCl: -2.4** to -1.4** (no exp.)	AgI (if $n_I \geq n_{Ag}$) AgCl (if $n_I < n_{Ag}$)
Cs	0	0	0	none
Mo(VI)	-4.7* to -3.5* (min pcH 6.8)	-5.1 to -3.5	-5.1* to -4.1* (max pcH 11.6)	$CaMoO_4$
Ni	-2.6 To 0* (min pcH 8)	-6.5 to -1.5	-7.4 to -4.9	$Ni(OH)_2$
Pb	-2.3* to -1.0* (no exp.)	-4.8 to -1.3* (min pcH 8.5)	-6.1* to -4.1 (max pcH 11.5)	$K_2Pb(SO_4)_2$? PbClOH
Rb	0	0	0	none
Sn(IV)	-6.4** to -4.7** (min pcH 7.3)	-6.9 to -4.7	-7.2* to -5.7* (max pcH 11.5)	$SnO_2 \cdot xH_2O$? $CaSn(OH)_6(cr)$?
Sr	-5.1* to -3.5*	-5.1 to -3.5	-5.1 to -3.5	$SrSO_4$

Tab. 8.9   Solubility limits in IP21 solution

Ele-ment	log c [mol/kg] pcH 6-8	log c [mol/kg] pcH 8-10	log c [mol/kg] pcH 10-12	Solubility limiting phase
Ag(I)	AgI: -4.2** to -3.2** (min pcH 7.4) AgCl: -2.3** to -1.3** (no exp.)	AgI: -4.2 to -3.2 AgCl: -2.3** to -1.3** (no exp.)	AgI: -4.2** to -3.2** (max pcH 10.3) AgCl: -2.3** to -1.3** (no exp.)	AgI (if $n_I \geq n_{Ag}$) AgCl (if $n_I < n_{Ag}$)
Cs	0	0	0	None
Mo(VI)	-4.1 to -2.9	-4.9 to -2.9 (max pcH 9.9)	-4.9* to -3.7* (no exp.)	$CaMoO_4$?
Nb	≤-7.9 to -5.6	-7.6 to -4.3 (max pcH 9.3)	-6.1** to -1.5** (no exp.)	$CaNb_4O_{11} \cdot 8H_2O$?
Ni	-2.6 to 0* (min pcH 7)	-7.1 to -1.5	-7.1* to -4.8* (max pcH 10)	$Ni(OH)_2$?
Pb	-2.1* to -1.0* (min pcH 6.3)	-4.4* to -1.1 (max pcH 9.8)	-6.3* to -2.7 (no exp.)	$KCl \cdot 2PbCl_2$?/ $PbCl(OH)$?
Pd	0	-6.8** to -2.0**	Not determined (no exp.)	$Pd(OH)_2$?
Rb	0	0	0	none
Se(IV)	-2.8 to -0.6	-3.4 to -1.7	-3.5 to -2.3 (max. pcH 11.1)	$MgSeO_3.6H_2O$?/ $CaSeO_3 \cdot H_2O$
Sr	-5.2* to -4.1* (min pcH 6.5)	-5.3 to -3.4 (max pcH 9.6)	-4.9** to -3.2* (no exp.)	$SrSO_4$?
Sn(II)	-4.7 to 0* (min pcH 6.6)	-5.7 to -2.8	-5.7 to -3*(max. pcH 10.5)	SnO?
Sn(IV)	-5.8 to -4.3	-9.3 to -4.5	- 9.3 to -8.3 (max pcH 10.2)	$SnO_2 \cdot xH_2O$?
Zr	-6.8** to -5.6** (min pcH 6.96)	-6.8 to -5.6	-7.0** to -5.3** (max pcH 10.4)	$ZrO_2 \cdot xH_2O$?

Tab. 8.10 Solubility limits in Lower Cretaceous model pore (UK) water

Ele-ment	log c [mol/kg] pcH 6-8	log c [mol/kg] pcH 8-10	log c [mol/kg] pcH 10-12.5	Solubility limiting phase
Ag(I)	AgI: -5.9** to -4.9** (min pcH 7.9) AgCl: -3.3** to -2.3** (no exp.)	AgI: -5.9** to -4.9** (max pcH 9.5) AgCl: -3.3** to -3.3** (no exp.)	AgI: -5.9** to -4.9** (no exp.) AgCl: -3.3** to -2.3** (no exp.)	AgI (if $n_I \geq n_{Ag}$) AgCl (if $n_I < n_{Ag}$)
Cs	0	0	0	none
Mo(VI)	-5.9** to -4.3** (min. pcH 7.0)	-6.0 to -4.6	-6.0 to -4.6 (max pcH 11.0)	$CaMoO_4$
Ni	-3.5 to 0* (min pcH 7.3)	-6.1 to -1.5	-6.1 to -2.2** (max. pcH 11.5)	$Ni(OH)_2$
Nb	-8** to -7** (min. pcH 6.5)	-8 to -5.8	-7.4** to -6.2** (max pcH 10.2)	?
Pb	-4.5 to -2.6* (min. pcH 7.5)	-5.7 to -3.1	-6.1 to -2.7 (max. pcH 11.8)	$PbCl_2(CO_3)_2$, PbClOH, $3PbO \cdot PbCl_2 \cdot H_2O$?
Pd	-3.8 to 0* (min pcH 6.9)	-6.5 to -2.9	-6.5 to -2.5** (max. pcH 11.3)	$Pd(OH)_2$?
Rb	0	0	0	none
Se(IV)	-4.2 to -1.7	-4.4 to -3.1	-4.5* to -3.3* (max pcH 10.7)	$CaSeO_3 \cdot H_2O$?
Sm	-7.2 to -4.5** (min. pcH 6.5)	-8.8 to -6.3	-8.8 to -8.0 (max pcH 10.9)	$Sm(OH)CO_3 \cdot 0.5H_2O$? $Sm(OH)CO_3$?
Sn(II)	-7.8 to -6.2	-7.7 to -5.6	-6.6 to -3.0** (max. pcH 10.7)	SnO?
Sn(IV)	-7.5 to -5.9 (min pcH 7.1)	-7.2 to -5.1	-7.2 to -5.5	$SnO_2 \cdot xH_2O$/ $CaSn(OH)_6$?
Sr	-3.2 to -2.0* (min pcH 7.3)	-3.2 to -2.2	-3.8 to -2.2	$SrSO_4$
Zr	-6.8** to -5.4** (min pcH 7.0)	-6.8 to -5.4	-6.8 to -3.8* (max pcH 11.2)	$ZrO_2 \cdot xH_2O$?

8.11.2   Comparison of solubility limits for a repository in salt rock

For salt rock formations, it is typically not known in advance which type of salt solutions may enter the disposal drift after a hypothetical consecutive failure of technical barriers. Principally, a range of solution compositions has to be considered (see discussion in chapter 2.3). In that case, solubility limits for a couple of solution types needs to be combined to allow for a whole picture of possible solubility characteristics. Although UK water is not a solution that would occur in a salt rock formation, its rather high calcium concentration represents a feature of many naturally occurring brines that is not covered by halite/ anhydrite saturated, IP9 or IP21 solution. UK water is therefore included in the comparison.

Tab. 8.11 summarizes the data from Tab. 8.6 to Tab. 8.10 and also combines solubility limits for different oxidation states. Which oxidation states have to be considered in the long-term needs to be investigated in more detail because purely thermodynamic considerations do not necessarily reflect the real behaviour of elements. Certain reduction, oxidation, or disproportion processes may not take place because of slow kinetics. It should be noted that solubility experiments have not been conducted for all oxidation state/ solution type combinations. Only few experimental gaps remain for these elements so that little change is expected when such experiments were conducted. Due to the very similar chemical behaviour of rare earth elements, the solubility limits of europium were assumed to be identical to those of samarium.

This new set of solubilities was compared with previous data from Buhmann et al. /BUH 91/and Kienzler et al. /KIE 12/ (Tab. 8.12). For simplicity, only data for moderately alkaline solutions are considered. Following container corrosion, the pcH is expected to increase but buffered by the presence of magnesium both in potentially inflowing solutions or in the crushed salt used as backfill. Another buffering process is the equilibrium between the iron corrosion phases $Fe(OH)_3Cl$ and $Fe(OH)_2$. PcH values around 8 to 10 are considered to be likely in that case. In addition, calculations from Kienzler et al. on the maximum, inventory driven radionuclide concentration in disposal drifts are included. While it is not likely that all waste material gets dissolved in the rather low volumes of brines that could fill the pores of the backfill in a drift, the numbers represent a 'natural' concentration maximum.

A visual comparison of previous and current solubility limits shows that the upper solubility limit could be reduced for six elements (Fig. 8.57). This includes molybdenum,

nickel, niobium, samarium, strontium, and tin. Only for palladium the upper limit of the solubility limit needs to be increased. For caesium, iodine, rubidium, selenium, and zirconium the upper limits remained the same or nearly the same. For silver and lead, solubility limits were derived for the first time. No new limits were derived for cobalt, europium, and radium. At least for Eu, the solubility limits for Sm may be adapted as a good guess. The confidence interval was extended for nearly all elements, mainly because new lower solubility limits were determined. That especially applies to those elements that may be reduced to the metallic state in the presence of metallic iron or iron(II) hydroxide (silver, lead, nickel, palladium).

If the calculated inventory controlled maximum radionuclide concentrations for clay rock (this work) and salt rock /KIE 12/ are taken as an orientation, Cs, I, Rb and Ag (only clay) are probably inventory-controlled. All other elements may be solubility limited.

The new solubility limits cannot directly be compared with literature data on foreign repository projects because the geochemical conditions are always different. One of the solution compositions considered in Canada (NaCl/ $CaCl_2$ I=4.5, /DUR 10/) comes at least close to the compositions in 'HalAnh' and in the 'UK' solutions. The solubility limits in this source are also listed in Tab. 8.12. For Nb, Se, Sn, and Zr the values are within the confidence interval derived in the present study. For Pd and Pb, the solubility was considered unlimited. For molybdenum, the solubility was thought to be eight orders of magnitudes lower than the lower limit of our confidence interval. That is mainly because the thermodynamically very stable MoO_2 was considered as the solubility limiting phase. As our experiments show, the actual solubility of Mo(IV) this phase is considerably higher even if MoO_2 is used as a starting material. This is a good example for the potentially harmful effect of using tabulated thermochemical data to derive real world equilibrium concentrations. In individual cases, they can feign a strong retention of elements that in reality are much more mobile. Without at least some experimental solubility investigations to proof the validity of thermodynamic data no conclusion should be drawn about solubility limiting processes.

Tab. 8.11 Solubility limits in unspecified neutral to alkaline brines in salt rock formations (halite/ anhydrite saturated, IP9, IP21, UK water) with iron possibly present

Element	pcH 6-8	pcH 8-10	pcH 10-12
Ag	-7* to -1.3** (min pcH 7.95)	-7* to -1.3**	-7* to -1.3**
Co	No data	No data	No data
Cs	0	0	0
Eu (1)	0	-8.1 to -2.9* (min. pcH 9.0)	-9.3 to -5.2
I	0	0	0
Mo	-8.7 to -2.9	-8.7 to -2.9	IV: -8.7 to -1.7 max pcH 10.9)
Nb	-8.2 to -5.6 (min pcH 7.7)	-8.2 to -4.3	-7.7** to -1.5 (max. pcH 11.5)
Ni	-9.2* to 0*	-12.9* to -2.0	-13.2* to -4.8* (max. pcH 10.4)
Pb	-7.3* to -0.5	-11.4* to -2.0	-15 to -3.0
Pd	-31.6* - 0	-35.7* to 0*	-37.9* to -5.0** (max pcH 11.9)
Ra	No data	No data	No data
Rb	0	0	0
Se	-11.8* to 0	-10.2* to 0	-9 to 0
Sm	0	-8.1 to -2.9* (min. pcH 9.0)	-9.3 to -5.2
Sn	-8.2* to -2	-9.3 to -2.1	-9.3 to -2.0 (max. pcH 11.5)
Sr	-5.1* to -2.8* (min pcH 7.4)	-5.1 to -2.8	-5.1 to -2.8
Zr	-7.2 to – 5.6 (min pcH 7.7)	-7.2 to – 5.6	-7.2 to -4.8*

(1) assumed to be identical with Sm

Tab. 8.12 Comparison of solubility limits for moderately alkaline brines (halite/ anhydrite saturated, IP9 or IP21) in the presence of Fe(cr) (highlighted in green: if upper new solubility limit is below previously reported, highlighted in red, if new limits are higher)

Element	Buhmann et al. (1991) "alkaline"	Kienzler et al. pcH 9	Canada I=4.50 pH 8.1 (SR-270 NF)	This study pcH 8-10	Clay rock CSD-V [log mol/l]	Clay rock SF [log mol/l]	Inventory controlled [mol/l] /KIE 12/
Ag	No data	No data	No data	-7 to -1.3	-6.7	-7.0	No data
Co	-7 to -1	No data	No data	No data	No data	No data	No data
Cs	0	No data	No data	0	-2.1	-2.2	-2.3
Eu[1]	-7 to -1	No data	No data	**-8.1 to -2.9**	No data	No data	-2.4
I	0	No data	No data	0	-2.6	-2.8	-2.2
Mo	-7 to -1	No data	**-16.2**	**-8.7 to -2.9**	-7.7	-6.0	-0.8
Nb	-7 to -1	No data	**-6.7**	**-8.2 to -4.3**	-7.4	-3.4	-5.1
Ni	-7 to -1	No data	No data	**-12.9 to -2.0**	-6.0	-3.0	No data
Pb	No data	No data	0	-11.4 to -2.0	No data	No data	No data
Pd	-7 to -1	No data	0	-35.7 to 0	-2.4	-2.5	-1.5
Ra	No data	No data	-4.8	No data	-10.5	-10.4	No data
Rb	0	No data	No data	0	-2.2	-2.4	-1.8
Se	-8 to 0	No data	-8.8	-10.2 to 0	-3.8	-4.1	-2.6
Sm	-7 to -1	-4.5 to -4	No data	**-8.1 to -2.9**	-2.4	-2.7	-1.6
Sn	-7 to -1	No data	**-7.0**	**-9.3 to -2.1**	-3.1	-3.3	-2.7
Sr	-6 to 0	No data	No data	**-5.1 to -2.8**	-2.7	-2.7	-1.8
Zr	-10 to -4	-6	-9.3 to -7.7	-7.2 to – 5.6	-1.8	-2.0	-0.7

(1) assumed to be identical with Sm
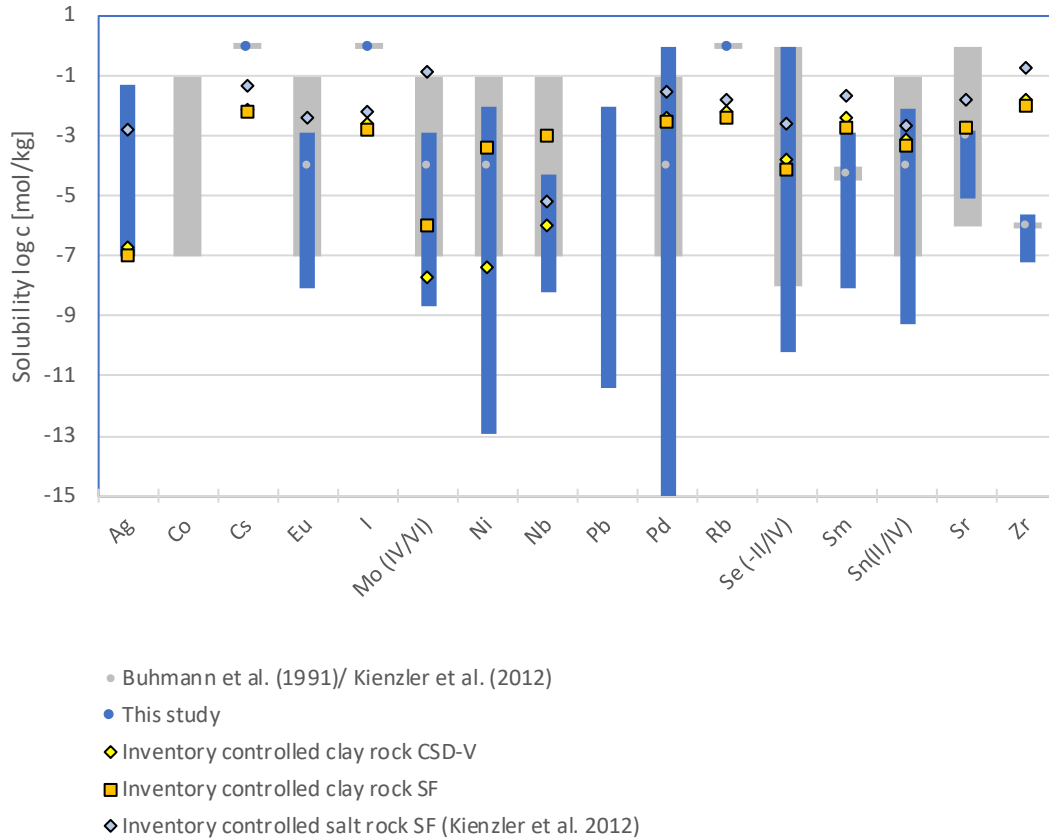
Fig. 8.57 Comparison of solubility limits for radionuclides in salt rock formations

8.12 Summary of knowledge gaps that should be addressed in future research

Tab. 8.13 contains an overview of thermodynamic properties and chemical processes that require additional attention in order to reduce uncertainties in the prediction of radionuclide solution behaviour.

Tab. 8.13 Summary of identified knowledge gaps (Al to Mo(IV))

Element	Experimental	Identity and stability of aqueous complexes	Stability of solid phases	Ion interaction coefficients
All	- Oxidation state of radionuclides in waste forms and oxidation state after release from the waste matrix - Impact of bromide and borates on the solubility - Inventory of fission and activation products in nuclear waste (including inactive isotopes)	Bromo and borato complexes Stability of mixed complexes (also by using estimation methods) Stability of ternary Ca/Mg – M- OH complexes	Bromides Stability of mixed hydroxide (chloride/ sulphate/ carbonate compounds) (also by using estimation methods)	Bromide, borates Reliable estimation methods for unknown interaction coefficients
Ag(0)	Kinetics of Ag(I) reduction to Ag(0) in saline media	Ag(aq)	Solubility of elemental silver	
Ag(I)	More solubility data for HalAnh, IP9, IP21 and UK	$AgCl_3^{2-}$, $AgCl_4^{3-}$		$Na^+/K^+/Mg^{2+}/Ca^{2+}$ - $AgCl(aq)$, $AgCl_2^-$, $AgCl_3^{2-}$
Mo(III)	Relevance of Mo(III) in a repository system. Solubility in salt solutions Mo corrosion products and oxidations states of Mo containing steels	$Mo(OH)_3(aq)$, $Mo(OH)_4^-$	$Mo(OH)_3$	$Na^+/K^+/Mg^{2+}$ - $Mo(OH)_4^-$
Mo(IV)	Solubility of MoO_2/ $MoO_2.xH_2O$ under defined redox conditions Reduction/ oxidation processes under saline conditions Solubility in IP9, IP21 and UK	$Mo(OH)_4(aq)$, $Mo(OH)_6^{2-}$ possibly ternary complex with Ca^{2+}	HalAnh: Identity of solubility limiting phase $MoO_2.xH_2O$	$Na^+/K^+/Mg^{2+}$ - $Mo(OH)6^{2-}$

Tab. 8.14 Summary of identified knowledge gaps (Mo(V) to Ni)

Element	Experimental	Identity and stability of aqueous complexes	Stability of solid phases	Ion interaction coefficients
Mo(V)	Relevance of Mo(V) in aqueous solutions under reducing conditions	$MoO_2(OH)_{1+x}^{-x}$	$MoO_2(OH).xH_2O$	$Na^+/K^+/Mg^{2+}$ - $MoO_2(OH)_2^-$
Mo(VI)	IP21: solubility at pcH >9.9 Reduction of Mo(VI) in the presence of corroding steel	$CaMoO_4(aq)$ $MgMoO_4(aq)$		K^+/Mg^{2+}-MoO_4^{2-}
Nb	IP21: solubility at pcH >9.3. UK: solubility at pcH <7 and pcH >10.5. All solutions: Identity of solid phase with Ca present or absent. Check the influence of ultrafiltration on analytical results Solubility in IP9 solution	Nature of dominating species between pcH 6 and 12	Nature of solubility limiting phases in salt solutions Validate or, if necessary, extend the empirical model of Talerico et al (2004) at high ionic strength	$Na^+/K^+/Mg^{2+}/Ca^{2+}$ - all dominating Nb species
Ni	Hal/ Anh: solubility at pcH >10.4 IP21: solubility at pcH >10. Identity of solid phase Kinetics of Ni(II) reduction to Ni(0) in saline media	Nature of dominating species at pcH > 9, Stability of $Ni(OH)_3^-$	$Ni_2(OH)Cl_3$ Mixed Ni(II)/Fe(II) phases Nullaginite and other nickel carbonates	Na^+/K^+ - $Ni(OH)_{2(aq)}$

Tab. 8.15   Summary of identified knowledge gaps (Pb to Se(0))

Element	Experimental	Identity and stability of aqueous complexes	Stability of solid phases	Ion interaction coefficients
Pb	Hal /Anh: solubility at pcH <9.2 and >10.8 Nature of solid phase at pcH >10.7 IP9: solubility at pcH <8.5 IP21: solubility at pcH >9.8 UK: Nature of the solid phase Kinetics of reduction in the presence of Fe(s) or Fe(II) corrosion phases	Mixed chloro hydroxo complexes Ternary Calcium lead hydroxo complexes	Blixite and other lead oxychlorides Symesite and other lead hydroxysulphates	$Ca^{2+}-Pb(OH)_3^-$
Pd	Hal/ Anh: solubility at 9< pcH <11 IP21: solubility at 6.8< pcH <8.6 and pcH > 9.6 UK: solubility at pcH >10 Kinetics of reduction in the presence of Fe(s) or Fe(II) corrosion phases. Solubility in IP9 solution Identity of the solubility limiting phase	Dominating species at high pcH and high chloride concentration Ternary Calcium and possibly magnesium Pd(II) hydroxo complexes carbonato complexes	$CaPd(OH)_4$ $MgPd(OH)_4(?)$	$Na+/K+/Ca^{2+}/Mg^{2+}$ - $Pd(Cl_xOH_y)$
Se(-II)	Solubility of FeSe under defined redox conditions Solubility in IP9, IP21 and UK	Acid dissociation constants of polyselanes, Fe(II) selenido complexes	Fe(II)selenides	$Na^+/K^+/Mg^{2+}$ - HSe^- $Na^+/K^+/Mg^{2+}$ - HSe_n^- $Na^+/K^+/Mg^{2+}$ - Se_n^{2-}
Se(0)	Solubility of selenium allotropes in equilibrium with Se(aq)	Composition of the aqueous Se(0) species		$Se(aq)/ Na^+, K^+, Mg^{2+}$

Tab. 8.16 Summary of identified knowledge gaps (Se(IV) to Sn(II))

Element	Experimental	Identity and stability of aqueous complexes	Stability of solid phases	Ion interaction coefficients
Se (IV)	Hal/ Anh: solubility at pcH >10.8 IP21: Identity of the solid phase UK: solubility at pcH >10.7	$CaSeO_3(aq)$, $MgSeO_3(aq)$	Transformation of Ca-$SeO_3 \cdot H_2O$ into $MgSeO_3 \cdot 5H_2O$	Na+/K+/Ca^{2+}/Mg^{2+}-$HSeO_3^-$ Mg^{2+}- SeO_3^{2-}
Sm	Hal/ Anh: solubility at pcH <9.0. IP21: Solubility in IP21 solutions UK: Solubility at pcH >9.4, All solutions: influence of ultrafiltration on analytical results, identity of solid phase. Solubility in IP9 solution	Ternary calcium samarium hydroxo complexes	$Sm(OH)CO_3 \cdot 0.5H_2O$, kozoite-Sm, hydroxylbastnäsite-Sm	
Sn(II)	Hal/ Anh: solubility at pcH <7.4. IP21: solubility at pcH <6.5 and pcH >10.5. UK: solubility at pcH >9.6 All solutions: nature of the solid phase Kinetics of disproportionation. Solubility in IP9 solution	Speciation at pcH >8 Mixed chloro/ hydroxo complexes $SnCO_3(aq)$ $Sn(OH)_2(aq)$ Ternary calcium tin(II) hydroxo complexes	$Sn_3O_2(OH)_2$	Na^+/K^+/Ca^{2+}/Mg^{2+}-$SnCl_3^-$ Na^+/K^+/Ca^{2+}/Mg^{2+}-$SnCl_4^{2-}$ Na^+/K^+/Ca^{2+} - $Sn(OH)_3^-$

Tab. 8.17 Summary of identified knowledge gaps (Sn(IV) to Zr)

Element	Experimental	Identity and stability of aqueous complexes	Stability of solid phases	Ion interaction coefficients
Sn(IV)	Hal/ Anh: solubility at pcH <7.6 IP21: solubility at pcH >8.5 UK: solubility at 10< pcH <12 All solutions: nature of the solid phase, influence of ultrafiltration on analytical results Chemical form of tin in nuclear waste	Ternary calcium tin(IV) hydroxo complexes Ternary magnesium tin(IV) hydroxo complexes Mixed chloro/ hydroxo complexes	Burtite, $CaSn(OH)_6$, schoenfliesite, $MgSn(OH)_6$ Influence of $MgCl_2$ concentration on the solubility of $SnO_2 \cdot xH_2O$	Na^+/K^+-$Sn(OH)_6^{2-}$
Sr	IP21: solubility at pcH >9.6.		Kalistrontite, $K_2Sr(SO_4)_2$	K^+/Mg^{2+}-Sr-SO_4
Zr	IP21: solubility at pcH >10.4 UK: solubility at pcH >11.2 All solutions: Identity of the solid phase, influence of ultrafiltration on analytical results	$Zr(OH)_4(aq)$, ternary calcium zirconium hydroxo complexes Ternary zirconium carbonato complexes		$Na^+/K^+/Ca^{2+}$ - Ca-Zr-OH complexes

9 Summary and outlook

Sequences of events in a repository system may lead to a contact of solutions with the emplaced waste containers. This will result in corrosion of the waste containers and other metallic components in the near field and will eventually lead to the failure of the containers and subsequent mobilisation of the radionuclides from the waste matrix. According to the present state of knowledge, even if the safety concept for a repository in a clay formation is consistently implemented, such developments are to be expected and have to be considered in a safety case. For the evaluation of these event sequences, a long-term safety analysis has to be performed.

The mobility of radionuclides along the migration path from the waste containers through the near field is often limited by solubility. In transport calculations, the maximum concentration a radionuclide may achieve taking into account solubility limiting and solubility enhancing chemical processes (complexation, retention in solid phases, etc.) is often expressed by so-called solubility limits. Usage of such limits allows to avoid the implementation of time-consuming chemical models in performance assessment codes.

Solubility limits are not rigid quantities but depend strongly on the local chemical environment (e.g., salinity, pH, redox status, presence of complexing ions). In probabilistic long-term safety analyses, the uncertainties regarding the chemical conditions and the specific chemical behaviour of radionuclides in the near-field are usually represented by confidence intervals. Low solubilities (and solubility limits) are not always an indication of overall safety because they may contribute to the accumulation of radionuclides at one place and potentially lead to criticality.

Solubility limits, which are applicable for Lower Cretaceous formations in Northern Germany, have not been derived so far. Therefore, the consideration of chemical retention effects in radionuclide dispersion calculations is currently not reliable. For repository sites in rock salt formations, current pH-dependent solubility limits are only available for important actinides (e.g., U, Pu, Th), technetium and zirconium. For other fission products, experimental investigations have not yet been carried out. The only relevant literature source on solubility limits in salt systems was prepared in the early 1990s. It was largely based on undocumented expert guesses and cannot be reliably used for future performance assessments. In the present study, solubility limits for relevant fission elements were estimated based on experimental investigations and additional thermodynamical modelling.

The following chemical elements were the subject of the present work: Ag, Cs, I, Mo, Nb, Ni, Pb, Pd, Rb, Se, Sm, Sn, Sr, and Zr. These elements are considered in long-term safety analyses, and some of them contribute to certain time ranges to the calculated indicator values for the evaluation of the safety of the containment of radionuclides. Only elements were considered which also contain non-radioactive isotopes so that an experimental investigation was possible in the GRS laboratory. Under the expected geochemical conditions in the near field, some elements can occur in several oxidation states whose solubility was determined separately. For the elements Mo, Se, and Sn, two different oxidation states were investigated separately.

As an introduction to the topic, solubility limits and solubility-determining solid phases from various international repository projects were compiled. Some of these studies also derived values for saline solutions which can serve as an orientation for solution types relevant for potential repository formations in Germany.

The composition of solutions that may occur in the near-field of a repository is always site-dependent. As no site for repositories for heat-generating waste has been defined in Germany yet, it is not possible to narrow down the range of possible compositions at present. For salt formations, a rough classification was carried out based on historical solution data from a large number of mainly central German salt mines. A total of ten solution types were described. The most frequent are solutions with a medium to high $MgCl_2$ content (about 1 to 4 mol/kg), sometimes also with considerable amounts of $CaCl_2$ (up to 1.9 mol/kg). Given the lack of published data for pore waters in northern German Lower Cretaceous clay, the range of possible solution compositions can only be estimated. Results of the parallelly completed project KOPRHA show that in formations of the Apt and older (≥ 113 million years old) the occurrence of strongly saline pore waters is highly probable, whereas in younger formations pore waters of rather low salinity are thought to prevail. The following solution types were selected for solubility experiments within this study:

- A model pore water, whose composition was calculated for a generic site in the Lower Cretaceous clay based on a salinity gradient encountered in Northern Germany. It is a NaCl/ $CaCl_2$ dominated solution which is in equilibrium with the minerals found in the clay. As a variant, an alkaline solution was used, which results from contact of the pore water with portlandite. This mineral is the main constituent of portlandite cement, which may be used for the lining of roadways and the sealing of boreholes.

- A salt solution saturated with halite and anhydrite

- IP21 solution, a solution rich in $MgCl_2$, which is formed by contact of salt solutions with the potash rocks sylvite, carnallite and kainite as well as Polyhalite. Solutions of similar composition also occur as limited solution reservoirs in salt formations, even if the above-mentioned potash rocks are not or only partially present in the environment. A reaction solution was used as a variant, which results when IP21 solution becomes more basic due to corrosion of iron and magnesium precipitation occurs.

- IP9 solution, which results from the dissolution of polyhalitic rock salt. It has an increased $MgCl_2$ content but is not saturated with potassium minerals. Solutions of this type are also frequently found in reservoirs. A variant was also used for the IP9 solution, which results from the precipitation of magnesium due to iron corrosion. A further variant describes an IP9 solution after contact with Sorel concrete, which is being discussed for road closures.

For the determination of the fission or activation product solubilities, the salt solutions mentioned were mixed with a suitable solid phase of the fission product (if possible, the one which is probably solubility-determining based on previous investigations). Subsequently, the pH value was changed to the target value by adding acid or base.

For most of the element/ solution combinations investigated, a pH-dependent solubility profile (pcH 6 to 12) could be established based on the experimental findings. In some cases, the planned pH spectrum could not be completely covered, because the pH values were too far away from the planned values due buffering and conversion processes. Where possible, the solubility determining solid phases were identified by X-ray diffraction. For some elements, however, a clear assignment was not possible, probably because only X-ray amorphous phases were present. This concerned experiments with palladium, molybdenum, samarium, tin, niobium, and zirconium.

The experiments and the derivation of the solubility limits were supported by geochemical modelling. Most of the thermodynamic data required for this purpose were not available as a database up to now. An orienting database was developed for most of the concerned chemical elements (with the exception of Ag and Nb). The THEREDA database was supplemented with available data from the literature and estimated model parameters to allow modelling in the relevant pH/ salinity range. For many elements, good

agreement was found between the models and the solubilities observed in the experiments.

Sometimes, assumptions had to be used which should be confirmed by additional scientific investigations. For a couple of element/ solution combinations uncertainties remained because the nature of the solubility-determining phases and the predominant solution species could not be determined. This became apparent in considerable deviations between experiment and modelling. Several approaches were discussed that allow the estimation of equilibrium constants and ion interaction coefficients. They have been applied for numerous species where an experimental was so far lacking. It is recommended to further develop, test, and qualify these methods so that they can be reliably used in the preparation of thermodynamic databases.

The impact of metallic iron or iron(II) corrosion phases on the solubility of some redox active elements was checked by means of geochemical modelling. It could be shown that the solubility of silver, palladium, lead, nickel and probably also selenium would be lower by many orders of magnitude if these elements are reduced to the elemental state as the thermodynamic data suggests. The presence of iron would have little impact on molybdenum solubilities. In the case of tin, the solubility may be higher if tin is present in the lower oxidation state. No definite judgement could be made for selenium because its solubility depends on the initial Fe/ Se ratio and the progress of iron corrosion. For all these six considered elements the kinetics of redox reaction in the presence of Fe(s) and Fe(II) corrosion phases is unknown. Speed and product of redox reactions need to be investigated further before credit could be taken from the predicted, often strongly reduced solubilities.

The newly determined solubility limits provide a more reliable basis to include chemical effects into performance assessment models. For many elements, the upper limit of the assumed solubility could be considerably reduced. Comparison with one set of solubility limits that has been derived for a saline system of a potential repository system in Canada showed consistency for many elements. In one case (molybdenum), the predicted solubility was thought to be eight orders of magnitudes lower than the lower limit of our confidence interval – even though the starting material in our experiments was the same as the considered solubility limiting phase in the Canadian study. This is a good example for the potentially harmful effect of using tabulated thermochemical data to derive real world equilibrium concentrations. Without at least some experimental solubility

investigations to proof the validity of thermodynamic data no conclusion should be drawn about solubility limiting processes.

Based on the experimental results and the current capabilities of geochemical modelling, this study identified critical knowledge gaps that should be addressed in future research activities. This includes the clarification of the following questions:

- For the redox-sensitive elements, e.g., molybdenum, selenium, silver, tin, palladium, it should be clarified which oxidation states can be expected after passing through a container corrosion zone.
- In some cases, the composition of the solubility determining phase is still unclear, e.g., for Sn(IV), Zr, Nb, Pd
- For some identified or assumed solid phases, solubility and solubility constant data are unreliable or not available, e.g., for $MoO_2 \cdot xH_2O$, $Na_2Sn(OH)_6$, $Ni(OH)_3Cl$
- For the relevant oxidation states, the species which predominate in the relevant pH range and in the solution types under consideration must be identified, e.g., Sn(IV) at higher pH values, Sn(II), Mo(III, IV, V), Nb
- For calcium-rich solutions, there are indications of the formation of ternary calcium hydroxide complexes, which strongly increase the solubility of fission elements in alkaline solutions. Such complexes are known for trivalent and tetravalent radionuclide ions, but for divalent metal ions their relevance should be examined more closely
- Interaction parameters are required which allow the calculation of activity coefficients of hydroxide and carbonate complexes. For some species, such parameters have already been derived by analogy methods. However, the database still contains relevant gaps, especially for hydroxide species of medium to heavy radionuclides where few suitable analogues exist. In such cases, interaction parameters should be estimated based on specific experimental investigations.

10 References

/D'A 08/   D'Ans, J.: Neutrale Tripelsulfate des Calciums. Ber. Dtsch. Chem. Ges., pp. 1777–1779, 1908.

/ABD 95/   Abdelouas, A., Crovisier, J. L., Lutze, W.: Structure and chemical properties of surface layers developed on R7T7 simulated nuclear waste altered in brine at 190 °C. Eur. J. Mineral., vol. 7, pp. 1101–1113, 1995.

/ABD 97/   Abdelouas, A., Crovisier, J. L., Lutze, W.: Surface layers on a borosilicate nuclear waste glass corroded in $MgCl_2$ solution. J. Nucl. Mater., vol. 240, pp. 100–111, 1997.

/ABR 90/   Abrajano, T. A.: Secondary phase formation during nuclear waste-glass dissolution. Clay. Clay Min., vol. 38, no. 5, pp. 537–548, 1990.

/AKS 60/   Akselrud', N. V., Spivakovskii, V. B.: Basic chloride and hydroxide of samarium. Russ. J. Inorg. Chem., vol. 5, pp. 163–167, 1960.

/ALF 20/   Alfarra, A., Bertrams, N., Bollingerfehr, W., Eickemeier, R., Flügge, J., Frenzel, B., Maßmann, J., Mayer, K.-M., Mönig, J., Mrugalla, S., Müller-Hoeppe, N., Reinhold, K., Rübel, A., Schubarth-Engelschall, N., et al.: RESUS. Grundlagen zur Bewertung eines Endlagersystems in einer Tongesteinsformation größerer Mächtigkeit. GRS-Ber., No. 571, 186 p., 2020.

/ALT 04/   Altmaier, M., Neck, V., Fanghänel, T.: Solubility and colloid formation of Th(IV) in concentrated NaCl and $MgCl_2$ solution. Radiochim. Acta, vol. 92, pp. 537–543, 2004.

/ALT 08/   Altmaier, M., Neck, V., Fanghänel, T.: Solubility of Zr(IV), Th(IV) and Pu(IV) hydrous oxides in $CaCl_2$ solutions and the formation of ternary Ca-M(IV)-OH complexes. Radiochim. Acta, vol. 96, No. 9-11, 2008.

/ALT 11/   Altmaier, M., Brendler, V., Bube, C., Neck, V., Marquardt, C., Moog, H. C., Richter, A., Scharge, T., Voigt, W., Wilhelm, S., Willms, T., Wollmann, G.: THEREDA - Thermodynamische Referenz-Datenbasis. GRS-Ber., vol. 265, 2011.

/AME 07/   Amelung, P., Jobmann, M., Uhlig, L.: Untersuchungen zur sicherheitstechnischen Auslegung eines generischen Endlagers im Tonstein in Deutschland - GENESIS - Anlagenband Geologie der Referenzregionen im Tonstein. Deutsche Gesellschaft zum Bau und Betrieb von Endlagern für Abfallstoffe mbH, 2007.

/AND 99/   Andersson, J.: SR 97. Data and data uncertainties. Compilation of data and data uncertainties for radionuclide transport calculations. SKB Tech. Rep., Vol. TR-99-09, 1999.

/AND 05a/   ANDRA: Dossier 2005 Argile. Tome Safety evaluation of a geological repository. Paris, 2005.

/AND 05b/   ANDRA: Dossier Argile. Tome Phenomenological evolution of a geological repository. 2005.

/ANT 09/   Antonio, M. R., Nyman, M., Anderson, T. M.: Direct observation of contact ion-pair formation in aqueous solution. Angew. Chem., vol. 121, no. 33, pp. 6252–6256, 2009.

/ATE 10/   Atencio, D., Andrade, M. B., Christy, A. G., Giere, R., Kartashov, P. M.: The pyrochlore supergroup of minerals: nomenclature. Can. Min., vol. 48, no. 3, pp. 673–698, 2010.

/AUT 58/   Autenrieth, H.: Untersuchungen im Sechs-Komponenten-System K, Na, Mg, Ca, SO_4" (Cl'), H_2O mit Schlussfolgerung für die Verarbeitung der Kalisalze. Kali und Steinsalz, vol. 2, no. 6, pp. 181–200, 1958.

/AZU 99/   Azuma, J., Shibata, M., Yui, M., Shibutani, T., Notoya, S., Yoshida, Y.: Solubility and speciation of radioactive elements of high-level radioactive waste disposal system. JNC Tech. Note, TN8400 99-071, 1999.

/BAA 77/   Baar, C.: Applied Salt-Rock Mechanics 1, The in-situ behavior of salt rocks. 302 p., ISBN 0444601651, Elsevier Science: Amsterdam, 1977.

/BAE 76/   Baes, C. F., Mesmer, R. E.: The Hydrolysis of Cations. ISBN 0-471-03985-3, Wiley Interscience, 1976.

/BAS 98/   Basciano, L. C., Peterson, R. C., Roder, P. L., Swainson, I.: Description of schoenfliesite, $MgSn(OH)_6$, and roxbyite, $Cu_{1.72}S$, from a 1375 BC shipwreck, Rietveld neutron-diffraction refinement of synthetic schoenfliesite, wickmanite, $MnSn(OH)_6$, and burtite, $CaSn(OH)_6$. Can. Min., vol. 36, pp. 1203–1210, 1998.

/BAU 28/   Baumert, B.: Über Laugen- und Wasserzuflüsse im deutschen Kalibergbau. 90 p., Aachen: Technische Hochschule, 1928.

/BEC 90/   Beck, M. T., Nagypal, I.: Chemistry of complex equilibria. 410 p., ISBN 0131730630, Ellis Horwood: Chichester, 1990.

/BEC 94/   Becht, A.: Photophysik und Photochemie von Zinn-Chloro- und Blei-Hydroxkomplexen. Diss., Universität Regensburg: Regensburg, 1994.

/BEN 04/   Bentouhami, E., Bouet, G. M., Meullemeestre, J., Vierling, F., Khan, M. A.: Physicochemical study of the hydrolysis of rare-earth elements (III) and thorium (IV). Compt. Rend. Chim., vol. 7, no. 5, pp. 537–545, 2004.

/BEN 14/   Bennett, D. G.: Radionuclide solubility limits in SKB's safety case. Ed.: Strålsäkerhetsmyndigheten, SSM 2014:11, 62 p., 2014.

/BER 13/   Berner, U., Hummel, W., Curti, E., Kulik, D., Thoenen, T., Thien, B.: Geochemical Modelling. In: Paul-Scherrer-Insititut (Ed.), pp. 17–28, 2013: Progress Report 2013. Laboratory for Waste Management. Nuclear Energy and Safety Department.

/BER 14a/ Berner, U.: Solubility of radionuclides in a bentonite environment for provisional safety analyses for sgt-e2. Nagra Tech. Rep., vol. 14, no. 06, 2014.

/BER 14b/ Berner, U.: Solubility of radionuclides in a concrete environment for provisional safety analyses for SGT-E2. Nagra Tech. Rep., 14-07, 2014.

/BER 14c/ Berner, U.: The PSI/Nagra Chemical Thermodynamic Database 12/07 (update oft he Nagra/PSI TDB 01/01): Data Selection of Selenium. PSI Rep., TM, No. 44-14-, 2014.

/BER 14d/ Berner, U., Hummel, W., Curti, E., Kulik, D., Thoenen, T., Thien, B.: Geochemical modelling. PSI Progr. Rep., vol. 2013, pp. 17–28, 2014.

/BER 19/ Berger, D., Soles, J. S., Giumlia-Mair, A. R., Brügmann, G., Galili, E., Lockhoff, N., Pernicka, E.: Isotope systematics and chemical composition of tin ingots from Mochlos (Crete) and other Late Bronze Age sites in the eastern Mediterranean Sea: An ultimate key to tin provenance? PloS one, vol. 14, no. 6, pp. e0218326, 2019.

/BER 20/ Bertrams, N., Bollingerfehr, W., Eickemeier, R., Fahland, S., Flügge, J., Frenzel, B., Hammer, J., Kindlein, J., Liu, W., Maßmann, J., Mayer, K.-M., Mönig, J., Mrugalla, S., et al.: Grundlagen zur Bewertung eines Endlagersystems in steil lagernden Salzformationen. GRS-Ber., No. 569, 240 p., 2020.

/BET 16/ Bette, S., Rincke, C., Dinnebier, R. E., Voigt, W.: Crystal structure and hydrate water content of synthetic hellyerite, $NiCO_3 \cdot 5 \cdot 5H_2O$. Z. Anorg. Allg. Chem., vol. 642, No. 9-10, pp. 652–659, 2016.

/BET 17/ Bette, S., Pannach, M., Dinnebier, R. E., Freyer, D.: Phase formation and solubilities in the ternary System $Ni(OH)_2$ -$NiCl_2$ -H_2O at 25 and 200 °C. Eur. J. Inorg. Chem., vol. 2017, no. 11, pp. 1488–1497, 2017.

/BEU 12/ Beuth, T., Bracke, G., Buhmann, D., Dresbach, C., Keller, S., Krone, J., Lommerzheim, A., Mönig, J., Mrigalle, S., Rübel, A., Wolf, J.: Szenarienentwicklung: Methodik und Anwendung. Bericht zum Arbeitspaket 8. Vorgezogene Sicherheitsanalyse für den Standort Gorleben. GRS-Ber., vol. 284, 2012.

/BGR 16/ BGR: Salze in Deutschland. 103 p., 2016.

/BIN 11/   Bingham, P. A., Connelly, A. J., Cassingham, N. J., Hyatt, N. C.: Oxidation state and local environment of selenium in alkali borosilicate glasses for radioactive waste immobilisation. J. Non-Cryst. Solids, vol. 357, no. 14, pp. 2726–2734, 2011.

/BIS 09/   Biswas, K. C., Woodards, N. A., Xu, H. Barton, L. L.: Reduction of molybdate by sulfate-reducing bacteria. BioMetals, vol. 22, no. 1, pp. 131–139, 2009.

/BIS 16/   Bischofer, B., Hagemann, S., Altmaier, M., Banik, N., Bosbach, D., Bracke, G., Brendler, V., Curtius, H., Finck, N., Franzen, C., Gaona, X., Geckeis, H., Hebrling, F., Herm, M., Kindlein, J., et al.: Behaviour of long-lived fission and activation products in the nearfield of a nuclear waste repository and the possibilities of their retention. GRS-Ber., No. 374, 2016.

/BLA 70/   Blandamer, M. J.: Structure and properties of aqueous salt solutions. Q. Rev., Chem. Soc., vol. 24, no. 2, pp. 169, 1970.

/BLO 68/   Block, J., Waters, O. B., JR.: The $CaSO_4$-Na_2SO_4-$NaCl$-H_2O system at 25°. J. Chem. Eng. Data, vol. 13, pp. 336–344, 1968.

/BOH 13/   Bohn, A.: Hydrogeochemische Analyse und Modellierung von Lösungs- und Reaktionsprozessen im Salinar- und Deckgebirge am Staßfurter Sattel. 189 p., Technischen Universität Cottbus - Senftenberg, 2013.

/BOI 07/   Boily, J.-F., Seward, T. M., Charnock, J. M.: The hydrolysis and precipitation of Pd(II) in 0.6 mol kg 1 NaCl: A potentiometric, spectrophotometric, and EXAFS study. Geochim. Cosmochim. Acta, vol. 71, pp. 4834–4845, 2007.

/BOL 11/   Bollingerfehr, W., Filbert, W., Lerch, C., Tholen, M.: Endlagerkonzepte. Bericht zum Arbeitspaket 5. Vorläufige Sicherheitsanalyse für den Standort Gorleben, Technical Report. Gesellschaft für Anlagen- und Reaktorsicherheit (GRS) mbH, DBE Technology GmbH (DBE Tec), GRS-272, ISBN 978-3-939355-48-9: Köln, 2011.

/BOL 12/   Bollingerfehr, W., Filber, W., Dörr, S., Herold, P., Lerch, C., Burgwinke, P., Charlier, F., Thomauske, B., Bracke, G., Kilger, R.: Endlagerauslegung und -optimierung. Bericht zum Arbeitspaket 6. Vorläufige Sicherheitsanalyse für den Standort Gorleben. GRS-Ber., vol. 281, 2012.

/BOR 12/   Borg, S., Liu, W., Etschmann, B., Tian, Y., Brugger, J.: An XAS study of molybdenum speciation in hydrothermal chloride solutions from 25–385°C and 600 bar. Geochim. Cosmochim. Acta, vol. 92, pp. 292–307, 2012.

/BÖR 18/   Börsig, N., Scheinost, A. C., Shaw, S., Schild, D., Neumann, T.: Retention and multiphase transformation of selenium oxyanions during the formation of magnetite via iron(ii) hydroxide and green rust. Dalton Trans., vol. 47, no. 32, pp. 11002–11015, 2018.

/BOS 09/   Bosbach, D., Luckscheiter, B., Brendebach, B., Denecke, M. A., Finck, N.: High level nuclear waste glass corrosion in synthetic clay pore solution and retention of actinides in secondary phases. J. Nucl. Mater., vol. 385, no. 2, pp. 456–460, 2009.

/BOU 78/   Boulegue, J.: Solubility of elemental sulfur in water at 298 K. Phosphorus Sulfur Relat. Elem., vol. 5, no. 1, pp. 127–128, 1978.

/BRA 62/   Braitsch, O.: Entstehung und Stoffbestand der Salzlagerstätten. Springer-Verlag, Berlin, 1962.

/BRE 98/   Brennecke, P.: Prüfung und Bewertung einer möglichen Verschmutzung des Grundwassers durch bestimmte gefährliche Stoffe. Ed.: Bundesamt für Strahlenschutz (BfS), BfS Interner Arbeitsbericht, ET-I8-94-REV-3, 1998.

/BRE 07/   Brendebach, B., Altmaier, M., Rothe, J., Neck, V., Denecke, M. A.: EXAFS study of aqueous Zr^{IV} and Th^{IV} complexes in alkaline $CaCl_2$ solutions: $Ca_3[Zr(OH)_6]^{4+}$ and $Ca_4[Th(OH)_8]^{4+}$. Inorg. Chem., vol. 46, no. 16, pp. 6804–6810, 2007.

/BRO 87a/ Brown, P. L., Sylva, R. N.: Unified theory of metal ion complex formations constants. Australian Atomic Energy Commission, AAEC, E656, 72 p., 1987.

/BRO 87b/ Brown, P. L., Wanner, H.: Predicted formation constants using the unified theory of metal ion complexation. Ed.: OECD Nuclear Energy Agency: Paris, 1987.

/BRO 16/ Brown, P. L., Ekberg, C.: Hydrolysis of Metal Ions. 1. ed., 917 p., ISBN 9783527330102, Wiley-VCH, 2016.

/BRÖ 22/ Brönsted, J. N.: Studies on solubility. IV. The principle of the specific interaction of ions. J. Am. Chem. Soc., vol. 44, no. 5, pp. 877–898, 1922.

/BUC 16/ Bucher, K., Stober, I.: Large-scale chemical stratification of fluids in the crust: hydraulic and chemical data from the geothermal research site Urach, Germany. Geofluids, vol. 16, no. 5, pp. 813–825, 2016.

/BUG 13/ Bugaris, D. E., Smith, M. D., zur Loye, H.-C.: Hydroflux crystal growth of platinum group metal hydroxides: $Sr_6NaPd_2(OH)_{17}$, $Li_2Pt(OH)_6$, $Na_2Pt(OH)_6$, $Sr_2Pt(OH)_8$, and $Ba_2Pt(OH)_8$. Inorg. Chem., vol. 52, no. 7, pp. 3836–3844, 2013.

/BUH 91/ Buhmann, D., Nies, A., Storck, R.: Analyse der Langzeitsicherheit von Endlagerkonzepten für wärmeerzeugende radioaktive Abfälle. GSF (Gesellschaft für Umwelt und Gesundheit mbH), GSF-Ber., 27/91: Braunschweig, 1991.

/BUH 08/ Buhmann, D., Mönig, J., Wolf, J.: Untersuchungen zur Ermittlung und Bewertung von Freisetzungsszenarien. Teilbericht zum Projekt ISIBEL: "Überprüfung und Bewertung des Instrumentariums für eine sicherheitliche Bewertung von Endlagern für HAW", Technical Report. GRS (Gesellschaft für Anlagen- und Reaktorsicherheit mbH), GRS-Ber., No. 233: Braunschweig, 2008.

/BUN 95/ Bundesanstalt für Geowissenschaften und Rohstoffe (BGR): Endlagerung stark wärmeentwickelnder radioaktiver Abfälle in tiefen geologischen Formationen Deutschlands, Untersuchung und Bewertung von Salzformationen. 138 p., 1995.

/BUN 06/ Richtlinie zur Emissions- und Immissionsüberwachung kerntechnischer An-
lagen (REI) as amended on 23 June 2006, last changed 2006 (Ge-
meinsames Ministerialblatt 2006, No. 14-17, p. 253).

/BUN 15/ Bundesministerium für Umwelt, Naturschutz, Bau und Reaktorsicherheit
(BMUB) (Ed.): Programm für eine verantwortungsvolle und sichere En-
tsorgung bestrahlter Brennelemente und radioaktiver Abfälle (Nationales
Entsorgungsprogramm). 2015.

/BUN 20/ Bundesgesellschaft für Endlagerung (BGE) (Ed.): Sub-areas interim report
pursuant to Section 13 StandAG. SG01101/16-1/2-2021#1 – Object ID:
850052 – Revision: 00, 2034 p., 2020.

/BUS 88/ Bushuev, N. N., Nikonova, N. S., Mishenina, N. V.: The $SrSO_4$-$CaSO_4$ sys-
tem. Russ. J. Inorg. Chem., vol. 33, pp. 299–301, 1988.

/BYR 00/ Byrne, R. H., Yao, W.: Formation of palladium(II) hydroxychlorirde com-
plexes and precipitates in sodium chloride solutions and seawater. Geo-
chim. Cosmochim. Acta, vol. 64, pp. 4153–4156, 2000.

/CAN 10/ Cannìere, P. D., Maes, A., Williams, S. J.: Behaviour of selenium in Boom
Clay. SCK, CEN, No. ER-120, 2010.

/CAR 17/ Carriere, C., Neff, D., Foy, E., Martin, C., Linard, Y., Michau, N., Dynes, J.,
Dillmann, P.: Influence of iron corrosion on nuclear glass alteration pro-
cesses: nanoscale investigations of the iron-bearing phases. Corr. Engin.
Sci. Techn., vol. 52, sup1, pp. 166–172, 2017.

/CAS 13/ Cassingham, N. J.: Structure and Durability of UK Simulated High Level
Nuclear Waste Glasses. University of Sheffield: Sheffield, 2013.

/CHA 14/ Charykova, M. V., Krivovichev, V. G., Lelet, M. I., Yakovenko, O. S., Su-
leimanov, E. V., Depmeier, W., Semenova, V. V., Zorina, M. L.: A calori-
metric and thermodynamic investigation of the synthetic analogs of cobalto-
menite, $CoSeO_3 \cdot 2H_2O$, and ahlfeldite, $NiSeO_3 \cdot 2H_2O$. Am. Mineral., vol. 99,
no. 4, pp. 742–748, 2014.

/CHA 17/ Charykova, M. V., Krivovichev, V. G.: Mineral systems and the thermodynamics of selenites and selenates in the oxidation zone of sulfide ores – a review. Mineralogy and Petrology, vol. 111, no. 1, pp. 121–134, 2017.

/CIA 80/ Ciavatta, L.: The specific interaction theory in evaluating ionic equilibria. Ann. Chim. (Roma), vol. 70, pp. 551–567, 1980.

/CIG 12/ Cigala, R. M., Crea, F., Stefano, C. d.: The inorganic speciation of tin(II) in aqueous solution. Geochim. Cosmochim. Acta, vol. 87, pp. 1–20, 2012.

/CLE 80/ Clever, H. L., Johnston, F. J.: The Solubility of Some sparingly Soluble Lead Salts: An Evaluation of the Solubility in Water and Aqueous Electrolyte Solution. J. Phys. Chem. Ref. Data, vol. 9, no. 4, pp. 751–784, 1980.

/COE 84/ Coetzee, P. P., Förster, M., Lieser, K. H.: Solubility of AgI in saturated NaCl solution. Radiochim. Acta, vol. 37, no. 3, pp. 159–160, 1984.

/COL 08/ Colombo, C., Oates, C. J., Monhemius, A. J., Plant, J. A.: Complexation of platinum, palladium and rhodium with inorganic ligands in the environment. Geochem. Explor. Environm. Anal., vol. 8, no. 1, pp. 91–101, 2008.

/COU 98/ Coucouvanis, D.: Syntheses, Structures, and Reactions of Binary and Tertiary Thiomolybdate Complexes Containing the (O)Mo(Sx) AND (S)Mo(Sx) Functional Groups (x = 1, 2, 4). In: Advances in Inorganic Chemistry. no. 45, pp. 1–73, ISBN 9780120236459, Elsevier, 1998.

/CUR 03/ Curti, E.: Glass Dissolution Parameters: Update for Entsorgungsnachweis. NAGRA, NAGRA Tech. Rep., 02-21, 2003.

/CUR 06/ Curti, E., Crovisier, J. L., Morvan, G., Karpoff, A. M.: Long-term corrosion of two nuclear waste reference glasses (MW and SON68): A kinetic and mineral alteration study. Appl. Geochem., vol. 21, no. 7, pp. 1152–1168, 2006.

/CUR 09/ Curti, E., Dähn, R., Farges, F., Vespa, M.: Na, Mg, Ni and Cs distribution and speciation after long-term alteration of a simulated nuclear waste glass: A micro-XAS/XRF/XRD and wet chemical study. Geochim. Cosmochim. Acta, vol. 73, no. 8, pp. 2283–2298, 2009.

/CUR 15/ Curti, E., Puranen, A., Grolimund, D., Jädernas, D., Sheptyakov, D., Mesbah, A.: Characterization of selenium in UO_2 spent nuclear fuel by micro X-ray absorption spectroscopy and its thermodynamic stability. Environ. Sci. Process. Impacts, vol. 17, no. 10, pp. 1760–1768, 2015.

/DAL 75/ Dal Negro, A., Rossi, G., Tazzoli, V.: The crystal structure of ancylite,$(RE)_x,(Ca,Sr)_{2-x}(CO_3)_2(OH)_x(2-x)H_2O$. Am. Mineral., vol. 60, pp. 280–284, 1975.

/DEB 15/ Deblonde, J.-P., Chagnes, A., Bélair, S., Cote, G.: Solubility of niobium(V) and tantalum(V) under mild alkaline conditions. Hydromet., vol. 156, pp. 99–106, 2015.

/DEB 16/ Deblonde, G. J.-P., Chagnes, A., Weigel, V., Cote, G.: Direct precipitation of niobium and tantalum from alkaline solutions using calcium-bearing reagents. Hydromet., vol. 165, pp. 345–350, 2016.

/DOB 63/ Dobrowolski, J., Oglaza, J.: Zastowanie izotopu [110]Ag do badania rozpuszsczalnosci srebra metalicznego i chorku srebra w roztorach wodnych sierczanu cynku. Nukleonika, vol. 8, pp. 79–81, 1963.

/DOI 09/ Doi, R., Kitamura, A., Yui, M.: JAEA Thermodynamic Database for Performance Assessment of Geological Disposal of High-level and TRU Wastes: Selection of Thermodynamic Data of Selenium. Ed.: Japan Atomic Energy Agency (JAEA), 26 p., 2009.

/DUB 22/ Dubrovinskaia, N., Messingschlager, M., Dubrovinsky, L.: Tin weathering experiment set by nature for 300 years: natural crystals of the anthropogenic mineral hydroromarchite from Creussen, Bavaria, Germany. Eur. J. Mineral., vol. 34, no. 6, pp. 563–572, 2022.

/DUN 03/ Dunkle, S., Craig, J. R., Rimstidt, J. D., Lusardi, W.: Romarchite, hydroromarchite and abhurite formed during thecorrosion of pewter artifacts from the Queen Anne's Revenge (1718). Can. Min., vol. 41, pp. 659–669, 2003.

/DUN 04/   Dunkle, S. E., Craig, J. R., Lusardi, W. R.: Romarchite and associated phases as common corrosion products on pewter artifacts from marine archaeological sites. Geoarchaeol., vol. 19, no. 6, pp. 531–552, 2004.

/DUR 06a/   Duro, L., Grivé, M., Cera, E.: Update of a thermodynamic database for redionuclides to assist solubility limits calculation for performance assessment. SKB Tech. Rep., TR, No. 06-17, 2006.

/DUR 06b/   Duro, L., Grivé, M., Cera, E., Gaona, X., Domènech, C., Bruno, J.: Determination and assessment of the concentration limits to be used in SR-Can. 135 p., 2006.

/DUR 10/   Duro, L., Montoya, V., Colás, E., García, D.: Groundwater equilibration and radionuclide solubility calculations. Ed.: Nuclear Waste Management Organization (NWMO), NWMO TR-2010-02, 108 p., 2010.

/EDW 92/   Edwards, R., Gillard, R. D., Williams, P. A.: The stabilities of secondary tin minerals: abhurite and its relationships to Sn(II) and Sn(IV) oxides and oxyhydroxides. Mineral. Mag., vol. 56, no. 383, pp. 221–226, 1992.

/EDW 96/   Edwards, R., Gillard, R. D., Williams, P. A.: The stabilities of secondary tin minerals. Part 2: The hydrolysis of tin(II) sulphate and the stability of $Sn_3O(OH)_2SO_4$. Mineral. Mag., vol. 60, no. 400, pp. 427–432, 1996.

/ENG 63/   Engelhardt, W. V., Gaida, K. H.: Concentration changes of pore solutions during compaction of clay sediments. J. Sedim. Res., vol. 33, no. 4, pp. 919–930, 1963.

/ESS 88/   Essington, M. E.: Estimation of the standard free energy of formation of metal arsenates, selenates, and selenites. Soil Sci. Soc. Am. J., vol. 52, pp. 1574–1579, 1988.

/ESS 92/   Essington, M. E.: Formation of Calcium and Magnesium Molybdate Complexes in Dilute Aqueous Solutions. Soil Sci. Soc. Am. J., vol. 56, no. 4, pp. 1124–1127, 1992.

/FAT 78/ Fatouros, N., Rouelle, F., Chemla, M.: Influence de la formation de complexes chlorures sur la réduction électrochimique de Sn IV en milieu perchlorique acide. J. Chim. Phys. Phys. Biol., vol. 75, pp. 476–483, 1978.

/FAU 71/ Faust, G. T., Schaller, W. T.: Schoenfliesite, $MgSn(OH)_6$. Z. Krist., vol. 134, No. 1-2, 1971.

/FED 79/ Fedorov, V. A., Kuznechikhina, M. A., Kanarsh, I. V., Kirnyuk, G. M., Chernikova, G. E.: Formation of mixed zinc halide complexes in aqueous solutions. Soviet J. Coord. Chem., vol. 4, pp. 33–38, 1979.

/FEI 36/ Feitknecht, W., Collet, A.: Über die Konstitution der festen basischen Salze zweiwertiger Metalle. II Basische Nickelhalogenide mit "Einfachschichtengittern". Helv. Chim. Acta, vol. 19, pp. 831–841, 1936.

/FEL 92/ Felmy, A. R., Rai, D., Mason, M. J.: The solubility of $CaMoO_4(c)$ and an aqueous thermodynamic model for Ca^{2+} - MoO_4^{2-} ion-interactions. J. Solution Chem., vol. 21, pp. 525–532, 1992.

/FEL 16a/ Felipe-Sotelo, M., Hinchliff, J., Field, L. P., Milodowski, A. E., Holt, J. D., Taylor, S. E., Read, D.: The solubility of nickel and its migration through the cementitious backfill of a geological disposal facility for nuclear waste. J. Hazard. Mater., vol. 314, pp. 211–219, 2016.

/FEL 16b/ Felipe-Sotelo, M., Hinchliff, J., Evans, N. D. M., Read, D.: Solubility constraints affecting the migration of selenium through the cementitious backfill of a geological disposal facility. J. Hazard. Mater., vol. 305, pp. 21–29, 2016.

/FIL 20/ Filella, M., May, P. M.: The aqueous solution thermodynamics of niobium under conditions of environmental and biological interest. Appl. Geochem., vol. 122, pp. 104729, 2020.

/FRI 85/ Fritz, J. J.: Thermodynamic properties of chloro-complexes of silver chloride in aqueous solution. J. Solution Chem., vol. 14, pp. 865–879, 1985.

/GAL 08/   Galuskin, E. V., Gazeev, V. M., Armbruster, T., Zadov, A. E., Galuskina, I. O., Pertsev, N. N., Dzierzanowski, P., Kadiyski, M., Gurbanov, A. G., Wrzalik, R., Winiarski, A.: Lakargiite CaZrO3: A new mineral of the perovskite group from the North Caucasus, Kabardino-Balkaria, Russia. Am. Miner., vol. 93, No. 11-12, pp. 1903–1910, 2008.

/GAM 97/   Gammons, C. H., Yu, Y.: The stability of aqueous silver bromide and iodide complexes at 25–300°C: Experiments, theory and geologic applications. Chem. Geol., vol. 137, No. 3-4, pp. 155–173, 1997.

/GAM 01/   Gamsjäger, H., Preis, W., Wallner, H.: Solid-solute phase equilibria in aqueous solutions XIV [1]. Thermodynamic analysis of the solubility of hellyrite in Water. Monatsh. Chem., vol. 132, pp. 411–415, 2001.

/GAM 05/   Gamsjäger, H., Bugajski, J., Gajda, T.: Chemical thermodynamics of nickel. 645-, Elsevier, Amsterdam, 2005.

/GAM 12/   Gamsjäger, H., Gajda, T., Sangster, J., Saxena, S. K., Voigt, W.: Chemical thermodynamics of tin. Chemical Thermodynamics, vol. 12, 646 p., OECD, 2012.

/GAT 09/   Gatta, G. D., Rotiroti, N., Boffa Ballaran, T., Sanchez-Valle, C., Pavese, A.: Elastic behavior and phase stability of pollucite, a potential host for nuclear waste. Am. Mineral., vol. 94, No. 8-9, pp. 1137–1143, 2009.

/GAY 49/   Gayer, K. H., Garrett, A. B.: The Equilibria of Nickel Hydroxide, $Ni(OH)_2$, in Solutions of Hydrochloric Acid and Sodium Hydroxide at 25°. J. Am. Chem. Soc., vol. 71, no. 9, pp. 2973–2975, 1949.

/GIE 93/   Giester, G.: Crystal structure of $KFe[SeO_3]_2$. Z. Krist., vol. 207, no. 1, pp. 1–7, 1993.

/GIE 96a/   Giester, G., Pertlik, F., Brandstätter, F.: A revision of the formula $Fe_2(SeO_3)_3 \cdot 6H_2O$ to $Fe_2(SeO_3) \cdot 3H_2O$. Mat. Res. Bull., vol. 31, no. 10, pp. 1189–1193, 1996.

/GIE 96b/ Giester, G.: Syntheses and Crystal Structures of $Ca_3Fe_2(SeO_3)_6$ and $Sr_3Fe_2(SeO_3)_6$. Z. Anorg. Allg. Chem., vol. 622, no. 10, pp. 1788–1792, 1996.

/GIE 96c/ Giester, G.: Crystal structure of $Fe_2O(SeO_3)_2$, a new oxoselenite compound with ferric iron in distorted tetrahedral coordination. Z. Krist., vol. 211, no. 9, 1996.

/GIN 21/ Gin, S., Delaye, J.-M., Angeli, F., Schuller, S.: Aqueous alteration of silicate glass: state of knowledge and perspectives. npj Mater. Degrad., vol. 5, no. 1, 2021.

/GME 89/ Gmelin-Institut für Anorganische Chemie: Gmelin handbook of inorganic chemistry. 8th edition. Molybdenum. B 3b, Springer-Verlag: Berlin, 1989.

/GOD 88/ Godon, N., Thomassin, J. H., Touray, J. C., Vernaz, E.: Experimental alteration of R7T7 nuclear model glass in solutions with different salinities (90C, 1 bar): implications for the selection of geological repositories. J. Mater. Sci., vol. 23, no. 1, pp. 126–134, 1988.

/GON 18/ González-Siso, M. R., Gaona, X., Duro, L., Altmaier, M., Bruno, J.: Thermodynamic model of Ni(II) solubility, hydrolysis and complex formation with ISA. Radiochim. Acta, vol. 106, no. 1, pp. 31–45, 2018.

/GRA 90/ Grambow, B., Müller, R.: Chemistry of glass corrosion in high saline brines. Mat. Res. Soc. Symp. Proc., vol. 176, pp. 229–240, 1990.

/GRA 92/ Grambow, B., Müller, R., Rother, A.: Determination of molybdate mean ionic activity coefficients for the assessment of radionuclide mobility. Radiochimica Acta, vol. 58, no. 59, pp. 71–77, 1992.

/GRA 96a/ Grambow, B., Lutze, W., Kahl, L., Geckeis, H., Bohnert, E., Loida, A., Dressler, P.: Long-term safety of radioactive waste disposal. Retention of Pu, Am, Np and Tc in the corrosion of COGEMA glass R7T7 in salt solutions. Final report. Ed.: Forschungszentrum Karlsruhe, Forschungsz. Karlsruhe Wiss. Ber., FZKA-5767, 1996.

/GRA 96b/ Grambow, B., Loida, A., Dressler, P., Geckeis, H., Gago, J., Casas, I., de Pablo, J., Giménez, J., Torrero, M. E.: Long-term safety of radioactive waste disposal: Chemical reaction of fabricated and high burnup spent UO_2 fuel with saline brines, Final report. Forschungsz. Karlsruhe Wiss. Ber., vol. 5702, FZKA 5702, 1996.

/GRA 97a/ Grauer, R.: Solubility Limitations: An "Old Timer's" View. In: Grenthe, I., Puigdomenech, I. (Eds.): Modelling in aquatic chemistry. pp. 131–152, ISBN 92-64-15569-4, OECD-Publications, 1997.

/GRA 97b/ Grambow, B., Loida, A., Dressier, P., Geckeis, H., Gago, J., Casas, I., de Pablo, J., Giménez, J., Torrero, M. E.: Chemical reaction of fabricated and high burn-up spent UO_2 fuel with saline brines, Final report. Europäische Kommission, EUR Nuclear science and technology, vol. 17111, EUR 17111, 166 p., ISBN 92-827-9572-1, Off. for Off. Publ. of the Europ. Communities: Luxembourg, 1997.

/GRA 99/ Grambow, B., Bernotat, W., Kelm, M.: Erstellung eines integrierten Nahfeldmodells von Gebinden hochaktiver Abfälle im Salzstock Gorleben: geochemisch fundierter Quellterm für HAW-Glas, abgebrannte Brennelemente und Zement. Forschungszentrum Karlsruhe - Institut für Nukleare Entsorgungstechnik, vol. 07, no. 99, 1999.

/GRA 08/ Grambow, B.: Mobile fission and activation products in nuclear waste disposal. J. Contam. Hydrol., vol. 102, pp. 180–186, 2008.

/GRA 13/ Grambow, B.: Waste forms for actinides: borosilicate glasses. In: Burns, P. C., Sigmon, G. E. (Eds.): Uranium, Cradle to grave. Mineralogical Association of Canada, Short course series, volume 43, pp. 301–3016, ISBN 978-0-921294-53-5, Mineralogical Association of Canada: Québec, 2013.

/GRE 92/ Grenthe, I., Fuger, J., Konings, R. J. M.: Chemical thermodynamics of uranium. North-Holland, 1992.

/GRE 97/ Grenthe, I., Puigdomenech, I. (Eds.): Modelling in aquatic chemistry. ISBN 92-64-15569-4, OECD-Publications, 1997.

/GRI 10a/ Grivé, M., Domènech, C., Montoya, V., Garcia, D., Duro, L.: Determination and assessment of the concentration limits to be used in SR-Can - Supplement to TR-06-32. Ed.: Svensk Kärnbränslehantering AB (SKB), SKB Report, R-10-50, 28 p., 2010.

/GRI 10b/ Grivé, M., Domènech, C., Montoya, V., Garcia, D., Duro, L.: Simple functions spreadsheet tool presentation. SKB Tech. Rep, TR-10-61, 2010.

/GUG 55/ Guggenheim, E. A., Turgeon, J. C.: Specific interaction of ions. Trans. Faraday Soc., vol. 51, pp. 747, 1955.

/GUI 03/ Guillaumont, R., Mompean, F. J.: Update on the chemical thermodynamics of uranium, neptunium, plutonium, americium and technetium. Elsevier B.V., Amsterdam, 2003.

/HA 11/ Ha, Y.-K., Kim, J.-G., Park, Y.-S., Park, S.-D., Song, K.-S.: Behaviours of molybdenum in UO_2 fuel matrix. Nucl. Engin. Technol., vol. 43, no. 3, pp. 309–316, 2011.

/HAA 21/ Haase, P., Christensen, H. G., Nielsen, U. G., Koch, C. B., Galazka, Z., Majzlan, J.: Stability and solubility of members of tin perovskites in the schoenfliesite subgroup, $\square_2$ ($B$$Sn^{4+}$)$(OH,O)_6$ (B = Ca, Fe^{3+}, Mg, Mn^{2+}, Zn, Cu). Chem. Thermodyn. Therm. Anal., Vol. 1-2, pp. 100005, 2021.

/HAG 99/ Hagemann, S.: Thermodynamische Eigenschaften des Bleis in Lösungen der ozeanischen Salze. Diss., DOI 10.24355/dbbs.084-200511080100-200, 152-, Technische Universität Braunschweig: Braunschweig, 1999.

/HAG 12a/ Hagemann, S., Moog, H. C., Herbert, H.-J.: Rückhaltung und thermodynamische Modellierung von Iod und Selen in hochsalinaren Lösungen. GRS-Ber., vol. 245, pp. 167, 2012.

/HAG 12b/ Hagemann, S.: Entwicklung eines thermodynamischen Modells für Zink, Blei und Cadmium in salinaren Lösungen. GRS-Ber., vol. 219, 2012.

/HAG 14/ Hagemann, S., Bischofer, B., Scharge, T.: Entwicklung von Methoden und Modellen zur Bestimmung des Redoxpotentials salinarer Lösungen. GRS-Ber., vol. 260, 2014.

/HAG 15a/ Hagemann, S., Scharge, T., Willms, T.: Entwicklung einer thermodynamischen Datenbasis für ausgewählte Schwermetalle. GRS-Ber., vol. 244, 2015.

/HAG 15b/ Hagemann, S., Schönwiese, D., Scharge, T.: Werkzeuge und Daten für die Geochemische Modellierung - Thermodynamische Daten für Schwefelspezies und Hintergrundsalze sowie Tools zur Unsicherheitsanalyse. GRS-Ber., vol. 373, 2015.

/HAG 21/ Hagemann, S., Mönig, H.: Stability of iron corrosion phases expected in a repository in Lower Cretaceous clay. GRS-Ber., No. 587, 181 p., 2021.

/HAG 23/ Hagemann, S.: Entwicklung eines thermodynamischen Modells für Zink, Blei und Cadmium in salinaren Lösungen. GRS-Ber., vol. 219, 219 rev., 2023.

/HAG 24/ Hagemann, S., Bischofer, B.: Behaviour of long-lived fission and activation products in the near field of a repository and possibilities of their retention (VESPA II) - Subproject GRS (in print). GRS-Ber., No. 708, 2024.

/HAR 84/ Harvie, C. E., Moeller, N., Weare, J. H.: The prediction of mineral solubilities in natural waters: The Na-K-Mg-Ca-H-Cl-SO_4-OH-HCO_3-CO_3-CO_2-H_2O system to high ionic strengths at 25°C. Geochim. Cosmochim. Acta, vol. 48, pp. 723–751, 1984.

/HAR 14/ Haring, M. M. M., McDonald, A. M.: Franconite, $NaNb_2O_5(OH)\cdot3H_2O$: structure determination and the role of H bonding, with comments on the crystal chemistry of franconite-related minerals. Mineral. Mag., vol. 78, no. 3, pp. 591–607, 2014.

/HER 61/ Herrmann, A. G.: Über das Vorkommen einiger Spurenelemente in Salzlösungen aus dem deutschen Zechstein. Kali und Steinsalz, vol. 3, no. 7, pp. 210–220, 1961.

/HER 00/ Herbert, H.-J.: Zur Geochemie und geochemischen Modellierung hochsalinarer Lösungen mineralischer Rohstoffe. Geol. Jb. Sonderh. D, vol. 1, ISBN 3-510-95845-4, Schweizerbart: Stuttgart, 2000.

/HER 01/ Herbert, H. J., Sander, W.: Wassergehaltsbestimmung an Steinsalz (Erkundsungssohle). Abschlussbericht. Projekt Gorleben. PSP-Element 9G 412 2210 00. GRS-A-Bericht, 2001.

/HER 07/ Herbert, H.-J., Schwandt, A.: Salzlösungszuflüsse im Salzbergbau Mitteldeutschlands. GRS-Ber., vol. 226, No. 226, 198 p., 2007.

/HOL 18/ Holzheid, A., Charykova, M. V., Krivovichev, V. G., Ledwig, B., Fokina, E. L., Poroshina, K. L., Platonova, N. V., Gurzhiy, V. V.: Thermal behavior of ferric selenite hydrates ($Fe_2(SeO_3)_3 \cdot 3H_2O$, $Fe_2(SeO_3)_3 \cdot 5H_2O$) and the water content in the natural ferric selenite mandarinoite. Geochem., vol. 78, no. 2, pp. 228–240, 2018.

/HÖL 41/ Höltje, R., Geyer, R.: Das Verhalten von Molybdänlösungen gegen Reduktionsmittel. Z. Anorg. Allg. Chem., vol. 246, no. 3, pp. 243–257, 1941.

/HOT 97/ Hoth, P., Seibt, A., Kellner, T., Huenges, E.: Geowissenschaftliche Bewertungsgrundlagen zur Nutzung hydrogeothermaler Ressourcen in Norddeutschland. Ed.: GFZ, GFZ Sci. Tech. Rep., 97-1, 149 p.: Potsdam, 1997.

/HOT 07/ Hoth, P., Wirth, H., Reinhold, K., Bräuer, V., Krull, P., Feldrappe, H.: Endlagerung radioaktiver Abfälle in tiefen geologischen Formationen Deutschlands - Untersuchung und Bewertung von Tongesteinsformationen. Ed.: Bundesanstalt für Geowissenschaften und Rohstoffe (BGR), 124 p., 2007.

/HU 13/ Hu, S., Johnsson, M.: Synthesis and crystal structure of $Fe_6Ca_2(SeO_3)_9Cl_4$ - a porous oxohalide. Dalton Trans., vol. 42, pp. 7859–7862, 2013.

/HUM 02/ Hummel, W., Berner, U., Curti, E.: NAGRA / PSI Chemical Thermodynamic Data Base 01/01. Nagra Tech. Rep., vol. 02, no. 16, 2002.

/HUM 22/   Humphreys, M. P., Waters, J. F., Turner, D. R., Dickson, A. G., Clegg, S. L.: Chemical speciation models based upon the Pitzer activity coefficient equations, including the propagation of uncertainties: artificial seawater from 0 to 45 °C. Marine Chem., vol. 244, pp. 901–904, 2022.

/IID 10/   Iida, Y., Yamaguchi, T., Tanaka, T., Nakayama, S.: Solubility of selenium at high ionic strength under anoxic conditions. J. Nucl. Sci. Techn., vol. 47, pp. 431–438, 2010.

/ISA 63/   Isaacs, T.: The mineralogy and chemistry of the nickel carbonates. Mineral. mag. j. Mineral. Soc., vol. 33, no. 263, pp. 663–678, 1963.

/IVA 84/   Ivanov-Emin, B. N., Petrishcheva, L. P., Zaitsev, B. E., Ivlieva, V. I., Izmailovich, A. S., Dolganev, V. P.: Strontium and barium tetrahydroxopalladates(II). Russ. J. Inorg. Chem., vol. 29, pp. 1169–1171, 1984.

/IVA 85/   Ivanov-Emin, B. N., Zaitsev, B. E., Petrishcheva, L. P.: Alkaline solutions of hydrated palladium(II) oxide. Russ. J. Inorg. Chem., vol. 30, pp. 1786–1788, 1985.

/JAH 13/   Jahn, S., Sönnke, J.: Endlagerstandortmodell Nord (AnSichT) - Teil II: Zusammenstellung von Gesteinseigenschaften für den Langzeitsicherheitsnachweis. Zwischenbericht. Bundesanstalt für Geowissenschaften und Rohstoffe, 2013.

/JAM 84/   Jambor, J. L., Sabina, A. P., Roberts, A. C., Bonardi, M., Ramik, R. A., Sturman, B. D.: Franconite, a new hydrated Na-Nb oxide mineral from Montreal Island, Quebec. Can. Min., vol. 22, pp. 239–243, 1984.

/JEH 91/   Jehng, J. -M., Wachs, I. E.: Niobium oxide solution chemistry. J. Raman Spectr., vol. 22, pp. 83–89, 1991.

/JNC 00/   JNC: Second progress report on research and development for geological disposal of HLW in Japan. H12: project to establish the scientific and technical basis for HLW disposal in Japan. Supporting report 3. Safety assessment of the geological disposal system. JNC Tech. Note, TN1410 2000-004, 2000.

/JOR 66/   Jordanov, N., Havezov, I.: Löslichkeitsprodukte der normalen Carbonate einiger dreiwertiger Seltener Erden ($E_2(CO_3)_3 \cdot nH_2O$). Z. Anorg. Allg. Chem., vol. 347, No. 1-2, pp. 101–106, 1966.

/KAM 04/   Kamyshny, A., Goifman, A., Gun, J.: Equilibrium distribution of polysulfide ions in aqueous solutions at 25 (degree)C: A new approach for the study of polysulfides' equilibria. Env. Sci. Tech., vol. 38, pp. 6633–6644, 2004.

/KAM 09/   Kamyshny, A.: Solubility of cyclooctasulfur in pure water and sea water at different temperatures. Geochim. Cosmochim. Acta, vol. 73, pp. 6022–6028, 2009.

/KEE 05/   Keesmann, S., Noseck, U., Buhmann, D., Fein, E., Schneider, A.: Modellrechnungen zur Langzeitsicherheit von Endlagern für abgebrannte Brennelemente in Salz- und Granitformationen. GRS (Gesellschaft für Anlagen- und Reaktorsicherheit mbH), GRS-Ber., No. 206, ISBN 3-931995-73-9: Braunschweig, 2005.

/KEL 07a/   Keller, S.: Langzeitsicherheitsanalyse für ein HAW-Endlager im Salz. Geologisches Referenzmodell für einen HAW-Endlagerstandort im Salz. Beitrag für das Projekt ISIBEL. BGR Tech. Ber, 2007.

/KEL 07b/   Kelly, S. D., Kemner, K. M., Brooks, S. C.: X-ray absorption spectroscopy identifies calcium-uranyl-carbonate complexes at environmental concentrations. Geochim. Cosmochim. Acta, vol. 71, no. 4, pp. 821–834, 2007.

/KEM 78/   Kemper, E., Zimmerle, W.: Die anoxischen Sedimente der präoberaptischen Unterkreide NW-Deutschlands und ihr paläograpischer Rahmen. Geol. Jb., A 45, pp. 3–41, 1978.

/KES 99/   Kessi, J., Ramuz, M., Wehrli, E., Spycher, M., Bachofen, R.: Reduction of selenite and detoxification of elemental selenium by the phototrophic bacterium Rhodospirillum rubrum. Appl. Environ. Microbiol., vol. 65, no. 11, pp. 4734–4740, 1999.

/KIE 12/ Kienzler, B., Altmaier, M., Bube, C.: Radionuclide Source Term for HLW Glass, Spent Nuclear Fuel, and Compacted Hulls and End Pieces (CSD-C Waste). KIT Sci. Rep., vol. 7624, 2012.

/KIE 13/ Kienzler, B., Altmaier, M., Bube, C., Metz, V.: Radionuclide source term for irradiated fuel from prototype, research and education reactors, for waste forms with negligible heat generation and for uranium tails. KIT Sci. Rep, vol. 7635, 2013.

/KIM 88a/ Kim, H. -T., Frederick, W. J.: Evaluation of Pitzer Ion Interaction Parameters of Aqueous Mixed Electrolyte Solutions at 25 °C. 1. Single Salt Parameters. J. Chem. Eng. Data, vol. 33, no. 2, pp. 177–184, 1988.

/KIM 88b/ Kim, H.-T.: Prediction of Thermodynamic Properties of Aqueous Electrolyte Solutions. PhD, Oregon State University: Corvallis, 1988.

/KIM 91/ Kim, H.-T., Bae, S.-Y., Yoo, K.-O.: Correlation of pitzer ion interaction parameters. Korean J. Chem. Eng., vol. 8, no. 2, pp. 105–113, 1991.

/KIM 03/ Kim, E., Boulègue, J.: Chemistry of rhenium as an analogue of technetium: Experimental studies of the dissolution of rhenium oxides in aqueous solutions. Radiochim. Acta, vol. 91, no. 4, 2003.

/KIM 12/ Kim, S. -S., Min, J. -H., Baik, M. -H.: Estimation of the behaviour of selenium in the near field of repository. Nucl. Engin. Technol., vol. 44, pp. 945–952, 2012.

/KIT 10a/ Kitamura, A., Kirishima, A., Saito, T., Shibutami, S., Tochiyama, O.: JAEA Thermodyanamic database for performance assessment of geological disposal of high-level and TRU wastes: slection of thermodynamic data of molybdenum. JAEA-Review, 2020-010, 86 p., 2010.

/KIT 10b/ Kitamura, A., Yui, M.: Reevaluation of thermodynamic data for hydroxide and hydrolysis species of palladium(II) using the Brønsted-Guggenheim-Scatchard model. J. Nucl. Sci. Tech., vol. 47, no. 8, pp. 760–770, 2010.

/KIT 12/ Kitamura, A., Fujiwara, K., Doi, R., Yoshida, Y.: Update of JAEA-TDB: Additional Selection of Thermodynamic Data for Solid and Gaseous Phases on Nickel, Selenium, Zirconium, Technetium, Thorium, Uranium, Neptunium Plutonium and Americium, Update of Thermodynamic Data on Iodine, and Some Modifications. JAEA-Data/Code, 2012-006, 76 p., 2012.

/KLA 08/ Klaus, J.: Evaluation of 87Sr/86Sr, δ18O, δ2H, and cation contents as geochemical tracers for provenance and flow paths of saline solutions in German Zechstein deposits. Dissertation, 182 p., Georg-August-Universität zu Göttingen: Göttingen, 2008.

/KLI 92/ Klinge, H., Vogel, P., Schelkes, K.: Chemical composition and origin of saline formation waters from the Konrad mine, Germany. 1117-1120, 1992.

/KLU 00/ Klungness, G. D., Byrne, R. H.: Comparative hydrolysis behavior of the rare earths and yttrium: the influence of temperature and ionic strength. Polyhedr., vol. 19, no. 1, pp. 99–107, 2000.

/KOB 17/ Kobayashi, T., Sasaki, T.: Solubility of $Zr(OH)_4$(am) and the Formation of Zr(IV) Carbonate Complexes in Carbonate Solutions Containing 0.1–5.0 $mol \cdot dm^{-3}$ $NaNO_3$. J. Solution Chem., vol. 46, No. 9-10, pp. 1741–1759, 2017.

/KOC 12/ Kock, I., Eickemeier, R., Frieling, G., Heusermann, S., Knauth, M., Minkley, W., Navarro, M., Nipp, H.-K., Vogel, P.: Integritätsanalyse der geologischen Barriere. Bericht zum Arbeitspaket 9.1. Vorläufige Sicherheitsanalyse für den Standort Gorleben, Technical Report. Gesellschaft für Anlagen- und Reaktorsicherheit (GRS) mbH, Bundesanstalt für Geowissenschaften und Rohstoffe (BGR), Institut für Gebirgsmechanik GmbH (IfG), GRS-286, ISBN 978-3-939355-62-5: Köln, 2012.

/KON 16/ Konstantinou, K., Sushko, P. V., Duffy, D. M.: Modelling the local atomic structure of molybdenum in nuclear waste glasses with ab initio molecular dynamics simulations. Phys. Chem. Chem. Phys., vol. 18, no. 37, pp. 26125–26132, 2016.

/KOP 20/ Kopeikin, V. A.: Physicochemical model of silver behavior in a weathering profile. Geochem. Int., vol. 58, no. 6, pp. 746–752, 2020.

/KOZ 83/ Kozlov, V. K., Khodakovskii, I. L.: Eksperimental'noe izuchenie termodinamicheskikh svoystv atomarnogo seerbra v vodnykh rastvorakh v intervale temperatur 25-280°C. Geokhim., no. 6, pp. 836–848, 1983.

/KRA 10/ Kramer, J., Kelly, B., Manivannan, V.: Synthesis of $MSn(OH)_6$ (where M = Mg, Ca, Zn, Mn, or Cu) materials at room temperature. Open Chem., vol. 8, no. 1, pp. 65–69, 2010.

/KRI 06/ Krivovichev, S. V., Burns, P. C.: The crystal structure of $Pb_8O_5(OH)_2Cl_4$, a synthetic analogue of blixite? Can. Mineral., vol. 44, no. 2, pp. 515–522, 2006.

/KRI 11/ Krivovichev, V. G., Charykova, M. V., Yakovenko, O. S., Depmeier, W.: Thermodynamics of arsenates, selenites, and sulfates in the oxidation zone of sulfide ores: IV. Eh-pH diagrams of the Me-Se-H_2O systems (Me = Co, Ni, Fe, Cu, Zn, Pb) at 25°C. Geol. Ore Depos., vol. 53, no. 7, pp. 514–527, 2011.

/KÜP 11/ Küppers, C., Ustohalova, V., Steinhoff, M.: Neuberechnungen zu den Auswirkungen eines auslegungsüberschreitenden Lösungszutritts in der Schachtanlage Asse II : Weiterentwicklung der radioökologischen Modellierung ; Fortschreibung des Berichts vom 16.06.2010. Ed.: Öko-Institut, 216 p., 2011.

/LAR 13/ Larue, J., Baltes, B., Fischer, H., Frieling, G., Kock, I., Navarro, M., Seher, H.: Radiologische Konsequenzenanalyse. Bericht zum Arbeitspaket 10. Vorläufige Sicherheitsanalyse für den Standort Gorleben. Gesellschaft für Anlagen- und Reaktorsicherheit (GRS) mbH, GRS-Ber., No. 289, ISBN 978-3-939355-65-6: Köln, 2013.

/LÉB 66/ Lébl, M.: Absorption bands of lead in alkali chlorides in the presence of hydroxyl ions. Czech. J. Phys., B16, pp. 902–904, 1966.

/LEL 18/ Lelet, M. I., Charykova, M. V., Holzheid, A., Ledwig, B., Krivovichev, V. G., Suleimanov, E. V.: A Calorimetric and Thermodynamic Investigation of the Synthetic Analogue of Mandarinoite, $Fe_2(SeO_3)3 \cdot 5H_2O$. Geosci., vol. 8, no. 11, pp. 391, 2018.

/LEM 20/ Lemire, R. J., Palmer, D. A., Taylor, P., Schlenz, H.: Chemical thermodynamics of iron Part 2. OECD Nuclear Energy Agency, Chemical Thermodynamics, 13b, 1082 p., 2020.

/LEV 87/ Levason, W., Spicer, M. D.: The chemistry of copper and silver in their higher oxidation states. Coord. Chem. Rev., vol. 76, pp. 45–120, 1987.

/LI 04/ Li, G., Yang, J., Zhang, L.: Relationships between Pitzer's ion interaction coefficients and ionic parameters of electrolyte solutions. Trans. Nornferr. Met. Soc. China, vol. 14, pp. 1029–1032, 2004.

/LID 17/ Lidman, F., Källström, K., Kautsky, F.: Mo-93 from the grave to the cradle. Report from a workshop on molybdenum in radioactive waste and in the environment. SKB-Rep., P-16-22, 2017.

/LIM 12/ Lim, H. K., Syed, M. A., Shukor, M. Y.: Reduction of molybdate to molybdenum blue by Klebsiella sp. Strain hkeem. J. Basic Microbiol., vol. 52, no. 3, pp. 296–305, 2012.

/LIN 07/ Lindgren, M., Petterson, M., Wiborgh, M.: Correlation factors for C-14, Cl-36, Ni-59, Ni-63, Mo-93, Tc-99, I-129 and Cs-135 in operational waste for SFR 1. SKB Rapport, R-07-05, 2007.

/LIP 55/ Lippmann, F.: Ton, Geoden und Minerale des Barrême von Hoheneggelsen. Geol. Rundsch., vol. 43, no. 2, pp. 475–503, 1955.

/LIU 98/ Liu, X., Byrne, R. H.: Comprehensive Investigation of Yttrium and Rare Earth element complexation by carbonate ions using ICP–mass spectrometry. J. Solution Chem., vol. 27, no. 9, pp. 803–815, 1998.

/LOI 05/   Loida, A., Metz, V., Kienzler, B., Geckeis, H.: Radionuclide release from high burnup spent fuel during corrosion in salt brine in the presence of hydrogen overpressure. J. Nucl. Mater., vol. 346, no. 1, pp. 24–31, 2005.

/LOM 15/   Lommerzheim, A., Jobmann, M.: Projekt ANSICHT. Endlagerkonzept sowie Verfüll- und Verschlusskonzept für das Endlagerstandortmodell NORD. Technischer Bericht. DBETec Techn. Ber., TEC-14-2015-TB, 2015.

/LOT 99/   Lothenbach, B., Ochs, M., Wanner, H.: Thermodynamic data for the speciation and solubility of Pd, Pb, Sn, Sb, Nb and Bi in aqueous Solution. Japan Nuclear Cycle Development Institute (JNCDI), JNC Rep., TN8400, TN8400 99-011, 1999.

/LOT 00/   Lothenbach, B., Ochs, M., Hager, D.: Thermodynamic data for the solubility of tin (IV) in aqueous cementitious environments. Radiochimica Acta, vol. 88, pp. 521–526, 2000.

/LU 89/   Lu, Y. C., Clayton, C. R.: An XPS study of the passive and transpassive behavior of molybdenum in deaerated 0.1 M HCl. Corr. Sci., vol. 29, no. 8, pp. 927–937, 1989.

/LUC 96/   Luckscheiter, B., Nesovic, M.: Langzeitsicherheit der Endlagerung radioaktiver Abfälle: Entwicklung und Charakterisierung eines Glasprodukts für den HAWC der WAK. Ed.: Forschungszentrum Karlsruhe, Forschungszentrum Karlsruhe Tech. Rep., No. 5825, Forschungszentrum Karlsruhe, Institut für Nukleare Entsorgungstechnik, 1996.

/LUT 93/   Lutze, W.: Verglasung von toxischen, insbesondere hochradioaktiven Abfällen. Ed.: Kernforschungszentrum Karlsruhe, KfK 5267, 1993.

/MAK 69/   Makovskaya, G. V., Spivakovskii, V. B.: Nickel(II) and cobalt(II) hydroxides and hydroxide chlorides and the conditions for their precipitation from chloride solutions. Russ. J. Inorg. Chem., vol. 14, No. 773-776, 1969.

/MAR 88/   Marcus, Y.: Ionic radii in aqueous solutions. Chem. Rev., vol. 88, no. 8, pp. 1475–1498, 1988.

/MAR 94/ Marcus, Y.: Viscosity B-coefficients, structural entropies and heat capacities, and the effects of ions on the structure of water. J. Solution Chem., vol. 23, no. 7, pp. 831–848, 1994.

/MAY 11/ May, P. M., Rowland, D., Hefter, G.: A generic and updatable Pitzer characterization of aqueous binary electrolyte solutions at 1 bar and 25°C. J. Chem. Eng. Data, vol. 56, pp. 5066–5077, 2011.

/MAY 18/ May, P. M., Batka, D., Hefter, G., Königsberger, E., Rowland, D.: Goodbye to S^{2-} in aqueous solution. Chem. Commun. (Camb .), 2018.

/MER 96/ Merli, L., Fuger, J.: Thermochemistry of selected lanthanide and actinide hydroxycarbonates and carbonates. Radiochim. Acta, vol. 74, s1, 1996.

/MET 08/ Metz, V., Loida, A., Bohnert, E., Schild, D., Dardenne, K.: Effects of hydrogen and bromide on the corrosion of spent nuclear fuel and γ-irradiated UO_2 (s) in NaCl brine. Radiochim. Acta, vol. 96, No. 9-11, pp. 637–648, 2008.

/MIL 92/ Millero, F. J.: Stability constants for the formation of rare earth inorganic complexes as a function of ionic strength. Geochim. Cosmochim. Acta, vol. 56, pp. 3123–3132, 1992.

/MIN 05/ Minaev, V. S., Timoshenkov, S. P., Kalugin, V. V.: Structural and phase transformations in condensed selenium. J. Optoelectr. Adv. Mater., vol. 7, pp. 1717–1741, 2005.

/MIT 78/ Mit'kina, L. I., Mel'chakova, N. V., Peshkova, V. M.: Complex formation by Mo^{III} with hydroxide ions. Russ. J. Inorg. Chem., vol. 23, pp. 693–695, 1978.

/MÖN 12/ Mönig, J., Buhmann, D., Rübel, A., Wolf, J., Baltes, B., Fischer-Appelt, K.: Sicherheits- und Nachweiskonzept. Bericht zum Arbeitspaket 4. Vorläufige Sicherheitsanalyse für den Standort Gorleben. Gesellschaft für Anlagen- und Reaktorsicherheit (GRS) mbH, GRS-Ber., No. 277, ISBN 978-3-939355-53-3: Köln, 2012.

/MOO 15/ Moog, H. C., Bok, F., Marquardt, C. M., Brendler, V.: Disposal of nuclear waste in host rock formations featuring high-saline solutions – Implementation of a thermodynamic reference database (THEREDA). Appl. Geochem., vol. 55, pp. 72–84, 2015.

/MÜL 75/ Müller, E. P., Papendieck, G.: Zur Verteilung, Genese und Dynamik von Tiefenwässern unter besonderer Berücksichtigung des Zechsteins. Z. Dtsch. Ges. Geowiss., vol. 3, no. 2, pp. 167–196, 1975.

/MÜL 95/ Müller, E.: Geochemische und sedimentologische Untersuchung der grenzsschichten Barreme-Apt unter Berücksichtigung der Laminite. Geol. Jb., A141, pp. 533–549, 1995.

/NAB 84/ Nabivanets, V. I., Gorina, D. O.: Rastvorimost' gidroksila i monoyadernyi gidroliz molibdena(V) v perchloratnykh rastvorakh. Zh. Neorg. Khim., vol. 29, pp. 1738–1741, 1984.

/NAD 19/ Nadoll, P., Sośnicka, M., Kraemer, D., Duschl, F.: Post-Variscan structurally-controlled hydrothermal Zn-Fe-Pb sulfide and F-Ba mineralization in deep-seated Paleozoic units of the North German Basin: A review. Ore Geology Reviews, vol. 106, pp. 273–299, 2019.

/NAG 02/ NAGRA: Project Opalinus Clay. Safety Report. Demonstration of disposal feasibility for spent fuel, vitrified high-level waste and long-lived intermediate-level waste (Entsorgungsnachweis). Nagra Tech. Rep., vol. 02, 02-05, 2002.

/NEC 09/ Neck, V., Altmaier, M., Rabung, T.: Thermodynamics of trivalent actinides and neodymium in NaCl, $MgCl_2$, and $CaCl_2$ solutions: Solubility, hydrolysis, and ternary Ca-M(III)-OH complexes. Pure Appl. Chem., vol. 81, no. 9, pp. 1555–1568, 2009.

/NEC 11/ Neck, V., Moog, H., Brendler, V., Wilhelm, S.: THEREDA. Handbuch Teil 3. Richtlinien zur Datenauswahl. Version 1.0. 2011.

/NIC 77/ Nickel, E., Robinson, B. W., Davis, C. E. S.: Otwayite, a new nickel mineral from Western Australia. Am. Mineral., vol. 62, pp. 999–1002, 1977.

/NIC 85/ Nickel, E., Robinson, B. W.: Kambaldaite - a new hydrated Ni-Na carbonate mineral from Kambalda, Western Australia. Am. Mineral., vol. 70, pp. 419–422, 1985.

/NIC 87/ Nickel, E., Graham, J.: Paraotwayite, a new nickel hydroxide mineral from Western Australia. Can. Min., vol. 25, pp. 409–411, 1987.

/NIC 93/ Nickel, E. H., Robinson, B. W., Mumme, W. G.: Widgiemootthalite: The new Ni analogue of hydromagnesite from Western Australia. Am. Mineral., vol. 78, pp. 819–821, 1993.

/NIE 02/ Niedersächisches Ministerium für Umwelt (Ed.): Planfeststellungsbeschluss für die Errichtung und den Betrieb des Bergwerkes Konrad in Salzgitter. 2002.

/NIK 12/ Nikishina, E. E., Lebedeva, E. N., Drobot, D. V.: Niobium- and tantalum-containing oxide materials: synthesis, properties, and application. Inorg. Mat., vol. 48, pp. 1243–1260, 2012.

/NIN 16/ Ning, P., Xu, W., Cao, H., Lin, X., Xu, H.: Determination and modeling for the solubility of $Na_2MoO_4 \cdot 2H_2O$ in the ($Na^+ + MoO_4^{2-} + SO_4^{2-}$) system. J. Chem. Thermodyn., vol. 94, pp. 67–73, 2016.

/NIR 97/ NIREX: An assessment of the post-closure performance of a deep waste repository at Sellafield. Nirex Sci. Rep., S/97/012, 1997.

/NIR 03/ NIREX: Generic repository studies. Generic post-closure performance assessment. Nirex Rep, N/080, 2003.

/NIS 07/ Nishimura, T., Hata, R.: Chemistry of the Ca-Se(IV)-H_2O and Ca-Se(IV)-H_2O systems at 25°C. Hydromet., vol. 89, pp. 346–356, 2007.

/NOW 13/ Nowak, T., Maßmann, J.: Endlagerstandortmodell Nord (AnSichT) - Teil III: Auswahl von Gesteins- und Fluideigenschaften für numerische Modellberechnungen im Rahmen des Langzeitsicherheitsnachweises. Zwischenbericht. Bundesanstalt für Geowissenschaften und Rohstoffe, 2013.

/NUC 10/ Nuclear Decommissioning Authority (NDA): Geological Disposal. Radionuclide behaviour status report, Technical Report. NDA Report, NDA/RWMD/034, 2010.

/OHT 00/ Ohta, A., Kawabe, I.: Rare earth element partitioning between Fe oxyhydroxide precipitates and aqueous NaCl solutions doped with $NaHCO_3$: Determinations of rare earth element complexation constants with carbonate ions. Geochemical Journal, vol. 34, no. 6, pp. 439–454, 2000.

/OLI 05/ Olin, A., Noläng, B., Osadchii, E. G.: Chemical thermodynamics of selenium. 851-, Elsevier B.V., Amsterdam, 2005.

/PAL 84/ Palmer, D., Ramette, R. W., Mesmer, R. E.: Triiodide ion formation equilibrium and activity coefficients in aqueous solution. J. Solution Chem., vol. 13, no. 9, pp. 673–683, 1984.

/PAL 04/ Palmer, D. A., Bénézeth, P., Wesolowski, D. J.: Solubility of nickel oxide and hydroxide in water. In: Nakahara, M., Matubayasi, N., Ueno, M., Yasuoka, K., Watanabe, K. (Eds.): Proceedings of the 14th International Conference on the Properties of Water and Steam. Kyoto, Japan, 29 August - 3 September 2004, 2004.

/PEI 10/ Peiffert, C., Nguyen-Trung, C., Palmer, D. A., Laval, J. P., Giffaut, E.: Solubility of b-Nb2O5 and the hydrolysis of niobium(V) in aqueous solution as a function of temperature and ionic strength. J. Solution Chem., vol. 39, pp. 197–218, 2010.

/PET 81/ Pettine, M., Millero, F. J., Macchi, G.: Hydrolysis of tin(II) in aqueous solutions. Anal. Chem., vol. 53, pp. 1039–1043, 1981.

/PFE 11/ Pfeiffer, F., McStocker, B., Gründler, D., Ewig, F., Thomauske, B., Havenith, A., Kettler, J.: Abfallspezifikation und Mengengerüst. Basis Ausstieg aus der Kernenergienutzung (Juli 2011). Bericht zum Arbeitspaket 3. Vorläufige Sicherheitsanalyse für den Standort Gorleben. GRS-Ber., No. 278, 2011.

/PIN 15/   Pinzke, G.: Retrospektive über Zuflüsse von Wässern und Salzlösungen in die Grubenbaue ehemaliger mecklenburgischer Salzbergwerke (NE-Deutschland). Z. Geol. Wiss., vol. 43, No. 1-2, pp. 105–127, 2015.

/PIT 73/   Pitzer, K. S., Mayorga, G.: Thermodynamics of electrolytes. II. Activity and osmotic coefficients for strong electrolytes with one or both ions univalent. J. Phys. Chem., vol. 77, pp. 2300–2308, 1973.

/PIT 78/   Pitzer, K. S., Silvester, L. F.: Thermodynamics of electrolytes. 11. Properties of 3:2, 4:2, and other high-valence types. J. Phys. Chem., vol. 82, pp. 1239–1242, 1978.

/PIT 91/   Pitzer, K. S. (Ed.): Activity coefficients in electrolyte solutions. 2nd ed. CRC Press, Boca raton, 1991.

/PLY 98/   Plyasunov, A., Fanghänel, T., Grenthe, I.: Estimation of the Pitzer equation parameters for aqueous complexes. A case study for uranium at 298.15 K and 1 atm. Acta Chem. Scand., vol. 52, pp. 250–260, 1998.

/POT 78/   Potter, R. W., Clynne, M. A.: The solubility of the noble gases He, Ne, Ar, Kr, and Xe in water up to the critical point. J. Solution Chem., vol. 7, no. 11, pp. 837–844, 1978.

/RAG 98/   Raghavan, R., Mohanan, P., Patnaik, S.: Innovative processing technique to produce zinc concentrate from zinc leach residue with simultaneous recovery of lead and silver. Hydromet., vol. 48, no. 2, pp. 225–237, 1998.

/RAI 88/   Rai, D., Mattigod, S. V., Moore, D. A.: Characterization of $Fe_2(SeO_3)_3 \cdot 6H_2O$, a new synthetic ferric selenite. Mat. Res. Bull., vol. 23, pp. 1621–1628, 1988.

/RAI 95/   Rai, D., Felmy, A. R., Moore, D. A.: The solubility product of crystalline ferric selenite hexahydrate and the complexation constant of $FeSeO_3^+$. J. Solution Chem., vol. 24, pp. 735–752, 1995.

/RAI 99/   Rai, D., Rao, L., Weger, H. T., Felmy, A. R., Choppin, G. R., Yui, M.: Thermodynamic data for predicting concentrations of Pu(III), Am(III), and Cm(III) in geologic environments. Japan Nuclear Cycle Development Institute (JNCDI), JNC TN8400 99-010, 105 p., 1999.

/RAI 01/   Rai, D., Xia, Y., Hess, N. J., Strachan, D. M., McGrail, B. P.: Hydroxo and chloro complexes/ion interactions of Hf^{4+} and the solubility product of HfO_2(am). J. Solution Chem., vol. 30, no. 11, pp. 949–967, 2001.

/RAI 11a/   Rai, D., Yui, M., Kitamura, A., Grambow, B.: Thermodynamic approach for predicting actinide and rare earth concentrations in leachates from radioactive waste glasses. J. Solution Chem., vol. 40, no. 8, pp. 1473–1504, 2011.

/RAI 11b/   Rai, D., Yui, M., Schaef, H. T., Kitamura, A.: Thermodynamic model for SnO_2(cr) and SnO_2(am) solubility in the aqueous Na^+-H^+-OH^--Cl^--H_2O system. J. Solution Chem., vol. 40, pp. 1155–1172, 2011.

/RAI 12/   Rai, D., Yui, M., Kitamura, A.: Thermodynamic model for amorphous $Pd(OH)_2$ solubility in the aqueous Na^+-K^+-H^+-OH^--Cl^--ClO_4^- system at 25°C: a critical review. J. Solution Chem., vol. 41, pp. 1965–1985, 2012.

/RAI 18/   Rai, D., Kitamura, A., Altmaier, M., Rosso, K. M., Sasaki, T., Kobayashi, T.: A thermodynamic model for ZrO_2(am) solubility at 25 °C in the Ca^{2+}–Na^+–H^+–Cl^-–OH^-–H_2O system. A critical review. J. Solution Chem., vol. 47, no. 5, pp. 855–891, 2018.

/RAM 65/   Ramette, R. W., Sandford, R. W.: Thermodynamics of iodine solubility and triiodide ion formation in water and in deuterium oxide. J. Am. Chem. Soc., vol. 87, no. 22, pp. 5001–5005, 1965.

/REA 90/   Reardon, E. J.: An ion interaction model for the determination of chemical equilibria in cement/water systems. Cement Concr. Res., vol. 20, pp. 175–192, 1990.

/REI 39/   Reiff, F., Toussaint, S. M.: Stability and solubility of sodium stannates. Z. Anorg. Allg. Chem., vol. 241, pp. 372–380, 1939.

283

/REI 13/   Reinhold, K., Jahn, S., Kühnlenz, T.: Endlagerstandortmodell Nord (An-SichT) - Teil I: Beschreibung des geologischen Endlagerstandortmodells. Bundesanstalt für Geowissenschaften und Rohstoffe, 2013.

/RES 10/   Resele, G., Holocher, J., Mayer, G., Niemeyer, M.: Prozesse und Modellkonzepte Tonstein. AF-Colenco AG, 1313/04, 158 p., 2010.

/RIC 51/   Ricci, J. E., Linke, W. F.: The system magnesium molybdate-water and the 25° isotherm of the system $MgMoO_4$ - $MgCl_2$ - H_2O. J. Am. Chem. Soc., vol. 73, no. 8, pp. 3603–3607, 1951.

/RIC 13/   Richens, D. T.: Chapter 4: Molybdenum Aqua Ions. In: Molybdenum, Its biological and coordination chemistry and industrial applications. Chemistry Research and Applications, ISBN 1-62417-285-7, Nova Science Publishers Inc: Hauppauge, New York, 2013.

/RIN 15/   Rincke, C., Bette, S., Dinnebier, R. E., Voigt, W.: Nickel bicarbonate revealed as a basic carbonate. Eur. J. Inorg. Chem., no. 36, pp. 5913–5920, 2015.

/ROB 95/   Robie, R. A., Hemingway, B. S.: Thermodynamic properties of minerals and related substances at 298,15 K and 1 bar (10^5 Pascals) pressure and at higher temperatures. US Geol. Survey Bull., vol. 2131, pp. 1–41, 1995.

/ROS 68/   Rosenblum, P.: Solubility in the potassium stannate – potassium hydroxide – water system at 0 to 95.0 °C. Can. J. Chem., vol. 46, no. 16, pp. 2715–2719, 1968.

/ROS 11/   Rosenberg, Y. O., Metz, V., Ganor, J.: Co-precipitation of radium in high ionic strength systems. 1. Thermodynamic properties of the Na-Ra-Cl-SO_4-H_2O system - Estimating Pitzer parameters for $RaCl_2$. Geochim. Cosmochim. Acta, vol. 75, no. 19, pp. 5389–5402, 2011.

/ROS 14/   Rosenberg, Y. O., Sadeh, Y., Metz, V., Pina, C. M., Ganor, J.: Nucleation and growth kinetics of $Ra_xBa_{1-x}SO_4$ solid solution in NaCl aqueous solutions. Geochim. Cosmochim. Acta, vol. 125, pp. 290–307, 2014.

/ROW 12/ Rowland, D., May, P. M.: An investigation of Zdanovskii's rule for predicting the water activity of multicomponent aqueous strong electrolyte solutions. J. Chem. Eng. Data, vol. 57, pp. 2589–2602, 2012.

/RÜB 07/ Rübel, A., Becker, D.-A., Fein, E.: Radionuclide transport modelling. Performance assessment of repositories in clays. GRS-Ber., vol. 228, No. 228, 219 p., Ges. für Anlagen- und Reaktorsicherheit (GRS): Köln, 2007.

/RÜB 10/ Rübel, A., Mönig, J.: Prozesse, Modellkonzepte und sicherheitsanalytische Rechnungen für ein Endlager im Salz. GRS-A-Bericht, No. 3521, 2010.

/SAL 17/ Salah, S., Wang, L.: Speciation and solubility calculations for waste relevant radionuclides in Boom Clay. Ed.: SCK CEN, SCK-CEN, No. 26188888, 156 p., 2017.

/SAS 08/ Sasaki, T., Kobayashi, T., Tagaki, I., Moriyama, H.: Hydrolysis constant and coordination geometry of zirconium(IV). J. Nucl. Sci. Tech., vol. 45, no. 8, pp. 735–739, 2008.

/SAS 10/ Sasaki, T., Nakaoka, O., Arakawa, R., Kobayashi, T., Tagaki, I., Moriyama, H.: Detection of polynuclear zirconium hydroxide species in aqueous solution by desktop ESI-MS. J. Nucl. Sci. Tech., vol. 47, no. 12, pp. 1211–1218, 2010.

/SAV 18/ Savage, D., Cloet, V.: A review of cement-clay modelling. NAGRA Arbeitsbericht, NAB 18-24, 2018.

/SCH 62/ Scholder, R., Giesler, E.: Über Hydroxoniccolate(II) und Hydroxocobaltate(II). Z. Anorg. Allg. Chem., vol. 316, No. 3-4, pp. 237–246, 1962.

/SCH 69/ Schöneshöfer, M., Karmann, W., Henglein, A.: Die Pulsradiolyse des Selenwasserstoffes in wässriger Lösung. Intl. J. Radiation Phys. Chem., vol. 1, no. 3, pp. 407–423, 1969.

/SCH 81/ Schnering, H. G. v., Nesper, R., Pelshenke, H.: $Sn_{21}Cl_{16}(OH)_{14}O_6$, das sogenannte basische Zinn(II)-chlorid [1] / $Sn_{21}Cl_{16}(OH)_{14}O_6$, the so-called basic tin(II) chloride. Z. Naturforsch. B, vol. 36, no. 12, pp. 1551–1560, 1981.

/SCH 03/ Scheidegger, A. M., Grolimund, D., Cui, D., Devoy, J., Spahiu, K., Wersin, P., Bonhoure, I., Janousch, M.: Reduction of selenite on iron surfaces: A micro-spectroscopic study. J. Phys. IV France, vol. 104, pp. 417–420, 2003.

/SCH 08/ Scheinost, A. C., Charlet, L.: Selenite reduction by mackinawite, magnetie and siderite: XAS characterization of nansized redox products. Environ. Sci. Technol., vol. 42, pp. 1984–1989, 2008.

/SCH 09/ Schramm, M., Kühnlenz, T., Mingerzahn, G., Hammer, J.: Lösungen im Salzstock Gorleben - eine Dokumentation und genetische Interpretation. Bundesanstalt für Geowissenschaften und Rohstoffe (BGR), 145 p.: Hannover, 2009.

/SCH 12/ Scharge, T., Muñoz, A. G., Moog, H. C.: Activity coefficients of fission products in higly salinary solutions of Na^+, K^+, Mg^{2+}, Ca^{2+}, Cl^-, and SO_4^{2-}: Cs+. J. Chem. Eng. Data, vol. 57, pp. 1637–1647, 2012.

/SCH 13/ Scharge, T., Muñoz, A. G., Moog, H. C.: Addition to "Activity coefficients of fission products in highly salinary solutions of Na+, K^+, Mg^{2+}, Ca^{2+}, Cl^-, and SO_4^{2-}: Cs^+. J. Chem. Eng. Data, vol. 58, pp. 187–188, 2013.

/SÉB 01/ Séby, F., Potin-Gautier, M., Giffaut, E.: A critical review of thermodynamic data for inorganic tin species. Geochim. Cosmochim. Acta, vol. 65, pp. 3041–3053, 2001.

/SHO 02/ Short, R. J., Hand, R. J., Hyatt, N. C.: Molybdenum in nuclear waste glasses - incorporation and redox state. MRS Proc., vol. 757, 2002.

/SHU 09/ Shukor, M. Y., Rahman, M. F., Shamaan, N. A., Syed, M. A.: Reduction of molybdate to molybdenum blue by Enterobacter sp. Strain Dr.Y13. J. Basic Microbiol., 49 Suppl. 1, pp. S43-54, 2009.

/SIM 16/ Simoes, M. C., Hughes, K. J., Ingham, D. B., Ma, L., Pourkashanian, M.: Estimation of the Pitzer parameters for 1–1, 2–1, 3–1, 4–1, and 2–2 single electrolytes at 25 °C. J. Chem. Eng. Data, vol. 61, no. 7, pp. 2536–2554, 2016.

/SIM 17/ Simoes, M. C., Hughes, K. J., Ingham, D. B., Ma, L., Pourkashanian, M.: Estimation of the thermochemical radii and ionic volumes of complex ions. Inorg. Chem., vol. 56, no. 13, pp. 7566–7573, 2017.

/SKB 11/ SKB: Long-term safety for the final repository for spent nuclear fuel at For-smark - Main report of the SR-Site project - Volume I - SKB Technical Report TR-11-01, Technical Report. SKB Berichte (Svensk Kärnbränslehan-tering AB, Schweden), SKB TR-11-01, Svensk Kärnbränslehantering AB, Swedish Nuclear Fuel and Waste Management Co., Box 250, SE-101 24 Stockholm, 2011.

/SOU 70/ Souchay, P., Cadiot, M., Viossat, B.: Quelques propriétés nouvelles des hy-droxydes des Mo^{IV} et Mo^V. Bull. Soc. Chim. Fr., pp. 892–898, 1970.

/STO 99/ Stober, Bucher: Origin of salinity of deep groundwater in crystalline rocks. Terra Nova, vol. 11, no. 4, pp. 181–185, 1999.

/SUN 92/ Sun, W., Li, Y., Chen, X.: Relationships between ionic radii and Pitzer's pa-rameters in 1:1 type electrolyte solutions. Trans. Nonferrous Met. Soc. China, vol. 2, no. 4, pp. 34–38, 1992.

/TAL 04/ Talerico, C., Ochs, M., Giffaut, E.: Solubility of niobium(V) under cementi-tious conditions: importance of Ca-niobate. Mat. Res. Soc. Symp. Proc., vol. 824, pp. 443–448, 2004.

/TAR 05/ Tarantino, S. C., Zema, M.: Mixing and ordering behavior in manganoco-lumbite-ferrocolumbite solid solution: A single-crystal X-ray diffraction study. Am. Mineral., vol. 90, No. 8-9, pp. 1291–1300, 2005.

/TAU 02/   Taube, F., Andersson, I., Pettersson, L.: Molybdate speciation in systems related to the bleaching of kraft pulp. In: Pope, M. T., Müller, A. (Eds.): Polyoxometalate Chemistry From Topology via Self-Assembly to Applications. no. 3, pp. 161–173, ISBN 0-7923-7011-2, DOI 10.1007/0-306-47625-8_12, Kluwer Academic Publishers: Dordrecht, 2002.

/THO 14/   Thoenen, T., Hummel, W., Berner, U. Curti, E.: The PSI/Nagra Chemical Thermodynamic Database 12/07, Other. Paul Scherrer Institut, PSI Bericht, 14-04, 1 January 2014.

/THO 21/   Thorpe, C. L., Neeway, J. J., Pearce, C. I., Hand, R. J., Fisher, A. J., Walling, S. A., Hyatt, N. C., Kruger, A. A., Schweiger, M., Kosson, D. S., Arendt, C. L., Marcial, J., Corkhill, C. L.: Forty years of durability assessment of nuclear waste glass by standard methods. npj Mater. Degrad., vol. 5, no. 1, 2021.

/TIT 86/   Tittel, G., Hollmann, A., StierFriedland, G., Warnecke, E.: Schachtanlage Konrad - Ableitung von Sorptionsdaten aus experimentellen Untersuchungen. PTB Interner Arbeitsbericht, PTB-SE-IB-7, 1986.

/TYT 86/   Tytko, K.-H.: Mo Molybdenum, Molybdenum oxide hydrates. Oxomolybdenum species in aqueous solutions. Eds.: Katscher, H., Schröder, F., Gmelin Handbook of Inorganic Chemistry, M-o / A-B / B / 3 / a, 8. ed., 360 p., ISBN 9783662088395, DOI 10.1007/978-3-662-08837-1, Springer Berlin Heidelberg: Berlin, Heidelberg, s.l., 1986.

/TYT 87/   Tytko, K.-H., Trobisch, U.: Gmelin handbook of inorganic chemistry. 8th edition. Mo Molybdenum. Supplement Volume B 3a. Molybdenum oxide hydrates. Oxomolybdenum species in aqueous solutions. 360 p., Springer-Verlag: Berlin, 1987.

/USD 98/   Usdowski, E., Dietzel, M.: Atlas and data of solid-solution equilibria of marine evaporites. Springer: Berlin, 1998.

/UZA 59/   Uzarov, G. G., Lipshits, B. M., Lovchikov, V. S.: Izotermy rastvorimosti v sisteme $Na_2O-H_2O-SnO_2$ pri 25 i 75°. Zh. Neorg. Khim., vol. 4, pp. 2380–2383, 1959.

/VAN 06/ van Iseghem, P., Lemmens, K., Aertsens, M., Gin, S., Ribet, I., Grambow, B., Crovisier, J. L., Del Nero, M., Curti, E., Schwyn, B., Luckscheiter, B., McMenamin, T.: Chemical durability of high-level waste glass in repository environment: main conclusions and remaining uncertainties from the GLASTAB and GLAMOR projects. MRS Proc., vol. 932, pp. 293–304, 2006.

/VLE 77/ Vlek, P. L. G., Lindsay, W. L.: Thermodynamic stability and solubility of molybdenum minerals in soils. Soil Sci. Soc. Am. J., vol. 41, no. 1, pp. 42–46, 1977.

/VOI 16/ Voigt, M., Rodriguez-Blanco, J. D., Vallina, B., Benning, L. G., Oelkers, E. H.: An experimental study of hydroxylbastnasite solubility in aqueous solutions at 25 °C. Chem. Geol., vol. 430, pp. 70–77, 2016.

/VON 92/ von Borstel, L. E.: Lösungen in marinen Zechsteinevaporiten Deutschlands. Technische Universität Clausthal (TU Clausthal), 1992.

/WAL 07/ Walter, R.: Geologie von Mitteleuropa (7. Aufl.). Schweizerbart'sche Verlagsbuchhandlung, Stuttgart, 2007.

/WAL 11/ Walke, R., Humphreys, P., King, F., Little, R., Metcalfe, R., Penfold, J., Towler, G., Walsh, R., Wilson, J.: OPG's deep geologic repository for low & intermediate level waste. Postclosure safety assessment: data. NWMO Tech. Rep, NWMO DGR-TR-2011-32, 2011.

/WAN 10a/ Wang, F., Hu, B.: Solubility prediction of $RbCl$-Rb_2SO_4-H_2O system at 25°C using Pitzer ion-interaction model. Russ. J. Inorg. Chem., vol. 55, no. 3, pp. 441–443, 2010.

/WAN 10b/ Wang, P., Wilson, L. L., Wesolowski, D. J., Rosenqvist, J., Anderko, A.: Solution chemistry of Mo(III) and Mo(IV), Thermodynamic foundation for modeling localized corrosion. Corr. Sci., vol. 52, no. 5, pp. 1625–1634, 2010.

/WAN 13a/ Wang, L.: Solubility of radionuclides in supercontainer concrete. SCK CEN External Rep, SCK CEN-ER-239, 2013.

/WAN 13b/ Wang, F. Y.: Thermodynamic simulation on Rb_2SO_4-Cs_2SO_4-$MgSO_4$-H_2O system at 25 °C. Asian J. Chem., vol. 25, no. 13, pp. 7631–7632, 2013.

/WEA 90/ Weast, R. C., Lide, D. R., Astle, M. J., Beyer W. H.: CRC Handbock of Chemistry and Physics 70th ed. CRC Press: Boca Raton, 1990.

/WER 14/ Wersin, P., Kiczka, M., Rosch, D.: Safety case for the disposal of spent nuclear fuel at Olkiluoto. Radionuclide solubility limits and migration parameters for the canister and buffer. Posiva Rep, 2012-39, 2014.

/WOL 11/ Wolfgramm, M., Thorwart, K., Rauppach, K.: Zusammensetzung, Herkunft und Genese geothermaler Tiefengrundwässer im Norddeutschen Becken (NDB) und deren Relevanz für die geothermische Nutzung. Z. Dtsch. Ges. Geowiss., vol. 339, pp. 173–193, 2011.

/WOL 12/ Wolf, J., Behlau, J., Beuth, T., Bracke, G., Bube, C., Buhmann, D., Dresbach, C., Hammer, J., Keller, S., Kienzler, B., Klinge, H., Krone, J., Lommerzheim, A., Metz, V., et al.: FEP-Katalog für die VSG. Dokumentation. Bericht zum Arbeitspaket 7. Vorläufige Sicherheitsanalyse für den Standort Gorleben. Gesellschaft für Anlagen- und Reaktorsicherheit (GRS) mbH, Bundesanstalt für Geowissenschaften und Rohstoffe (BGR), DBE Technology GmbH (DBE Tec), Institut für Gebirgsmechanik GmbH (IfG), Karlsruhe Institut für Technologie \textendash Institut für Nukleare Entsorgung (KIT-INE), GRS-Ber., No. 283: Köln, 2012.

/WOO 84/ Wood, S. A., Crerar, D. A., Brantley, S. L.: Mean molal stoichiometric activity coefficients of alkali halides and related electrolytics in hydrothermal solutions. Am. J. Sci., vol. 284, no. 6, pp. 668–705, 1984.

/XIE 12/ Xie, M., Herbert, H.-J.: Vorgezogene Sicherheitsanalyse Gorleben. Geochemical Analysis of the Sealing System - Technical Report to Work Package 9.1.2. GRS-Ber., No. 308, 322 p., 2012.

/YAL 16/ Yalçıntaş, E., Gaona, X., Altmaier, M., Dardenne, K., Polly, R., Geckeis, H.: Thermodynamic description of Tc(iv) solubility and hydrolysis in dilute to concentrated NaCl, $MgCl_2$ and $CaCl_2$ solutions. Dalton Trans., vol. 45, no. 21, pp. 8916–8936, 2016.

/YUI 99/ Yui, M., Azuma, J., Shibata, M.: JNC thermodynamic database for performance assessment of high-level radioactive waste disposal system. JNC Tech. Note, TN8400 99-070, 1999.

/ZAI 91/ Zaitsev, B. E., Ivanov-Emin, B. N., Petrishcheva, L. P., Il'inets, A. M., Baturin, N. A., Regel' L. L., Dolganev, V. P.: Preparation and structure of alkaline-earth metal hydroxopalladates(II). Russ. J. Inorg. Chem., vol. 36, pp. 74–77, 1991.

/ZDA 38/ Zdanovskij, A. B.: Funkcional'naja svjaz' svojstv smesannych i otdelnych rastvorov. Zh. Fiz. Khim., vol. 12, pp. 106–108, 1938.

/ZIM 03/ Zimmer, P.: Bildung von Sekundärphasen bei der Korrosion von verglasten Nuklear-Abfällen. Ed.: Forschungszentrum Karlsruhe, Forschungsz. Karlsruhe Wiss. Ber., No. 6910, 194 p.: Karlsruhe, 2003.

/ZOC 20/ Zocher, H.: Über zinnsaure und bleisaure Salze. Z. Anorg. Allg. Chem., vol. 112, pp. 1–66, 1920.

/ZOT 95/ Zotov, A. V., Kudrin, A. V., Levin, K. A., Shikina, N. D., Var'yash, L. N.: Experimental studies of the solubility and complexing of selected ore elements (Au, Ag, Cu, Mo, As, Sb, Hg) in aqueous solutions. In: Shmulovich, K. I., Yardley, B. W. D., Gonchar, G. G. (Eds.): Fluids in the Crust, Equilibrium and transport properties. pp. 95–137, ISBN 978-94-010-4536-0, DOI 10.1007/978-94-011-1226-0_5, Springer Netherlands: Dordrecht, s.l., 1995.

A   Annex

A.1   Table of appendices

A.2 Overview of considered solubility limits in previous geochemical studies

The various geochemical studies did not address all elements considered in this study. In that case, the study is not mentioned in the tables for these elements.

Abbreviations:

UL: Considered upper solubility limit [mol/l] (M) or [mol/kg] (m)

LL: Considered lower solubility limit [mol/l] (M) or [mol/kg] (m)

RV/ Rec. Value: Recommended solubility value

Phase: assumed solubility limiting solid phase

Tab A. 1   Considered sources of solubility limits

No.	Country	Source
1	Belgium	/SAL 17/
2	Belgium	/WAN 13a/
3	Canada	/WAL 11/
4	Canada	/DUR 10/
5	Finland	/WER 14/
6	France	/AND 05b/
7a	Germany	/NIE 02/ (based on /BRE 98/)
7b	Germany	/BUH 91/
8	Germany	/KIE 12/
9	Germany	/KIE 13/
10	Great Britain	/NUC 10/ taken from /NIR 03/
11	Japan	/AZU 99/, /JNC 00/
12	Sweden	/BEN 14/ based on /GRI 10a/ /GRI 10b/ and /DUR 06b/
13	Switzerland	/BER 14a/, /BER 14b/

Tab A. 2 Solubility limiting solid phases and solubilities for caesium in earlier studies (I)

Country	Study	Solution type	Phase	Lower Limit	Rec. value	Upper Limit
Belgium	1	Boom clay pore water I=0.0085 pH 8.36	none	No limit		No limit
Belgium	2	Cement pore water I ≤ 0.08. state I: pH 13.5 - 12.5 state II: 12.5 state III: 12.5 - 10.5	none	No limit		No limit
Finland	5	Altered groundwaters (six different) inside the canisters NaCl/CaCl$_2$ I= 0.001 to 1.3 mol/l pH 7.33 to 10	none			No limit
Finland	5	Altered ground waters (six different) at the buffer/ host rock interface NaCl/CaCl$_2$ I= 0.001 to 1.3 mol/l pH 7.12 to 10	none			No limit
Finland	5	Bentonite porewater (six different) NaCl/CaCl$_2$ I=0.002 to 2.9, pH 7.23 to 10	none			No limit
France	6	Pore water in bentonite Buffer (unspecified)	none			No limit
France	6	Pore water of cement-based materials (unspecified)	none			No limit
France	6	Pore water of Callovo-Oxfordian clay rock NaCl/CaCl$_2$ I=0.09-0.12 mol/l pH 6.9-7.6	none			No limit

Tab A. 3 Solubility limiting solid phases and solubilities for caesium in earlier studies (II)

Country	Study	Solution type	Phase	Lower Limit	Rec. value	Upper Limit
Germany	7a	Unspecified solution expected to occur in the Konrad mine <pH12, possibly up to 3.3 mol/l Cl (NaCl/ CaCl$_2$/ MgCl$_2$)	none			$1 \cdot 10^{-2}$ M
Germany	7b	Unspecified brine under alkaline, neutral, and acidic conditions	none			No limit
Great Britain	10	Cementitious system (not specified)	none	No limit		No limit
Great Britain	10	Bentonite pore water (not specified)	none	No limit		No limit
Japan	11	Bentonite porewater based on fresh groundwater Na$_2$CO$_3$ I=0.026 pH 8.4	none	No limit		No limit
Japan	11	Bentonite porewater based on saline groundwater NaCl/ Na$_2$CO$_3$ I=0.615 pH 7.8	none	No limit		No limit
Japan	11	Bentonite porewater based on fresh groundwater after contact with cement Na$_2$CO$_3$ I=0.0181 pH 8.7	none	No limit		No limit
Japan	11	Bentonite porewater based on fresh groundwater Na$_2$CO$_3$/ Na$_2$SO$_4$ I=0.211 pH 7.2	none	No limit		No limit
Japan	11	Bentonite porewater based on fresh groundwater Na$_2$CO$_3$ I=0.0083 pH 9.7	none	No limit		No limit
Japan	11	Bentonite porewater based on fresh groundwater, oxidizing Na$_2$CO$_3$ I=0.0223 pH 8.4	none	No limit		No limit
Sweden	12	Forsmark reference water (NaCl/ CaCl$_2$ I= 0.19 mol/l)	none	No limit		No limit

Tab A. 4   Solubility limiting solid phases and solubilities for caesium in earlier studies (III)

Country	Study	Solution type	Phase	Lower Limit	Rec. value	Upper Limit
Sweden	12	Saline water (NaCl/ CaCl$_2$ I=1.86 mol/l)	none	No limit		No limit
Sweden	12	Ice-melting water (Na/Ca/Cl,HCO3/F,Si) I=0.0012 mol/l)	none	No limit		No limit
Switzerland	13	Cement/ concrete system equilibrated with Opalinus clay porewater: NaCl/ CaCl$_2$ I=0.09 mol/kg pH12.5	none	No limit		No limit
Switzerland	13	Bentonite porewater system equilibrated with Opalinus clay porewater NaCl/ Na$_2$SO$_4$ I=0.239 mol/kg pH 7.79	none	No limit		No limit

Tab A. 5   Solubility limiting solid phases and solubilities for iodine in earlier studies

Country	Study	Solution type	Phase	Lower Limit	Rec. value	Upper Limit
Germany	7a	Unspecified solution expected to occur in the Konrad mine <pH12, possibly up to 3.3 mol/l Cl (NaCl/ CaCl$_2$/ MgCl$_2$)	none			$1 \cdot 10^{-2}$ M

Tab A. 6 Solubility limiting solid phases and solubilities for lead in earlier studies (I)

Country	Study	Solution type	Phase	Lower Limit	Rec. value	Upper Limit
Belgium	2	Cement pore water I ≤ 0.08. state I: pH 13.5 - 12.5 state II: 12.5 state III: 12.5 - 10.5	PbO (litharge)	I: No limit II: $5 \cdot 10^{-2}$ M III: $1 \cdot 10^{-4}$ M		No limit
Canada	3	Argillaceous limestone model porewater (Guelph): Concentrated NaCl/ CaCl$_2$ brine I=7.2 mol/kg pH 6.5	none	No limit		No limit
Canada	3	Argillaceous limestone model porewater (Cobourg 2): NaCl/KCl/CaCl$_2$ brine I=3.8 mol/kg pH 6.5	none	No limit		No limit
Canada	3	ditto, but equilibrated with cement pH 11.9	none	No limit		No limit
Canada	4	Model groundwater for crystalline rock Na/Ca/Cl/SO4 I=0.24 mol/l pH 7.1 (CR-10 eq)	PbCO$_3$ (cerussite) or Pb$_3$(CO$_3$)$_2$(OH)$_2$ (hydrocerussite) or Pb$_3$(PO$_4$)$_2$			PbCO$_3$: $3.11 \cdot 10^{-6}$ m Pb$_3$(CO$_3$)$_2$(OH)$_2$: $7.96 \cdot 10^{-6}$ m Pb$_3$(PO$_4$)$_2$: $7.1 \cdot 10^{-6}$ m
Canada	4	Model groundwater for crystalline rock equilibrated with bentonite and steel I=0.32 pH 8.7 (CR-10 NF)	Pb$_3$(PO$_4$)$_2$			$1.4 \cdot 10^{-5}$ m

Tab A. 7 Solubility limiting solid phases and solubilities for lead in earlier studies (II)

Country	Study	Solution type	Phase	Lower Limit	Rec. value	Upper Limit
Canada	4	Brine from salt formation NaCl/ CaCl$_2$ I=4.51 pH 5.8 (SR-270 eq)	none			No limit
Canada	4	Brine from salt formation equilibrated with bentonite and steel NaCl/ CaCl$_2$ I=4.50 pH 8.1 (SR-270 NF)	none			No limit
France	6	Pore water in bentonite buffer (unspecified)	not determined	No limit		No limit
France	6	Pore water of cement-based materials (unspecified)	not determined	No limit		No limit
France	6	Pore water of Callovo-Oxfordian clay rock NaCl/ CaCl$_2$ I=0.09-0.12 mol/l pH 6.9-7.6	not determined	No limit		No limit
Germany	7a	Unspecified solution expected to occur in the Konrad mine <pH12, possibly up to 3.3 mol/l Cl (NaCl/ CaCl$_2$/ MgCl$_2$)	not determined			$1 \cdot 10^{-4}$ M
Great Britain	10	Cementitious system (not specified)	not determined	No limit		No limit
Great Britain	10	Bentonite pore water (not specified)	not determined	No limit		No limit
Japan	11	Bentonite porewater based on fresh groundwater Na$_2$CO$_3$ I=0.026 pH 8.4	PbCO$_3$ (cerussite)	Japan		$2 \cdot 10^{-6}$ M
Japan	11	Bentonite porewater based on saline groundwater NaCl/ Na$_2$CO$_3$ I=0.615 pH 7.8	PbCO$_3$ (cerussite)	Japan		$6 \cdot 10^{-6}$ M
Japan	11	Bentonite porewater based on fresh groundwater after contact with cement Na$_2$CO$_3$ I=0.0181 pH 8.7	PbCO$_3$ (cerussite)	Japan		$2 \cdot 10^{-6}$ M
Japan	11	Bentonite porewater based on fresh groundwater Na$_2$CO$_3$/ Na$_2$SO$_4$ I=0.211 pH 7.2	PbCO$_3$ (cerussite)	Japan		$2 \cdot 10^{-6}$ M

Tab A. 8   Solubility limiting solid phases and solubilities for lead in earlier studies (III)

Country	Study	Solution type	Phase	Lower Limit	Rec. value	Upper Limit
Japan	11	Bentonite porewater based on fresh groundwater Na_2CO_3 I=0.0083 pH 9.7	$PbCO_3$ (cerussite)	Japan		$3 \cdot 10^{-6}$ M
Japan	11	Bentonite porewater based on fresh groundwater, oxidizing Na_2CO_3 I=0.0223 pH 8.4	$PbCO_3$ (cerussite)	Japan		$2 \cdot 10^{-6}$ M
Sweden	12	Forsmark reference water (NaCl/ $CaCl_2$ I= 0.19 mol/l)	$PbCO_3$ (cerussite)			$1.07 \cdot 10^{-6}$ M
Sweden	12	Saline water (NaCl/ $CaCl_2$ I=1.86 mol/l)	$Pb_3(CO_3)_2(OH)_2$ (hydrocerussite)			$2.82 \cdot 10^{-7}$ M
Sweden	12	Ice-melting water (Na/Ca/Cl,HCO3/F,Si I=0.0012 mol/l)	Pb(OH)Cl (laurionite)			$7.41 \cdot 10^{-7}$ M
Switzerland	13	Cement/ concrete system equilibrated with Opalinus clay porewater: NaCl/ $CaCl_2$ I=0.09 mol/kg pH12.5	UL, RV: $Pb(OH)_2$ LL: PbO(red) (litharge)	$1.7 \cdot 10^{-3}$ M	$4.6 \cdot 10^{-3}$ M	$4.6 \cdot 10^{-3}$ M
Switzerland	13	Bentonite porewater system equilibrated with Opalinus clay porewater NaCl/ Na_2SO_4 I=0.239 mol/kg pH 7.79	UL: $PbSO_4$ (anglesite) RV: $PbCO_3$ (cerussite) LL: PbS (galena)	$2.4 \cdot 10^{-8}$ M	$8.8 \cdot 10^{-7}$ M	$6.5 \cdot 10^{-5}$ M

Tab A. 9 Solubility limiting solid phases and solubilities for molybdenum in earlier studies (I)

Country	Study	Solution type	Phase	Lower Limit	Rec. value	Upper Limit
Belgium	1	Boom clay pore water I=0.0085 pH 8.36	UL: MoO_2 (tugari-novite) LL: MoS2	$1.966 \cdot 10^{-13}$		$1.661 \cdot 10^{-6}$ M
Belgium	2	Cement pore water I ≤ 0.08. state I: pH 13.5 - 12.5 state II: 12.5 state III: 12.5 - 10.5	$CaMoO_4$	I: $5 \cdot 10^{-6}$ m II: $5 \cdot 10^{-6}$ m III: $5 \cdot 10^{-6}$ m		I: $9 \cdot 10^{-4}$ m II: $5 \cdot 10^{-6}$ m III: $5 \cdot 10^{-5}$ m
Canada	4	Model groundwater for crystalline rock Na/Ca/Cl/SO4 I=0.24 mol/l pH 7.1 (CR-10 eq)	MoO_2			$8.72 \cdot 10^{-9}$ m
Canada	4	Model groundwater for crystalline rock equilibrated with bentonite and steel I=0.32 pH 8.7 (CR-10 NF)	MoO_2			$3.64 \cdot 10^{-15}$ m
Canada	4	Brine from salt formation NaCl/ $CaCl_2$ I=4.51 pH 5.8 (SR-270 eq)	MoO_2			$2.34 \cdot 10^{-13}$ m
Canada	4	Brine from salt formation equilibrated with bentonite and steel NaCl/ $CaCl_2$ I=4.50 pH 8.1 (SR-270 NF)	MoO_2			$6.29 \cdot 10^{-17}$ m
Finland	5	Altered groundwaters (six different) inside the canisters NaCl/ $CaCl_2$ I= 0.001 to 1.3 mol/l pH 7.33 to 10	MoO_2 or $CaMoO_4$	$2.4 \cdot 10^{-6}$ M		No limit

Tab A. 10 Solubility limiting solid phases and solubilities for molybdenum in earlier studies (II)

Country	Study	Solution type	Phase	Lower Limit	Rec. value	Upper Limit
Finland	5	Altered ground waters (six different) at the buffer/ host rock interface NaCl/ CaCl$_2$ I= 0.001 to 1.3 mol/l pH 7.12 to 10	MoO$_2$ or CaMoO$_4$	$8.8 \cdot 10^{-9}$ M		No limit
Finland	5	Bentonite porewater (six different) NaCl/ CaCl$_2$ I=0.002 to 2.9, pH 7.23 to 10				
Germany	7a	Unspecified solution expected to occur in the Konrad mine <pH12, possibly up to 3.3 mol/l Cl (NaCl/ CaCl$_2$/ MgCl$_2$)	none			$1 \cdot 10^{-4}$ M
Germany	7b	Unspecified brine under acidic conditions	none	$1 \cdot 10^{-3}$ M	$1 \cdot 10^{-2}$ M	$1 \cdot 10^{-1}$ M
Germany	7b	Unspecified brine under neutral conditions	none	$1 \cdot 10^{-7}$ M	$1 \cdot 10^{-4}$ M	$1 \cdot 10^{-1}$ M
Germany	7b	Unspecified brine under alkaline conditions	none	$1 \cdot 10^{-7}$ M	$1 \cdot 10^{-4}$ M	$1 \cdot 10^{-1}$ M
Great Britain	10	Cementitious system (not specified)	not specified	$1 \cdot 10^{-12}$ M		$1 \cdot 10^{-1}$ M
Switzerland	13	Cement/ concrete system equilibrated with Opalinus clay porewater: NaCl/ CaCl$_2$ I=0.09 mol/kg pH12.5	CaMoO$_4$ (powellite)	$3.6 \cdot 10^{-5}$ M	$7.2 \cdot 10^{-6}$ M	$2.0 \cdot 10^{-5}$ M
Switzerland	13	Bentonite porewater system equilibrated with Opalinus clay porewater NaCl/ Na$_2$SO$_4$ I=0.239 mol/kg pH 7.79	CaMoO$_4$ (powellite)	$6.5 \cdot 10^{-6}$ M	$2.1 \cdot 10^{-5}$ M	$4.7 \cdot 10^{-5}$ M

Tab A. 11 Solubility limiting solid phases and solubilities for nickel in earlier studies (I)

Country	Study	Solution type	Phase	Lower Limit	Rec. value	Upper Limit
Belgium	1	Boom clay pore water I=0.0085 pH 8.36	UL: β-Ni(OH)$_2$ LL: FeNi$_2$S$_4$ (violarite)	$9.522 \cdot 10^{-9}$		$7.2 \cdot 10^{-4}$
Belgium	2	Cement pore water I ≤ 0.08. state I: pH 13.5 - 12.5 state II: 12.5 state III: 12.5 - 10.5	Ni-Al-LDH	I: $2.4 \cdot 10^{-7}$ m II: $2.4 \cdot 10^{-7}$ m III: $2.4 \cdot 10^{-7}$ m		I: $3.4 \cdot 10^{-7}$ m II: $3.4 \cdot 10^{-7}$ m III: $3.4 \cdot 10^{-7}$ m
Finland	5	Altered groundwaters (six different) inside the canisters NaCl/ CaCl$_2$ I= 0.001 to 1.3 mol/l pH 7.33 to 10	Ni(OH)$_2$	$9.3 \cdot 10^{-5}$ M		$8.3 \cdot 10^{-4}$ M
Finland	5	Altered ground waters (six different) at the buffer/ host rock interface NaCl/ CaCl$_2$ I= 0.001 to 1.3 mol/l pH 7.12 to 10	Ni(OH)$_2$	$1.5 \cdot 10^{-3}$ M		No limit
Finland	5	Bentonite porewater (six different) NaCl/ CaCl$_2$ I=0.002 to 2.9, pH 7.23 to 10	Ni(OH)$_2$	$1.9 \cdot 10^{-4}$ M		$1.5 \cdot 10^{-3}$ M
France	6	Pore water in bentonite buffer (unspecified)	not specified	$1 \cdot 10^{-6}$ M		$1 \cdot 10^{-5}$ M

Tab A. 12 Solubility limiting solid phases and solubilities for nickel in earlier studies (II)

Country	Study	Solution type	Phase	Lower Limit	Rec. value	Upper Limit
France	6	Pore water of cement-based materials (unspecified)	not specified			$2 \cdot 10^{-7}$ M
France	6	Pore water of Callovo-Oxfordian clay rock NaCl/ CaCl$_2$ I=0.09-0.12 mol/l pH 6.9-7.6	not specified	$1 \cdot 10^{-6}$ M		$1 \cdot 10^{-5}$ M
Germany	7a	Unspecified solution expected to occur in the Konrad mine <pH12, possibly up to 3.3 mol/l Cl (NaCl/ CaCl$_2$/ MgCl$_2$)	not deter-mined			$1 \cdot 10^{-3}$ M
Germany	7b	Unspecified brine under acidic conditions	none	$1 \cdot 10^{-3}$ M	$1 \cdot 10^{-2}$ M	$1 \cdot 10^{-1}$ M
Germany	7b	Unspecified brine under neutral conditions	none	$1 \cdot 10^{-7}$ M	$1 \cdot 10^{-4}$ M	$1 \cdot 10^{-1}$ M
Germany	7b	Unspecified brine under alkaline conditions	none	$1 \cdot 10^{-7}$ M	$1 \cdot 10^{-5}$ M	$1 \cdot 10^{-3}$ M
Great Britain	10	Cementitious system (not specified)	not specified	$1 \cdot 10^{-9}$ M		$5 \cdot 10^{-6}$ M
Great Britain	10	Bentonite pore water (not specified)	none	No limit		No limit
Sweden	12	Forsmark reference water (NaCl/ CaCl$_2$ I= 0.19 mol/l)	β-Ni(OH)$_2$ (theophrasite)		$1.55 \cdot 10^{-3}$ M	
Sweden	12	Saline water (NaCl/ CaCl$_2$ I=1.86 mol/l)	β-Ni(OH)$_2$ (theophrasite)		$1.35 \cdot 10^{-7}$ M	

Tab A. 13   Solubility limiting solid phases and solubilities for nickel in earlier studies (III)

Country	Study	Solution type	Phase	Lower Limit	Rec. value	Upper Limit
Sweden	12	Ice-melting water (Na/Ca/Cl,HCO3/F,Si I=0.0012 mol/l)	β-Ni(OH)$_2$ (theophrasite)		$5.62 \cdot 10^{-5}$ M	
Switzerland	13	Cement/ concrete system equilibrated with Opalinus clay porewater: NaCl/ CaCl$_2$ I=0.09 mol/kg pH12.5	β-Ni(OH)$_2$ (theophrasite)	$1.0 \cdot 10^{-7}$ M	$3.0 \cdot 10^{-6}$ M	$2.3 \cdot 10^{-4}$ M
Switzerland	13	Bentonite porewater system equilibrated with Opalinus clay porewater NaCl/ Na$_2$SO$_4$ I=0.239 mol/kg pH 7.79	NiCO$_3$	$2.8 \cdot 10^{-5}$ M	$5.5 \cdot 10^{-5}$ M	$4.9 \cdot 10^{-3}$ M

Tab A. 14 Solubility limiting solid phases and solubilities for niobium in earlier studies (I)

Country	Study	Solution type	Phase	Lower Limit	Rec. value	Upper Limit
Belgium	1	Boom clay pore water I=0.0085 pH 8.36	Nb_2O_5	$1\cdot10^{-8}$		$1\cdot10^{-3}$
Belgium	2	Cement pore water I ≤ 0.08. state I: pH 13.5 - 12.5 state II: 12.5 state III: 12.5 - 10.5	"calcium niobate"	I: $4\cdot10^{-9}$ m II: $4\cdot10^{-9}$ m III: $4\cdot10^{-9}$ m		I: $2\cdot10^{-5}$ m II: $8\cdot10^{-9}$ m III: $4.2\cdot10^{-7}$ m
Canada	3	ditto, but equilibrated with cement pH 11.9	none	No limit		No limit
Canada	4	Model groundwater for crystalline rock Na/Ca/Cl/SO$_4$ I=0.24 mol/l pH 7.1 (CR-10 eq)	Nb_2O_5			$1.07\cdot10^{-7}$ m
Canada	4	Model groundwater for crystalline rock equilibrated with bentonite and steel I=0.32 pH 8.7 (CR-10 NF)	Nb_2O_5			$1.30\cdot10^{-5}$ m
Canada	4	Brine from salt formation NaCl/ CaCl$_2$ I=4.51 pH 5.8 (SR-270 eq)	Nb_2O_5			$1.30\cdot10^{-5}$ m
Canada	4	Brine from salt formation equilibrated with bentonite and steel NaCl/ CaCl$_2$ I=4.50 pH 8.1 (SR-270 NF)	Nb_2O_5			$2.01\cdot10^{-7}$ m
Finland	5	Altered groundwaters (six different) inside the canisters NaCl/ CaCl$_2$ I= 0.001 to 1.3 mol/l pH 7.33 to 10	Nb_2O_5	$1.9\cdot10^{-7}$ M		No limit

Tab A. 15 Solubility limiting solid phases and solubilities for niobium in earlier studies (II)

Country	Study	Solution type	Phase	Lower Limit	Rec. value	Upper Limit
Finland	5	Altered ground waters (six different) at the buffer/ host rock interface NaCl/ CaCl$_2$ I= 0.001 to 1.3 mol/l pH 7.12 to 10	Nb$_2$O$_5$	$1.2 \cdot 10^{-7}$ M		No limit
Finland	5	Bentonite porewater (six different) NaCl/ CaCl$_2$ I=0.002 to 2.9, pH 7.23 to 10	Nb$_2$O$_5$	$1.5 \cdot 10^{-7}$ M		No limit
France	6	Pore water in bentonite buffer (unspecified)	not specified			$<5 \cdot 10^{-7}$ M
France	6	Pore water of cement-based materials (unspecified)	not specified			$1 \cdot 10^{-9}$ M
France	6	Pore water of Callovo-Oxfordian clay rock NaCl/ CaCl$_2$ I=0.09-0.12 mol/l pH 6.9-7.6	not specified			$2 \cdot 10^{-7}$ M
Germany	7a	Unspecified solution expected to occur in the Konrad mine <pH12, possibly up to 3.3 mol/l Cl (NaCl/ CaCl$_2$/ MgCl$_2$)	not deter-mined			10^{-7} M
Germany	7b	Unspecified brine under acidic conditions	none	$1 \cdot 10^{-3}$ M	$1 \cdot 10^{-2}$ M	$1 \cdot 10^{-1}$ M
Germany	7b	Unspecified brine under neutral conditions	none	$1 \cdot 10^{-7}$ M	$1 \cdot 10^{-4}$ M	$1 \cdot 10^{-1}$ M

Tab A. 16   Solubility limiting solid phases and solubilities for niobium in earlier studies (III)

Country	Study	Solution type	Phase	Lower Limit	Rec. value	Upper Limit
Germany	7b	Unspecified brine under alkaline conditions	none	$1 \cdot 10^{-7}$ M	$1 \cdot 10^{-4}$ M	$1 \cdot 10^{-1}$ M
Great Britain	10	Cementitious system (not specified)	not specified	$1 \cdot 10^{-12}$ M		$1 \cdot 10^{-2}$ M
Great Britain	10	Bentonite pore water (not specified)	not specified	$4.69 \cdot 10^{-5}$ M		$4 \cdot 10^{-2}$ M
Japan	11	Bentonite porewater based on fresh groundwater Na_2CO_3 I=0.026 pH 8.4	Nb_2O_5(am)			$1 \cdot 10^{-4}$ M
Japan	11	Bentonite porewater based on saline groundwater NaCl/ Na_2CO_3 I=0.615 pH 7.8	Nb_2O_5(s)			$1 \cdot 10^{-4}$ M
Japan	11	Bentonite porewater based on fresh groundwater after contact with cement Na_2CO_3 I=0.0181 pH 8.7	Nb_2O_5(s)			$1 \cdot 10^{-4}$ M
Japan	11	Bentonite porewater based on fresh groundwater Na_2CO_3/ Na_2SO_4 I=0.211 pH 7.2	Nb_2O_5(s)			$1 \cdot 10^{-6}$ M
Japan	11	Bentonite porewater based on fresh groundwater Na_2CO_3 I=0.0083 pH 9.7	Nb_2O_5(s)			$1 \cdot 10^{-4}$ M
Japan	11	Bentonite porewater based on fresh groundwater, oxidizing Na_2CO_3 I=0.0223 pH 8.4	Nb_2O_5(s)			$1 \cdot 10^{-4}$ M

Tab A. 17 Solubility limiting solid phases and solubilities for niobium in earlier studies (III)

Country	Study	Solution type	Phase	Lower Limit	Rec. value	Upper Limit
Sweden	12	Forsmark reference water (NaCl/ CaCl$_2$ I= 0.19 mol/l)	Nb$_2$O$_5$			$3.09 \cdot 10^{-5}$ M
Sweden	12	Saline water (NaCl/ CaCl$_2$ I=1.86 mol/l)	Nb$_2$O$_5$			$2.88 \cdot 10^{-3}$ M
Sweden	12	Ice-melting water (Na/Ca/Cl,HCO3/F,Si I=0.0012 mol/l)	Nb$_2$O$_5$			$1.07 \cdot 10^{-4}$ M
Switzerland	13	Cement/ concrete system equilibrated with Opalinus clay porewater: NaCl/ CaCl$_2$ I=0.09 mol/kg pH12.5	none	No limit	No limit	No limit
Switzerland	13	Bentonite porewater system equilibrated with Opalinus clay porewater NaCl/ Na$_2$SO$_4$ I=0.239 mol/kg pH 7.79	Nb$_2$O$_5$	$3.8 \cdot 10^{-5}$ M	$7.1 \cdot 10^{-5}$ M	$1 \cdot 10^{-4}$ M

Tab A. 18 Solubility limiting solid phases and solubilities for palladium in earlier studies (I)

Country	Study	Solution type	Phase	Lower Limit	Rec. value	Upper Limit
Belgium	1	Boom clay pore water I=0.0085 pH 8.36	UL: $Pd(OH)_2$ LL: PdS	$7.936 \cdot 10^{-35}$ M		$4 \cdot 10^{-5}$ M
Belgium	2	Cement pore water I ≤ 0.08. state I: pH 13.5 - 12.5 state II: 12.5 state III: 12.5 - 10.5	$Pd(OH)_2$	I: $1 \cdot 10^{-5}$ m II: $1 \cdot 10^{-5}$ m III: $4 \cdot 10^{-6}$ m		I: $1 \cdot 10^{-4}$ m II: $1 \cdot 10^{-5}$ m III: $1 \cdot 10^{-5}$ m
Canada	4	Model groundwater for crystalline rock Na/Ca/Cl/SO_4 I=0.24 mol/l pH 7.1 (CR-10 eq)	$Pd(OH)_2$			$4.11 \cdot 10^{-6}$ m
Canada	4	Model groundwater for crystalline rock equilibrated with bentonite and steel I=0.32 pH 8.7 (CR-10 NF)	$Pd(OH)_2$			$3.98 \cdot 10^{-6}$ m
Canada	4	Brine from salt formation NaCl/ $CaCl_2$ I=4.51 pH 5.8 (SR-270 eq)	none			No limit
Canada	4	Brine from salt formation equilibrated with bentonite and steel NaCl/ $CaCl_2$ I=4.50 pH 8.1 (SR-270 NF)	none			No limit
Finland	5	Altered groundwaters (six different) inside the canisters NaCl/ $CaCl_2$ I= 0.001 to 1.3 mol/l pH 7.33 to 10	$Pd(OH)_2$	$3.7 \cdot 10^{-6}$ M		$1.2 \cdot 10^{-5}$ M

Tab A. 19 Solubility limiting solid phases and solubilities for palladium in earlier studies (II)

Country	Study	Solution type	Phase	Lower Limit	Rec. value	Upper Limit
Finland	5	Altered ground waters (six different) at the buffer/ host rock interface NaCl/ CaCl$_2$ I= 0.001 to 1.3 mol/l pH 7.12 to 10	Pd(OH)$_2$	$3.9 \cdot 10^{-6}$ M		$8.5 \cdot 10^{-5}$ M
Finland	5	Bentonite porewater (six different) NaCl/ CaCl$_2$ I=0.002 to 2.9, pH 7.23 to 10	Pd(OH)$_2$	$3.4 \cdot 10^{-6}$ M		$1.5 \cdot 10^{-4}$ M
Germany	7a	Unspecified solution expected to occur in the Konrad mine <pH12, possibly up to 3.3 mol/l Cl (NaCl/ CaCl$_2$/ MgCl$_2$)	not deter-mined			$1 \cdot 10^{-4}$ M
Germany	7b	Unspecified brine under acidic conditions	none	$1 \cdot 10^{-3}$ M	$1 \cdot 10^{-2}$ M	$1 \cdot 10^{-1}$ M
Germany	7b	Unspecified brine under neutral conditions	none	$1 \cdot 10^{-7}$ M	$1 \cdot 10^{-4}$ M	$1 \cdot 10^{-1}$ M
Germany	7b	Unspecified brine under alkaline conditions	none	$1 \cdot 10^{-7}$ M	$1 \cdot 10^{-5}$ M	$1 \cdot 10^{-3}$ M
Great Britain	10	Cementitious system (not specified)	none			No limit
Great Britain	10	Bentonite pore water (not specified)	not specified	$2.17 \cdot 10^{-9}$ M		$8 \cdot 10^{-9}$ M
Japan	11	Bentonite porewater based on fresh groundwater Na$_2$CO$_3$ I=0.026 pH 8.4	Pd (metal)			$1 \cdot 10^{-9}$ M

Tab A. 20 Solubility limiting solid phases and solubilities for palladium in earlier studies (III)

Country	Study	Solution type	Phase	Lower Limit	Rec. value	Upper Limit
Japan	11	Bentonite porewater based on saline groundwater NaCl/ Na$_2$CO$_3$ I=0.615 pH 7.8	Pd (metal)			$1 \cdot 10^{-9}$ M
Japan	11	Bentonite porewater based on fresh groundwater after contact with cement Na$_2$CO$_3$ I=0.0181 pH 8.7	Pd (metal)			$1 \cdot 10^{-9}$ M
Japan	11	Bentonite porewater based on fresh groundwater Na$_2$CO$_3$/ Na$_2$SO$_4$ I=0.211 pH 7.2	Pd (metal)			$1 \cdot 10^{-9}$ M
Japan	11	Bentonite porewater based on fresh groundwater Na$_2$CO$_3$ I=0.0083 pH 9.7	Pd (metal)			$1 \cdot 10^{-9}$ M
Japan	11	Bentonite porewater based on fresh groundwater, oxidizing Na$_2$CO$_3$ I=0.0223 pH 8.4	Pd (metal)			$1 \cdot 10^{-7}$ M
Sweden	12	Forsmark reference water (NaCl/ CaCl$_2$ I= 0.19 mol/l)	Pd(OH)$_2$			$3.47 \cdot 10^{-6}$ M
Sweden	12	Saline water (NaCl/ CaCl$_2$ I=1.86 mol/l)	Pd(OH)$_2$			$3.98 \cdot 10^{-6}$ M
Sweden	12	Ice-melting water (Na/Ca/Cl,HCO3/F,Si I=0.0012 mol/l)	Pvd(OH)$_2$			$3.47 \cdot 10^{-6}$ M

Tab A. 21   Solubility limiting solid phases and solubilities for palladium in earlier studies (IV)

Country	Study	Solution type	Phase	Lower Limit	Rec. value	Upper Limit
Switzerland	13	Cement/ concrete system equilibrated with Opalinus clay porewater: NaCl/ CaCl$_2$ I=0.09 mol/kg pH12.5	UL,RV: Pd(OH)$_2$ LL: Pd (metal)	insignificant	$8.5 \cdot 10^{-7}$ M	$2.5 \cdot 10^{-5}$ M
Switzerland	13	Bentonite porewater system equilibrated with Opalinus clay porewater NaCl/ Na$_2$SO$_4$ I=0.239 mol/kg pH 7.79	UL,RV: Pd(OH)$_2$ LL: Pd (metal)	insignificant	$5.7 \cdot 10^{-8}$ M	$1.8 \cdot 10^{-7}$ M

Tab A. 22 Solubility limiting solid phases and solubilities for radium in earlier studies (I)

Country	Study	Solution type	Phase	Lower Limit	Rec. value	Upper Limit
Belgium	1	Boom clay pore water I=0.0085 pH 8.36	UL: $RaCO_3$ LL: $RaSO_4$	$7.033 \cdot 10^{-6}$ M		$1.2 \cdot 10^{-4}$ M
Belgium	2	Cement pore water I ≤ 0.08. state I: pH 13.5 - 12.5 state II: 12.5 state III: 12.5 - 10.5	$RaSO_4$	I: $7 \cdot 10^{-9}$ m II: $1 \cdot 10^{-6}$ m III: $1 \cdot 10^{-8}$ m		I: $1 \cdot 10^{-6}$ m II: $1 \cdot 10^{-6}$ m III: $1 \cdot 10^{-6}$ m
Canada	3	Argillaceous limestone model porewater (Guelph): Concentrated NaCl/ $CaCl_2$ brine I=7.2 mol/kg pH 6.5	none	No limit		No limit
Canada	3	Argillaceous limestone model porewater (Cobourg 2): NaCl/ KCl/ $CaCl_2$ brine I=3.8 mol/kg pH 6.5	none	No limit		No limit
Canada	3	ditto, but equilibrated with cement pH 11.9	none	No limit		No limit
Canada	4	Model groundwater for crystalline rock Na/Ca/Cl/SO_4 I=0.24 mol/l pH 7.1 (CR-10 eq)	$RaSO_4$			$1.56 \cdot 10^{-7}$ m
Canada	4	Model groundwater for crystalline rock equilibrated with bentonite and steel I=0.32 pH 8.7 (CR-10 NF)	$RaSO_4$			$7.20 \cdot 10^{-8}$ m
Canada	4	Brine from salt formation NaCl/ $CaCl_2$ I=4.51 pH 5.8 (SR-270 eq)	$RaSO_4$			$1.68 \cdot 10^{-5}$ m

Tab A. 23 Solubility limiting solid phases and solubilities for radium in earlier studies (II)

Country	Study	Solution type	Phase	Lower Limit	Rec. value	Upper Limit
Canada	4	Brine from salt formation equilibrated with bentonite and steel NaCl/ CaCl$_2$ I=4.50 pH 8.1 (SR-270 NF)	RaSO$_4$			$1.43 \cdot 10^{-5}$ m
Finland	5	Altered groundwaters (six different) inside the canisters NaCl/ CaCl$_2$ I= 0.001 to 1.3 mol/l pH 7.33 to 10	UL: RaSO$_4$ LL: (Ba,Ra)SO$_4$	$1.6 \cdot 10^{-11}$ M		$8.7 \cdot 10^{-5}$ M
Finland	5	Altered ground waters (six different) at the buffer/ host rock interface NaCl/ CaCl$_2$ I= 0.001 to 1.3 mol/l pH 7.12 to 10	UL: RaSO$_4$ LL: (Ba,Ra)SO$_4$	$6.7 \cdot 10^{-11}$ M		$8.6 \cdot 10^{-5}$ M
Finland	5	Bentonite porewater (six different) NaCl/ CaCl$_2$ I=0.002 to 2.9, pH 7.23 to 10	UL: RaSO$_4$ LL: (Ba,Ra)SO$_4$	$1.4 \cdot 10^{-11}$ M		No limit
Germany	7a	Unspecified solution expected to occur in the Konrad mine <pH12, possibly up to 3.3 mol/l Cl (NaCl/ CaCl$_2$/ MgCl$_2$)	not determined			$1 \cdot 10^{-3}$ M
Germany	7b	Unspecified brine under acidic conditions	none	$1 \cdot 10^{-8}$ M	$1 \cdot 10^{-5}$ M	$1 \cdot 10^{-2}$ M
Germany	7b	Unspecified brine under neutral conditions	none	$1 \cdot 10^{-8}$ M	$1 \cdot 10^{-6}$ M	$1 \cdot 10^{-4}$ M
Germany	7b	Unspecified brine under alkaline conditions	none	1·10-8 M	1·10-6 M	1·10-4 M

Tab A. 24   Solubility limiting solid phases and solubilities for radium in earlier studies (III)

Country	Study	Solution type	Phase	Lower Limit	Rec. value	Upper Limit
Great Britain	10	Cementitious system (not specified)	none			No limit
Great Britain	10	Bentonite pore water (not specified)	not specified	$1.26 \cdot 10^{-9}$ M		$2 \cdot 10^{-4}$ M
Japan	11	Bentonite porewater based on fresh groundwater Na_2CO_3 I=0.026 pH 8.4	$(Ca,Ra)CO_3$			$1 \cdot 10^{-12}$ M
Japan	11	Bentonite porewater based on saline groundwater $NaCl/Na_2CO_3$ I=0.615 pH 7.8	$(Ca,Ra)CO_3$			$1 \cdot 10^{-10}$ M
Japan	11	Bentonite porewater based on fresh groundwater after contact with cement Na_2CO_3 I=0.0181 pH 8.7	$(Ca,Ra)CO_3$			$1 \cdot 10^{-12}$ M
Japan	11	Bentonite porewater based on fresh groundwater Na_2CO_3/ Na_2SO_4 I=0.211 pH 7.2	$(Ca,Ra)CO_3$			$1 \cdot 10^{-12}$ M
Japan	11	Bentonite porewater based on fresh groundwater Na_2CO_3 I=0.0083 pH 9.7	$(Ca,Ra)CO_3$			$1 \cdot 10^{-12}$ M
Japan	11	Bentonite porewater based on fresh groundwater, oxidizing Na_2CO_3 I=0.0223 pH 8.4	$(Ca,Ra)CO_3$			$1 \cdot 10^{-12}$ M

Tab A. 25 Solubility limiting solid phases and solubilities for radium in earlier studies (IV)

Country	Study	Solution type	Phase	Lower Limit	Rec. value	Upper Limit
Sweden	12	Forsmark reference water (NaCl/ CaCl$_2$ I= 0.19 mol/l)	RaSO$_4$			$2.40 \cdot 10^{-7}$ M
Sweden	12	Saline water (NaCl/ CaCl$_2$ I=1.86 mol/l)	RaSO$_4$			$1.51 \cdot 10^{-6}$ M
Sweden	12	Ice-melting water (Na/Ca/Cl,HCO$_3$/F,Si I=0.0012 mol/l)	RaSO$_4$			$2.95 \cdot 10^{-7}$ M
Switzerland	13	Cement/ concrete system equilibrated with Opalinus clay porewater: NaCl/ CaCl$_2$ I=0.09 mol/kg pH12.5	UL: RaSO$_4$ RV,LL: (Ba,Ra)SO$_4$	$2.1 \cdot 10^{-7}$ M	$9.7 \cdot 10^{-7}$ M	$1.7 \cdot 10^{-5}$ M
Switzerland	13	Bentonite porewater system equilibrated with Opalinus clay porewater NaCl/ Na$_2$SO$_4$ I=0.239 mol/kg pH 7.79	UL: RaSO$_4$ RV,LL: (Ba,Ra)SO$_4$	$5.1 \cdot 10^{-12}$ M	$3.4 \cdot 10^{-10}$ M	$1.1 \cdot 10^{-7}$ M

Tab A. 26 Solubility limiting solid phases and solubilities for rubidium in earlier studies

Country	Study	Solution type	Phase	Lower Limit	Rec. value	Upper Limit
Belgium	1	Boom clay pore water I=0.0085 pH 8.36	none	No limit		No limit
Germany	7a	Unspecified solution expected to occur in the Konrad mine <pH12, possibly up to 3.3 mol/l Cl (NaCl/ CaCl$_2$/ MgCl$_2$)	not deter-mined			$1\cdot10^{-2}$ M
Germany	7b	Unspecified brine under alkaline, neutral, and acidic conditions	none	No limit		No limit

Tab A. 27   Solubility limiting solid phases and solubilities for samarium in earlier studies (I)

Country	Study	Solution type	Phase	Lower Limit	Rec. value	Upper Limit
Belgium	1	Boom clay pore water I=0.0085 pH 8.36	UL: $Sm(OH)_3$ LL: $Sm(OH)CO_3$	$2 \cdot 10^{-8}$ M		$3.655 \cdot 10^{-4}$ M
Finland	5	Altered groundwaters (six different) inside the canisters NaCl/ $CaCl_2$ I= 0.001 to 1.3 mol/l pH 7.33 to 10	$Sm(OH)CO_3 \cdot 0.5H_2O$	$6.1 \cdot 10^{-8}$ M		$1.2 \cdot 10^{-5}$ M
Finland	5	Altered ground waters (six different) at the buffer/ host rock interface NaCl/ $CaCl_2$ I= 0.001 to 1.3 mol/l pH 7.12 to 10	$Sm(OH)CO_3 \cdot 0.5H_2O$	$5.3 \cdot 10^{-7}$ M		$2.1 \cdot 10^{-5}$ M
Finland	5	Bentonite porewater (six different) NaCl/ $CaCl_2$ I=0.002 to 2.9, pH 7.23 to 10	$Sm(OH)CO_3 \cdot 0.5H_2O$		$1.7 \cdot 10^{-7}$ M	$2.1 \cdot 10^{-5}$ M
France	6	Pore water in bentonite buffer (un-specified)	Incorporation into Ca phases			$1 \cdot 10^{-12}$ M
France	6	Pore water of cement-based materials (unspecified)	Incorporation into Ca phases			$1 \cdot 10^{-10}$ M
France	6	Pore water of Callovo-Oxfordian clay rock NaCl/ $CaCl_2$ I=0.09-0.12 mol/l pH 6.9-7.6	Incorporation into Ca phases			$1 \cdot 10^{-12}$ M

Tab A. 28 Solubility limiting solid phases and solubilities for samarium in earlier studies (II)

Country	Study	Solution type	Phase	Lower Limit	Rec. value	Upper Limit
Germany	7a	Unspecified solution expected to occur in the Konrad mine <pH12, possibly up to 3.3 mol/l Cl (NaCl/ CaCl$_2$/ MgCl$_2$)	not determined			$1 \cdot 10^{-4}$ M
Germany	7b	Unspecified brine under acidic conditions	none	$1 \cdot 10^{-3}$ M	$1 \cdot 10^{-2}$ M	$1 \cdot 10^{-1}$ M
Germany	7b	Unspecified brine under neutral conditions	none	$1 \cdot 10^{-7}$ M	$1 \cdot 10^{-5}$ M	$1 \cdot 10^{-3}$ M
Germany	7b	Unspecified brine under alkaline conditions	none	$1 \cdot 10^{-7}$ M	$1 \cdot 10^{-5}$ M	$1 \cdot 10^{-3}$ M
Great Britain	10	Cementitious system (not specified)	none	No limit		No limit
Great Britain	10	Bentonite pore water (not specified)	not specified	$3.22 \cdot 10^{-8}$ M		$2.0 \cdot 10^{-5}$ M
Japan	11	Bentonite porewater based on fresh groundwater Na$_2$CO$_3$ I=0.026 pH 8.4	Sm(OH)CO$_3$			$2 \cdot 10^{-7}$ M
Japan	11	Bentonite porewater based on saline groundwater NaCl/ Na$_2$CO$_3$ I=0.615 pH 7.8	Sm(OH)CO$_3$			$4 \cdot 10^{-7}$ M
Japan	11	Bentonite porewater based on fresh groundwater after contact with cement Na$_2$CO$_3$ I=0.0181 pH 8.7	Sm(OH)CO$_3$			$4 \cdot 10^{-8}$ M

Tab A. 29 Solubility limiting solid phases and solubilities for samarium in earlier studies (III)

Country	Study	Solution type	Phase	Lower Limit	Rec. value	Upper Limit
Japan	11	Bentonite porewater based on fresh groundwater Na_2CO_3/ Na_2SO_4 I=0.211 pH 7.2	$Sm(OH)CO_3$			$2 \cdot 10^{-6}$ M
Japan	11	Bentonite porewater based on fresh groundwater Na_2CO_3 I=0.0083 pH 9.7	$Sm(OH)CO_3$			$2 \cdot 10^{-8}$ M
Japan	11	Bentonite porewater based on fresh groundwater, oxidizing Na_2CO_3 I=0.0223 pH 8.4	$Sm(OH)CO_3$			$2 \cdot 10^{-7}$ M
Sweden	12	Forsmark reference water (NaCl/ CaCl2 I= 0.19 mol/l)	$Sm(OH)CO3$			$1.45 \cdot 10$-7 M
Sweden	12	Saline water (NaCl/CaCl2 I=1.86 mol/l)	$Sm(OH)CO3$			$2.57 \cdot 10$-9 M
Sweden	12	Ice-melting water (Na/Ca/Cl,HCO3/F,Si I=0.0012 mol/l)	$Sm(OH)CO3$			$4.27 \cdot 10$-8 M
Switzerland	13	Cement/ concrete system equilibrated with Opalinus clay porewater: NaCl/ $CaCl_2$ I=0.09 mol/kg pH12.5	UL, RV: Sm(OH)3 (am) LL: Sm(OH)3(cr)	$8.9 \cdot 10$-11 M	$4.6 \cdot 10$-7 M	$4.6 \cdot 10$-7 M
Switzerland	13	Bentonite porewater system equilibrated with Opalinus clay porewater NaCl/ Na_2SO_4 I=0.239 mol/kg pH 7.79	UL: Sm(OH)3 RV: Sm(OH)CO3·0.5H2O LL: SmPO4	$2.4 \cdot 10$-11 M	$1.5 \cdot 10$-7 M	$1.8 \cdot 10$-5 M

Tab A. 30 Solubility limiting solid phases and solubilities for selenium in earlier studies (I)

Country	Study	Solution type	Phase	Lower Limit	Rec. value	Upper Limit
Belgium	1	Boom clay pore water I=0.0085 pH 8.36	UL: Se (mono) LL: $FeSe_2$ (achávalite)	$6.6 \cdot 10^{-12}$ M		$2.36 \cdot 10^{-6}$ M
Belgium	2	Cement pore water I ≤ 0.08. state I: pH 13.5 - 12.5 state II: 12.5 state III: 12.5 - 10.5	I: Se(0) or Ca-SeO_3 II: Se(0) or Ca-SeO_3 III: Se(0)	I: $5 \cdot 10^{-4}$ m II: $2 \cdot 10^{-5}$ m III: $1 \cdot 10^{-11}$ m		I: No limit II: No limit III: No limit
Canada	4	Model groundwater for crystalline rock Na/Ca/Cl/SO4 I=0.24 mol/l pH 7.1 (CR-10 eq)	$FeSe_2$ (fer-roselite)			$1.15 \cdot 10^{-10}$ m
Canada	4	Model groundwater for crystalline rock equilibrated with bentonite and steel I=0.32 pH 8.7 (CR-10 NF)	β-$Fe_{1.04}Se$			$1.15 \cdot 10^{-10}$ m
Canada	4	Brine from salt formation NaCl/ $CaCl_2$ I=4.51 pH 5.8 (SR-270 eq)	$FeSe_2$ (fer-roselite)			$3.43 \cdot 10^{-9}$ m
Canada	4	Brine from salt formation equilibrated with bentonite and steel NaCl/ $CaCl_2$ I=4.50 pH 8.1 (SR-270 NF)	β-$Fe_{1.04}Se$			$1.77 \cdot 10^{-9}$ m
Finland	5	Altered groundwaters (six different) inside the canisters NaCl/ $CaCl_2$ I= 0.001 to 1.3 mol/l pH 7.33 to 10	FeS_2 or Se(0)	$5.9 \cdot 10^{-11}$ M		$3.4 \cdot 10^{-7}$ M

Tab A. 31 Solubility limiting solid phases and solubilities for selenium in earlier studies (II)

Country	Study	Solution type	Phase	Lower Limit	Rec. value	Upper Limit
Finland	5	Altered ground waters (six different) at the buffer/ host rock interface NaCl/ CaCl$_2$ I= 0.001 to 1.3 mol/l pH 7.12 to 10	FeS$_2$ or Se(0)	$4.9 \cdot 10^{-10}$ M		$1 \cdot 10^{-6}$ M
Finland	5	Bentonite porewater (six different) NaCl/ CaCl$_2$ I=0.002 to 2.9, pH 7.23 to 10	FeS$_2$	$4.3 \cdot 10^{-10}$ M		$8.1 \cdot 10^{-7}$ M
France	6	Pore water in bentonite buffer (unspecified)	Incorporation into FeS$_2$	$1 \cdot 10^{-14}$ M		$5 \cdot 10^{-10}$ M
France	6	Pore water of cement-based materials (unspecified)	CaSeO$_3$ or solid solution with ettringite			$1 \cdot 10^{-5}$ M
France	6	Pore water of Callovo-Oxfordian clay rock NaCl/ CaCl$_2$ I=0.09-0.12 mol/l pH 6.9-7.6	Incorporation into FeS$_2$	$1 \cdot 10^{-14}$ M		$5 \cdot 10^{-10}$ M
Germany	7a	Unspecified solution expected to occur in the Konrad mine <pH12, possibly up to 3.3 mol/l Cl (NaCl/ CaCl$_2$/ MgCl$_2$)	not deter-mined			$1 \cdot 10^{-2}$ M

Tab A. 32 Solubility limiting solid phases and solubilities for selenium in earlier studies (III)

Country	Study	Solution type	Phase	Lower Limit	Rec. value	Upper Limit
Germany	7b	Unspecified brine under acidic conditions	none	$1 \cdot 10^{-8}$ M	$1 \cdot 10^{-4}$ M	$1 \cdot 10^{-0}$ M
Germany	7b	Unspecified brine under neutral conditions	none	$1 \cdot 10^{-8}$ M	$1 \cdot 10^{-4}$ M	$1 \cdot 10^{-0}$ M
Germany	7b	Unspecified brine under alkaline conditions	none	$1 \cdot 10^{-8}$ M	$1 \cdot 10^{-4}$ M	$1 \cdot 10^{-0}$ M
Great Britain	10	Cementitious system (not specified)	not specified	$1 \cdot 10^{-9}$ M		1 M
Great Britain	10	Bentonite pore water (not specified)	not specified	$3.22 \cdot 10^{-8}$ M		$4.1 \cdot 10^{-3}$ M
Japan	11	Bentonite porewater based on fresh groundwater Na_2CO_3 I=0.026 pH 8.4	$FeSe_2$			$3 \cdot 10^{-9}$ M
Japan	11	Bentonite porewater based on saline groundwater NaCl/ Na_2CO_3 I=0.615 pH 7.8	$FeSe_2$			$6 \cdot 10^{-9}$ M
Japan	11	Bentonite porewater based on fresh groundwater after contact with cement Na_2CO_3 I=0.0181 pH 8.7	$FeSe_2$			$4 \cdot 10^{-9}$ M
Japan	11	Bentonite porewater based on fresh groundwater Na_2CO_3/ Na_2SO_4 I=0.211 pH 7.2	$FeSe_2$			$1 \cdot 10^{-10}$ M
Japan	11	Bentonite porewater based on fresh groundwater Na_2CO_3 I=0.0083 pH 9.7	$FeSe_2$			$7 \cdot 10^{-9}$ M

Tab A. 33   Solubility limiting solid phases and solubilities for selenium in earlier studies (IV)

Country	Study	Solution type	Phase	Lower Limit	Rec. value	Upper Limit
Japan	11	Bentonite porewater based on fresh groundwater, oxidizing Na_2CO_3 I=0.0223 pH 8.4	none			No limit
Sweden	12	Forsmark reference water (NaCl/ $CaCl_2$ I= 0.19 mol/l)	FeS_2			$1.82 \cdot 10^{-11}$ M
Sweden	12	Saline water (NaCl/ $CaCl_2$ I=1.86 mol/l)	Se			$3.80 \cdot 10^{-11}$ M
Sweden	12	Ice-melting water (Na/Ca/Cl,HCO3/F,Si I=0.0012 mol/l)	FeS_2			$4.07 \cdot 10^{-7}$ M
Switzerland	13	Cement/ concrete system equilibrated with Opalinus clay porewater: NaCl/ $CaCl_2$ I=0.09 mol/kg pH12.5	$CoSe_2$	$7.2 \cdot 10^{-11}$ M	$2.1 \cdot 10^{-6}$ M	No limit
Switzerland	13	Bentonite porewater system equilibrated with Opalinus clay porewater NaCl/ Na_2SO_4 I=0.239 mol/kg pH 7.79	UL, RV: Se LL: $CoSe_2$	$4.1 \cdot 10^{-12}$ M	$5.3 \cdot 10^{-9}$ M	$1.6 \cdot 10^{-7}$ M

Tab A. 34   Solubility limiting solid phases and solubilities for silver in earlier studies (I)

Country	Study	Solution type	Phase	Lower Limit	Rec. value	Upper Limit
Belgium	1	Boom clay pore water I=0.0085 pH 8.36	none			No limit
Belgium	2	Cement pore water I ≤ 0.08. state I: pH 13.5 - 12.5 state II: 12.5 state III: 12.5 - 10.5	none			No limit
Canada	3	Argillaceous limestone model porewater (Guelph): Concentrated NaCl/ CaCl$_2$ brine I=7.2 mol/kg pH 6.5	none	No limit		No limit
Canada	3	Argillaceous limestone model porewater (Cobourg 2): NaCl/ KCl/ CaCl$_2$ brine I=3.8 mol/kg pH 6.5	none	No limit		No limit
Canada	3	ditto, but equilibrated with cement pH 11.9	none	No limit		No limit
Finland	5	Altered groundwaters (six different) inside the canisters NaCl/ CaCl$_2$ I= 0.001 to 1.3 mol/l pH 7.33 to 10	none	No limit		No limit
Finland	5	Altered ground waters (six different) at the buffer/ host rock interface NaCl/ CaCl$_2$ I= 0.001 to 1.3 mol/l pH 7.12 to 10	none	No limit		No limit
Finland	5	Bentonite porewater (six different) NaCl/ CaCl$_2$ I=0.002 to 2.9, pH 7.23 to 10	none	No limit		No limit
France	6	Pore water in bentonite buffer (unspecified)	none			No limit
France	6	Pore water of cement-based materials (unspecified)	none			No limit

Tab A. 35 Solubility limiting solid phases and solubilities for silver in earlier studies (II)

Country	Study	Solution type	Phase	Lower Limit	Rec. value	Upper Limit
France	6	Pore water of Callovo-Oxfordian clay rock NaCl/ CaCl$_2$ I=0.09-0.12 mol/l pH 6.9-7.6	none			No limit
Great Brit-ain	10	Cementitious system (not specified)	none			No limit
Great Brit-ain	10	Bentonite pore water (not specified)	none			No limit
Sweden	12	Forsmark reference water (NaCl/ CaCl$_2$ I= 0.19 mol/l)	none	No limit		No limit
Sweden	12	Saline water (NaCl/ CaCl$_2$ I=1.86 mol/l)	none	No limit		No limit
Sweden	12	Ice-melting water (Na/Ca/Cl,HCO3/F,Si I=0.0012 mol/l)	none	No limit		No limit
Switzerland	13	Cement/concrete system equilibrated with Opalinus clay porewater: NaCl/ CaCl$_2$ I=0.09 mol/kg pH12.5	AgI	$1.8 \cdot 10^{-7}$ M	$1.8 \cdot 10^{-7}$ M	$1.8 \cdot 10^{-7}$ M
Switzerland	13	Bentonite porewater system equilibrated with Opalinus clay porewater NaCl/ Na$_2$SO$_4$ I=0.239 mol/kg pH 7.79	LL, RV: AgI UL: none	$7.7 \cdot 10^{-8}$ M	$9.0 \cdot 10^{-7}$ M	No limit

Tab A. 36 Solubility limiting solid phases and solubilities for strontium in earlier studies (I)

Country	Study	Solution type	Phase	Lower Limit	Rec. value	Upper Limit
Belgium	1	Boom clay pore water I=0.0085 pH 8.36	$SrCO_3$ (strontianite)	$4.7 \cdot 10^{-6}$ M		$1.3 \cdot 10^{-5}$ M
Belgium	2	Cement pore water I ≤ 0.08. state I: pH 13.5 - 12.5 state II: 12.5 state III: 12.5 - 10.5	$SrCO_3$ (strontianite)	I: $1 \cdot 10^{-4}$ m II: $2.5 \cdot 10^{-3}$ m III: $3.4 \cdot 10^{-4}$ m		I: $2.5 \cdot 10^{-3}$ m II: $2.5 \cdot 10^{-3}$ m III: $2.5 \cdot 10^{-3}$ m
Finland	5	Altered groundwaters (six different) inside the canisters NaCl/ CaCl$_2$ I= 0.001 to 1.3 mol/l pH 7.33 to 10	$SrSO_4$ (strontianite) or $SrCO_3$ (celestite)	$1.3 \cdot 10^{-4}$ M		No limit
Finland	5	Altered ground waters (six different) at the buffer/ host rock interface NaCl/ CaCl$_2$ I= 0.001 to 1.3 mol/l pH 7.12 to 10	$SrSO_4$ (strontianite) or $SrCO_3$ (celestite)	$8.7 \cdot 10^{-4}$ M		No limit
Finland	5	Bentonite porewater (six different) NaCl/ CaCl$_2$ I=0.002 to 2.9, pH 7.23 to 10	$SrSO_4$ (strontianite) or $SrCO_3$ (celestite)	$6.7 \cdot 10^{-4}$ M		No limit
Germany	7a	Unspecified solution expected to occur in the Konrad mine <pH12, possibly up to mol/l Cl (NaCl/ CaCl$_2$/ MgCl$_2$)	not determined			$1 \cdot 10^{-2}$ M

Tab A. 37 Solubility limiting solid phases and solubilities for strontium in earlier studies (II)

Country	Study	Solution type	Phase	Lower Limit	Rec. value	Upper Limit
Germany	7b	Unspecified brine under acidic conditions	none	$1\cdot10^{-6}$ M	$1\cdot10^{-3}$ M	$1\cdot10^{-0}$ M
Germany	7b	Unspecified brine under neutral conditions	none	$1\cdot10^{-6}$ M	$1\cdot10^{-3}$ M	$1\cdot10^{-0}$ M
Germany	7b	Unspecified brine under alkaline conditions	none	$1\cdot10^{-6}$ M	$1\cdot10^{-5}$ M	$1\cdot10^{-4}$ M
Great Britain	10	Cementitious system (not specified)	not specified	No limit		No limit
Great Britain	10	Bentonite pore water (not specified)	not specified	$2.39\cdot10^{-4}$ M		$4\cdot10^{-2}$ M
Sweden	12	Forsmark reference water (NaCl/ CaCl$_2$ I= 0.19 mol/l)	$SrCO_3$ (celestite)		$9.77\cdot10^{-4}$ M	
Sweden	12	Saline water (NaCl/ CaCl$_2$ I=1.86 mol/l)	$SrSO_4$ (strontianite)		$1.12\cdot10^{-5}$ M	
Sweden	12	Ice-melting water (Na/Ca/Cl,HCO3/F,Si I=0.0012 mol/l)	$SrCO_3$ (celestite)		$1.51\cdot10^{-3}$ M	

Tab A. 38   Solubility limiting solid phases and solubilities for strontium in earlier studies (III)

Country	Study	Solution type	Phase	Lower Limit	Rec. value	Upper Limit
Switzerland	13	Cement/ concrete system equilibrated with Opalinus clay porewater: NaCl/ CaCl$_2$ I=0.09 mol/kg pH12.5	SrSO$_4$ (strontianite)		2.1·10^{-6} M	
Switzerland	13	Bentonite porewater system equilibrated with Opalinus clay porewater NaCl/ Na$_2$SO$_4$ I=0.239 mol/kg pH 7.79	UL: SrCO$_3$ (celestite) RV, LL: basis solution composition (ion exchange with montmorillonite)	1.9·10^{-6} M	5.6·10^{-5} M	1.4·10^{-4} M

Tab A. 39   Solubility limiting solid phases and solubilities for tin in earlier studies (I)

Country	Study	Solution type	Phase	Lower Limit	Rec. value	Upper Limit
Belgium	1	Boom clay pore water I=0.0085 pH 8.36	SnO_2(am)	$1.1 \cdot 10^{-6}$ M		$3.3 \cdot 10^{-6}$ M
Belgium	2	Cement pore water I ≤ 0.08. state I: pH 13.5 - 12.5 state II: 12.5 state III: 12.5 - 10.5	$CaSn(OH)_6$ (burtite)	I: $1 \cdot 10^{-8}$ m II: $1 \cdot 10^{-8}$ m III: $1 \cdot 10^{-8}$ m		I: $3 \cdot 10^{-6}$ m II: $1 \cdot 10^{-8}$ m III: $1 \cdot 10^{-7}$ m
Canada	4	Model groundwater for crystalline rock Na/Ca/Cl/SO4 I=0.24 mol/l pH 7.1 (CR-10 eq)	SnO_2 (am)			$5.81 \cdot 10^{-8}$ m
Canada	4	Model groundwater for crystalline rock equilibrated with bentonite and steel I=0.32 pH 8.7 (CR-10 NF)	SnO_2 (am) or $CaSn(OH)_6$			SnO_2 (am): $4.85 \cdot 10^{-7}$ m $CaSn(OH)_6$: $9.63 \cdot 10^{-7}$ m
Canada	4	Brine from salt formation NaCl/ $CaCl_2$ I=4.51 pH 5.8 (SR-270 eq)	SnO_2 (am)			$3.91 \cdot 10^{-8}$ m
Canada	4	Brine from salt formation equilibrated with bentonite and steel NaCl/ $CaCl_2$ I=4.50 pH 8.1 (SR-270 NF)	SnO_2 (am)			$9.06 \cdot 10^{-8}$ m
Finland	5	Altered groundwaters (six different) inside the canisters NaCl/ $CaCl_2$ I= 0.001 to 1.3 mol/l pH 7.33 to 10	SnO_2 (am)	$6.3 \cdot 10^{-8}$ M		$1.3 \cdot 10^{-5}$ M

Tab A. 40   Solubility limiting solid phases and solubilities for tin in earlier studies (II)

Country	Study	Solution type	Phase	Lower Limit	Rec. value	Upper Limit
Finland	5	Altered ground waters (six different) at the buffer/ host rock interface NaCl/ CaCl$_2$ I= 0.001 to 1.3 mol/l pH 7.12 to 10	SnO$_2$ (am)	$5.7 \cdot 10^{-8}$ M		$1.3 \cdot 10^{-5}$ M
Finland	5	Bentonite porewater (six different) NaCl/ CaCl$_2$ I=0.002 to 2.9, pH 7.23 to 10	SnO$_2$ (am)	$5.9 \cdot 10^{-8}$ M		$1.2 \cdot 10^{-5}$ M
Germany	7a	Unspecified solution expected to occur in the Konrad mine <pH12, possibly up to 3.3 mol/l Cl (NaCl/ CaCl$_2$/ MgCl$_2$)	not deter- mined			$1 \cdot 10^{-4}$ M
Germany	7b	Unspecified brine under acidic conditions	none	$1 \cdot 10^{-3}$ M	$1 \cdot 10^{-2}$ M	$1 \cdot 10^{-1}$ M
Germany	7b	Unspecified brine under neutral conditions	none	$1 \cdot 10^{-7}$ M	$1 \cdot 10^{-4}$ M	$1 \cdot 10^{-1}$ M
Germany	7b	Unspecified brine under alkaline conditions	none	$1 \cdot 10^{-7}$ M	$1 \cdot 10^{-5}$ M	$1 \cdot 10^{-3}$ M
Great Britain	10	Cementitious system (not specified)	not specified	$1 \cdot 10^{-9}$ M		5 M
Great Britain	10	Bentonite pore water (not specified)	not specified	$2.01 \cdot 10^{-12}$ M		$1 \cdot 10^{-5}$ M
Japan	11	Bentonite porewater based on fresh groundwater Na$_2$CO$_3$ I=0.026 pH 8.4	SnO$_2$(am)			$5 \cdot 10^{-6}$ M

Tab A. 41 Solubility limiting solid phases and solubilities for tin in earlier studies (III)

Country	Study	Solution type	Phase	Lower Limit	Rec. value	Upper Limit
Japan	11	Bentonite porewater based on saline groundwater NaCl/ Na_2CO_3 I=0.615 pH 7.8	SnO_2(am)			$5 \cdot 10^{-6}$ M
Japan	11	Bentonite porewater based on fresh groundwater after contact with cement Na_2CO_3 I=0.0181 pH 8.7	SnO_2(am)			$5 \cdot 10^{-6}$ M
Japan	11	Bentonite porewater based on fresh groundwater Na_2CO_3/ Na_2SO_4 I=0.211 pH 7.2	SnO_2(am)			$5 \cdot 10^{-6}$ M
Japan	11	Bentonite porewater based on fresh groundwater Na_2CO_3 I=0.0083 pH 9.7	SnO_2(am)			$5 \cdot 10^{-6}$ M
Japan	11	Bentonite porewater based on fresh groundwater, oxidizing Na_2CO_3 I=0.0223 pH 8.4	SnO_2(am)			$5 \cdot 10^{-6}$ M
Sweden	12	Forsmark reference water (NaCl/ $CaCl_2$ I= 0.19 mol/l)	SnO_2(am)			$5.89 \cdot 10^{-8}$ M
Sweden	12	Saline water (NaCl/ $CaCl_2$ I=1.86 mol/l)	SnO_2(am)			$2.69 \cdot 10^{-6}$ M
Sweden	12	Ice-melting water (Na/Ca/Cl,HCO3/F,Si I=0.0012 mol/l)	SnO_2(am)			$8.51 \cdot 10^{-8}$ M

Tab A. 42 Solubility limiting solid phases and solubilities for tin in earlier studies (IV)

Country	Study	Solution type	Phase	Lower Limit	Rec. value	Upper Limit
Switzerland	13	Cement/ concrete system equilibrated with Opalinus clay porewater: NaCl/ CaCl$_2$ I=0.09 mol/kg pH12.5	CaSn(OH)$_6$	$5.0 \cdot 10^{-8}$ M	$1.0 \cdot 10^{-7}$ M	$2.0 \cdot 10^{-7}$ M
Switzerland	13	Bentonite porewater system equilibrated with Opalinus clay porewater NaCl/ Na$_2$SO$_4$ I=0.239 mol/kg pH 7.79	LL: SnO$_2$(cr) (cassiterite) RV: SnO$_2$ (am) UL: CaSn(OH)$_6$	$9.0 \cdot 10^{-9}$ M	$9.2 \cdot 10^{-8}$ M	$2.2 \cdot 10^{-4}$ M

Tab A. 43 Solubility limiting solid phases and solubilities for zirconium in earlier studies (I)

Country	Study	Solution type	Phase	Lower Limit	Rec. value	Upper Limit
Belgium	1	Boom clay pore water I=0.0085 pH 8.36	UL: $Zr(OH)_4$ (am, fresh) LL: $Zr(OH)_4$ (am, a-ged)	$3.5 \cdot 10^{-10}$ M		$1.1 \cdot 10^{-4}$ M
Belgium	2	Cement pore water I ≤ 0.08. state I: pH 13.5 - 12.5 state II: 12.5 state III: 12.5 - 10.5	$Zr(OH)_4$ (am, aged)	I: $3.6 \cdot 10^{-10}$ m II: $3.6 \cdot 10^{-10}$ m III: $3.6 \cdot 10^{-10}$ m		I: $1 \cdot 10^{-7}$ m II: $1 \cdot 10^{-6}$ m III: $1 \cdot 10^{-6}$ m
Canada	3	Argillaceous limestone model porewater (Guelph): Concentrated NaCl/ CaCl$_2$ brine I=7.2 mol/kg pH 6.5	ZrO_2 (baddeleyite)			$6 \cdot 10^{-10}$)1
Canada	3	Argillaceous limestone model porewater (Cobourg 2): NaCl/ KCl/ CaCl$_2$ brine I=3.8 mol/kg pH 6.5	ZrO_2 (baddeleyite)			$6 \cdot 10^{-10}$
Canada	3	ditto, but equilibrated with cement pH 11.9	ZrO_2 (baddeleyite)			$6 \cdot 10^{-10}$
Canada	4	Model groundwater for crystalline rock Na/Ca/Cl/SO4 I=0.24 mol/l pH 7.1 (CR-10 eq)	$Zr(OH)_4$ (am) or ZrO_2			$Zr(OH)_4$ (am): $1.82 \cdot 10^{-8}$ m ZrO_2: $6.4 \cdot 10^{-10}$ m

Tab A. 44 Solubility limiting solid phases and solubilities for zirconium in earlier studies (II)

Country	Study	Solution type	Phase	Lower Limit	Rec. value	Upper Limit
Canada	4	Model groundwater for crystalline rock equilibrated with bentonite and steel I=0.32 pH 8.7 (CR-10 NF)	$Zr(OH)_4$ (am) or ZrO_2			$Zr(OH)_4$ (am): $1.82 \cdot 10^{-8}$ m ZrO_2: $6.4 \cdot 10^{-10}$ m
Canada	4	Brine from salt formation NaCl/ $CaCl_2$ I=4.51 pH 5.8 (SR-270 eq)	$Zr(OH)_4$ (am) or ZrO_2			$Zr(OH)_4$ (am): $1.82 \cdot 10^{-8}$ m ZrO_2: $4.7 \cdot 10^{-10}$ m
Canada	4	Brine from salt formation equilibrated with bentonite and steel NaCl/ $CaCl_2$ I=4.50 pH 8.1 (SR-270 NF)	$Zr(OH)_4$ (am) or ZrO_2			$Zr(OH)_4$ (am): $1.82 \cdot 10^{-8}$ m ZrO_2: $4.7 \cdot 10^{-10}$ m
Finland	5	Altered groundwaters (six different) inside the canisters NaCl/ $CaCl_2$ I= 0.001 to 1.3 mol/l pH 7.33 to 10	$Zr(OH)_4$ (am, aged)	$1.7 \cdot 10^{-8}$ M		$9.2 \cdot 10^{-7}$ M
Finland	5	Altered ground waters (six different) at the buffer/ host rock interface NaCl/ $CaCl_2$ I= 0.001 to 1.3 mol/l pH 7.12 to 10	$Zr(OH)_4$ (am, aged)	$1.7 \cdot 10^{-8}$ M		$9.2 \cdot 10^{-7}$ M
Finland	5	Bentonite porewater (six different) NaCl/ $CaCl_2$ I=0.002 to 2.9, pH 7.23 to 10	$Zr(OH)_4$ (am, aged)	$1.5 \cdot 10^{-8}$ M		$9.2 \cdot 10^{-7}$ M

Tab A. 45   Solubility limiting solid phases and solubilities for zirconium in earlier studies (III)

Country	Study	Solution type	Phase	Lower Limit	Rec. value	Upper Limit
France	6	Pore water in bentonite buffer (un-specified)	not specified	$1 \cdot 10^{-11}$ M		$3 \cdot 10^{-6}$ M
France	6	Pore water of cement-based materials (unspecified)	not specified			$1 \cdot 10^{-8}$ M
France	6	Pore water of Callovo-Oxfordian clay rock NaCl/ CaCl$_2$ I=0.09-0.12 mol/l pH 6.9-7.6	not specified	$1 \cdot 10^{-11}$ M		$3 \cdot 10^{-6}$ M
Germany	7a	Unspecified solution expected to occur in the Konrad mine <pH12, possibly up to 3.3 mol/l Cl (NaCl/ CaCl$_2$/ MgCl$_2$)	not determined			10^{-7} M
Germany	7b	Unspecified brine under acidic conditions	none	$1 \cdot 10^{-8}$ M	$1 \cdot 10^{-6}$ M	$1 \cdot 10^{-4}$ M
Germany	7b	Unspecified brine under neutral conditions	none	$1 \cdot 10^{-8}$ M	$1 \cdot 10^{-6}$ M	$1 \cdot 10^{-4}$ M
Germany	7b	Unspecified brine under alkaline conditions	none	$1 \cdot 10^{-10}$ M	$1 \cdot 10^{-8}$ M	$1 \cdot 10^{-6}$ M
Germany	9	NaCl 5 mol/l pcH 6	Zr(OH)$_4$(am)	not determined		$1 \cdot 10^{-6}$ M
Germany	9	NaCl 5 mol/l pcH 9	Zr(OH)$_4$(am)	not determined		$1 \cdot 10^{-6}$ M

Tab A. 46   Solubility limiting solid phases and solubilities for zirconium in earlier studies (IV)

Country	Study	Solution type	Phase	Lower Limit	Rec. value	Upper Limit
Germany	9	$MgCl_2$ 4.5 mol/l pcH 6	$Zr(OH)_4(am)$	not deter-mined		$1 \cdot 10^{-6}$ M
Germany	9	$MgCl_2$ 4.5 mol/l pcH 9	$Zr(OH)_4(am)$	not deter-mined		$1 \cdot 10^{-6}$ M
Germany	9	NaCl 5.6 mol/kg pcH 12.8	$Zr(OH)_4(am)$	not deter-mined		$1 \cdot 10^{-6}$ M
Germany	9	$MgCl_2$ 4 mol/kg pcH 9	$Zr(OH)_4(am)$	not deter-mined		$1 \cdot 10^{-6}$ M
Germany	9	$CaCl_2$ 2 mol/kg pcH 12	$Zr(OH)_4(am)$	not deter-mined		$>1 \cdot 10^{-2}$ M
Great Britain	10	Cementitious system (not specified)	not specified	$1 \cdot 10^{-10}$ M		$1 \cdot 10^{-6}$ M
Great Britain	10	Bentonite pore water (not specified)	not specified	$2.1\ 10^{-9}$ M		$3 \cdot 10^{-9}$ M
Japan	11	Bentonite porewater based on fresh groundwater Na_2CO_3 I=0.026 pH 8.4	$ZrO_2(am)$			$1 \cdot 10^{-6}$ M
Japan	11	Bentonite porewater based on saline groundwater NaCl/Na_2CO_3 I=0.615 pH 7.8	$ZrO_2(am)$			$1 \cdot 10^{-6}$ M

Tab A. 47 Solubility limiting solid phases and solubilities for zirconium in earlier studies (V)

Country	Study	Solution type	Phase	Lower Limit	Rec. value	Upper Limit
Japan	11	Bentonite porewater based on fresh groundwater after contact with cement Na_2CO_3 I=0.0181 pH 8.7	ZrO_2(am)			$1 \cdot 10^{-6}$ M
Japan	11	Bentonite porewater based on fresh groundwater Na_2CO_3/ Na_2SO_4 I=0.211 pH 7.2	ZrO_2(am)			$1 \cdot 10^{-6}$ M
Japan	11	Bentonite porewater based on fresh groundwater Na_2CO_3 I=0.0083 pH 9.7	ZrO_2(am)			$1 \cdot 10^{-6}$ M
Japan	11	Bentonite porewater based on fresh groundwater, oxidizing Na_2CO_3 I=0.0223 pH 8.4	ZrO_2(am)			$1 \cdot 10^{-6}$ M
Sweden	12	Forsmark reference water (NaCl/ $CaCl_2$ I= 0.19 mol/l)	ZrO_2(am, aged)			$1.74 \cdot 10^{-8}$ M
Sweden	12	Saline water (NaCl/ $CaCl_2$ I=1.86 mol/l)	ZrO_2(am, aged)			$1.82 \cdot 10^{-8}$ M
Sweden	12	Ice-melting water (Na/Ca/Cl,HCO_3/F,Si I=0.0012 mol/l)	ZrO_2(am, aged)			$1.41 \cdot 10^{-8}$ M

Tab A. 48   Solubility limiting solid phases and solubilities for zirconium in earlier studies (VI)

Country	Study	Solution type	Phase	Lower Limit	Rec. value	Upper Limit
Switzerland	13	Cement/ concrete system equilibrated with Opalinus clay porewater: NaCl/ $CaCl_2$ I=0.09 mol/kg pH12.5	LL, RV: ZrO_2 (baddeleyite) UL: $Zr(OH)_4$(am, fresh)	$6.8 \cdot 10^{-11}$ M	$4.5 \cdot 10^{-9}$ M	$1.3 \cdot 10^{-4}$ M
Switzerland	13	Bentonite porewater system equilibrated with Opalinus clay porewater NaCl/ Na_2SO_4 I=0.239 mol/kg pH 7.79	LL, RV: ZrO_2 (baddeleyite) UL: $Zr(OH)_4$(am, fresh)	$1.6 \cdot 10^{-11}$ M	$1.0 \cdot 10^{-7}$ M	$1.1 \cdot 10^{-4}$ M

)1   In table C.10 of the publication values between $3.65 \cdot 10^{-39}$ and $2.31 \cdot 10^{-28}$ mol/kg are given but in analogy to the assumptions made for the Cobourg 2 water the same value of $6 \cdot 10^{-10}$ mol/kg would be logical

A 1.1   Radioactive inventory

Tab A. 49 Radioactive inventory calculated for the year 2075 /LAR 13/

Radionuclide	Structure parts [Bq]	Spent fuel (DWR/SWR/WWER) [Bq]	Vitrified waste CSD-V [Bq]	Vitrified waste CSD-C [Bq]	Vitrified waste CSD-B [Bq]	Vitrified waste AVR [Bq]	Thorium high temperature reactor THTR [Bq]	Prototype and research reactors (FRM II, BER II,	Other radioactive mixed waste [Bq]	Uranium tails [Bq]	Graphite waste [Bq]	Total [Bq]	half-life [a⁻¹]	Molecular weight [g/mol]	Mass [g]
Be-10	1.35E+07	1.47E+11	4.01E+10	8.69E+07	0.00E+00	0.00E+00	2.11E+09	1.28E+09	0.00E+00	0.00E+00	0.00E+00	1.91E+11	1.60E+06	10.013534	2.31E+02
C-14	6.23E+12	3.98E+14	6.63E+13	5.62E+13	0.00E+00	2.99E+12	1.60E+12	1.90E+12	2.94E+12	0.00E+00	2.78E+14	8.14E+14	5.73E+03	14.003241	4.94E+03
Cl-36	2.32E+11	1.14E+13	1.88E+12	2.04E+12	0.00E+00	9.26E+10	4.11E+10	0.00E+00	7.67E+09	0.00E+00	5.80E+10	1.58E+13	3.00E+05	35.968306	1.28E+04
Ca-41	7.46E+09	6.33E+11	1.41E+11	6.93E+10	0.00E+00	0.00E+00	4.49E+08	0.00E+00	0.00E+00	0.00E+00	0.00E+00	8.51E+11	1.03E+05	40.962278	2.71E+02
Ni-59	4.03E+14	2.23E+15	3.19E+11	9.05E+14	0.00E+00	4.11E+09	1.54E+09	0.00E+00	8.85E+12	0.00E+00	0.00E+00	3.55E+15	7.50E+04	58.943349	1.18E+06
Ni-63	3.76E+16	2.16E+17	2.73E+13	7.15E+16	0.00E+00	9.48E+08	1.20E+11	2.83E+04	1.06E+15	0.00E+00	0.00E+00	3.26E+17	1.00E+02	62.929669	1.55E+05
Se-79	8.81E+06	2.95E+13	8.53E+12	7.60E+07	0.00E+00	2.75E+10	1.99E+11	1.11E+11	2.79E+08	0.00E+00	0.00E+00	3.84E+13	4.80E+05	78.918498	1.10E+05
Rb-87	3.35E+02	1.33E+10	4.08E+09	7.12E+03	0.00E+00	8.38E+06	1.23E+07	1.13E+08	0.00E+00	0.00E+00	0.00E+00	1.75E+10	4.80E+10	86.909187	5.52E+06
Sr-90	3.55E+11	1.15E+19	2.02E+18	3.45E+12	4.36E+15	4.08E+15	6.46E+15	1.35E+17	6.55E+14	0.00E+00	3.19E+12	1.37E+19	2.86E+01	89.907738	2.66E+06
Zr-93	1.51E+12	1.21E+15	3.41E+14	1.78E+13	0.00E+00	7.42E+11	8.77E+11	1.03E+13	2.48E+11	0.00E+00	0.00E+00	1.58E+15	1.50E+06	92.906474	1.67E+07
Nb-94	9.66E+13	3.54E+15	5.71E+10	1.04E+15	0.00E+00	2.54E+07	2.12E+10	1.99E+09	3.97E+07	0.00E+00	0.00E+00	4.68E+15	2.00E+04	93.90728	6.64E+05
Mo-93	1.75E+12	4.92E+13	1.77E+11	1.33E+13	0.00E+00	8.45E+08	9.10E+08	0.00E+00	6.30E+06	0.00E+00	0.00E+00	6.44E+13	3.50E+03	92.906813	1.58E+03
Tc-99	2.27E+11	9.04E+15	2.64E+15	1.61E+12	0.00E+00	4.08E+12	5.42E+12	8.10E+13	7.61E+11	0.00E+00	0.00E+00	1.18E+16	2.10E+05	98.906254	1.85E+07
Pd-107	5.31E+06	9.25E+13	1.97E+13	1.61E+08	0.00E+00	6.20E+09	4.79E+09	8.07E+11	0.00E+00	0.00E+00	0.00E+00	1.13E+14	6.50E+06	106.905127	5.93E+06
Ag-108m	4.46E+06	4.19E+13	1.33E+13	2.12E+08	0.00E+00	0.00E+00	2.03E+10	1.37E+08	0.00E+00	0.00E+00	0.00E+00	5.52E+13	4.18E+02	107.905952	1.88E+02
Sn-126	2.27E+07	3.87E+14	9.60E+13	6.15E+08	0.00E+00	1.40E+11	1.77E+11	3.41E+12	1.40E+10	0.00E+00	0.00E+00	4.87E+14	2.35E+05	125.907654	1.09E+06

344

Radionuclide	Structure parts [Bq]	Spent fuel (DWR/ SWR/ WWER) [Bq]	Vitrified waste CSD-V [Bq]	Vitrified waste CSD-C [Bq]	Vitrified waste CSD-B [Bq]	Vitrified waste AVR [Bq]	Thorium high temperature reactor THTR [Bq]	Prototype and research reactors (FRM II, BER II,	Other radioactive mixed waste [Bq]	Uranium tails [Bq]	Graphite waste [Bq]	Total [Bq]	half-life [a^{-1}]	Molecular weight [g/mol]	Mass [g]
I-129	9.98E+05	1.92E+13	4.97E+12	2.50E+07	0.00E+00	8.01E+09	1.14E+10	1.68E+11	3.25E+12	0.00E+00	0.00E+00	2.76E+13	1.57E+07	128.904986	4.22E+06
Cs-135	2.12E+07	3.17E+14	8.21E+13	2.93E+08	0.00E+00	1.43E+11	1.34E+11	2.31E+12	9.79E+09	0.00E+00	0.00E+00	4.02E+14	2.00E+06	134.905885	8.19E+06
Cs-137	8.86E+11	1.93E+19	3.08E+18	1.10E+13	1.44E+16	4.66E+15	6.94E+15	2.19E+17	1.32E+15	0.00E+00	6.93E+11	2.26E+19	3.02E+01	136.907073	7.06E+06
Sm-147	2.16E+02	3.06E+09	1.12E+09	3.46E+03	0.00E+00	0.00E+00	2.87E+06	2.57E+07	0.00E+00	0.00E+00	0.00E+00	4.21E+09	1.06E+11	146.914895	4.95E+06
Sm-151	1.83E+10	1.60E+17	3.49E+16	1.97E+11	0.00E+00	2.66E+13	6.40E+13	1.31E+15	8.17E+11	0.00E+00	0.00E+00	1.96E+17	9.30E+01	150.919929	2.08E+05
Ho-166m	9.25E+03	8.60E+11	8.18E+10	2.56E+03	0.00E+00	3.62E+05	2.38E+09	8.11E+09	0.00E+00	0.00E+00	0.00E+00	9.52E+11	1.20E+03	165.932281	1.43E+01
Cm-248	1.11E-03	3.63E+09	1.70E+07	1.08E+03	0.00E+00	0.00E+00	4.36E+01	1.22E+07	0.00E+00	0.00E+00	0.00E+00	3.66E+09	3.40E+05	248.072343	2.33E+01
Pu-244+	8.99E+01	3.19E+11	8.45E+09	2.39E+05	0.00E+00	2.35E+06	2.10E+05	5.24E+09	8.10E+06	0.00E+00	0.00E+00	3.33E+11	8.00E+07	244.064199	4.91E+05
Pu-240	5.16E+10	4.54E+17	1.14E+15	4.00E+11	0.00E+00	1.29E+13	4.52E+12	3.01E+15	2.43E+13	0.00E+00	0.00E+00	4.58E+17	6.56E+03	240.053808	5.45E+07
U-236	1.64E+06	1.38E+14	7.72E+10	1.12E+07	0.00E+00	9.38E+10	1.50E+11	1.10E+12	1.13E+10	0.00E+00	0.00E+00	1.39E+14	2.34E+07	236.045562	5.82E+07
Th-232	3.84E-03	2.29E+08	1.09E+08	4.29E-02	0.00E+00	5.17E+09	2.56E+10	2.74E+03	2.41E+11	0.00E+00	0.00E+00	2.72E+11	1.41E+10	232.038054	6.73E+07
U-232	2.23E+04	2.32E+13	8.13E+09	1.04E+06	0.00E+00	4.55E+12	2.36E+13	1.59E+11	0.00E+00	0.00E+00	0.00E+00	5.15E+13	6.89E+01	232.03713	6.22E+01
Cm-245	5.52E+04	1.55E+15	2.41E+13	7.11E+08	0.00E+00	5.68E+08	2.01E+08	3.71E+12	9.02E+08	0.00E+00	0.00E+00	1.58E+15	8.50E+03	246.067218	2.49E+05
Am-241+	3.06E+11	4.05E+18	1.55E+17	8.32E+12	3.56E+13	1.07E+14	3.33E+13	2.52E+16	1.83E+14	0.00E+00	0.00E+00	4.23E+18	4.32E+02	241.056823	3.33E+07
Np-237	4.08E+06	2.85E+14	6.29E+13	1.95E+08	4.51E+08	8.32E+10	8.02E+10	2.18E+12	2.52E+10	0.00E+00	0.00E+00	3.50E+14	2.14E+06	237.048167	1.34E+07
U-233	5.99E+02	1.18E+12	2.13E+10	3.38E+04	3.77E+04	8.91E+12	4.79E+13	5.07E+08	8.90E+05	0.00E+00	0.00E+00	5.80E+13	1.59E+05	233.039628	1.62E+05

Radionuclide	Structure parts [Bq]	Spent fuel (DWR/SWR/WWER) [Bq]	Vitrified waste CSD-V [Bq]	Vitrified waste CSD-C [Bq]	Vitrified waste CSD-B [Bq]	Vitrified waste AVR [Bq]	Thorium high temperature reactor THTR [Bq]	Prototype and research reactors (FRM II, BER II,)	Other radioactive mixed waste [Bq]	Uranium tails [Bq]	Graphite waste [Bq]	Total [Bq]	half-life [a^{-1}]	Molecular weight [g/mol]	Mass [g]
Th-229	1.51E+00	6.21E+09	2.74E+08	9.13E+01	4.22E+01	7.58E+10	3.42E+11	3.04E+06	3.20E+02	0.00E+00	0.00E+00	4.24E+11	7.88E+03	229.031755	5.79E+01
Cm-246	3.31E+03	2.55E+14	3.41E+12	1.30E+08	0.00E+00	2.60E+08	2.81E+07	9.58E+11	0.00E+00	0.00E+00	0.00E+00	2.59E+14	4.73E+03	246.067218	2.28E+04
Pu-242	4.13E+07	2.76E+15	2.13E+12	3.82E+09	0.00E+00	8.60E+10	1.88E+10	1.70E+13	4.56E+10	0.00E+00	0.00E+00	2.78E+15	3.75E+05	242.058737	1.91E+07
U-238	1.71E+07	1.27E+14	9.11E+10	5.29E+07	0.00E+00	5.16E+09	5.24E+08	1.40E+12	8.14E+10	1.18E+15	0.00E+00	1.31E+15	4.47E+09	238.050784	1.05E+11
Am-242m	2.85E+08	1.34E+16	8.42E+14	7.85E+09	0.00E+00	1.42E+11	2.03E+10	3.37E+13	6.07E+10	0.00E+00	0.00E+00	1.43E+16	1.41E+02	242.05941	3.68E+04
Pu-238	1.00E+10	2.76E+18	2.04E+15	5.90E+11	0.00E+00	3.40E+14	2.68E+14	1.58E+16	1.41E+14	0.00E+00	0.00E+00	2.78E+18	8.77E+01	238.049554	4.38E+06
U-234	1.59E+07	8.94E+14	9.19E+11	2.18E+08	0.00E+00	1.22E+12	3.64E+12	6.29E+12	3.37E+09	1.99E+14	0.00E+00	1.11E+15	2.46E+05	234.040946	4.81E+06
Th-230	6.87E+03	3.52E+11	1.56E+10	9.96E+04	0.00E+00	1.06E+09	1.42E+10	2.40E+09	1.28E+05	1.32E+11	0.00E+00	5.17E+11	7.54E+04	230.033127	6.78E+02
Ra-226+	7.34E+01	4.03E+09	5.33E+08	1.34E+03	0.00E+00	1.39E+07	4.42E+08	2.48E+07	1.29E+11	2.07E+09	0.00E+00	1.36E+11	1.60E+03	226.025402	3.72E+00
Cm-247	1.86E-03	1.41E+09	8.89E+06	3.95E+02	0.00E+00	0.00E+00	3.71E+01	3.91E+06	0.00E+00	0.00E+00	0.00E+00	1.42E+09	1.56E+07	247.070347	4.14E+02
Am-243	9.32E+07	3.59E+16	2.76E+15	4.58E+10	0.00E+00	5.30E+11	7.96E+10	1.99E+14	1.34E+11	0.00E+00	0.00E+00	3.89E+16	7.37E+03	243.061375	5.26E+06
Pu-239	7.36E+10	2.06E+17	4.09E+14	5.34E+11	0.00E+00	6.31E+12	1.66E+12	1.70E+15	1.60E+13	0.00E+00	0.00E+00	2.08E+17	2.41E+04	239.052157	9.06E+07
U-235	5.31E+05	5.56E+12	6.15E+09	9.86E+05	0.00E+00	4.73E+09	2.01E+10	5.56E+10	5.22E+09	1.58E+13	0.00E+00	2.15E+13	7.04E+08	235.043924	2.68E+08
Pa-231	6.43E+02	3.09E+10	7.53E+09	2.16E+03	0.00E+00	6.08E+09	8.00E+10	1.95E+08	9.05E+05	2.45E+10	0.00E+00	1.49E+11	3.28E+04	231.03588	8.54E+01
Ac-227	3.45E+02	2.42E+10	7.05E+09	1.54E+03	0.00E+00	6.16E+09	7.43E+10	1.38E+08	1.09E+05	1.51E+10	0.00E+00	1.27E+11	2.18E+01	227.02775	4.74E-02

A.3 Composition of vitrified glass and inactive simulates

Tab A. 50 Composition of glasses used in selected glass corrosion studies (wt.- %) (part I)

Oxide	MW (inactive) (1)	MW (inactive) (2)	SON68 (inactive) (3)	R7T7 simulate (inactive) (4)	R7T7 (active) (4)	GP WAK I (active) (4)	GP WAK Ia (inactive) (4)
Ag$_2$O				0.03	0.03	0.02	0.02
Al$_2$O$_3$	6.6	4.86	4.91	1.36	4.91	2.62	2.62
B$_2$O$_3$	16	16.43	14.02	16.82	14.02	14.78	14.78
BaO		0.4	0.6	1.1	0.6	0.46	0.5
CaO	0.03		4.04		4.04	4.59	4.6
CdO				0.06	0.03	0.02	0.02
Ce$_2$O$_3$	0.9		0.93				
CeO$_2$		2.23		1.76	0.93	0.35	0.38
CoO					0.12		
Cr$_2$O$_3$		0.68	0.51	0.22	0.51	0.49	0.54
Cs$_2$O	1.1	1.17	1.42	1.67	1.42	0.59	0.64
Eu$_2$O$_3$				0.1		0.03	
Fe$_2$O$_3$	3.1	3.15	2.91	1.07	2.91	1.87	2.04
Gd$_2$O$_3$		0.12		3.06		0.06	0.07
K$_2$O						0.05	0.05
La$_2$O$_3$	0.4	0.66	0.9	0.89	0.9	0.43	0.46
Li$_2$O		3.98	1.98	3.91	1.98	2.9	2.9
MgO	5.9	5.05		1.46		1.92	1.93
MnO$_2$			0.72	0.02	0.72	0.35	0.38
MoO$_3$		1.52	1.7	3.03	1.7	0.9	0.98
Na$_2$O	8.5	8.33	9.86	8.31	9.86	10.38	10.76
Nb$_2$O$_5$				0.01			
Nd$_2$O$_3$	1.4	1.94	1.59	2.82	1.59	1.29	1.41

Tab A. 51   Composition of glasses used in selected glass corrosion studies (wt.- %) (part II)

Oxide	MW (inactive) (1)	MW (inactive) (2)	SON68 (inactive) (3)	R7T7 simulate (inactive) (4)	R7T7 (active) (4)	GP WAK I (active) (4)	GP WAK Ia (inactive) (4)
NiO		0.45	0.74	0.14	0.74	0.29	0.32
P_2O_5	0.2		0.28	0.15	0.28	0.38	0.41
PdO						0.26	0.29
Pr_2O_3	0.4	0.61	0.44	0.86	0.44	0.29	0.32
Rb_2O				0.23		0.06	0.06
Rh_2O_3						0.13	0.14
RuO_2		0.42				0.52	0.57
Sb_2O_3				0.01	0.01	<0.01	<0.01
SeO_2				0.04		0.02	0.02
SiO_2	46.7	45.82	45.82	45.99	45.48	50.4	50.4
Sm_2O_3		0.43		0.57		0.25	0.27
SnO_2				0.04	0.02	0.01	0.01
SO_4				0.02			
SrO		0.31	0.33	0.6	0.33	0.1	0.11
TeO_2		0.18	0.23	0.32	0.23	0.13	0.14
ThO_2					0.33		
TiO_2						1.01	1.01
UO_2					0.52	1.27	
Y_2O_3		0.2	0.2	0.35	0.2	0.13	0.14
ZnO			2.5	0.03	2.5	<0.01	<0.01
ZrO_2	1.4	1.59	2.65	2.95	2.65	0.65	0.71
other oxides	7.4		0.08				

1 /CUR 03/
2 /CAS 13/
3 /CAR 17/
4 /ZIM 03/

A.4 Preparation of salt minerals and equilibrium solutions

A.4.1 General remarks

For the preparation of the solid compounds and salt solutions, the procedures in the following chapters were described in this chapter. The identity of the solids was confirmed by XRD measurements.

The equilibrium solutions were analysed chemically several times in order to make sure that the composition is stable and close to the expected concentrations. In the case of IP21 solution a difference between the solution concentrations found reported in the literature and our values pertained. Also, it was not possible to detect all minerals that were added during the experiment in the final solid mixture. Either their concentration was too small, or they were not present because they have been transformed into a different mineral. The solution was nevertheless used for the experiments as it had similar characteristics as a 'real' IP21 solution: high $MgCl_2$ content and considerable concentrations of potassium and sulphate.

A.4.2 Polyhalite, $K_2MgCa_2(SO_4)_4 \cdot 2H_2O$

The preparation of polyhalite followed the recipe of Autenrieth /AUT 58/. In the first step 1247.1 g $MgCl_2 \cdot 6H_2O$ (Merck Emsure, crist.), 192.6 g $MgSO_4 \cdot 7H_2O$ (Merck Emsure, p.a.), and KCl (VWR 99.0-100.5 %) were dissolved in 1250 g water at 70°C. Not reacted KCl was removed by vacuum filtration. The clear solution was heated to 95°C under reflux and a solution of 10.3 g $CaCl_2 \cdot 2H_2O$ (Merck Emprove) in 38.8 ml water was added over the course of two hours and the mixture stirred for another 3h. The hot slurry underwent vacuum filtration. The precipitate was washed first with 85 % alcohol then with 95 % alcohol and dried at the air. The yield was 24 g. The identity of the solid was confirmed by XRD.

A second batch was prepared based on a method described by D'Ans /D'A 08/: 620 g $MgSO_4 \cdot 7H_2O$ (Merck Emsure, p.a.), 71 g K_2SO_4 (Merck, p.a.), 70 g $CaSO \cdot 2H_2O$, and 685 g water were mixed and heated under reflux. The precipitate was sucked dry. Drying in a desiccator lead to a yield of 138 g.

A.4.3 Syngenite, $K_2Ca(SO_4)_2 \cdot H_2O$

A solution of 227 g K_2SO_4 (Merck, p.a.) in 2 kg water was mixed with a solution prepared from 43.8 g $CaCl_2 \cdot 2H_2O$ (Merck Emprove) and 39 g water. The white precipitate was dried in a desiccator. The yield was 96 g. The identity of the solid was confirmed by XRD.

A.4.4 Glauberite, $CaSO_4 \cdot Na_2SO_4$

The solubility experiments by Block and Waters /BLO 68/ served as a basis to develop the procedure. 116.9 g NaCl and 49.7 g Na_2SO_4 were dissolved in 0.5 kg water. Then a mixture of 113.6 g Na_2SO_4 and 137.7 g $CaSO_4 \cdot 2H_2O$ was added in three batches (53 g, 82 g, remainder). The slurry was heated to 100°C under reflux and constant stirring. Clumps of gypsum dissolved after about one hour. After a day 60 g water were added. The mixture underwent vacuum filtration. The filtrate was dried in a heating cabinet at 105 °C. The yield was 201 g. The identity of the solid was confirmed by XRD.

A.4.5 Carnallite, $KMgCl_3 \cdot 6H_2O$

189 g water were added to 556 g $MgCl_2 \cdot 6H_2O$ (Merck Emsure). The mixture was stirred under slight heating until the solid has disappeared. A solid mixture of 365 g $MgCl_2 \cdot 6H_2O$ and 134 g KCl (VWR Ph.EUR) were added in batches under cautious heating. The slurry contained a considerable amount of undissolved cubic crystals (KCl). A solution consisting of 235 g $MgCl_2 \cdot 6H_2O$, and 126 g water was added and the mixture stirred for five days. The precipitate was sucked dry and was further dried in a desiccator. The yield was 328 g. The identity of the solid was confirmed by XRD.

A.4.6 Kainite, $KMgClSO_4 \cdot 2.75H_2O$

A solution was prepared by dissolving 17.5 g K_2SO_4 (Merck p.a.), 324 g $MgCl_2 \cdot 6H_2O$ (Merck Emsure) in 246.1 g water. A mixture of 97 g $MgSO_4$ (Applichem reinst), 200 g $MgSO_4 \cdot 7H_2O$ (Merck p.a. Emsure) and 95.4 g KCl (VWR Ph.EUR) were added in three batches and the mixture stirred by means of an overhead stirrer (two days). At one point the stirrer was clogged by unreacted salts and needed to be free by slight heating. The mixture underwent vacuum filtration. The identity of the solid was confirmed by XRD

A.4.7   Anhydrite, CaSO₄

Gypsum was weighed in a porcelain cup and heated to 500 °C for several hours. The cup was allowed to cool in a dry desiccator above silica gel.

A.4.8   Synthetic clay pore water 'UK solution' (lower cretaceous clay, Northern Germany)

The UK solution was prepared by dissolving 577 g NaCl (SigmaAldrich p.a., 106 g $CaCl_2 \cdot 2H_2O$ (Merck Emprove), 61.5 g $MgCl_2 \cdot 6H_2O$, 2.32 g NaBr, 0.014 g $NaHCO_3$ (Merck Emsure p.a.), 25.1 g $Na_2SO_4 \cdot 10H_2O$ (Merck Emsure p.a.), 3.2 g KCl (Merck Emsure p.a.), and 1.9 ml of a 11.5 w.- % $FeCl_2$ solution in 3917 g water. In addition, 20 g $CaSO_4 \cdot 2H_2O$ (Merck p.a.), 20 g Siderite (prepared in the GRS lab, see /HAG 21/), and 20 g $CaCO_3$ were added. The mixture was stirred for several weeks.

The UK-Portlandite solution was prepared by adding 5.68 g Ca(OH)2 (Merck Emsure p.a.), 2.51 $CaCO_3$ (Merck, p.a.), and 2.56 g $CaSO_4 \cdot 2H_2O$ (Merck p.a.) to 500 ml UK solution.

A.4.9   Solution saturated with halite and anhydrite

This solution (HalAnh) was prepared by adding 2959 g halite to 8.8 kg water and subsequent stirring until the salt was dissolved. 53.5 g $CaCl_2 \cdot 2H_2O$ were dissolved. After that, a solution consisting of 200 ml water and 52.13 g Na_2SO_4 were added. Further water was added to achieve a total volume of approximately 10 l and left standing. The mixture was stirred for several days. 10 g anhydrite and 200 g halite were added, and the mixture stirred again for several weeks.

A.4.10   IP9 solution and IP9 Reak solution

IP9 solution was prepared by adding 1062 g NaCl, 574 g $MgCl_2 \cdot 6H_2O$, 8.24 g $Na_2SO_4 \cdot 10H_2O$, 425 g $MgSO_4 \cdot 7H_2O$, 299 KCl, and 2.84 g $CaCl_2$ to 3832 g water. The mixture was stirred for several weeks. A first analysis showed that the concentrations differed slightly from the expected composition. To ensure a saturation with the equilibrium minerals, 100 g NaCl, 15 g polyhalite, 15 g glauberite, 15 g syngenite, and 15 g anhydrite were added, and the mixture stirred again for several weeks.

IP9 Reak was prepared by dissolving 575 g NaCl (SigmaAldrich p.a.), 79.7 g K_2SO_4 (Merck p.a.), 53.8 g KCl (Merck Emsure p.a.), and 1.75 g $CaCl_2$ (Merck Emprove) to 1650 g water. To ensure a saturation with the equilibrium minerals, 50 g NaCl, 10 g glauberite, 10 g $Mg(OH)_2$, (Fluka > 99 %) were added and the mixture stirred again for several weeks.

A.4.11 IP21 solution and IP21 Reak solution

IP21 solution was prepared by adding, by the following sequence, 0.31 g $CaCl_2$, 0.39 g Na_2SO_4, 210 g KCl, 119 g NaCl, 149 g $MgSO_4$, 3386 g $MgCl_2 \cdot 6H_2O$ to 2593 g water. The mixture was stirred for several weeks. A first analysis showed that the concentrations differed slightly from the expected composition. To ensure a saturation with the equilibrium minerals, 20 g NaCl, 20 g KCl, 20 g carnallite, 20 kainite, 15 g polyhalite were added and the mixture stirred again for several weeks.

IP21 Reak was prepared by dissolving 75.3 g KCl (Applichem p.a.), 115.3 g K_2SO_4 (Merck, p.a.), 693 g NaCl (SigmaAldrich p.a.), 1.7 g $CaCl_2 \cdot 2H_2O$ (Applichem p.a.) to 2000 g water. Further 49.6 g NaCl as well as 10 g syngenite and 10 g glauberite were added to saturate the solution. The mixture was stirred for several weeks.

95 % solutions (neutral, acidic, alkaline) were prepared by adding 5 % water, 2 M HCl or 5 % NaOH (e.g., 1.15 ml 45 w.- % NaOH and 3.85 ml water)

A.5 Commercial and prepared solid phases used as starting materials in solubility measurements

A.5.1 Overview

Tab A. 52 Solid starting materials

Substance	Source
AgI	Alfa Aesar 99.999 % (12111)
$CaSeO_3$ (nestolaite)	Prepared
Fe	Aldrich p.a. (44890)
FeSe	Alfa Aesar 99.9 % (31112)
$K_2Pb(SO_4)_2$ (palmierite)	Prepared
MoO_2	Alfa Aesar 99 % (48117)
$Nb_2O_5 \cdot xH_2O$	Prepared
$Ni(OH)_2$	Alfa Aesar (12517)
PbClOH (laurionite)	Prepared
$PbCl_2$	Alfa Aesar 99 % (12349)
$PdCl_2$	Alfa Aesar 99 % (39496)
$SmCl_3$	Alfa Aesar 99.9 % (11231)
$Sm(OH)_3$	Prepared
$Sn_{21}Cl_{16}(OH)_{14}O_6$ (abhurite)	Prepared
$SnCl_2 \cdot xH_2O$	Merck p.a. (1.07815)
$SnO_2 \cdot xH_2O$	Prepared
$SrSO_4$ (celestine)	Prepared
$ZrO_2 \cdot xH_2O$	Prepared

A.5.2 Lead chloride hydroxide, laurionite, PbClOH

338 g NaCl were dissolved in 1000 g deionised water. 27 g $PbCl_2$ were added in steps and the mixture stirred until the solution became clear. 96 ml of a 1 M NaOH solution were added dropwise until the pH was above 7. The precipitate was removed by filtration, washed with water, and later dried in a desiccator.

A.5.3   Potassium lead sulphate, palmierite, $K_2Pb(SO_4)_2$

13.16 g lead sulphate, $PbSO_4$ (Aldrich 98 % 307734), 21.9 g potassium sulphate, K_2SO_4 (Merck suprapur) and 179.5 g water were mixed and then stored at 90°C in a thermal cabinet for three days. During that time the mixture was shaken several times. After that it was removed and left to stand at room temperature for a month. The overstanding solution was removed by vacuum filtration through a Büchner funnel. The precipitate was washed two times with small amounts of water.

A.5.4   Niobium oxide hydrate

25 g of $NbCl_5$ (Alfa Aesar 99.9 %, 11548) were dissolved in 200 ml Ethanol (99 %). Dilution with 3000 ml water led to a milky suspension with very little precipitation. Addition of 27.5 g NaCl and 5 ml NaOH (0.1 M) forced a white precipitate to form. It was concentrated to a sludge by 2 hours centrifugation at 3000 rpm. The sludge was washed with 300 ml water and centrifuged again and then dried in a desiccator.

A.5.5   Samarium hydroxide, $Sm(OH)_3$

$Sm(OH)_3$ was prepared by mixing a $SmCl_3$ solution (18.12 g Alfa Aeasar 99.9 % to 200 ml carbonate-free deionised water) with carbonate-free NaOH solution (9.250 ml of a 46.9 % carbonate-free NaOH solution (ρ=1.510) added to 164 ml water) in the glovebox under exclusion of CO_2. The mixture was stirred for one day and allowed to settle. The precipitate was separated by filtration and washed with water to remove NaCl and $SmCl_3$ residues.

A.5.6   Calcium selenite, nestolaite, $CaSeO_3\cdot H_2O$

In the first step, aqueous sodium selenite was prepared by adding 20.9 g selenic acid, H_2SeO_3 (Aldrich 99.999 %, 229857) to a diluted NaOH solution prepared by adding 18.30 ml of a 46.9 % carbonate-free NaOH solution (ρ=1.510) to 200 g of carbonate-free deionised water. The solution should be neutral or slightly acidic. A second solution was prepared by dissolving 47.7 g $CaCl_2\cdot 6H_2O$ in 200 g carbonate-free deionised water. Both solutions were mixed, and the precipitate allowed to settle. It was separated from the resulting solution by filtration and later washed with water.

Calcium selenite was prepared by mixing a sodium selenite and $CaCl_2$ solutions. A precipitate formed that was washed with water and dried in a desiccator. The product was identified by XRD as $CaSeO_3 \cdot H_2O$ (nestolaite).

A.5.7 Strontium sulphate, celestine, $SrSO_4$

$SrSO_4$ was prepared by mixing a solution of $SrCl_2$ (Merck p.a. 1.07865; 43.5 g = 0.163 mol added to 200 ml H_2O) with a solution of Na_2SO_4 (24.4 g = 0.163 mol to 200 ml). The precipitate was allowed to settle. The overstanding solution was filtered off and the remaining solid washed with deionised water several times.

A.5.8 Tin(II) chloride hydroxide, $Sn_{21}Cl_{16}(OH)_{14}O_6$, abhurite

Under an argon stream 23.7 g of tin powder (Alfa Aesar 100 mesh 99.5 %, 10378) were added to 206 ml 2 M HCl in screw capped flask. When the formation of hydrogen ended, a clear solution resulted. The flask was moved to a glove box, where 6.7 g urea were added. This resulted in the precipitation of a white solid that was separated from the solution by filtration and washed with little water.

A.5.9 Tin(IV) dioxide hydrate, $SnO_2 \cdot xH_2O$

18 g $SnCl_4$ (Alfa Aesar 98 %, 11570) were added dropwise and under stirring to 100 ml water producing an opaque solution. Aqueous NaOH was added until the pH was around 7. A white voluminous solid appeared that was separated by filtering and washed several times with water. The solid was stored under a layer of water.

A.5.10 Zirconium dioxide hydrate, $ZrO_2 \cdot xH_2O$

22.8 g $ZrOCl_2 \cdot 8H_2O$ (Alfa 99.9 %, 86108) were added slowly to 150 ml water. A second solution was prepared by diluting 8 ml 47 w.- % NaOH with 150 ml water and added to the Zr solution. A white voluminous precipitate occurred that was allowed to settle. The precipitate was concentrated by centrifugation and washed with water / centrifugated several times. The precipitated was stored in wet condition. It was X-ray amorphous.

A.6 Solubility experiments

The following tables report about the analytically determined elemental concentrations at the end of the solubility experiments. The following abbreviations are used:

n.a.: not analysed
LoQ: limit of quantification

A.6.1 Determined solubilities in halite/ anhydrite saturated solution

Tab A. 53 Solubility of lead in halite/ anhydrite saturated solution [mol/kg]

No.	Na	Ca	Cl	SO$_4$	Pb	pH	pcH
2	6.00	0.0418	5.85	0.0444	2.84E-03	7.60	8.56
3	5.76	0.0416	5.76	0.0436	7.06E-04	8.27	9.19
4	5.35	0.0436	5.34	0.0459	3.79E-04	8.56	9.41
5	5.39	0.0455	5.39	0.0471	4.08E-04	8.55	9.41
6	6.49	0.0474	6.49	0.0497	4.89E-04	8.49	9.57
7	6.14	0.0427	6.14	0.0452	2.77E-04	8.70	9.70
8	5.87	0.0449	5.87	0.0469	2.97E-04	8.73	9.67
9	6.12	0.0458	6.11	0.0492	1.16E-04	9.20	10.20
10	5.92	0.0408	5.90	0.0516	7.10E-05	9.46	10.41
11	6.15	0.0422	6.13	0.0463	5.77E-05	9.66	10.66
12	6.06	0.0383	5.77	0.0409	9.09E-06	11.45	12.41

Tab A. 54   Solubility of molybdenum(IV) in halite/ anhydrite saturated solution [mol/kg]

No.	Na	Ca	Cl	SO$_4$	Mo	pH	pcH
1	5.30	0.0399	5.29	0.0474	1.19E-06	5.08	5.91
2	5.81	0.0378	5.80	0.0473	6.75E-06	6.80	7.73
3	5.78	0.0369	5.76	0.0464	6.94E-06	6.86	7.78
4	6.16	0.0361	6.13	0.0478	8.54E-06	7.11	8.11
5	5.96	0.0352	5.93	0.0479	7.41E-06	7.88	8.84
6	6.09	0.0360	6.06	0.0450	7.73E-06	8.07	9.05
7	6.06	0.0360	6.03	0.0471	7.88E-06	8.23	9.21
8	5.99	0.0407	5.96	0.0506	7.77E-06	8.77	9.74
9	5.80	0.0358	5.77	0.0509	8.05E-06	9.04	9.97
10	5.65	0.0365	5.61	0.0544	9.65E-06	9.95	10.85

Tab A. 55   Solubility of molybdenum(VI) in halite/ anhydrite saturated solution [mol/kg]

No.	Na	Ca	Cl	SO$_4$	Mo	pH	pcH
1	5.68	0.0399	5.66	0.0489	9.46E-06	4.43	5.34
2	6.25	0.0378	6.23	0.0494	8.77E-06	6.87	7.90
3	5.93	0.0369	5.91	0.0469	8.89E-06	5.02	5.97
4	5.97	0.0361	5.95	0.0473	< d.l.	6.46	7.43
5	5.99	0.0352	5.96	0.0509	< d.l.	9.74	10.71
6	5.97	0.0360	5.94	0.0475	5.61E-06	6.65	7.61
7	6.04	0.0360	6.02	0.0491	6.38E-06	8.73	9.71
8	6.95	0.0407	6.92	0.0557	5.96E-06	8.93	10.10
9	6.05	0.0358	6.02	0.0501	4.55E-06	9.46	10.45
10	6.00	0.0365	5.97	0.0527	5.39E-06	9.79	10.76
11	5.96	0.0355	5.46	0.0542	2.69E-06	10.09	11.00
12	6.20	0.0350	5.97	0.0454	7.25E-06	10.20	11.19

Tab A. 56   Solubility of nickel in halite/ anhydrite saturated solution [mol/kg]

No.	Na	Ca	Cl	SO$_4$	Ni	pH	pcH
1	6.07	0.0439	6.06	0.0501	9.63E-04	7.36	8.35
2	n.a.	n.a.	n.a.	n.a.	2.61E-05	8.18	9.13
3	6.10	0.0433	6.08	0.0519	6.60E-07	9.10	10.09
4	6.19	0.0429	6.17	0.0507	9.15E-07	8.94	9.95
5	6.09	0.0426	6.07	0.0510	6.61E-07	9.23	10.22
6	6.15	0.0431	6.14	0.0493	4.57E-05	8.08	9.08
7	6.01	0.0423	6.00	0.0502	1.54E-06	8.81	9.79
8	5.94	0.0400	5.91	0.0516	1.21E-06	9.00	9.96
9	6.08	0.0392	6.04	0.0573	9.72E-07	9.46	10.44
10	6.33	0.0394	6.30	0.0552	8.52E-07	8.94	9.98

Tab A. 57   Solubility of niobium in halite/ anhydrite saturated solution [mol/kg]

No.	Na	Ca	Cl	SO$_4$	Nb	pH	pcH
1	5.42	0.0368	5.37	0.0602	5.69E-08	10.69	11.54
2	6.06	0.0359	6.02	0.0553	8.40E-08	10.17	11.15
3	6.06	0.0348	6.03	0.0540	6.54E-08	10.01	10.99
4	5.93	0.0381	5.92	0.0450	3.20E-08	6.77	7.73
5	5.86	0.0373	5.84	0.0469	2.05E-08	7.78	8.73
6	5.93	0.0384	5.91	0.0486	3.16E-08	8.06	9.01
7	5.93	0.0380	5.91	0.0498	7.46E-08	8.44	9.40
8	5.93	0.0369	5.90	0.0524	9.08E-08	8.79	9.74
9	5.93	0.0351	5.89	0.0543	3.22E-07	9.33	10.29
10	5.92	0.0326	5.87	0.0582	1.05E-07	9.86	10.81

Tab A. 58 Solubility of palladium in halite/ anhydrite saturated solution [mol/kg]

No.	Na	Ca	Cl	SO$_4$	Pd	pH	pcH
1	6.08	0.0388	6.07	0.0472	2.44E-03	7.67	8.66
2	6.11	0.0478	6.14	0.0460	1.42E-02	5.76	6.76
3	6.02	0.0493	6.05	0.0463	1.37E-02	5.90	6.88
4	6.05	0.0462	6.08	0.0444	1.32E-02	7.31	8.30
5	5.79	0.0447	5.81	0.0450	1.12E-02	7.50	8.44
6	6.01	0.0449	6.02	0.0477	7.50E-03	7.45	8.43
7	5.98	0.0393	5.96	0.0489	4.35E-04	8.03	9.00
8	5.98	0.0396	5.96	0.0517	1.31E-06	9.95	10.92
9	5.99	0.0392	5.97	0.0524	1.43E-06	10.49	11.46
10	6.05	0.0412	6.02	0.0556	2.77E-06	10.93	11.91

Tab A. 59 Solubility of samarium in halite/ anhydrite saturated solution [mol/kg]

No.	Na	Ca	Cl	SO$_4$	Sm	pH	pcH
1	5.97	0.0493	5.98	0.0452	4.00E-07	8.01	8.98
2	5.97	0.0485	5.97	0.0458	2.86E-07	8.87	9.84
3	6.00	0.0463	6.00	0.0452	7.62E-08	9.37	10.34
4	6.01	0.0462	6.02	0.0448	2.36E-07	8.40	9.38
5	6.02	0.0492	6.03	0.0463	6.66E-07	9.93	10.91
6	5.93	0.0454	5.93	0.0440	4.83E-07	9.04	10.00
7	6.08	0.0524	6.09	0.0493	4.54E-07	9.13	10.12
8	6.01	0.0459	6.01	0.0452	3.70E-07	10.54	11.51
9	5.89	0.0460	5.89	0.0441	1.65E-06	9.42	10.37
10	6.12	0.0410	6.10	0.0480	1.93E-06	11.19	12.18

Tab A. 60   Solubility of selenium(II) in halite/ anhydrite saturated solution [mol/kg]

No.	Na	Ca	Cl	SO$_4$	Fe	Se	pH	pcH
1	5.38	0.0389	5.38	0.0431	4.63E-03	1.67E-05	4.90	5.74
2	4.96	0.0432	4.98	0.0482	1.37E-02	1.37E-07	6.11	6.87
3	5.12	0.0448	5.13	0.0487	1.06E-02	1.09E-07	6.64	7.43
4	5.80	0.0397	5.79	0.0444	1.60E-03	3.39E-07	7.08	8.01
5	6.02	0.0373	6.01	0.0415	2.50E-04	9.32E-07	7.44	8.41
6	6.45	0.0438	6.44	0.0478	3.35E-05	6.89E-07	7.76	8.82
7	5.89	0.0412	5.88	0.0459	5.83E-05	1.02E-05	8.07	9.02
8	5.98	0.0374	5.97	0.0416	1.01E-05	2.44E-05	8.60	9.56
9	6.16	0.0424	6.15	0.0468	6.64E-06	1.87E-05	9.09	10.10
10	5.84	0.0404	5.82	0.0483	9.80E-06	2.28E-05	9.61	10.55

Tab A. 61   Solubility of selenium(IV) in halite/ anhydrite saturated solution [mol/kg]

No.	Na	Ca	Cl	SO$_4$	Se	pH	pcH
1	6.07	0.0458	6.07	0.0471	1.86E-04	9.16	10.15
2	6.06	0.0431	6.05	0.0474	1.88E-04	9.78	10.77
3	6.08	0.0444	6.08	0.0449	1.51E-04	8.71	9.70
4	6.08	0.0444	6.07	0.0452	1.75E-04	9.23	10.22
5	6.14	0.0444	6.14	0.0440	1.54E-04	8.54	9.55
6	6.04	0.0450	6.05	0.0439	1.34E-04	8.43	9.42
7	6.03	0.0440	6.03	0.0431	1.77E-04	8.28	9.26
8	6.08	0.0436	6.08	0.0429	6.04E-04	6.82	7.81
9	6.07	0.0442	6.07	0.0434	3.82E-04	7.14	8.13
10	5.97	0.0448	5.97	0.0436	2.77E-04	7.40	8.37

Tab A. 62   Solubility of strontium in halite/ anhydrite saturated solution [mol/kg]

No.	Na	Ca	Cl	SO$_4$	Sr	pH	pcH
1	5.97	0.0441	5.85	0.0482	4.15E-04	8.51	8.31
2	6.47	0.0475	6.22	0.0523	4.42E-04	7.56	7.41
3	6.34	0.0477	6.15	0.0510	4.46E-04	8.23	8.06
4	6.10	0.0462	5.95	0.0489	4.29E-04	8.13	7.95
5	6.51	0.0489	6.26	0.0504	4.60E-04	8.09	7.93
6	6.23	0.0448	5.91	0.0491	4.11E-04	8.22	8.09
7	5.97	0.0424	5.86	0.0504	3.96E-04	8.99	8.79
8	6.22	0.0397	5.94	0.0545	3.70E-04	9.24	9.09
9	5.87	0.0416	5.84	0.0565	3.63E-04	9.41	9.18
10	6.07	0.0442	5.85	0.0485	4.02E-04	8.15	7.99
11	6.11	0.0404	5.65	0.0506	3.98E-04	9.95	10.89
12	5.84	0.0373	5.69	0.0458	3.85E-04	11.99	12.91

Tab A. 63   Solubility of tin(II) in halite/ anhydrite saturated solution [mol/kg]

No.	Na	Ca	Cl	SO$_4$	Sn	pH	pcH
1	n.a.	n.a.	n.a.	n.a.	3.53E-03	4.06	4.95
2	5.61	0.0371	5.60	0.0430	1.22E-05	6.76	7.65
3	5.68	0.0384	5.67	0.0424	1.54E-05	6.49	7.40
4	5.60	0.0386	5.59	0.0423	4.48E-06	8.10	8.99
5	5.70	0.0340	5.69	0.0383	9.21E-06	8.77	9.68
6	6.25	0.0432	6.24	0.0483	2.05E-05	9.08	10.10
7	5.61	0.0433	5.61	0.0435	9.64E-05	9.72	10.61
8	5.74	0.0411	5.74	0.0444	1.52E-04	10.17	11.09
10	5.79	0.0350	5.77	0.0411	1.91E-05	9.48	10.41
11	5.77	0.0344	5.74	0.0473	1.74E-04	10.55	11.47

Tab A. 64 Solubility of tin(IV) in halite/ anhydrite saturated solution [mol/kg]

No.	Na	Ca	Cl	SO$_4$	Sn	pH	pcH
1	5.79	0.0397	5.78	0.0448	2.29E-08	7.50	8.44
2	5.80	0.0387	5.79	0.0441	6.90E-08	7.14	8.07
3	5.93	0.0405	5.92	0.0460	6.63E-08	6.79	7.75
4	6.00	0.0406	5.99	0.0460	1.87E-07	6.61	7.58
5	6.00	0.0394	5.98	0.0469	2.52E-07	7.67	8.64
6	6.21	0.0374	6.19	0.0497	1.10E-07	9.37	10.39
7	6.07	0.0386	6.05	0.0491	4.25E-08	8.29	9.28
8	4.88	0.0296	4.85	0.0427	3.80E-08	9.50	10.25
10	6.14	0.0358	6.10	0.0521	5.50E-08	9.42	10.42
11	6.57	0.0398	6.53	0.0561	1.09E-07	9.02	10.11
12	6.12	0.0318	6.07	0.0566	1.69E-08	10.07	11.06

Tab A. 65 Solubility of zirconium in halite/ anhydrite saturated solution [mol/kg]

No.	Na	Ca	Cl	SO$_4$	Zr	pH	pcH
1	6.15	0.0457	6.15	0.0448	2.83E-07	7.14	8.14
2	5.96	0.0475	5.97	0.0459	2.22E-07	6.78	7.75
3	5.87	0.0435	5.87	0.0437	1.34E-07	7.55	8.50
4	6.07	0.0491	6.08	0.0481	2.93E-07	7.81	8.80
5	5.93	0.0413	5.92	0.0461	2.11E-07	9.09	10.05
6	5.87	0.0423	5.87	0.0446	1.59E-07	8.32	9.27
7	6.01	0.0399	5.99	0.0485	1.51E-07	9.65	10.62
8	5.97	0.0438	5.96	0.0465	1.69E-07	8.61	9.57
9	5.81	0.0424	5.80	0.0462	1.86E-07	8.70	9.63
10	6.02	0.0407	6.00	0.0493	1.87E-07	9.46	10.43

A.6.2 Determined solubilities in IP9 solution

Tab A. 66   Solubility of lead in IP9 / IP9 Reak solution [mol/kg]

No.	Na	K	Mg	Ca	Cl	SO$_4$	Pb	pH	pcH
1	4.70	0.881	1.21	0.00977	7.03	0.501	7.64E-03	7.182	8.48
2	3.99	0.749	1.02	0.00836	6.02	0.397	5.89E-03	7.552	8.62
3	3.93	0.740	1.01	0.00825	5.94	0.382	3.54E-03	7.739	8.79
4	4.16	0.769	1.07	0.00756	6.21	0.443	3.33E-03	7.775	8.89
5 Reak	6.10	0.969	0.00386	0.00595	6.49	0.302	1.57E-03	8.372	9.42
6 Reak	5.65	0.888	0.00391	0.00648	6.05	0.253	1.20E-03	8.538	9.49
7 Reak	5.82	0.918	0.00223	0.00603	6.21	0.273	9.87E-04	8.637	9.62
8 Reak	6.09	0.965	0.00149	0.00551	6.48	0.295	9.68E-04	8.631	9.67
9 Reak	5.52	0.816	< LoQ	0.00984	5.81	0.271	5.09E-05	9.958	10.85
10 Reak	5.26	0.816	< LoQ	0.00925	5.61	0.246	2.45E-05	10.736	11.59

Tab A. 67   Solubility of molybdenum(VI) in IP9/ IP9 Reak solution [mol/kg]

No.	Na	K	Mg	Ca	Cl	SO$_4$	Mo	pH	pcH
1	3.70	0.704	0.951	0.00666	5.59	0.365	7.12E-05	5.826	6.80
2	3.83	0.730	0.961	0.00781	5.77	0.364	6.54E-05	6.779	7.79
3	4.01	0.775	0.972	0.00739	5.97	0.387	7.05E-05	7.150	8.20
4	4.15	0.778	1.029	0.00712	6.17	0.414	7.16E-05	8.343	9.45
5 Reak	5.99	0.952	0.00381	0.00606	6.35	0.307	2.37E-05	7.737	8.76
6 Reak	5.96	0.936	0.00193	0.00644	6.34	0.286	2.46E-05	8.551	9.56
7 Reak	6.02	0.947	0.00315	0.00621	6.40	0.292	2.49E-05	8.659	9.69
8 Reak	5.51	0.840	< LoQ	0.00932	5.83	0.266	2.35E-05	9.379	10.29
9 Reak	6.02	0.941	< LoQ	0.00615	6.37	0.301	2.65E-05	9.649	10.67
10 Reak	5.60	0.844	< LoQ	0.00893	5.90	0.281	2.32E-05	10.629	11.56

Tab A. 68 Solubility of nickel in IP9/ IP9 Reak solution [mol/kg]

No.	Na	K	Mg	Ca	Cl	SO$_4$	Ni	pH	pcH
1	4.10	0.776	1.03	0.00797	6.12	0.415	4.10E-04	7.587	8.68
2	4.01	0.763	1.02	0.00680	5.99	0.415	6.44E-04	7.474	8.54
3	4.48	0.868	1.15	0.00789	6.75	0.457	2.81E-03	7.188	8.42
4	3.97	0.770	1.01	0.00740	6.01	0.392	8.13E-03	6.950	8.02
5 Reak	5.94	0.973	2.59E-3	0.00634	6.35	0.290	3.75E-05	8.241	9.25
6 Reak	5.87	0.965	6.87E-04	0.00565	6.27	0.289	6.89E-06	8.583	9.58
7 Reak	5.99	0.981	< LoQ	0.00672	6.44	0.270	3.55E-06	8.828	9.85
8 Reak	6.08	0.978	< LoQ	0.00658	6.46	0.301	2.81E-07	9.298	10.34
9 Reak	5.72	0.889	< LoQ	0.00845	6.04	0.289	5.65E-07	9.241	10.20
10 Reak	5.30	0.816	< LoQ	0.00900	5.59	0.270	1.27E-07	10.898	11.76

Tab A. 69 Solubility of strontium in IP9/ IP9 Reak solution [mol/kg]

No.	Na	K	Mg	Ca	Cl	SO$_4$	Sr	pH	pcH
1	3.86	0.757	0.999	0.00791	5.91	0.358	6.67E-05	7.013	8.06
2	3.90	0.760	0.996	0.00783	5.93	0.370	6.85E-05	7.391	8.44
3	4.45	0.778	0.611	0.00890	5.82	0.324	9.02E-05	8.533	9.51
4	4.23	0.807	0.978	0.00755	6.23	0.391	6.87E-05	8.335	9.44
5 Reak	5.96	0.672	0.00364	0.00370	6.27	0.189	9.71E-05	7.903	8.89
6 Reak	6.93	0.791	< LoQ	0.00648	7.25	0.241	8.64E-05	8.647	9.83
7 Reak	5.77	0.684	< LoQ	0.00323	6.07	0.193	8.58E-05	12.170	13.12
8 Reak	6.48	0.728	0.00346	0.00352	6.82	0.198	8.92E-05	8.372	9.47
9 Reak	5.57	0.836	< LoQ	0.00946	5.83	0.295	2.70E-05	10.100	11.00
10 Reak	5.61	0.879	< LoQ	0.00833	5.98	0.266	6.16E-05	8.876	9.80

Tab A. 70   Solubility of tin(IV) in IP9/ IP9 Reak solution [mol/kg]

No.	Na	K	Mg	Ca	Cl	SO$_4$	Sn	pH	pcH
1	3.91	0.723	0.982	0.00771	5.84	0.389	1.48E-06	6.308	7.34
2	4.08	0.748	1.000	0.00821	6.05	0.396	2.95E-06	6.627	7.70
3	3.88	0.707	0.946	0.00822	5.73	0.382	1.47E-04	7.031	8.04
4	4.08	0.746	0.959	0.00777	5.94	0.407	6.23E-06	7.559	8.61
5 Reak	6.19	0.975	< LoQ	0.00622	6.60	0.289	4.78E-07	7.701	8.74
6 Reak	5.98	0.939	< LoQ	0.00610	6.35	0.291	6.70E-07	8.172	9.17
7 Reak	5.75	0.907	< LoQ	0.00617	6.10	0.284	5.34E-07	8.584	9.53
8 Reak	5.98	0.936	< LoQ	0.00622	6.33	0.298	4.36E-07	9.059	10.05
9 Reak	5.66	0.863	< LoQ	0.00830	5.94	0.298	2.26E-07	10.025	10.95
10 Reak	5.62	0.867	< LoQ	0.00822	5.95	0.281	4.78E-07	10.547	11.46

A.6.3 Determined solubilities in IP21 solution

Tab A. 71 Solubility of lead in IP21/ IP21 Reak solution [mol/kg]

No.	Na	K	Mg	Ca	Cl	SO$_4$	Pb	pH	pcH
1	0.477	0.645	4.20	0.000475	8.96	0.313	2.59E-02	4.22	6.32
2	0.449	0.606	4.04	0.000507	8.58	0.303	2.42E-02	5.12	7.12
3	0.447	0.614	3.87	0.000459	8.26	0.290	2.44E-02	5.35	7.27
4	0.537	0.728	3.38	0.000536	7.58	0.244	2.46E-02	5.55	7.25
5	0.491	0.643	3.82	0.000488	8.24	0.292	2.38E-02	6.42	8.32
6	0.701	0.675	4.20	0.000519	9.16	0.333	2.37E-02	6.87	9.01
7 Reak	3.28	0.787	0.801	0.013020	5.14	0.285	3.11E-03	7.31	8.16
8 Reak	4.41	0.975	0.977	0.007069	6.70	0.325	1.92E-03	8.08	9.27
9 Reak	5.66	1.103	0.356	0.005736	6.79	0.349	7.66E-04	8.50	9.62
10 Reak	5.68	1.084	0.0882	0.003926	6.27	0.338	5.31E-04	8.79	9.77

Tab A. 72 Solubility of molybdenum(VI) in IP21/ IP21 Reak solution [mol/kg]

No.	Na	K	Mg	Ca	Cl	SO$_4$	Mo	pH	pcH
1	0.567	0.515	4.15	<7E-07	8.79	0.302	2.88E-04	3.51	5.59
2	0.559	0.510	4.00	<7E-07	8.48	0.294	3.28E-04	3.87	5.86
3	0.713	0.527	4.17	<7E-07	8.96	0.308	3.61E-04	4.05	6.16
4	0.619	0.514	4.16	<7E-07	8.86	0.293	3.51E-04	4.43	6.53
5	0.591	0.486	3.85	<7E-07	8.20	0.292	3.80E-04	5.68	7.59
6	0.870	0.512	3.80	<7E-07	8.38	0.295	3.93E-04	6.88	8.82
7 Reak	3.80	0.841	0.515	0.0125	5.13	0.281	5.67E-05	7.32	8.13
8 Reak	4.40	0.876	0.293	0.0114	5.36	0.265	4.94E-05	7.26	8.09
9 Reak	4.72	0.907	0.147	0.00930	5.40	0.272	4.67E-05	8.72	9.54
10 Reak	5.53	1.063	0.0250	0.00423	6.04	0.309	6.17E-05	9.01	9.93

Tab A. 73 Solubility of nickel in IP21/ IP21 Reak solution [mol/kg]

No.	Na	K	Mg	Ca	Cl	SO$_4$	Ni	pH	pcH
1	0.775	0.487	3.26	0.0023765	7.59	0.250	1.50E-01	5.31	7.00
2	0.701	0.480	3.48	<6E-07	7.77	0.259	7.60E-02	5.49	7.26
3	0.765	0.528	3.70	<6E-07	8.15	0.279	8.44E-03	6.13	8.01
4	0.639	0.508	3.79	<6E-07	8.19	0.278	4.13E-03	6.29	8.19
5	0.565	0.507	4.08	<6E-07	8.65	0.293	1.66E-03	6.47	8.51
6	0.805	0.508	3.71	<6E-07	8.17	0.280	1.61E-03	6.70	8.59
7 Reak	4.11	0.838	0.294	<6E-07	5.02	0.258	3.83E-04	7.63	8.39
8 Reak	4.09	0.838	0.274	<6E-07	4.96	0.258	2.52E-05	8.17	8.92
9 Reak	5.13	0.992	0.0981	<6E-07	5.73	0.294	3.99E-06	8.71	9.58
10 Reak	5.48	1.042	0.0117	<6E-07	5.93	0.308	4.07E-06	9.13	10.03

Tab A. 74 Solubility of niobium in IP21/ IP21 Reak solution [mol/kg]

No.	Na	K	Mg	Ca	Cl	SO$_4$	Nb	pH	pcH
1	0.670	0.481	4.01	0.000961	8.60	0.284	<5E-08	3.62	5.60
2	0.745	0.523	3.98	0.000852	8.65	0.292	<5E-08	4.49	6.47
3	0.723	0.489	3.88	0.001009	8.41	0.282	<5E-08	5.38	7.30
4	0.685	0.462	3.70	0.000908	7.97	0.287	7.85E-06	6.74	8.55
5	0.658	0.479	4.01	0.000826	8.58	0.287	9.73E-08	5.34	7.31
6	0.692	0.482	3.97	0.000888	8.55	0.285	7.30E-07	6.05	8.01
7 Reak	5.857	1.027	0.0177	0.005098	6.31	0.310	9.87E-08	7.04	8.05
8 Reak	5.907	1.044	0.0128	0.004620	6.37	0.310	2.29E-07	7.43	8.45
9 Reak	5.899	1.021	<0.00007	0.004712	6.31	0.309	1.29E-06	7.92	8.93
10 Reak	5.858	1.000	<0.00007	0.004535	6.24	0.314	2.68E-06	8.33	9.32

Tab A. 75   Solubility of palladium(II) in IP21/ IP21 Reak solution [mol/kg]

No.	Na	K	Mg	Ca	Cl	SO$_4$	Pd	pH	pcH
1	0.472	0.453	4.11	0.000777	8.59	0.294	1.56E-02	3.5	5.50
2	0.443	0.432	3.65	0.00201	7.64	0.266	0.00E+00	4.9	6.64
3	0.488	0.466	3.99	0.000973	8.39	0.289	1.54E-02	5.04	6.98
4	0.533	0.456	4.09	0.000735	8.60	0.299	1.54E-02	6.19	8.18
5	0.636	0.439	3.84	0.000843	8.23	0.278	1.79E-02	5.96	7.84
6	0.653	0.557	3.86	0.000794	8.33	0.316	1.79E-02	6.85	8.74
7 Reak	5.65	1.16	0.0687	0.00431	6.32	0.320	6.52E-05	8.81	9.81
8 Reak	5.63	1.06	0.0179	0.00389	6.10	0.317	2.94E-05	8.96	9.92
9 Reak	6.06	1.13	0.0104	0.00440	6.54	0.341	1.42E-05	9.13	10.18
10 Reak	5.86	1.09	< LoQ	0.00424	6.30	0.332	3.92E-06	9.56	10.56

Tab A. 76   Solubility of selenium(IV) in IP21/ IP21 Reak solution [mol/kg]

No.	Na	K	Mg	Ca	Cl	SO$_4$	SeO$_3$	pH	pcH
1	0.556	0.636	4.75	0.00529	10.09	0.243	6.69E-02	3.57	5.94
2	0.344	0.388	2.97	0.00327	6.36	0.154	1.27E-02	4.75	6.16
3	0.457	0.518	3.93	0.00423	8.42	0.201	9.00E-03	5.01	6.95
4	0.474	0.517	4.03	0.00416	8.63	0.206	5.94E-03	5.98	7.97
5	0.474	0.484	3.64	0.00404	7.85	0.190	4.84E-03	6.4	8.18
6	0.467	0.481	3.70	0.01723	7.97	0.200	5.08E-03	6.9	8.72
7 Reak	5.95	1.13	0.0397	0.00506	6.51	0.327	1.32E-03	8.32	9.37
8 Reak	5.90	1.07	0.0142	0.00469	6.36	0.323	1.34E-03	8.43	9.45
9 Reak	6.09	1.10	0.0069	0.00495	6.55	0.333	1.43E-03	8.68	9.74
10 Reak	5.75	1.10	0.00370	0.00509	6.22	0.326	1.21E-03	9.62	10.61

Tab A. 77   Solubility of strontium in IP21/ IP21 Reak solution [mol/kg]

No.	Na	K	Mg	Ca	Cl	SO$_4$	Sr	pH	pcH
1	0.549	0.479	3.79	0.000529	8.05	0.274	2.54E-05	4.66	6.50
2	0.579	0.456	3.76	0.000494	8.02	0.274	2.46E-05	4.99	6.82
3	0.431	0.451	3.95	0.000512	8.23	0.270	2.37E-05	5.31	7.22
4	0.441	0.465	3.88	0.000516	8.13	0.269	2.48E-05	5.61	7.48
5	0.442	0.487	3.94	0.000487	8.24	0.287	2.32E-05	6.24	8.14
6	0.545	0.475	3.69	0.000491	7.87	0.263	2.46E-05	6.84	8.63
7 Reak	4.42	0.876	0.295	0.0120	5.39	0.260	1.38E-04	7.01	7.85
8 Reak	4.37	0.866	0.289	0.0128	5.30	0.268	1.51E-04	7.11	7.94
9 Reak	5.02	0.802	0.103	0.00566	5.63	0.204	4.16E-05	8.69	9.56

Tab A. 78   Solubility of tin(II) in IP21/ IP21 Reak solution [mol/kg]

No.	Na	K	Mg	Ca	Cl	SO$_4$	Sn	pH	pcH
1	n.a.	n.a.	n.a.	n.a.	n.a.	n.a.	n.a.	3.58	
2	8.47	0.476	3.96	0.00095	8.47	0.280	2.61E-03	4.65	6.60
3	8.48	0.515	3.84	0.00133	8.48	0.269	4.87E-04	5.00	6.92
4	8.13	0.449	3.79	0.00145	8.13	0.265	6.81E-05	5.83	7.69
5	8.37	0.468	3.92	0.00106	8.37	0.276	2.02E-04	6.40	8.32
6	7.88	0.433	3.60	0.00204	7.88	0.254	4.81E-04	6.94	8.72
7 Reak	5.28	0.832	0.285	0.01135	5.28	0.301	2.03E-05	8.18	9.01
8 Reak	5.77	0.862	0.172	0.00980	5.77	0.286	1.67E-05	8.36	9.27
9 Reak	6.13	0.978	0.096	0.00637	6.13	0.308	7.09E-06	8.66	9.64
10 Reak	6.13	0.961	0.00248	0.00626	6.13	0.310	8.16E-06	9.51	10.49

Tab A. 79   Solubility of tin(IV) in IP21/ IP21 Reak solution [mol/kg]

No.	Na	K	Mg	Ca	Cl	SO$_4$	Sn	pH	pcH
1	0.454	0.496	4.10	0.000530	8.58	0.287	5.12E-06	3.75	5.78
2	0.555	0.548	4.48	0.000466	9.43	0.313	5.30E-06	4.97	7.22
3	0.539	0.520	4.14	0.000527	8.75	0.292	1.28E-05	5.33	7.40
4	0.551	0.487	3.86	0.000498	8.20	0.279	5.27E-06	5.73	7.65
5	0.594	0.502	3.85	0.000508	8.24	0.282	1.01E-05	6.24	8.16
6	0.689	0.505	3.71	0.000543	8.06	0.278	3.95E-06	6.74	8.61
7 Reak	4.07	0.847	0.340	0.0113	5.08	0.265	< 1.7E-09	7.31	8.09
8 Reak	4.15	0.838	0.283	0.0111	5.06	0.261	< 1.7E-09	7.66	8.43
9 Reak	5.14	1.01	0.072	0.00494	5.70	0.296	< 1.7E-09	8.80	9.67
10 Reak	5.68	1.10	0.005	0.00237	6.15	0.319	< 1.7E-09	9.27	10.21

Tab A. 80   Solubility of zirconium in IP21/ IP21 Reak solution [mol/kg]

No.	Na	K	Mg	Ca	Cl	SO$_4$	Zr	pH	pcH
1	0.53	0.48	3.92	0.00185	8.31	0.277	5.56E-07	6.03	7.94
2	0.46	0.49	4.02	0.00170	8.42	0.282	6.14E-07	4.99	6.94
3	0.48	0.48	3.95	0.00174	8.28	0.284	6.61E-07	5.61	7.52
4	0.52	0.52	4.06	0.00181	8.60	0.283	7.63E-07	6.04	8.02
5	0.46	0.48	3.99	0.00175	8.37	0.283	6.46E-07	6.19	8.12
6	0.50	0.50	3.97	0.00109	8.39	0.278	6.32E-07	6.87	8.80
7 Reak	5.00	0.95	0.311	0.00678	6.00	0.292	4.48E-07	8.41	9.38
8 Reak	5.34	1.00	0.111	0.00627	5.98	0.294	4.23E-07	8.7	9.64
9 Reak	5.53	1.02	0.00883	0.00552	5.96	0.310	3.84E-07	9.23	10.17
10 Reak	5.56	1.04	<0.00011	0.00512	5.99	0.314	1.53E-06	9.44	10.38

A.6.4 Determined solubilities in Lower Cretaceous clay pore water (UK water)

Tab A. 81   Solubility of lead in UK water [mol/kg]

No.	Na	K	Mg	Ca	Cl	SO$_4$	Pb	pH	pcH
1	2.61	0.0150	0.0755	0.187	3.00	0.0747	6.74E-04	6.807	7.21
2	2.61	0.0128	0.0786	0.187	3.12	0.0191	8.17E-04	7.005	7.43
3	2.52	0.0138	0.0749	0.177	3.00	0.0183	5.51E-04	7.245	7.64
4	2.66	0.0131	0.0767	0.181	3.15	0.0192	2.15E-04	7.660	8.09
5	2.62	0.0136	0.0711	0.173	3.09	0.0194	4.57E-04	8.034	8.45
6	2.33	0.0152	0.0736	0.169	2.79	0.0179	1.11E-04	7.897	8.25
7	2.36	0.0157	0.0614	0.168	2.79	0.0175	9.85E-06	9.156	9.51
8	2.45	0.0129	0.0277	0.174	2.83	0.0173	7.22E-06	9.450	9.81
9	2.59	0.0117	0.0031	0.174	2.92	0.0189	1.97E-05	9.919	10.29
10	2.49	0.0167	< LoQ	0.170	2.81	0.0192	2.20E-05	11.105	11.45
UK_Po_Mo sample L2	2.65	0.0104	0.0197	0.285	3.25	0.0114	6.18E-06	11.98	12.42
UK_Po_Ni sample L2	2.62	0.0146	< LoQ	0.345	3.30	0.0125	2.84E-06	9.12	9.58
UK_Po_Pb sample L2	2.57	0.0110	< LoQ	0.277	3.11	0.0130	3.19E-04	11.41	11.83
UK_Po_Sn sample L2	2.57	0.0124	< LoQ	0.261	3.08	0.0153	2.20E-07	12.01	12.42
UK_Po_Sr sample L2	2.58	0.0137	< LoQ	0.268	3.10	0.0152	2.63E-03	12.00	12.41
IP9_So_Mo sample L2	4.22	0.766	0.968	0.00467	6.21	0.358	9.34E-05	8.29	9.39
IP9_So_Ni sample L2	4.17	0.758	1.117	0.00710	6.49	0.340	2.40E-04	7.97	9.15
IP9_So_Pb sample L2	4.22	0.755	0.963	0.00567	6.27	0.324	2.06E-04	8.28	9.39
IP9_So_Sn sample L2	4.50	0.806	1.024	0.00609	6.67	0.348	<4E-08	8.30	9.50
IP9_So_Sr sample L2	4.31	0.741	0.961	0.00512	6.33	0.325	<5E-08	8.23	9.35

Tab A. 82   Solubility of molybdenum(VI) in UK water [mol/kg]

No.	Na	K	Mg	Ca	Cl	SO$_4$	Mo	pH	pcH
1	2.48	0.0124	0.0767	0.179	2.96	0.0194	1.03E-05	6.842	7.23
2	2.59	0.0108	0.0759	0.180	3.08	0.0195	5.52E-06	6.777	7.19
3	2.56	0.0119	0.0762	0.178	3.04	0.0196	5.47E-06	6.639	7.04
4	2.60	0.0115	0.0760	0.179	3.08	0.0199	5.68E-06	6.753	7.17
5	2.52	0.0112	0.0768	0.179	3.00	0.0195	5.00E-06	6.789	7.19
6	2.55	0.0110	0.0766	0.178	3.03	0.0197	4.78E-06	7.061	7.46
7	2.62	0.0131	0.0722	0.178	3.09	0.0197	3.96E-06	7.293	7.71
8	2.49	0.0117	0.0692	0.174	2.95	0.0197	4.44E-06	7.306	7.69
9	2.85	0.0117	< LoQ	0.174	3.17	0.0201	3.91E-06	9.599	10.02
10	2.63	0.0137	< LoQ	0.163	2.93	0.0210	4.06E-06	10.605	10.98

Tab A. 83   Solubility of nickel in UK water [mol/kg]

No.	Na	K	Mg	Ca	Cl	SO$_4$	Ni	pH	pcH
1	2.52	0.0142	0.0739	0.236	3.21	0.0167	4.45E-02	6.891	7.31
2	2.49	0.0137	0.0734	0.207	3.05	0.0179	1.46E-02	7.157	7.55
3	2.54	0.0136	0.0763	0.182	3.04	0.0204	4.29E-03	7.615	8.01
4	2.69	0.0127	0.0816	0.196	3.22	0.0204	8.66E-04	7.817	8.25
5	2.64	0.0128	< LoQ	0.170	2.95	0.0193	2.75E-04	11.144	11.51
6	2.49	0.0144	0.0718	0.173	2.96	0.0184	3.07E-04	8.014	8.39
7	2.59	0.0141	0.0672	0.175	3.05	0.0193	1.29E-04	8.204	8.60
8	2.60	0.0193	< LoQ	0.162	2.92	0.0200	5.34E-06	9.771	10.14
9	2.68	0.0153	0.0019	0.172	3.01	0.0195	5.62E-06	10.092	10.47
10	2.78	0.0144	0.0739	0.174	3.10	0.0196	1.57E-05	10.349	10.75

Tab A. 84   Solubility of niobium in UK water [mol/kg]

No.	Na	K	Mg	Ca	Cl	SO$_4$	Nb	pH	pcH
1	2.77	0.0126	0.0621	0.163	3.19	0.0187	<3.6E-08	6.26	6.68
2	2.92	0.0119	0.0595	0.166	3.34	0.0184	<3.6E-08	6.58	7.03
3	3.01	0.0126	0.0073	0.140	3.28	0.0210	2.75E-07	8.92	9.35
4	2.92	0.0114	0.0552	0.158	3.32	0.0178	<3.6E-08	7.38	7.83
5	2.63	0.0127	0.0591	0.141	3.00	0.0217	<3.6E-08	7.65	8.03
6	2.88	0.0126	0.0603	0.153	3.28	0.0203	1.05E-07	8.09	8.53
7	2.92	0.0130	0.0400	0.145	3.26	0.0214	2.38E-07	8.60	9.03
8	2.99	0.0143	0.0053	0.140	3.25	0.0221	1.98E-07	9.00	9.43
9	2.97	0.0144	<1.6E-5	0.125	3.18	0.0244	1.45E-07	9.75	10.16
10	2.82	0.0127	<1.6E-5	0.128	3.05	0.0228	2.49E-07	9.22	9.61

Tab A. 85   Solubility of palladium(II) in UK water [mol/kg]

No.	Na	K	Mg	Ca	Cl	SO$_4$	SeO$_3$	pH	pcH
1	2.56	0.0122	0.0689	0.206	3.18	0.0177	4.55E-02	6.16	6.57
2	2.51	0.0136	0.0714	0.184	3.09	0.0179	4.90E-02	6.54	6.94
3	2.56	0.0133	0.0695	0.183	3.14	0.0183	4.76E-02	6.72	7.13
4	2.57	0.0115	0.0670	0.184	3.14	0.0177	4.18E-02	6.52	6.93
5	2.59	0.0127	0.0716	0.181	3.07	0.0183	5.86E-04	7.34	7.74
6	2.70	0.0121	0.0670	0.173	3.16	0.0187	1.72E-05	8.24	8.66
7	2.61	0.0135	0.0671	0.180	3.08	0.0180	1.67E-05	8.23	8.63
8	2.67	0.0133	0.0383	0.176	3.08	0.0182	1.17E-06	9.1	9.50
9	2.75	0.0137	<LOQ	0.175	3.08	0.0184	1.11E-06	10.13	10.52
10	2.78	0.0129	<LOQ	0.172	3.10	0.0192	6.80E-06	10.86	11.26

Tab A. 86 Solubility of samarium in UK water [mol/kg]

No.	Na	K	Mg	Ca	Cl	SO$_4$	Sm	pH	pcH
1	2.09	0.0296	0.0577	0.213	2.63	0.0156	2.28E-07	6.319	6.63
2	2.09	0.0239	0.0583	0.201	2.60	0.0165	3.26E-07	7.018	7.33
3	2.42	0.0127	0.0658	0.218	2.97	0.0157	4.55E-08	8.2	8.58
4	2.10	0.0247	0.0561	0.200	2.60	0.0164	3.13E-07	7.337	7.65
5	2.50	0.0118	0.0626	0.187	2.98	0.0170	7.91E-08	8.41	8.79
6	2.45	0.0122	0.0652	0.184	2.92	0.0180	1.56E-08	9.02	9.39
7	2.38	0.0124	0.0645	0.182	2.85	0.0185	<1.5E-09	9.08	9.43
8	2.83	0.0153	0.0068	0.188	3.19	0.0212	<1.5E-09	9.55	9.96
9	2.62	0.0141	<1.8E-5	0.169	2.93	0.0195	<1.5E-09	9.94	10.30
10	2.63	0.0128	<1.8E-5	0.167	2.94	0.0196	<1.5E-09	10.08	10.44

Tab A. 87 Solubility of selenium(IV) in UK water [mol/kg]

No.	Na	K	Mg	Ca	Cl	SO$_4$	SeO$_3$	pH	pcH
1	2.51	0.0118	0.0704	0.188	3.00	0.0181	0.000968	6.50	6.89
2	2.56	0.0128	0.0744	0.185	3.05	0.0183	0.000489	6.95	7.35
3	2.63	0.0136	0.0765	0.191	3.14	0.0186	0.000299	7.33	7.75
4	2.41	0.0125	0.0678	0.214	2.95	0.0165	0.003322	5.89	6.27
5	2.44	0.0146	0.0676	0.190	2.93	0.0196	0.000229	7.83	8.20
6	2.73	0.0148	0.0800	0.223	3.31	0.0202	0.000219	7.83	8.28
7	2.48	0.0134	0.0680	0.180	2.95	0.0190	0.000224	7.87	8.25
8	2.40	0.0155	0.0219	0.170	2.75	0.0228	0.000180	9.40	9.73
9	2.74	0.0126	0.00872	0.186	3.10	0.0189	0.000141	9.46	9.86
10	2.68	0.0125	0.000111	0.181	3.02	0.0183	0.000105	10.33	10.71

Tab A. 88 Solubility of strontium in UK water [mol/kg]

No.	Na	K	Mg	Ca	Cl	SO$_4$	Sr	pH	pcH
1	2.47	0.0112	0.0710	0.167	2.93	0.0163	0.00188	6.897	7.28
2	2.42	0.0106	0.0780	0.184	2.93	0.0162	0.00188	7.078	7.46
3	2.49	0.0143	0.0743	0.175	2.97	0.0175	0.00185	7.121	7.51
4	2.52	0.0142	0.0754	0.177	3.01	0.0177	0.00187	7.158	7.56
5	2.55	0.0144	0.0631	0.173	3.01	0.0177	0.00188	8.691	9.09
7	2.47	0.0107	0.0739	0.176	2.96	0.0163	0.00191	7.836	8.22
8	2.55	0.0147	0.0703	0.169	3.01	0.0176	0.00187	7.773	8.17
9	2.68	0.0113	0.0021	0.172	3.01	0.0186	0.00184	10.019	10.41
10	2.62	0.0118	<1E-5	0.156	2.91	0.0191	0.00184	11.653	12.02

Tab A. 89 Solubility of tin(II) in UK water [mol/kg]

No.	Na	K	Mg	Ca	Cl	SO$_4$	Sn	pH	pcH
1	2.60	0.0136	0.0707	0.286	3.30	0.0127	1.38E-06	6.77	7.22
2	2.56	0.0139	0.0726	0.284	3.26	0.0127	1.62E-06	6.78	7.22
3	2.44	0.0159	0.0672	0.264	3.09	0.0137	4.08E-06	5.51	5.92
4	2.58	0.0137	0.0681	0.277	3.26	0.0126	7.21E-06	8.00	8.44
5	2.62	0.0134	0.0712	0.274	3.30	0.0131	1.50E-06	7.20	7.65
6	2.54	0.0134	0.0715	0.283	3.24	0.0127	1.66E-04	7.46	7.90
7	2.54	0.0138	0.0699	0.273	3.21	0.0133	1.50E-05	8.25	8.68
8	2.57	0.0149	0.0059	0.242	3.05	0.0137	1.81E-05	9.30	9.69
9	2.60	0.0131	0.0224	0.261	3.15	0.0129	1.09E-05	8.90	9.31
10	2.66	0.0138	0.0099	0.246	3.16	0.0137	1.46E-05	9.14	9.55

Tab A. 90   Solubility of tin(IV) in UK water [mol/kg]

No.	Na	K	Mg	Ca	Cl	SO$_4$	Sn	pH	pcH
1	2.53	0.0140	0.0631	0.257	3.16	0.0131	< 1e-07	6.668	7.10
2	2.51	0.0165	0.0619	0.239	3.10	0.0131	2.07E-07	6.877	7.30
3	2.54	0.0158	0.0618	0.235	3.12	0.0134	7.41E-08	6.909	7.33
4	2.62	0.0142	0.0658	0.247	3.24	0.0137	4.42E-07	6.842	7.29
5	2.69	0.0167	0.0084	0.195	3.11	< LoQ	8.35E-07	9.505	9.91
6	2.77	0.0314	< LoQ	0.136	3.07	< LoQ	2.02E-07	11.704	12.10
7	2.77	0.0123	0.0038	0.168	3.13	< LoQ	3.80E-07	9.481	9.89
8	2.67	0.0207	0.0367	0.175	3.11	< LoQ	1.29E-06	8.850	9.26
9	2.58	0.0204	0.0239	0.173	2.99	< LoQ	7.26E-07	9.093	9.48
10	2.81	0.0174	0.0058	0.169	3.18	< LoQ	2.02E-06	9.327	9.75

Tab A. 91   Solubility of zirconium in UK water [mol/kg]

No.	Na	K	Mg	Ca	Cl	SO$_4$	Zr	pH	pcH
1	2.52	0.0165	0.0755	0.183	3.02	0.0190	9.65E-07	6.69	7.05
2	2.73	0.0160	0.0837	0.197	3.26	0.0214	1.02E-06	7.12	7.52
3	2.59	0.0152	0.0787	0.185	3.09	0.0195	7.84E-07	7.29	7.66
4	2.55	0.0144	0.0708	0.173	3.02	0.0190	8.36E-07	7.73	8.09
5	2.67	0.0139	0.0743	0.186	3.16	0.0202	9.93E-07	7.85	8.24
6	2.59	0.0139	0.0721	0.178	3.07	0.0192	8.86E-07	7.74	8.11
7	2.47	0.0136	0.0666	0.171	2.92	0.0185	6.36E-07	7.73	8.07
8	2.57	0.0131	0.00518	0.165	2.88	0.0186	3.74E-07	9.63	9.96
9	2.77	0.0136	0.00158	0.172	3.09	0.0203	8.03E-07	9.90	10.26
10	2.65	0.0145	< LoQ	0.164	2.95	0.0205	6.07E-07	10.84	11.18

List of Tables

List of Figures